

UNIVERSITE DE LIEGE
FACULTE DES SCIENCES APPLIQUEES

RECENT ADVANCES IN THE FIELD OF STEEL JOINTS
COLUMN BASES AND FURTHER CONFIGURATIONS
FOR BEAM-TO-COLUMN JOINTS
AND BEAM SPLICES

par

J.P. JASPART
Chercheur qualifié du F.N.R.S.

Thèse présentée en vue de l'obtention du grade d'Agrégé de l'Enseignement Supérieur

Année académique 1996-1997

UNIVERSITE DE LIEGE

FACULTE DES SCIENCES APPLIQUEES

Le présent mémoire peut être livré à l'impression.

Liège le 7 février 1997

Le Secrétaire de la Faculté
des Sciences appliquées.
Secrétaire du Jury

J.ETIENNE

Le Doyen de la Faculté
des Sciences appliquées.
Président du Jury.

J.BOZET

Article 6 de l'Arrêté royal du 10 mars 1931 appliquant la loi du 21 mai 1929 sur la collation des grades académiques et les programmes des examens universitaires :
"En aucun cas, les opinions de l'auteur ne peuvent être considérées, par le fait de l'autorisation d'impression de la dissertation, comme étant celles du Jury ou de l'Université".

TABLE OF CONTENTS

	Pages
ACKNOWLEDGMENT	
FOREWORD	
PREFATORY CHAPTER	
PART I: GENERAL INTRODUCTION	
1. GENERAL INTRODUCTION	
1.1 Definitions	1.1
1.2 Sources of joint deformability	1.2.
<i>1.2.1 Beam-to-column joints</i>	1.3.
1.2.1.1 Major axis joints	1.3.
1.2.1.2 Minor axis joints	1.5.
1.2.1.3 Joints with beams on the major and minor column axes	1.6.
<i>1.2.2 Beam splices and column splices</i>	1.7.
<i>1.2.3 Beam-to-column joints</i>	1.8.
<i>1.2.4 Column bases</i>	1.8.
1.3 Joint modelling	1.9.
<i>1.3.1 General</i>	1.9.
<i>1.3.2 Modelling and sources of joint deformability</i>	1.12.
<i>1.3.3 Simplified modelling according to Eurocode 3</i>	1.12.
<i>1.3.4 Concentration of the joint deformability</i>	1.13.
1.3.4.1 Major axis beam-to column joint configurations	1.13.
1.3.4.2 Minor axis beam-to column joint configurations and beam-to-beam configurations	1.15.
<i>1.3.5 Notations</i>	1.15.
1.4 Joint idealization	1.15.

Table of contents

1.5	Joint characterization	1.19.
1.6	Joint classification	1.22.
	<i>1.6.1 General</i>	1.22.
	<i>1.6.2 Classification based on mechanical joint properties</i>	1.22.
1.7	Ductility classes of joints	1.23.
	<i>1.7.1 General concept</i>	1.23.
	<i>1.7.2 Requirements for classes of joints</i>	1.26.
 PART II: CHARACTERIZATION OF THE JOINTS		
2.	COMPONENT METHOD	2.1.
	2.1 Generals on the characterization	2.1.
	2.2 Principles of the component method	2.12.
	2.3 Levels of refinement	2.18.
3.	NEW CONTRIBUTIONS TO THE COMPONENT METHOD	3.1.
	3.1 Content of the chapter	3.1.
	3.2 Major axis beam-to-column joints and beam splices	3.2.
	<i>3.2.1 Behaviour of new components and additional considerations on existing ones</i>	3.2.
	3.2.1.1 Beam flange and web in compression	3.2.
	<u>Resistance</u>	3.2.
	<u>Stiffness</u>	3.4.
	<u>Deformation capacity</u>	3.4.
	3.2.1.2 Stiffening and strengthening of the extended part of an end-plate	3.5.
	<u>Resistance</u>	3.5.
	<u>Stiffness</u>	3.10.
	<u>Deformation capacity</u>	3.10.
	3.2.1.3 Intermediate stiffeners	3.11.

Table of contents

	<u>Resistance</u>	3.11.
	<u>Stiffness and deformation capacity</u>	3.12.
3.2.1.4	Haunches	3.12.
	<u>Geometrical and mechanical properties of the haunch</u>	3.14.
	<u>Resistance of the haunch flange</u>	3.15.
	<u>Resistance of the haunch web</u>	3.18.
	<u>Resistance of the column web in compression</u>	3.18.
	<u>Resistance of the beam web in transverse compression</u>	3.20.
	<u>Stiffness</u>	3.20.
	<u>Deformation capacity</u>	3.21.
3.2.1.5	Non-perpendicularly connected elements	3.21.
	<u>General</u>	3.21.
	<u>Loading</u>	3.22.
	<u>Distribution of internal forces</u>	3.23.
	<u>Component properties</u>	3.24.
3.2.1.6	Slender column web panels	
	<u>Context</u>	3.29.
	<u>Recommendations of Eurocode 3 Annex J</u>	3.30.
	<u>Design approaches for slender web panels</u>	3.32.
3.2.2	<i>Interaction between components</i>	3.37.
3.2.2.1	Generalities	3.37.
3.2.2.2	Physical description of the interactions	3.38.
	<u>Interactions in the column web panel</u>	3.38.
	<u>Interaction in the column flange for bolted connections</u>	3.41.
3.2.2.3	Numerical investigations	3.41.

Table of contents

	<u>Test specimens</u>	3.41.
	<u>Analysis of the results</u>	3.43.
3.2.2.4	Experimental investigations	3.53.
	<u>Test specimens</u>	3.53.
	<u>Definition of the experimental pseudo-plastic moment resistance</u>	3.55.
	<u>Analysis of WS test results</u>	3.56.
	<u>Analysis of WN test results</u>	3.58.
	<u>Analysis of EPN test results</u>	3.59.
3.2.2.5	Conclusions	3.61.
3.2.3	<i>Assembly of the components</i>	3.62.
3.2.3.1	Introduction	3.62.
3.2.3.2	Joint under bending and shear forces	3.65.
	<u>Stiffness assembly</u>	3.67.
	<u>Strength assembly</u>	3.70.
	<u>Validation through comparisons with tests</u>	3.76.
3.2.3.3	Joint under bending , shear and axial compressive or tensile forces	3.78.
	<u>Introduction</u>	3.78.
	<u>Similarities and specificities comparatively to joints under bending and shear</u>	3.79.
	<u>Recent works on joint assembly</u>	3.81.
	<u>Application of the software and conclusions</u>	3.89.
3.3	Minor axis beam-to-column joints	3.91.
	<i>3.3.3 Introduction</i>	3.91.
	<i>3.3.4 Local failure</i>	3.93.
	3.3.4.3 Flexural mechanisms	3.93.
	3.3.4.4 Punching shear mechanisms	3.96.

Table of contents

3.3.4.5	Combined flexural and punching shear mechanisms	3.96.
3.3.4.6	Correction to take into account the difference between Johansen and Von Mises criteria	3.98.
3.3.4.7	Comparison between the three modes of local failure	3.99.
3.3.5	<i>Global failure</i>	3.100.
3.3.6	<i>Design resistance</i>	3.101.
3.3.7	<i>Conclusions</i>	3.101.
3.4	Column bases	3.102.
3.4.1	<i>Introduction</i>	3.102.
3.4.2	<i>Experimental tests</i>	3.102.
3.4.2.1	Test set-up and general configuration of the specimens	3.102.
3.4.2.2	Measured geometrical and mechanical characteristics	3.106.
3.4.2.3	Instrumentation	3.108.
3.4.2.4	Moment-rotation curves	3.109.
	<u>Derivation of the curves</u>	3.109.
	<u>Comparison of the curves</u>	3.113.
	<u>Main characteristic values of the curves</u>	3.116.
3.4.3	<i>Analytical model</i>	3.117.
3.4.3.1	Evaluation of the resistance	3.118.
	<u>Introduction</u>	3.118.
	<u>Carrying capacity of the concrete block</u>	3.118.
	<u>Strength of the anchor bolts in tension and the base plate in bending</u>	3.120.
	<u>Resistance of the steel profile</u>	3.124.
	<u>Assembly of the components</u>	3.125.
	<u>Comparison with the experimental tests</u>	3.129.

Table of contents

3.4.3.2	Evaluation of the initial stiffness	3.132.
<i>3.4.4</i>	<i>Mechanical model</i>	3.133.
3.4.4.1	Background of the model	3.133.
3.4.4.2	Response of the individual components	3.136.
	<u>Concrete in compression</u>	3.136.
	<u>Anchor bolts in tension and base plate in bending</u>	3.138.
	<u>Steel profile</u>	3.144.
3.4.4.3	Assembly procedure	3.145.
3.4.4.4	Comparison with the experiments	3.151.
<i>3.4.5</i>	<i>Conclusions and further developments</i>	3.158.
3.5	Composite joints	3.159.
<i>3.5.1</i>	<i>Introduction</i>	3.159.
<i>3.5.2</i>	<i>Characterization</i>	3.161.
3.5.2.1	Concrete in tension	3.162.
3.5.2.2	Reinforcement bars in tension	3.162.
3.5.2.3	Encased columns	3.162.
3.5.2.4	Contact plates	3.163.
3.5.2.5	Assembly of the components	3.163.
<i>3.5.3</i>	<i>Classification</i>	3.163.
3.5.3.1	Classification by stiffness	3.163.
3.5.3.2	Classification by resistance	3.163.
3.5.3.3	Classification by ductility	3.163.
<i>3.5.4</i>	<i>Modelling</i>	3.163.
<i>3.5.5</i>	<i>Idealization</i>	3.164.
<i>3.5.6</i>	<i>Conclusions</i>	3.164.
3.6	Extension to high strength steels (HSS)	3.164.

Table of contents

3.6.1	<i>Introduction</i>	3.164.
3.6.2	<i>Steel grade limitation</i>	3.165.
3.6.3	<i>Column web in compression and HSS</i>	3.166.
3.6.3.1	Design resistance according to Eurocode 3 Annex J	3.166.
3.6.3.2	Comparisons with numerical simulations	3.167.
	<u>Available works with steel grades up to S355</u>	3.167.
	<u>Recent works with steel grades up to S460</u>	3.167.
3.6.3.2	Comparisons with experimental tests	3.169.
	<u>Available works with steel grades up to S355</u>	3.169.
	<u>Recent works with steel grades up to S460</u>	3.169.
3.6.4	<i>Conclusions</i>	3.170.

PART III: IDEALIZATION AND CLASSIFICATION OF THE JOINTS

4.	IDEALIZATION	4.1.
4.1	Introduction	4.1.
	<i>4.1.1 Elastic verification of the joint</i>	4.2.
	<i>4.1.2 Plastic verification of the joint</i>	4.3.
	<i>4.1.3 Equivalent stiffness for plastic joint verification</i>	4.3.
4.2	Rectangular frames	4.5.
4.3	Pitched-roof portal frames	4.8.
4.4	Accuracy of the proposed formulae	4.10.
	<i>4.4.1 Rectangular frames</i>	4.10.
	<i>4.4.2 Pitched-roof portal frames</i>	4.12.
4.5	Conclusions	4.13.
5.	CLASSIFICATION	5.1.

Table of contents

5.1	Introduction	5.1.
5.2	Eurocode 3 stiffness classification	5.1.
5.3	Ongoing research works on classification	5.4.
5.4	Classification criteria for joints in pitched-roof portal frames	5.6.
	<i>5.4.1 Objectives</i>	5.6.
	<i>5.4.2 Stiffness classification boundary</i>	5.7.
5.5	Conclusions	5.9.

PART IV: DESIGN TOOLS FOR PRACTITIONERS

6.	DESIGN TOOLS FOR PRACTITIONERS	6.1.
6.1	Introduction	6.1.
6.2	Content of the design handbook	6.2.
6.3	Design of the structural joints	6.3.
6.4	Design sheets and design tables	6.3.
	<i>6.4.1 The SPRINT project</i>	6.3.
	<i>6.4.2 The SPRINT document</i>	6.4.
	<i>6.4.3 The SPRINT design tools for joints</i>	6.4.
	<i>6.4.4 The different ways to use the SPRINT design tools</i>	6.6.
6.5	PC software DESIMAN for the design of joints	6.7.
	<i>6.5.1 Need for a software</i>	6.7.
	<i>6.5.2 Scope of DESIMAN</i>	6.7.
	<i>6.5.3 DESIMAN, a user's friendly software</i>	6.8.
	<i>6.5.4 How to use DESIMAN</i>	6.8.
6.6	Screens of DESIMAN and examples of design sheets and tables	6.10.
	6.6.1 Example of simplified design procedure	6.11.

Table of contents

6.6.2 Example of design table for standardized joints	6.15.
6.6.3 Input and output screens of DESIMAN software	6.16.
6.7 Conclusions	6.17.

PART V: GENERAL CONCLUSIONS

7. CONCLUSIONS AND FURTHER DEVELOPMENTS	7.1.
---	------

REFERENCES

Acknowledgment

Professor MAQUOI brought me his experience, his encouragements and his advices; he widely contributed so to the issue of the present work. Others brought me their help, at different levels, and their friendship. This thesis is not only mine but also theirs and, in a word, ours.

Jean-Pierre Jaspert

January 2, 1997.

FOREWORD

The present thesis is the outcome of several years of research and activity in the field of structural joints.

My first contact with this subject dates back to 1984 at the occasion of my diploma work devoted to the study of the carrying capacity of columns partially restrained at the ends by semi-rigid joints. As an assistant at the Department MSM of the University of Liège, I have then the opportunity to investigate more deeply the local behaviour of steel and composite joints and their influence on the resistance and stability of frames through different projects sponsored by CRIF (Centre de Recherches scientifiques et techniques de l'Industrie des Fabrications métalliques) and IRSIA (Institut pour la Recherche Scientifique dans l'Industrie et l'Agriculture) on one side, and by ECSC (European Convention for Steel and Coal) on the other hand. I carry out experimentation and develop theoretical models for joint characterization, frame analysis and verification of the serviceability and ultimate limit states. This material constitutes the background of the Ph.D. Thesis that I present in early 1991.

This favourable concatenation of circumstances is not casual; it clearly results from the action of Professor Maquoi who encourages me continuously since 1984 in my numerical, theoretical and experimental developments at the University and helps me in establishing links with scientists outside Belgium. In 1988, he gives me the opportunity to attend the meetings of the Technical Committee 8.1/8.2 « Structural Stability » of ECCS (European Convention for Constructional Steelwork) and in 1989, of the Technical Committee 10 « Connections » of ECCS. I become full member of TC10 some years later.

Since 1991, I concentrate my activity, through three main projects, on the local behaviour of the joints.

Two of these projects are funded by the European Community (SPRINT and ECSC) in the frame of international collaborations. Through these projects, a design handbook on « Frame Design including Joint Behaviour » and design tools for joint design are developed. The third one which is funded by the Walloon Region of Belgium in the frame of the European COST C1 Project extends over three years and allows to set up in Liège a research team of more or less four persons in which I ensure the coordination and the scientific guidance.

The contacts with international experts is quite important to select the research topics that I have to investigate with the highest priority. From that point of view, the Chairmanship of the COST C1 Working Group on « Steel and Composite Connections » offers me since 1992 opportunities to have a quite good overview of the ongoing researches in my field of activity.

Research in steel construction has to open on practical applications and to achieve this goal, a transfer of technologies is needed. In this context, two steps have to be contemplated. The first one is the codification of design rules in national or international codes. The second consists in the development of simplified design tools for practitioners.

Foreword

I have the chance to contribute to both in the last years, first as one of the three drafters of the revised Annex J of Eurocode 3 devoted to the design of steel joints, and then as a partner in the two aforementioned european ECSC and SPRINT projects.

I also take part in the drafting of a similar annex for Eurocode 4 dealing with composite joints.

It stands to reason that the contents of the thesis that you will discover all along the following pages profited by all these exchanges and fruitful contacts.

The context in which the thesis has been prepared being now specified, I wish you pleasant reading and hope you will feel interested in the following pages.

Jean-Pierre Jaspert

PREFATORY CHAPTER

Traditionally the design of a steel frame is achieved by assuming that the constitutive beam-to-column joints, beam splices, column splices and column bases are rigid or pinned.

Rigid joints are those where no relative rotation occurs between the connected members all along their loading. These joints transfer mainly bending moments, but also shear and axial forces.

In pinned joints, no bending moment is transferred between the connected members; their rotational response is characterized by a free rotation between the connected members.

Since decades, it is widely recognized that no actual joint exhibits such idealized behaviours; any joint transfer bending moments and enables a relative rotation to take place between the connected members. The joints are semi-rigid and the design of the frames should be performed accordingly, the degree of rotational flexibility of the joint influencing the distribution of internal forces in the frame, the field of displacements and the failure mode with regard to the traditional assumptions of rigid or pinned joints.

In these conditions, it may be asked why the concept of rigid and pinned joints is still widely used even though, as we will see later, the design of almost rigid and pinned joints is often difficult to achieve and costly.

To answer this question, let us follow the successive steps of the frame analysis and design process in cases where rigid or pinned joints and semi-rigid joints are used respectively.

In a traditional design (see Figure 1), the joints are assumed to be rigid or pinned right at the beginning of the design process. The design of the frame is then performed accordingly :

- *Predesign*, aimed at determining roughly beam and column profiles which would allow the frame to satisfy the design requirements in terms of deformability or resistance and stability under service and ultimate loads. The designer's experience is of great help to select appropriate profiles. But simple predesign procedures exist and may also be used.
- *Frame analysis*, aimed at defining the internal forces, and their distribution along the members.
- *Check of the limit states*, aimed at verifying whether the frame satisfies or not the design requirements : displacements, resistance of the section, stability of the members or global stability of the frame.

When the frame is not satisfying the design requirements, or does not satisfy them in an economical way (oversized members), new beam and column profiles are selected and the frame analysis is repeated.

An appropriate predesign limits obviously the number of iterations to perform before reaching the optimum solution, which is often considered as that leading to the minimum structural weight.

At the end of this process, the frame is defined; it remains than to design the joints. These ones have to satisfy the assumption made at the beginning of the design process - rigid or pinned - and to be able to transfer the maximum applied forces to which they are likely to be subjected. These applied forces are known from the frame analysis.

In fact, two possibilities exist for what regards the resistance of the joints :

- the joints are designed for the maximum applied forces; if these ones are lower than those that the connected members are able to support, the joints are called « partial strength ».
- the joints are designed in such a way that their resistance is at least equal to that of the connected members; the joints are then called « full strength ».

Figure 1 illustrates rather well the clear separation between frame and joint design. The two tasks are not interacting so much so that they are often carried out by different persons inside the same engineering office; in some countries, the engineer designs the frame and the constructor is responsible for the joint design.

Because of their high rotational stiffness, rigid joints attract high bending moments and relieve the beam and column elements. Their use allows to reduce the size of the members and therefore the weight of the structure. This gives to the designer the feeling of an optimum solution.

In reality, rigid joints are generally quite expensive as they require stiffening systems, such as transverse or diagonal column web stiffeners which increase substantially the fabrication and erection costs.

The manpower costs being significantly higher than the material ones, the benefit obtained through an optimum design in terms of structural weight is much more than counterbalanced by the fabrication and erection costs.

In fact, a rigid joint is nothing else than an idealization; all the joints have a certain degree of flexibility but some are so stiff that their behaviour may be assimilated to that of a perfect rigid joint. Until recently, no objective criterion was available to decide whether a joint is rigid or not and, to avoid any inconsistency between the actual joint behaviour and that considered in the frame analysis, stiffeners were more or less systematically recommended.

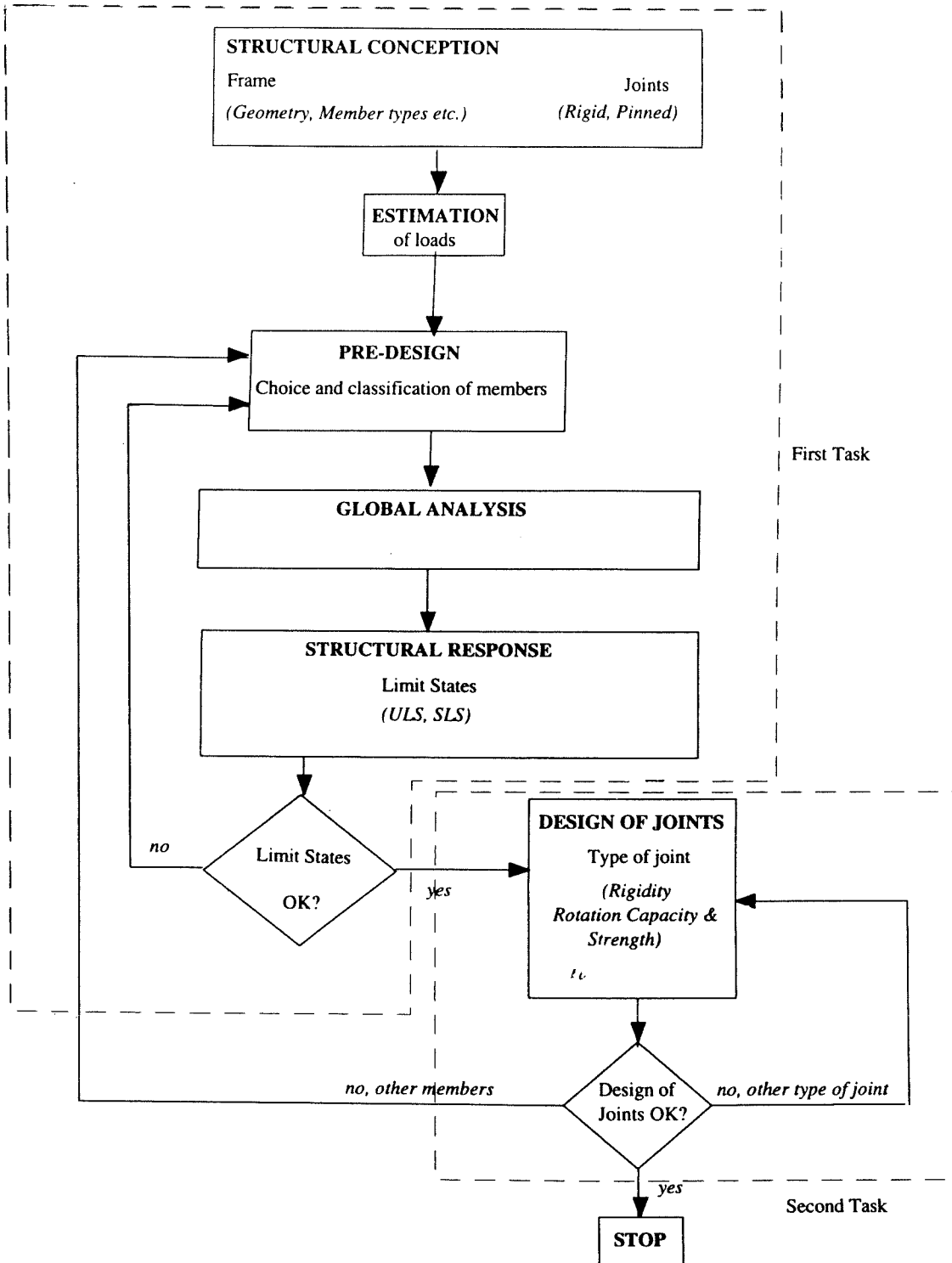


Figure 1 Traditional design procedure

Nowadays, classification criteria, that are introduced in Chapter 1, are available. They allow to determine the minimum rotational stiffness than the joints have to possess so as to be considered as rigid.

Through their use, some unstiffened joints are seen to be rigid. A rather optimum solution in terms now of structural weight and fabrication costs is then found. But in most of the cases, the unstiffened joints are semi-rigid and the design of the frame has to be performed accordingly.

This however requires an evaluation of the stiffness and resistance properties of these unstiffened joints and it is clear that the lack of knowledge on this so-called joint characterization is one of the main reasons to explain that the traditional design approach has been considered as the reference for decades.

In Figure 2, another design approach is followed, in which the joints are considered as actual frame elements, as beams and columns.

In the predesign step, beam and column members are selected, as usually, but also the connection type and detailing. Use can be made of tables of standardized joints as those presented in Chapter 6. The joints are chosen so as to be cheap for fabrication and erection, and not to fulfil stiffness requirements as in the traditional approach. The stiffness and/or resistance properties of the beams, column and joints are then evaluated before performing the frame analysis and checking the suitability of the frame for what regards serviceability and ultimate limit states. No design of the joints is needed as their mechanical properties have been taken into consideration in the frame analysis and design process.

Such an approach gives more freedom to the designer to optimize the total cost of the structure including material, fabrication and erection costs, but prevents at first sight any share of the design responsibility between, for instance, the designer and the constructor. The fact that the engineer, who is not necessarily aware of the fabrication and erection aspects which are largely dependent on the constructor's equipment, has to select what he considers as cheap joints may also appear as a detrimental aspect of this new design philosophy. But answers have been brought to these criticisms and appropriate solutions allowing simultaneously to design frames and joints for economy, to share the design responsibilities, if required, and let the final detailing of the joints in the hands of the more appropriate person, i.e. the constructor. These solutions are extensively described in [E4].

The new design approaches are linked to the recent research developments in the field of semi-rigid joints and frames including semi-rigid joints.

In fact, the inclusion of the joint properties in the frame design and analysis process required to investigate several aspects at the local joint level and at the frame level.

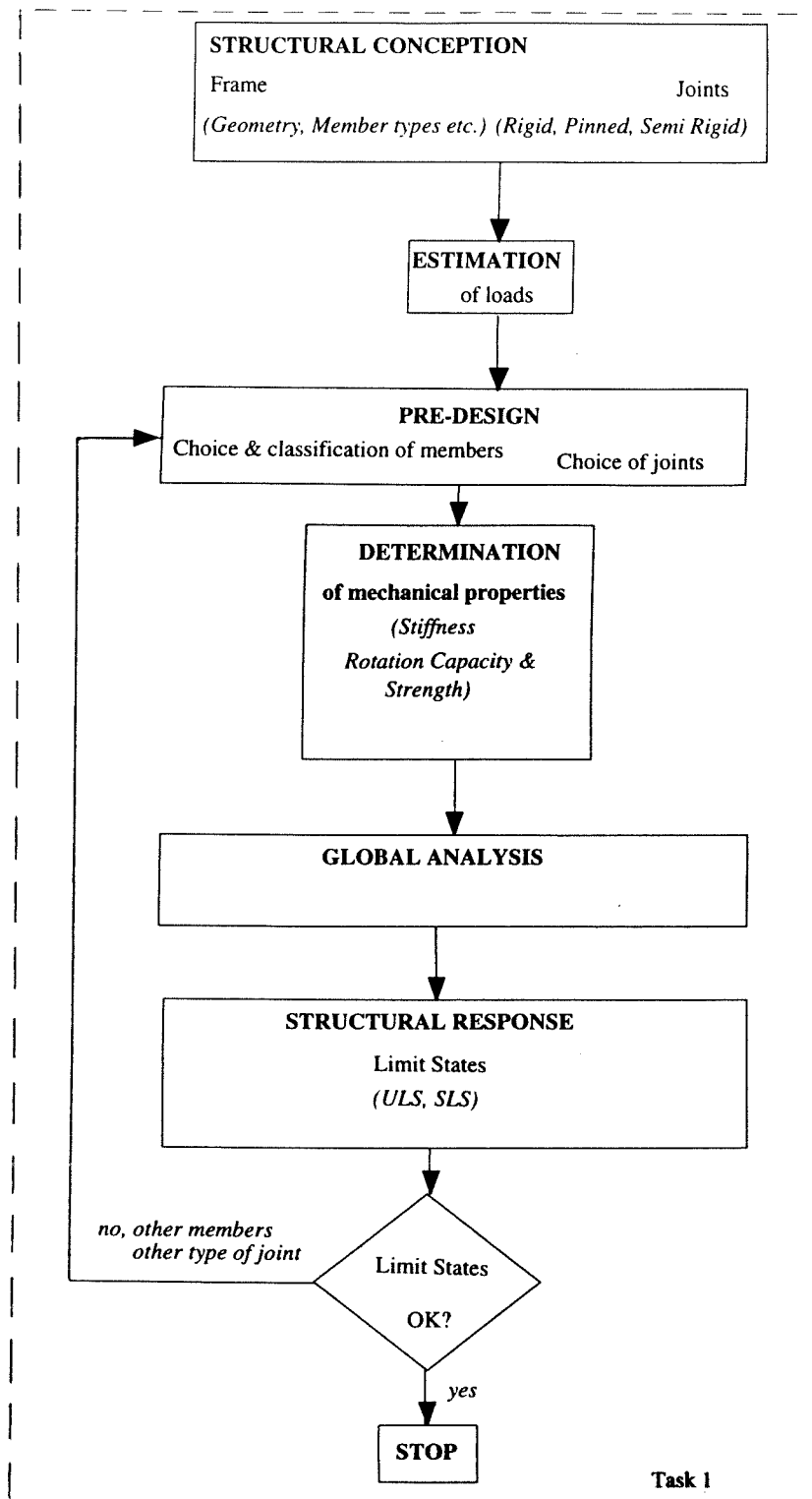


Figure 2 Other possible design procedure

Local joint level

- The *characterization* of the joint behaviour in terms of stiffness and resistance, but also rotation capacity is a key problem.
- The *classification* allows to distinguish rigid and pinned joints from semi-rigid ones, but also partial strength joints from full strength ones.
- The *modelling* of the joint defines the way in which the rotational response of the joints will be locally reflected at the frame level in view of the structural analysis.
- The *idealization* consists in idealizing the actual non-linear rotational response of the joints in view of the frame analysis. For instance, a linearization of the joint response is required for an elastic frame analysis.

Frame level

- Specific *predesign procedures* for frames including semi-rigid joints may be needed in a first step for designers whose experience with semi-rigid frames is not yet sufficient.
- *Methods of analysis* taking the rotational response of the joints into consideration have to be made available to designers.
- The *verification of the limit states* is an important step in the design process; it has also to integrate the presence of joints at the end of the structural members.

The four first aspects are described and commented in Chapter 1 of the present thesis. The three last ones have been extensively discussed in our Ph.D. Thesis [J1]. But that is in the design handbook for the Design of Frames including Joint Behaviour [E4] that the interested designer will find basic information, application rules and worked examples covering the whole design process. This handbook, which is presented in Chapter 6 of the present thesis, should be available in early 1997. Moreover Chapter 1 of the present thesis is largely inspired by one of the chapter that we have drafted for the handbook.

Most of the research works on joints carried out in the last decades focused on beam-to-column major axis joints with welded or end-plate connections and subjected to bending moments and shear forces. In these joints, the H or I beam and column profiles are bent about their major axes or, in other words, the beam is connected to the flange of the column.

As a result, the old Annex J of Eurocode 3 dealing with the design of joints was only covering these two joint configurations.

But it appears quickly to users that the number of cases covered by this annex was too limited to allow a use in daily practice; moreover the need for a single design philosophy for joints applicable to all the joints whatever is their connection types was expressed. And finally, some of the design rules contained in the old Annex J were shown to be either too conservative or a bit unconservative.

As a result, CEN (Comité Européen de Normalisation) took the decision to revise the so-called old Annex J.

When, in the present thesis, we refer to « Annex J » or to « revised Annex J », the new revised document is concerned. We systematically use the expression « old Annex J » to designate the previous one.

During the revision of the annex, its scope has been widened to beam splices and flange cleated connections following experimental and theoretical investigations on these joints and the adoption of the so-called component method described in Chapter 2 of the present thesis.

But to come to a wide acceptance of the new frame and joint design philosophies, the list of the joints for which characterization tools are available should not be limited to classical cases. This explains why, besides our activity as one of the drafters of Eurocode 3 revised Annex J, we devoted time in the last years to the extension of the component method to other types of joint configurations such as :

- minor axis joints;
- column bases;
- major axis joints with haunches, intermediate stiffeners, ...
- composite joints;
- joints made of high strength steels (HSS).

We also realized the need for more knowledge in the field of joints belonging to pitched-roof portal frames where :

- the members are not perpendicularly connected;
- the joints are subjected to high axial forces in addition to bending moments and shear forces;
- the use of rather slender built-up profiles leads to specific instability problems within the joints;
- the use of the classification and idealization as it is recommended in Eurocode 3 for « rectangular » frames where the members are perpendicularly connected is questionable.

In the present thesis, all these different aspects are dealt with.

For some of them, carried out in collaboration with young colleagues working under our guidance, we deliberately limit the contents of the related sections to a presentation of the main research results, without any background or detailed justification, so as to allow

Prefatory chapter

these young colleagues to valorize their work, by themselves, for instance in the frame of a Ph.D. Thesis.

The contribution to the design of composite joints that we reflect in the thesis is the outcome of the activities of a european working group in which we worked during the two last years. A publication emanating from this group is presently in the press. Only a brief summary of the group activities and of the contents of the publication is therefore given in this thesis.

For all the other parts of the thesis, the reader will find more background information and justification of the proposed design rules.

PART I : GENERAL INTRODUCTION

Chapter 1 : GENERAL INTRODUCTION

1. GENERAL INTRODUCTION

1.1 Definitions

Building frames consist of beams and columns, usually made of H- or I- shapes, that are assembled together by means of connections. These connections are between two beams, two columns, a beam and a column or a column and the foundation (Figure 1-1).

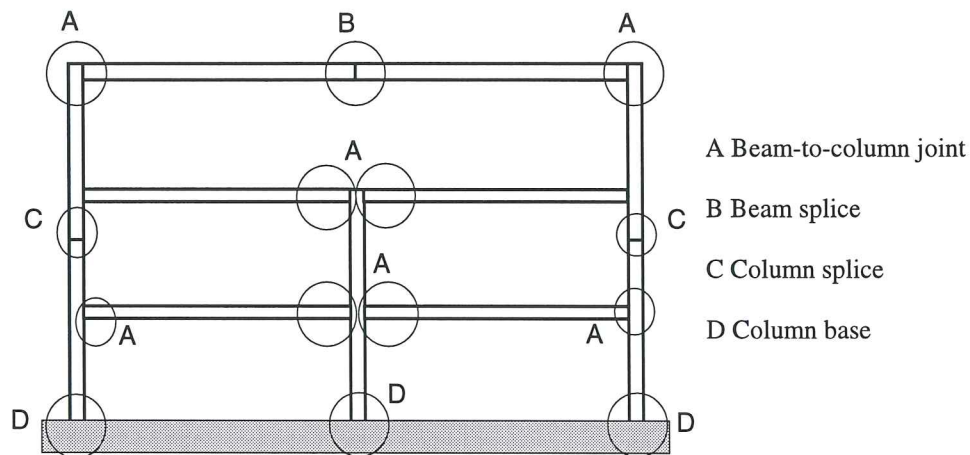


Figure 1-1 Different types of connections in a building frame

A *connection* is defined as the set of the physical components which mechanically fasten the connected elements. One considers the connection to be concentrated at the location where the fastening action occurs, for instance at the beam end/column interface in a major axis beam-to-column joint. When the connection as well as the corresponding zone of interaction between the connected members are considered together, the wording *joint* is then used (Figure 1-2.a).

Depending on the number of in-plane elements connected together, single-sided and double-sided joint configurations are defined (Figure 1-3). In a double-sided configuration (Figure 1-3.b), two joints - left and right - have to be considered (Figure 1-2.b.).

The definitions illustrated in Figure 1-2 are valid for other joint configurations and connection types.

As explained previously, the joints which are traditionally considered as rigid or pinned and are designed accordingly, possess, in reality, their own degree of flexibility resulting from the deformability of all the constitutive components. Section 1.2 is aimed at describing the main *joint deformability sources*. Section 1.3 provides information on how to *model* the joints in view of the frame analysis; this modelling depends on the level of joint flexibility. In Section 1.4, the way in which the shape of the non-linear joint deformability curves may be *idealized* is given. Section 1.5 refers to the *component method* as a general tool for the prediction of the main joint mechanical properties in

bending. The concept of *joint classification* is introduced in Section 1.6. Finally, it is commented on the *ductility classes* of joints in Section 1.7.

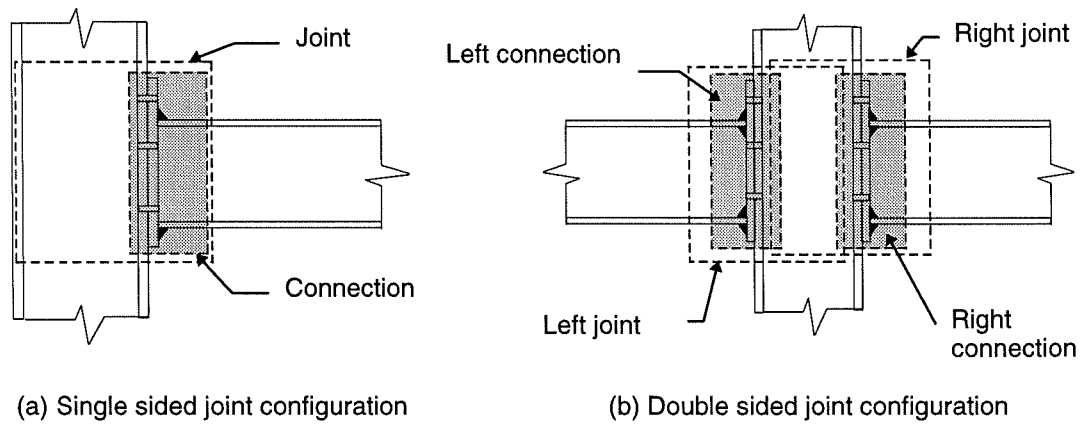


Figure 1-2 Joints and connections

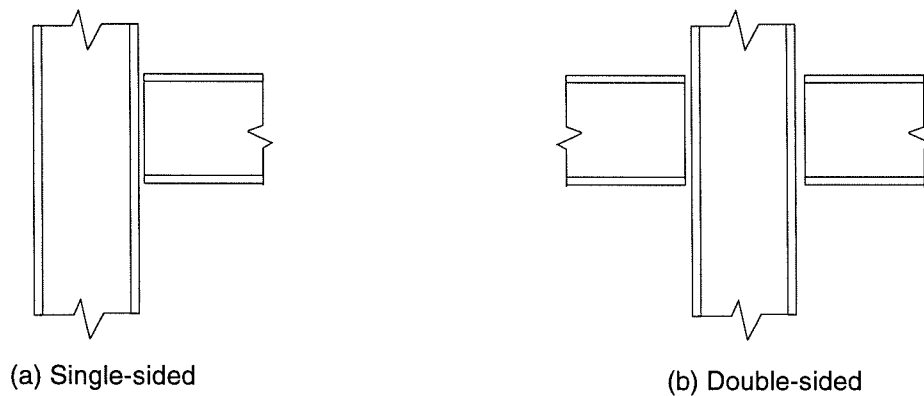


Figure 1-3 In-plane joint configurations

1.2 Sources of joint deformability

As said in the prefatory chapter, the rotational behaviour of the joints may affect the local and/or global structural response of the frames. In this section, the sources of rotational deformability are identified for beam-to-column joints, splices and column bases.

It is worthwhile mentioning that the rotational stiffness, the joint resistance and the rotation capacity are likely to be affected by the shear force and/or the axial force acting in the joint.

These shear and axial forces may obviously have contributions to the shear and axial deformability within the connections. However it is known that these contributions do not affect significantly the frame response; therefore, the shear and axial responses of the connection, in terms of rotational deformability, are neglected.

1.2.1 Beam-to-column joints

1.2.1.1 Major axis joints

In a major axis beam-to-column joint, different sources of deformability can be identified. For the particular case of a single-sided joint (Figure 1-4.a and Figure 1-5.a), these are:

- *The deformation of the connection.* It includes the deformation of the connection elements : column flange, bolts, end-plate or angles,... and the load-introduction deformation of the column web resulting from the transverse shortening and elongation of the column web under the compressive and tensile forces F_b acting on the column web. The couple of F_b forces are statically equivalent to the moment M_b at the beam end. These deformations result in a relative rotation ϕ_c between the beam and column axes; this rotation, which is equal to $\theta_b - \theta_c$ (see Figure 1-4.a) is concentrated mainly along edge BC and provides a flexural deformability curve $M_b - \phi_c$.
- *The shear deformation of the column web panel* associated to the shear force V_n acting in this panel. It leads to a relative rotation γ between the beam and column axes; this rotation makes it possible to establish a shear deformability curve $V_n - \gamma$

The deformability curve of a connection may obviously be influenced by the axial and shear forces possibly acting in the connected beam.

Similar definitions apply to double-sided joint configurations (Figure 1-4.b and Figure 1-5.b). For such configurations, two connections and a sheared web panel, forming two joints, must be considered.

In short, the main sources of deformability which must be contemplated in a beam-to-column major axis joint are :

Single-sided joint configuration :

- the connection deformability $M_b - \phi_c$ characteristic;
- the column web panel shear deformability $V_n - \gamma$ characteristic.

Double-sided joint configuration :

- the left hand side connection deformability $M_{b1} - \phi_{c1}$ characteristic;
- the right hand side connection deformability $M_{b2} - \phi_{c2}$ characteristic;
- the column web panel shear deformability $V_n - \gamma$ characteristic.

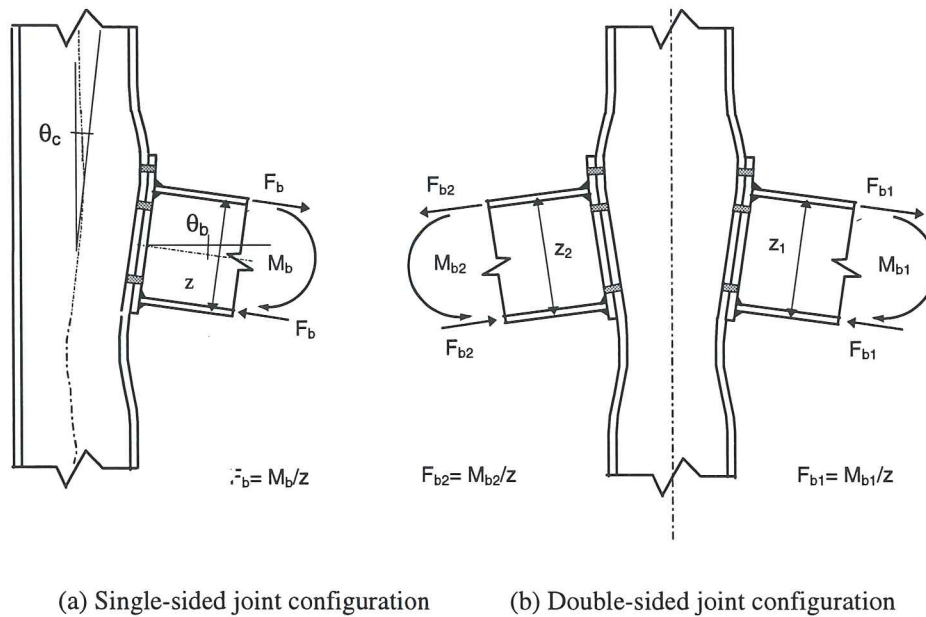


Figure 1-4 Sources of joint deformability

The deformability of the connection (connection elements + load-introduction) is only due to the couple of forces transferred by the flanges of the beam (equivalent to the beam end moment M_b). The shear deformability of the column web panel results from the combined action of these equal but opposite forces and of the shear forces in the column at the level of the beam flanges. Equilibrium equations of the web panel provide the shear force V_n (see Figure 1-5 for the sign convention) :

$$V_n = \frac{M_{b1} - M_{b2}}{z} - \frac{V_{c1} - V_{c2}}{2} \quad (1.1)$$

Another formula to which it is sometimes referred, i.e. :

$$V_n = \frac{M_{b1} - M_{b2}}{z} \quad (1.2)$$

is only a rough and conservative approximation of (1.1).

In both formulae, z is the lever arm of the resultant tensile and compressive forces in the connection(s). How to derive the value of z is explained in Chapter 3.

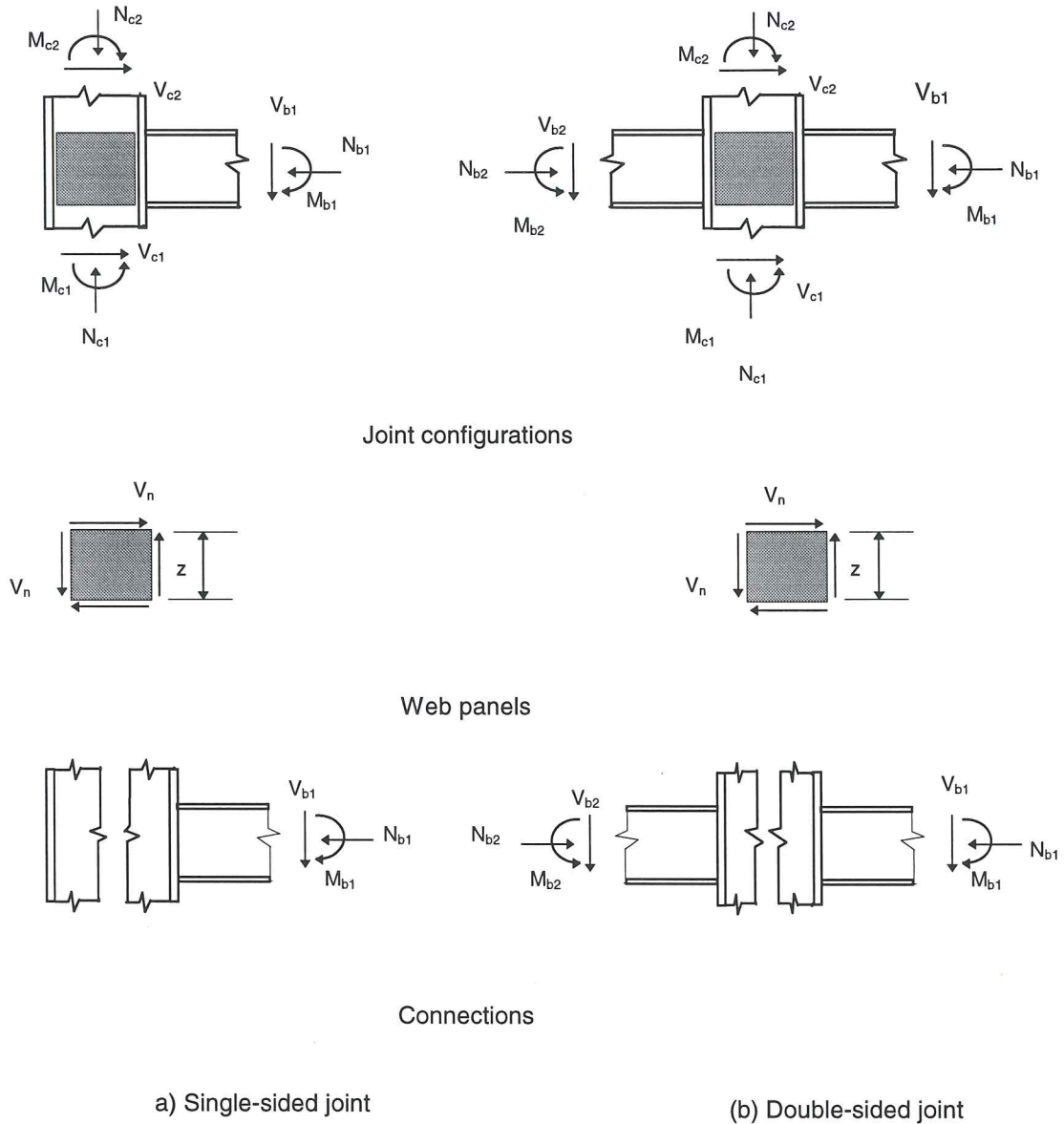


Figure 1-5 Loading of the web panel and the connections

1.2.1.2 Minor axis joints

A similar distinction between *web panel* and *connection* shall also be made for a minor axis joint (Figure 1-6). The column web exhibits a so-called out-of-plane deformability while the connection deforms in bending as it does in a major axis joint. However no load-introduction deformability is involved.

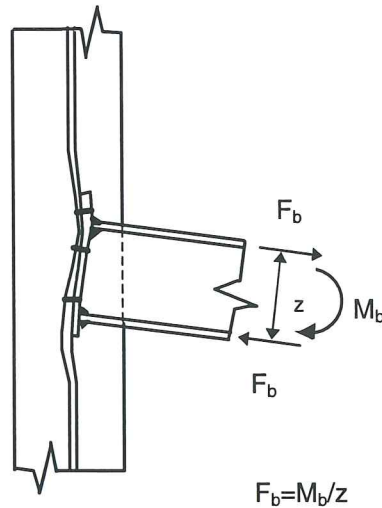


Figure 1-6 Deformability of a minor axis joint

In the double-sided joint configuration, the out-of-plane deformation of the column web depends on the bending moments experienced by the right and left connections (see Figure 1-7) :

$$\Delta M_b = M_{b1} - M_{b2} \quad (1.3.)$$

For a single-sided joint configuration (Figure 1-6), the value of ΔM_b equals that of M_b .

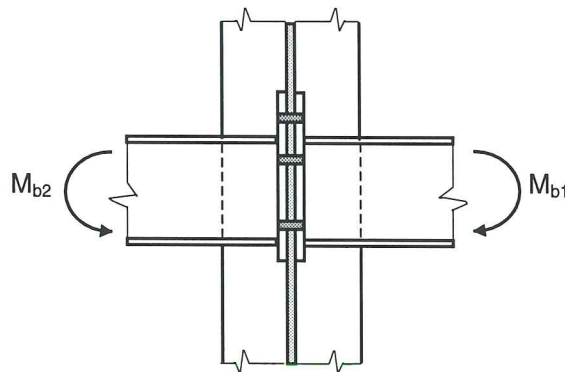


Figure 1-7 Loading of a double-sided minor axis joint

1.2.1.3 Joints with beams on both major and minor column axes

A 3-D joint is (Figure 1-8) characterized by the presence of beams connected to both the column flange(s) and web. In such joints, a shear deformation (see 1.2.1.1) and an out-of-plane deformation (see 1.2.1.2) of the column web develop coincidentally.

The loading of the web panel appears therefore as the superimposition of the shear loading given by formulae (1.1) or (1.2) and the out-of-plane loading given by formula (1.3).

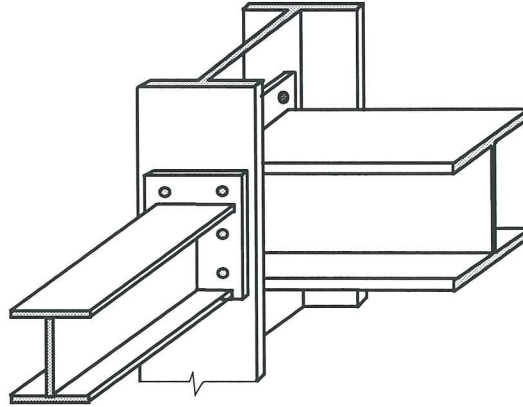


Figure 1-8 Example of a 3-D joint

The joint configuration of Figure 1-8 involves two beams only; configurations with three or four beams can also be met.

1.2.2 Beam splices and column splices

The sources of deformability in a beam splice (Figure 1-9) or in a column splice (Figure 1-10) are less than in a beam-to-column joint; indeed they are concerned with connections only. The deformability is depicted by the sole $M_b-\phi$ curve.

The single $M_b-\phi$ curve corresponds to the deformability of the whole joint, i.e. the two constituent connections (left connection and right one in a beam splice, upper connection and lower one in a column splice).

In a column splice where the compressive force is predominant, the axial force affects in a significant way the mechanical properties of the joint, i.e. its rotational stiffness, its strength and its rotation capacity. The influence, on the global frame response, of the axial deformability of splices is however limited; therefore it is neglected.

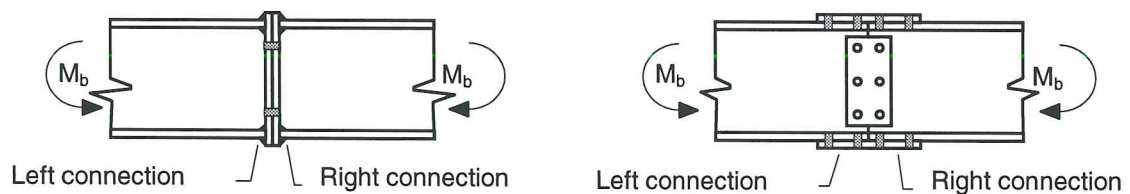


Figure 1-9 Deformation of a beam splice

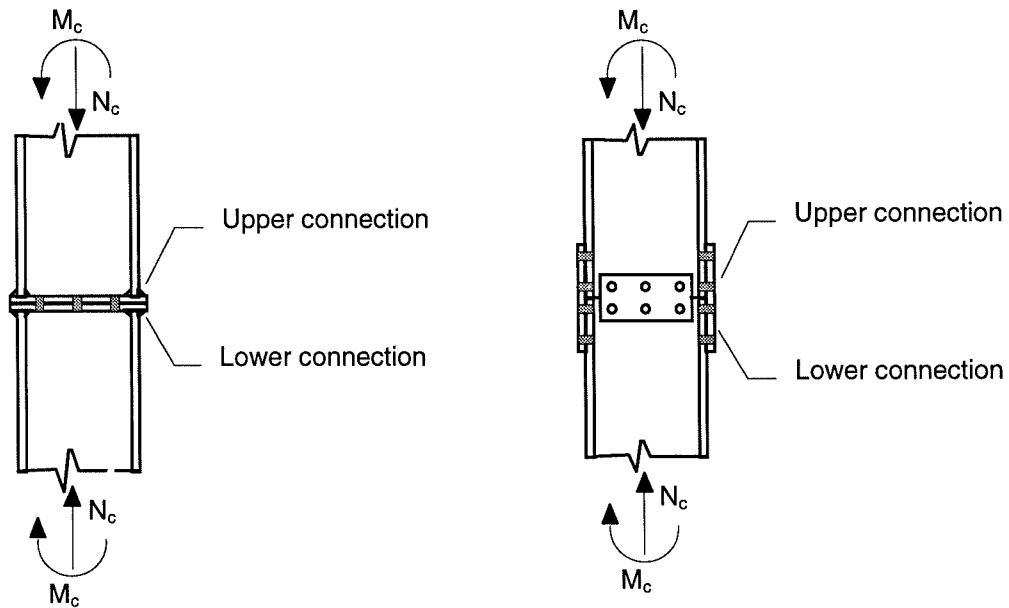


Figure 1-10 Deformation of a column splice

1.2.3 Beam-to-beam joints

The deformability of a beam-to-beam joint (Figure 1-11) is quite similar to the one of a minor axis beam-to-column joint; the loadings and the sources of deformability are similar to those expressed in 1.2.1.2 and can therefore be identified.

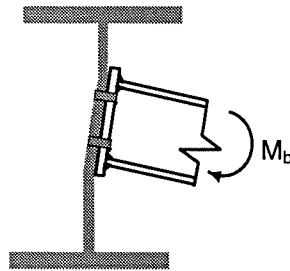


Figure 1-11 Deformation of a beam-to-beam joint

1.2.4 Column bases

In a column base, two connection deformabilities need to be distinguished (Figure 1-12):

- the deformability of the connection between the column and the concrete foundation (*column-to-concrete connection*);
- the deformability of the connection between the concrete foundation and the soil (*concrete-to-soil connection*).

For the column-to-concrete connection, the bending behaviour is represented by a $M_c-\phi$ curve, the shape of which is influenced by the ratio of the bending moment to the axial load at the bottom of the column.

For the connection between the concrete foundation and the soil, two basic deformability curves are identified:

- a N_c-u curve which corresponds to the soil settlement due to the axial compressive force in the column; in contrast with the other types of joint, this deformability curve may have a significant effect on the frame behaviour;
- a $M_c-\phi$ curve characterizing the rotation of the concrete block in the soil.

As for all the other joints described above, the deformability of the column base due to the shear force in the column may be neglected.

The column-to-concrete connection and concrete-to-soil connection $M_c-\phi$ characteristics are combined in order to derive the rotational stiffness at the bottom of the column and conduct the frame analysis and design accordingly.

Similar deformability sources exist in column bases subjected to biaxial bending and axial force. The connection $M_c-\phi$ characteristics are then defined respectively for both the major and the minor axes.

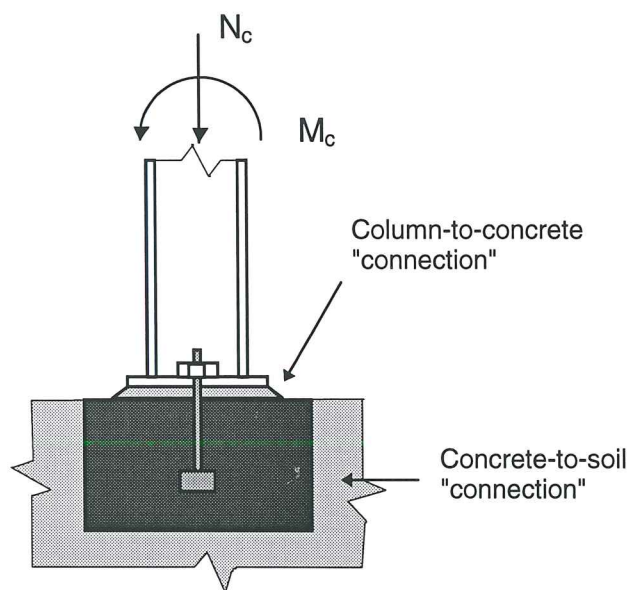


Figure 1-12 The connections in a column base

1.3 Joint modelling

1.3.1 General

Joint behaviour affects the structural frame response and shall therefore be modelled, just like beams and columns are, for the frame analysis and design. Traditionally, the following types of *joint modelling* are considered :

For rotational stiffness :

- rigid;
- pinned.

For resistance :

- full strength;
- partial strength;
- pinned.

When the joint rotational stiffness is of concern, the wording *rigid* means that no relative rotation occurs between the connected members whatever be the applied moment. The wording *pinned* postulates the existence of a perfect (i.e. frictionless) hinge between the members. In fact these definitions may be relaxed, as explained in Section 1.6 devoted to the joint classification. Indeed rather flexible but not fully pinned joints and rather stiff but not fully rigid joints may be considered as fairly pinned and fairly rigid respectively. The stiffness boundaries allowing one to classify joints as rigid or pinned are examined in Section 1.6.

For what regards the joint resistance, a *full-strength joint* is stronger than the weaker of the connected members, what is in contrast with a *partial-strength joint*. In the daily practice, partial-strength joints are used whenever the joints are designed to transfer the internal forces and not to resist the full capacity of the connected members. A *pinned joint* transfers no moment. Related classification criteria are conceptually discussed in Section 1.6.

Consideration of rotational stiffness and resistance joint properties leads to three significant joint modellings:

- rigid/full-strength;
- rigid/partial-strength;
- pinned.

However, as far as the joint rotational stiffness is considered, joints designed for economy may be neither rigid nor pinned but semi-rigid. There are thus new possibilities for joint modelling :

- semi-rigid/full-strength;
- semi-rigid/partial-strength.

STIFFNESS	RESISTANCE		
	Full-strength	Partial-strength	Pinned
Rigid	Continuous	Semi-continuous	-
Semi-rigid	Semi-continuous	Semi-continuous	-
Pinned	-	-	Simple
- : Without meaning			

Figure 1-13 Types of joint modelling

With a view to simplification, *Eurocode 3 Chapter 6* and *Annex J* account for these possibilities by introducing three joint models (Figure 1-13):

- *continuous* : covering the rigid/full-strength case only;
- *semi-continuous* : covering the rigid/partial-strength, the semi-rigid/full-strength and the semi-rigid/partial-strength cases;
- *simple* : covering the pinned case only.

The following meanings are given to these terms :

- *continuous* : the joint ensures a full rotational continuity between the connected members;
- *semi-continuous* : the joint ensures only a partial rotational continuity between the connected members;
- *simple* : the joint prevents from any rotational continuity between the connected members.

The interpretation to be given to these wordings depends on the type of frame analysis to be performed. In the case of an elastic global frame analysis, only the stiffness properties of the joint are relevant for the joint modelling. In the case of a rigid-plastic analysis, the main joint feature is the resistance. In all the other cases, both the stiffness and resistance properties govern the manner the joints shall be modelled. These possibilities are illustrated in Figure 1-14.

MODELLING	TYPE OF FRAME ANALYSIS		
	Elastic analysis	Rigid-plastic analysis	Elastic and elastic-plastic (or elastoplastic) analysis
Continuous	Rigid	Full-strength	Rigid/full-strength
Semi-continuous	Semi-rigid	Partial-strength	Rigid/partial-strength Semi-rigid/full-strength Semi-rigid/partial-strength
Simple	Pinned	Pinned	Pinned

Figure 1-14 Joint modelling and frame analysis

1.3.2 Modelling and sources of joint deformability

The difference between the loading of the connection and that of the column web in a beam-to-column joint (see Section 1.2) requires, from a theoretical point of view, that account be taken separately of both deformability sources when designing a building frame.

However doing so is only feasible when the frame is analysed by means of a sophisticated computer program which enables a separate modelling of both deformability sources. For most available softwares, the modelling of the joints has to be simplified by concentrating the sources of deformability into a single rotational spring located at the intersection of the axes of the connected members.

1.3.3 Simplified modelling according to *Eurocode 3*

For most applications, the separate modelling of the connection and of the web panel behaviour is neither useful nor feasible; therefore only the simplified modelling of the joint behaviour (see Section 1.3.2) will be considered in the present document. This idea is the one followed in the *ENV 1993-1-1* experimental standard (*Chapter 6* and *Annex J*). Figure 1-15, excerpted from the revised *Annex J*, shows how to relate the simplified modelling of typical joints to the basic wordings used for the joint modelling: simple, semi-continuous and continuous.

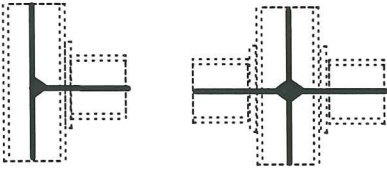
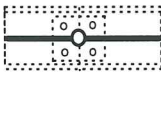
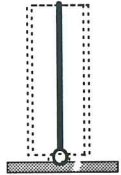
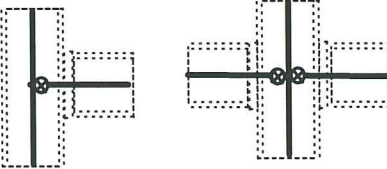
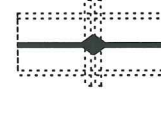
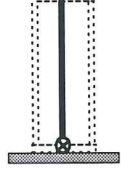
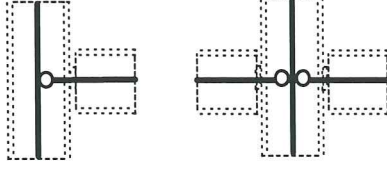
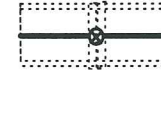
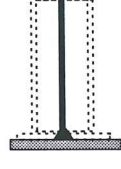
JOINT MODELLING	BEAM-TO-COLUMN JOINTS MAJOR AXIS BENDING	SPLICES	COLUMN BASES
SIMPLE			
SEMI-CONTINUOUS			
CONTINUOUS			

Figure 1-15 Simplified modelling for joints according to Eurocode 3

1.3.4 Concentration of the joint deformability

For the daily practice a separate account of both the flexural behaviour of the connection and the shear (major axis beam-to-column joint) or out-of-plane behaviour of the column web panel (minor axis beam-to-column joint configurations or beam-to-beam configurations) is not feasible. This section is aimed at explaining how to concentrate the two deformabilities into a single flexural spring located at the intersection of the axes of the connected members. The background of this concentration process and its justification are available in our Ph.D. Thesis [J1].

1.3.4.1 Major axis beam-to-column joint configurations

In a single-sided configuration, only one joint is concerned. The characteristic shear-rotation deformability curve of the column web panel (see Figure 1-4 and Figure 1-16.b) is first transformed into a M_b - γ curve through the use of the *transformation parameter* β . This parameter, defined in Figure 1-17.a, relates the web panel shear force to the (load-introduction) compressive and tensile forces connection (see also formulae 1.1 and 1.2).

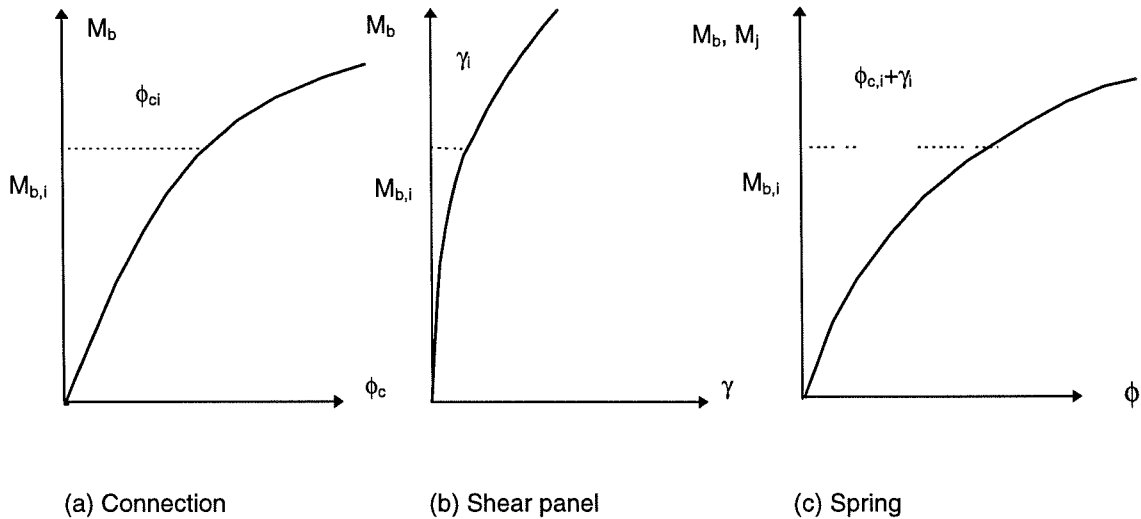


Figure 1-16 Flexural characteristic of the spring

The $M_b-\phi$ spring characteristic which represents the joint behaviour is shown in Figure 1-16.c; it is obtained by summing the contributions of rotation, from the connection (ϕ_c) and from the shear panel (γ). The $M_j-\phi$ characteristic of the joint rotational spring located at the beam-to-column interaction is assumed to identify itself to the $M_b-\phi$ characteristic obtained as indicated in Figure 1-16.c.

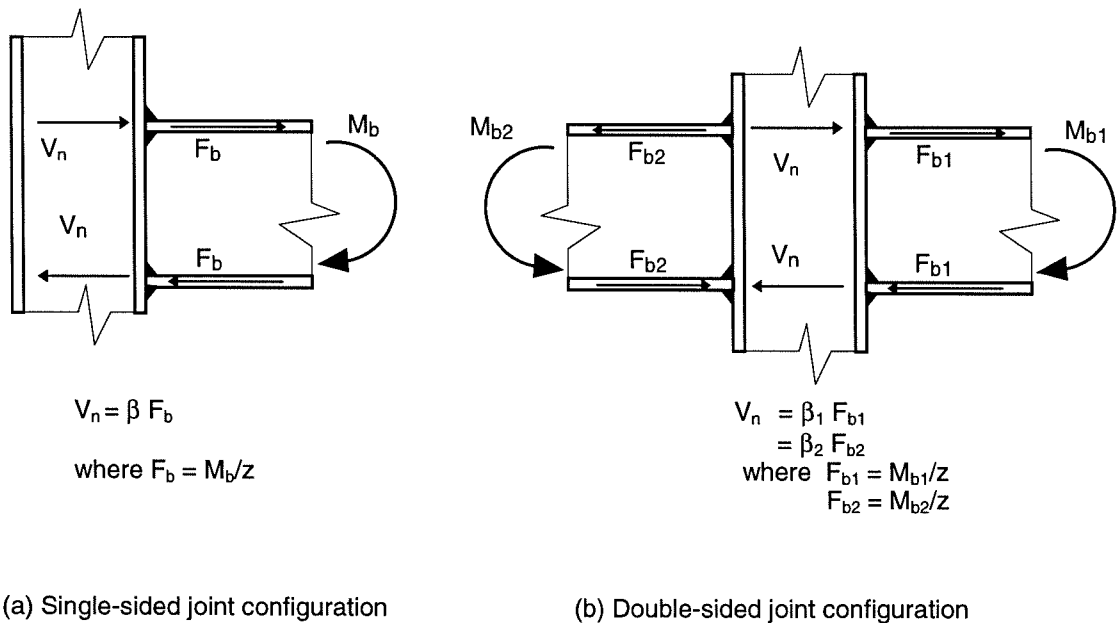


Figure 1-17 Definition of the transformation parameter β

In a double-sided configuration, two joints - the left one and the right one - are concerned. The derivation of their corresponding deformability curves is conducted

similarly as in a single-sided configuration by using transformation parameters β_1 and β_2 (Figure 1-17.b).

Because the values of the β parameters can only be determined once the internal forces are known, their accurate determination requires an iterative process in the global analysis. For practical applications, such an iterative process is hardly acceptable provided safe β values be available. These values may be used a priori to model the joints and, on the basis of such joint modelling, the frame analysis may be performed safely in a non-iterative way.

The recommended but approximate values of β , where β_1 is taken as equal to β_2 for double-sided configurations, are given in Eurocode 3 revised Annex J. They vary from $\beta = 0$ (double-sided joint configuration with balanced moments in the beams) to $\beta = 2$ (double-sided joint configuration with equal but unbalanced moments in the beams). These two extreme cases are illustrated in Figure 1-18.

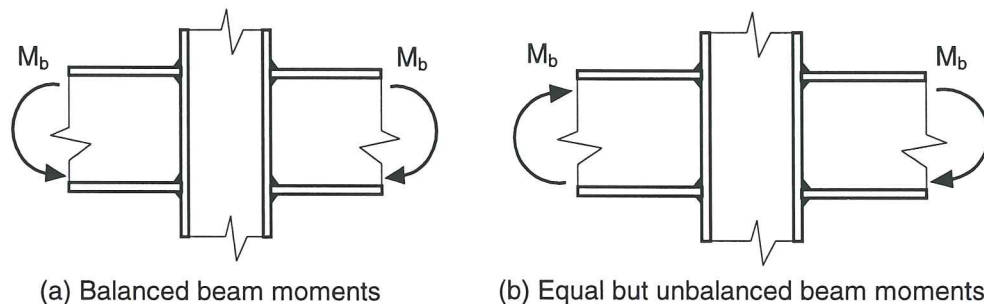


Figure 1-18 Extreme cases for β values

1.3.4.2 Minor axis beam-to-column joint configurations and beam-to-beam configurations

Similar concepts as those developed in Section 1.3.4.1 could be referred to for minor axis beam-to-column joint configurations and beam-to-beam configurations. The definition of the transformation parameter is somewhat different (see Figure 1-19).

Approximate values of β (assuming $\beta_1 = \beta_2$) for these joint configurations may be found in [E4].

1.3.5 Notations

For sake of consistency within the present Chapter, the moment in the joint is denoted M_j in the following sections. In the other chapters, a more simple notation M is used so as to lighten the figures and the formalism of the equations.

1.4 Joint idealization

The non-linear behaviour of the isolated flexural spring which characterizes the actual joint response does not lend itself towards everyday design practice. However the

moment-rotation characteristic curve may be idealized without significant loss of accuracy. One of the most simple idealizations possible is the elastic-perfectly plastic one (Figure 1-20.a). This modelling has the advantage of being quite similar to that used traditionally for the modelling of member cross-sections subjected to bending (Figure 1-20.b).

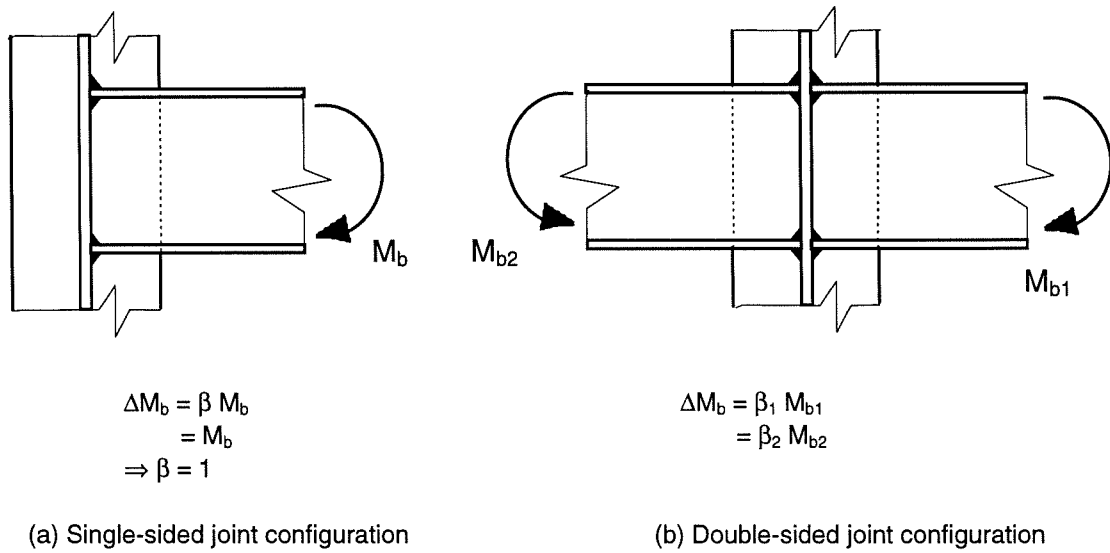


Figure 1-19 Definition of the transformation parameter β

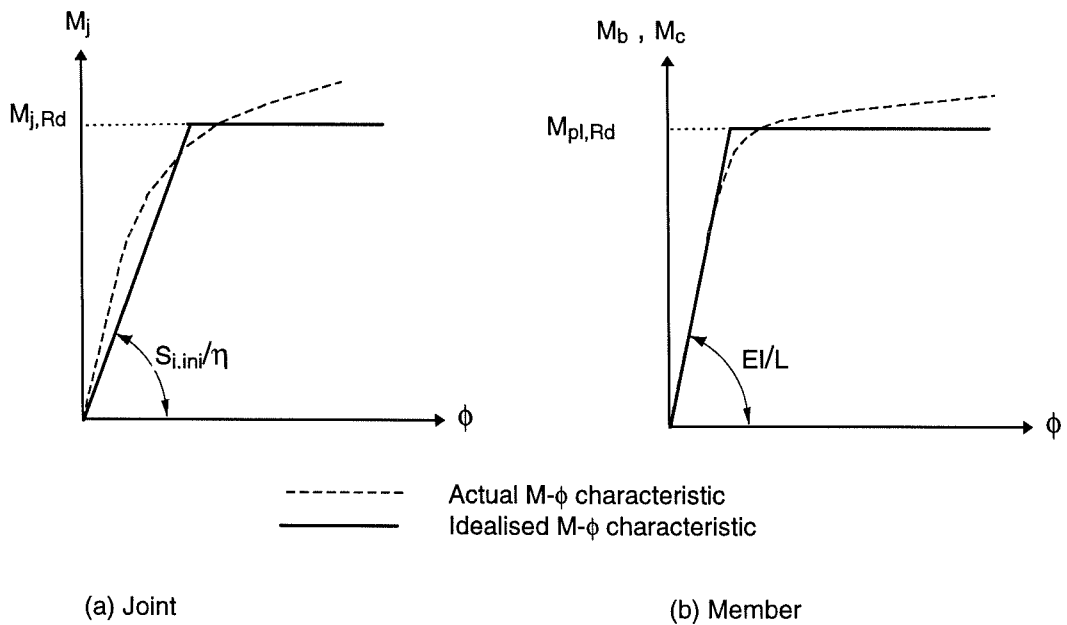


Figure 1-20 Bi-linearization of moment-rotation curves

The moment $M_{j,Rd}$ that corresponds to the yield plateau is termed *design moment resistance* in *Eurocode 3* (see Appendix 1). Strain-hardening effects and possible membrane effects are henceforth neglected; that explains the difference in Figure 1-20 between the actual $M_j-\phi$ characteristic and the *yield plateau* of the idealized one (see Appendix 2).

The value of the constant stiffness is discussed below.

In fact there are different possible ways to idealize a joint $M_j-\phi$ characteristic. The choice of one of them is subordinated to the type of frame analysis which is contemplated:

- *Elastic idealization for an elastic analysis* (Figure 1-21) :

The main joint characteristic is the constant rotational stiffness.

Two possibilities* are offered in *Eurocode 3 Annex J* :

- *Elastic verification of the joint resistance* (Figure 1-21.a) : the constant stiffness is taken equal to the initial stiffness $S_{j,ini}$; at the end of the frame analysis, it shall be checked that the design moment $M_{j,sd}$ experienced by the joint is less than the maximum elastic joint moment resistance defined as $2/3 M_{j,Rd}$;
- *Plastic verification of the joint resistance* (Figure 1-21.b) : the constant stiffness is taken equal to a fictitious stiffness, the value of which is intermediate between the initial stiffness and the secant stiffness relative to $M_{j,Rd}$; it is defined as $S_{j,ini}/\eta$ (values of η are given in Eurocode 3 revised Annex J and discussed in Chapter 4). This idealization is valid for $M_{j,sd}$ values less than or equal to $M_{j,Rd}$.

- *Rigid plastic idealization for a rigid-plastic analysis* (Figure 1-22).

Only the design resistance $M_{j,Rd}$ is needed. In order to allow the possible plastic hinges to form and rotate in the joint locations, it shall be checked that the joint has a sufficient rotation capacity.

- *Non-linear idealization for an elastic-plastic analysis* (Figure 1-23).

The stiffness and resistance properties are of equal importance in this case. The possible idealizations range from bi-linear, tri-linear representations, ... to the fully non-linear curve. Again rotation capacity is required in joints where plastic hinges are likely to form and rotate.

* A third possibility is expressed in Annex J. It leads to an iterative analysis procedure and is therefore not of practical interest. It is therefore not presented here.

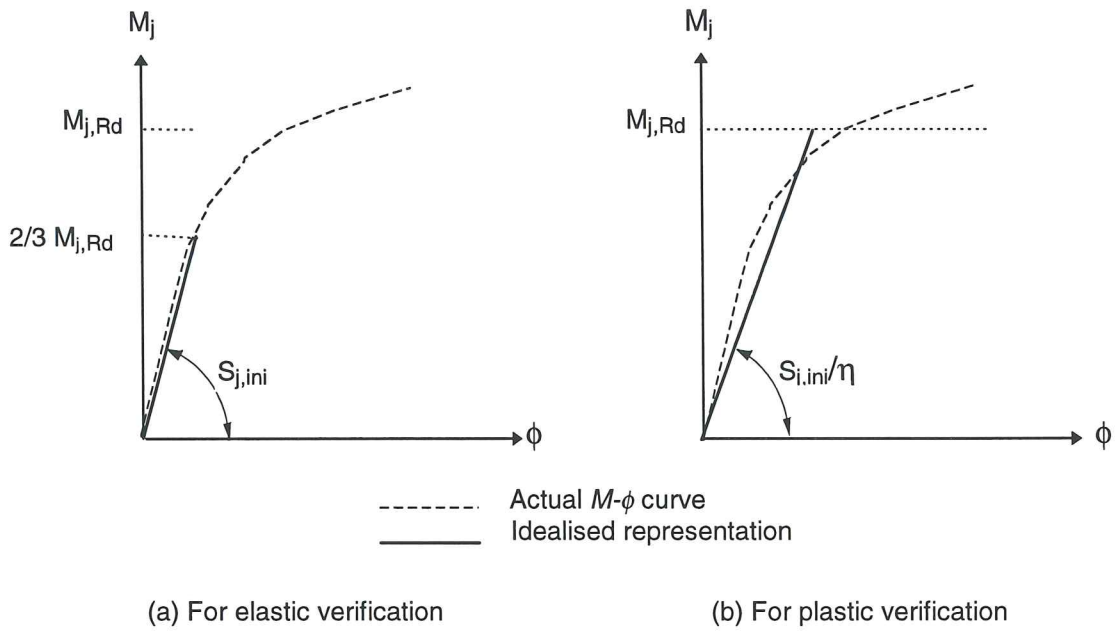


Figure 1-21 Linear representation of a $M_j-\phi$ curve

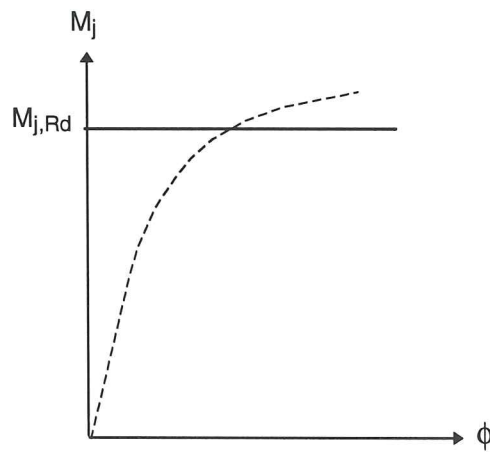


Figure 1-22 Rigid-plastic representation of a $M_j-\phi$ curve

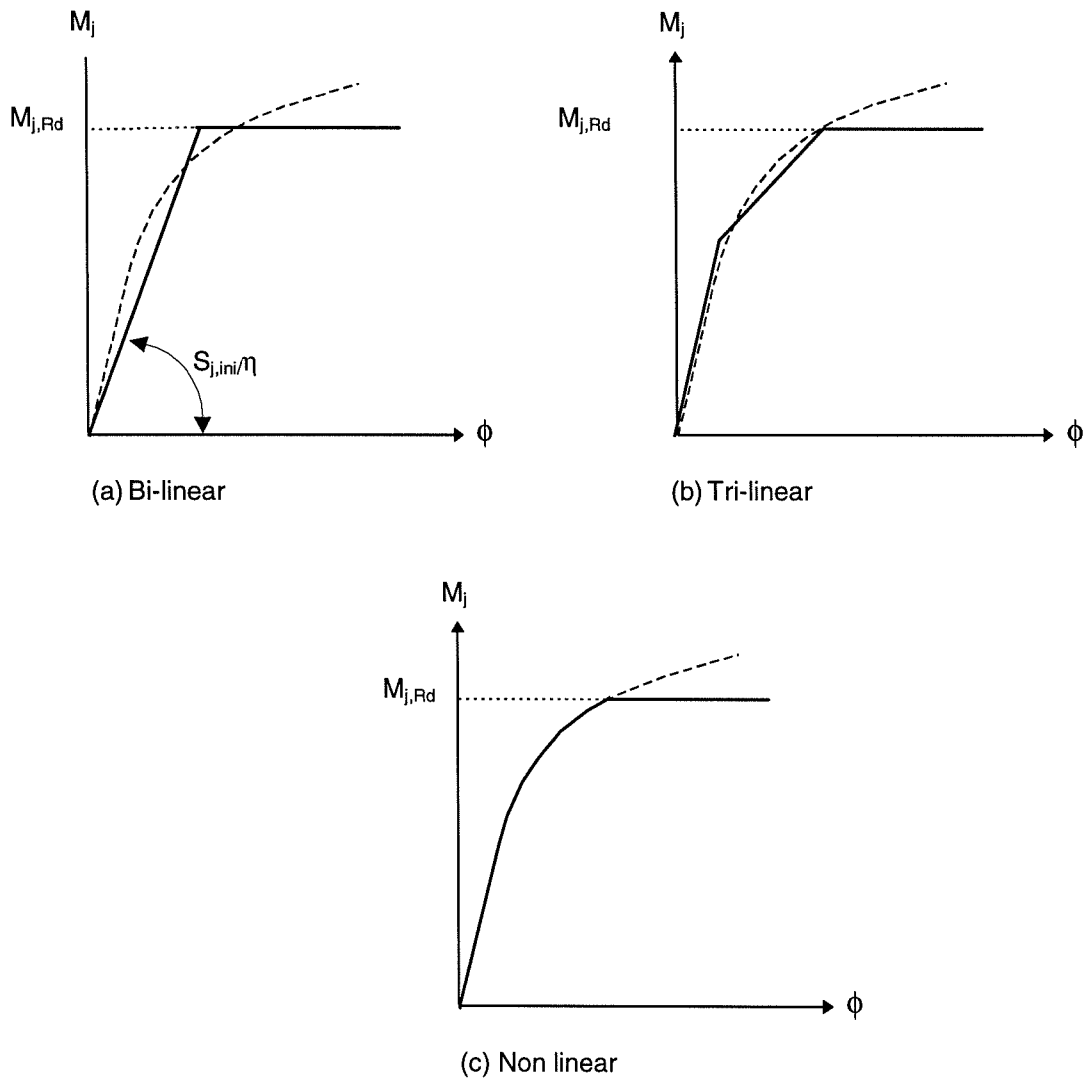


Figure 1-23 Non-linear representations of a M_j - ϕ curve

1.5 Joint characterization

An important step when designing a frame consists in the characterization of the rotational response of the joints.

Three main approaches may be followed :

- experimental;
- numerical;
- analytical.

The only practical one for the designer is the analytical approach. Analytical procedures enable a prediction of the joint response based on the knowledge of the mechanical and geometrical properties of the joint components.

In Chapter 2, a general analytical procedure, termed *component method*, is introduced. Its originality is to consider any joint as a set of *individual basic components*. For the

particular joint shown in Figure 1-4.a (joint with an extended end-plate connection subject to bending), the relevant components are the following :

- column web in compression;
- beam flange and web in compression;
- column web in tension;
- column flange in bending;
- bolts in tension;
- end-plate in bending;
- beam web in tension;
- column web panel in shear.

The procedure consists in deriving the mechanical properties of the whole joint from those of all the individual constitutive components.

In Eurocode 3 revised Annex J, the component method is used for the evaluation of the initial stiffness and the design moment resistance of the joint; these two properties enable to build design joint moment-rotation characteristics whatever the type of analysis (Figure 1-21 to Figure 1-23).

The application of the component method requires a sufficient knowledge of the behaviour of the basic components. The combination of the components allows one to cover a wide range of joint configurations, which should be largely sufficient to satisfy the needs of practitioners as far as major axis beam-to-column joints and beam splices in bending are concerned. Examples of such joints are given in Figure 1-24.

Some other fields of application could however be also contemplated :

- Joints subject to bending moment (and shear) and axial force;
- Column bases subject to combined bending moment, shear force and axial force;
- Minor axis joints.

These applications are however not yet covered, or only partially covered, by *Eurocode 3*. But as said in the prefatory chapter, the present thesis is aimed at investigating these topics in view of a possible further implementation of Eurocode 3 Annex J.

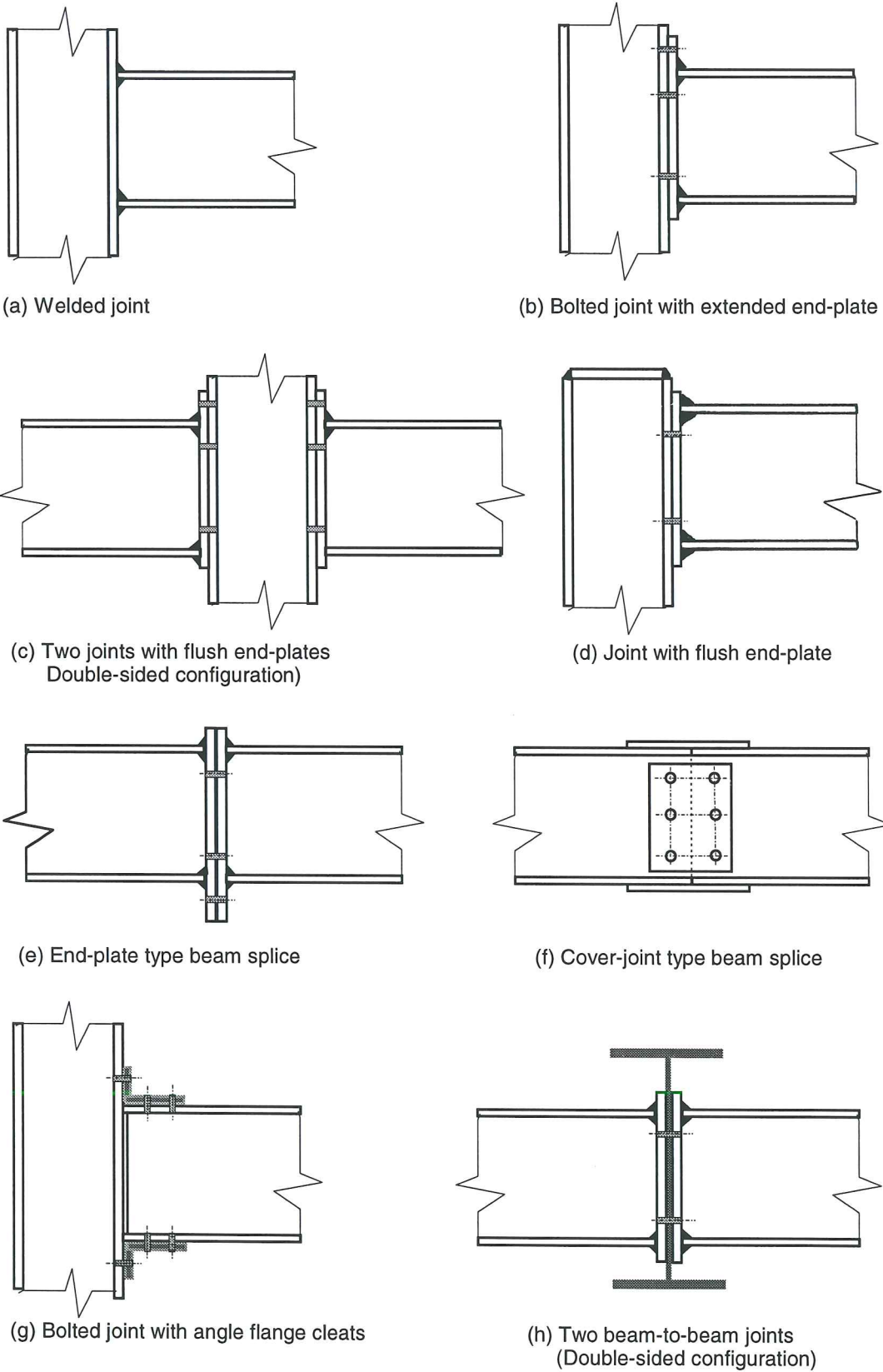


Figure 1-24 Examples of joints covered by Eurocode 3

1.6 Joint classification

1.6.1 General

In Section 1.3, it is shown that the joints need to be modelled for the global frame analysis and that three different types of joint modelling are introduced : simple, semi-continuous and continuous.

It has also been explained that the type of joint modelling to which it shall be referred is dependent both on the type of frame analysis and on the class of the joint in terms of stiffness and/or strength (Figure 1-13).

Classification criteria are used to define the stiffness class and the strength class to which the joint belong and also to determine the type of joint modelling which shall be adopted for analysis. Those available for beam-to-column joints are described in the following Section.

1.6.2 Classification based on mechanical joint properties¹

The *stiffness classification* is performed by comparing simply the design joint stiffness to two stiffness boundaries (Figure 1-25). For sake of simplicity, the stiffness boundaries have been derived so as to allow a direct comparison with the *initial design* joint stiffness, whatever the type of joint idealization that is used afterwards in the analysis (Figure 1-21 and Figure 1-23).

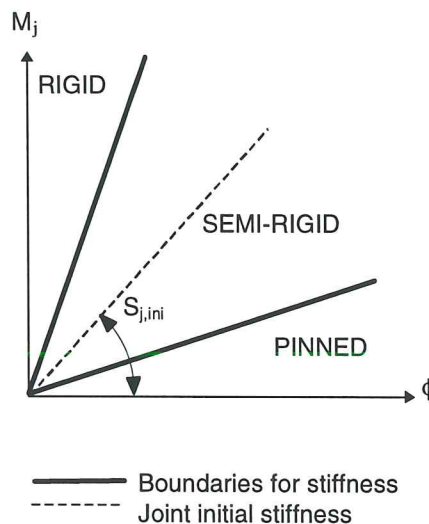


Figure 1-25 Stiffness classification boundaries

¹ These classification criteria are those given in revised *Eurocode 3-Annex J*. As *Annex J* is not fully compatible with the questionable classification diagram proposed in *Eurocode 3-Chapter 6.9*, no information on the latter is given here.

The *strength classification* simply consists in comparing the joint *design* moment resistance to "full strength" and "pinned" boundaries (Figure 1-26).

It is while stressing that a classification based on the *experimental* joint M_j - ϕ characteristics is not allowed, as *design* properties only are of concern.

The stiffness and strength boundaries for the joint classification are discussed in Chapter 5.

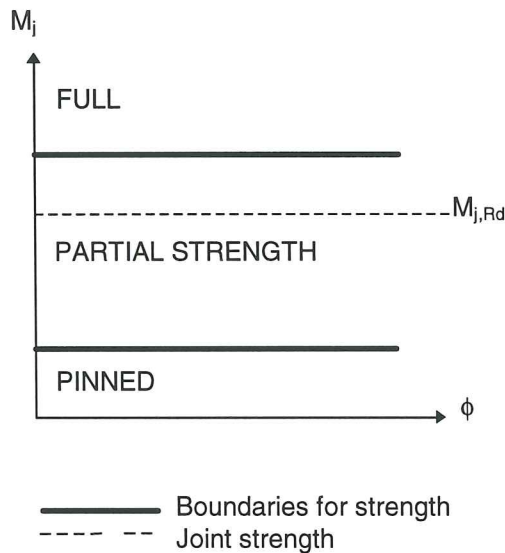


Figure 1-26 Strength classification boundaries

1.7 Ductility classes

1.7.1 General concept

Experience and proper detailing result in so-called *pinned* joints which exhibit a sufficient rotation capacity to sustain the rotations imposed on them.

For moment resistant joints the concept of ductility classes is introduced to deal with the question of rotation capacity.

For most of these structural joints, the shape of the M_j - ϕ characteristic is rather bi-linear (Figure 1-27.a). The initial slope $S_{j, ini}$ corresponds to the elastic deformation of the joint. It is followed by a progressive yielding of the joint (of one or some of the constituent components) until the design moment resistance $M_{j,Rd}$ is reached. Then a post-limit behaviour ($S_{j, post-lim}$) develops which corresponds to the onset of strain-hardening and possibly of membrane effects. The latter are especially important in components when rather thin plates are subject to transverse tensile forces as, for instance, in minor axis joints and in joints with columns made of rectangular hollow sections.

In many experimental tests (Figure 1-27.a) the collapse of the joints at a peak moment $M_{j,u}$ has practically never been reached because of high local deformations in the joints involving extremely high relative rotations. In the others (Figure 1-27.b) the collapse has involved an excessive yielding (rupture of the material) or, more often, the instability of one of the constituent components (ex : column web panel in compression or buckling of the beam flange and web in compression) or the brittle failure in the welds or in the bolts.

In some joints, the premature collapse of one of the components prevents the development of a high moment resistance and high rotation. The post-limit range is rather limited and the bi-linear character of the $M_j-\phi$ response is less obvious to detect (Figure 1-27.c).

As explained in Section 4.4, the actual $M_j-\phi$ curves are idealized before performing the global analysis. As for beam and column cross-sections, the usual concept of plastic hinge can be referred to for plastic global analysis.

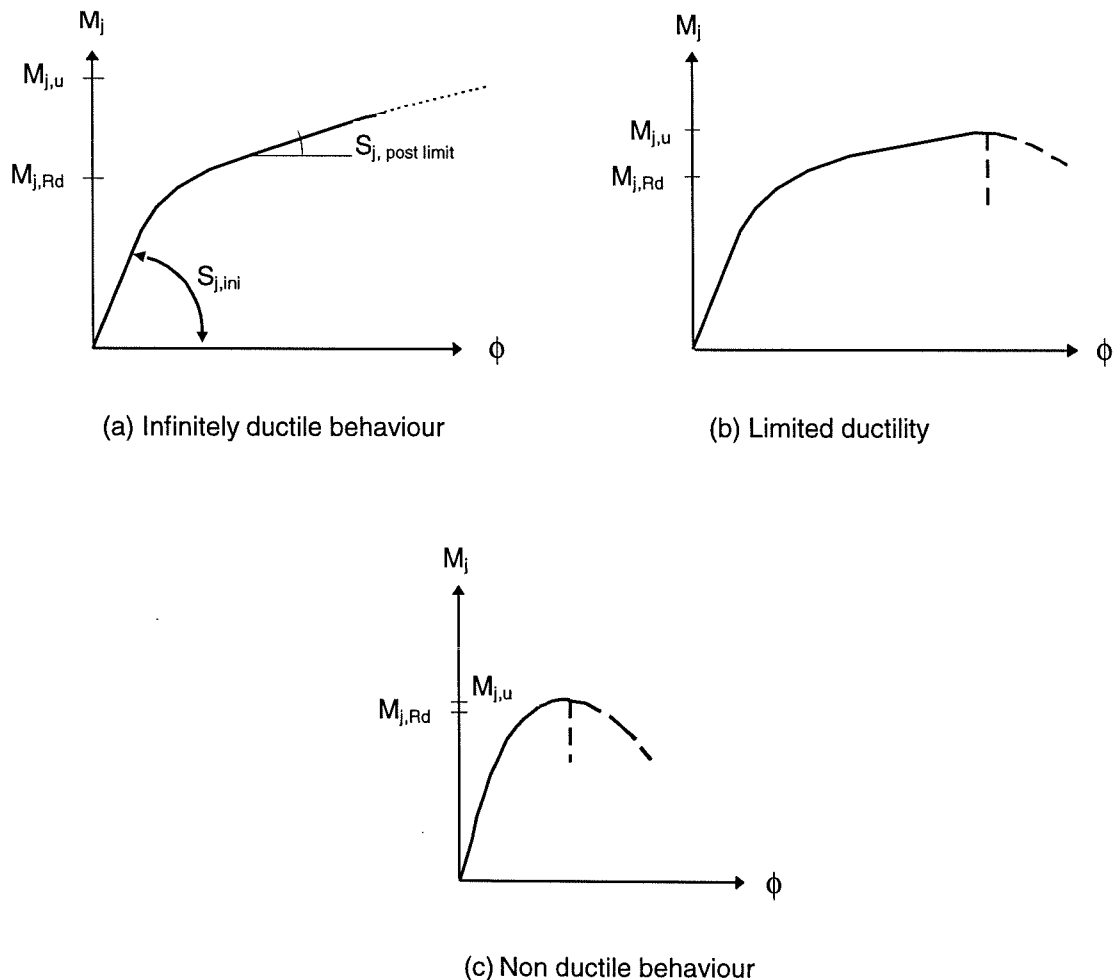


Figure 1-27 Shape of joint $M-\phi$ characteristics

The development of plastic hinges during the loading of the frame and the corresponding redistribution of internal forces in the frame require, from the joints where hinges are likely to occur, a sufficient rotation capacity. In other words, there must be a sufficiently long yield plateau ϕ_{pl} (Figure 1-28) to allow the redistribution of internal forces to take place.

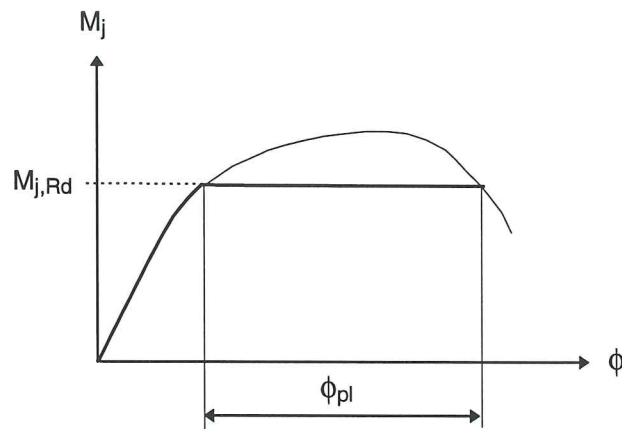


Figure 1-28 Plastic rotation capacity

For beam and column sections, deemed-to-satisfy criteria allow one to determine the class of the sections and therefore the type of global frame analysis which can be contemplated (see Chapter 3).

A strong similarity exists for what regards structural joints; moreover a similar classification may be referred to :

- *Class 1 joints* : $M_{j,Rd}$ is reached by full plastic redistribution of the internal forces within the joints and a sufficiently good rotation capacity is available to allow, without specific restrictions, a plastic frame analysis and design to be performed if required;
- *Class 2 joints* : $M_{j,Rd}$ is reached by full plastic redistribution of the internal forces within the joints but the rotation capacity is limited. An elastic frame analysis possibly combined with a plastic verification of the joints has to be performed. A plastic frame analysis is also allowed as long as it does not result in a too high required rotation capacity in the joints where hinges are likely to occur. The available and required rotation capacities have therefore to be compared before validating the analysis;
- *Class 3 joints* : brittle failure (or instability) limits the moment resistance and does not allow a full redistribution of the internal forces in the joints. It is compulsory to perform an elastic verification of the joints unless it is shown that no hinge occurs in the joint locations.

As the moment design resistance $M_{j,Rd}$ is known whatever the collapse mode and the resistance level, no Class 4 has to be defined as for member sections.

1.7.2 Requirements for classes of joints

In *Eurocode 3*, the procedure given for the evaluation of the design moment resistance of any joint provides the designer with other information such as :

- the collapse mode;
- the state of stresses inside the joint at collapse.

Through this procedure, the designer knows directly whether the full plastic redistribution of the forces within the joint has been reached - the joint is then Class 1 or 2 - or not - the joint is then classified as Class 3 (see Chapter 3).

For Class 1 or 2 joints, the knowledge of the collapse mode, and more especially of the component leading to collapse, gives an indication about whether there is adequate rotation capacity for a global plastic analysis to be permitted. The related criteria are expressed in Chapter 3.

PART II : CHARACTERIZATION OF THE JOINTS

Chapter 2 : COMPONENT METHOD

Chapter 3 : NEW CONTRIBUTIONS TO THE COMPONENT METHOD

2. COMPONENT METHOD

2.1 Generals on the characterization

In the present chapter, a general analytical procedure for the prediction of the mechanical properties of structural joints is introduced. This so-called component method, the name of which originates from the period where the Annex J of Eurocode 3 has been revised, appears as the outcome of several years of studies on joint characterization throughout Europe and North America. Its great advantage, contrary to other approaches proposed in the past, is the possibility to be applied to any steel or composite beam-to-column joints, to beam splices or to column bases.

Before describing the principles of the component method, and in view of a better understanding of its different levels of refinement, it appears quite interesting to present hereafter an overview of the other characterization procedures by particularly highlighting their advantages and drawbacks.

The more accurate but also expensive way to characterize the deformability and the resistance of joints is the experimentation in laboratory. The use of this technique - which requires much money and much time - is basically limited to research activities and can consequently not be recommended for daily practice.

The existence of numerous test results for a large variety of joint configurations and connection types led progressively some researchers to develop computerised databanks. The low probability for the designer to find informations for the specific joint he is studying and the risk to misinterpretate the results listed in the databank - no standardised procedure for the testing of joint exists at present - limit considerably the practical interest of these tools. On the other hand, it appears now clearly that the databanks have to be considered as quite valuable tools for the validation of mathematical models aimed at predicting the joint response on the basis of the geometrical and mechanical joint properties.

Most of the well-known mathematical models available in the literature are described in [N1] by Nethercot and Zandonini and in [B1] by Bursi. They can be classified in four main categories :

- A - curve fitting;
- B - simplified analytical models;
- C - mechanical models;
- D - finite element analysis;

The objective here is to highlight the differences and similarities between these categories through four tables focusing for each category, on :

- the definition;

- the advantages and disadvantages (practical interest, field of application, etc).

The description of a specific model as well as a list of available models - without any reference - see [N1] and [B1] if needed - complete also the information given in each table.

Such a synthetic presentation is aimed at helping the researchers who intend to develop mathematical predicting tools for joints - whatever is the material used - to choose on good grounds the type of modelling to which he will refer.

From the four tables, it may be concluded that :

1. The finite element analysis is not yet likely to be used to predict the semi-rigid response for any type of connection detailing and that its use is reserved to research activities.
2. The simplified analytical models and the mechanical models are characterized by a wider field of application than curve fitting; this results from the theoretical background of these two kinds of modelling.
They have however to be extended to other types of connections in order to cover the main needs of the designers.
3. The simplified analytical models are the only ones - with the formulae resulting from curve fitting - to be suitable for hand calculations.

A**CURVE FITTING****Definition**

- Attempt to fit a mathematical representation to characteristic $M-\phi$ curves obtained by means of :
 - experimental tests in laboratory;
 - numerical simulations;
- Possible attempt to link the coefficients of the mathematical representation with physical parameters of the joint.

Example

Frye and Morris formula :

$$\phi = C_1(kM) + C_2(kM)^3 + C_3(kM)^5$$

in which :

k is depending on the main parameters of the joint;

C coefficients are curve fitting constants.

List of existing modelsMathematical representationsAuthors

- | | |
|---|--|
| <ul style="list-style-type: none"> • Polynomial | Sommer, 1969
Kennedy, 1969
Frye and Morris, 1975 |
| <ul style="list-style-type: none"> • Cubic B-Spline | Jones and al, 1981 |
| <ul style="list-style-type: none"> • Béziers | Jaspert, 1985 |
| <ul style="list-style-type: none"> • Richard formula | Richard and al, 1980 |
| <ul style="list-style-type: none"> • Ramberg-Osgood | Ang and Morris, 1984 |
| <ul style="list-style-type: none"> • Exponential | Lui and Chen, 1986 |
| <ul style="list-style-type: none"> • Power | Krishnamurthy and al, 1979
Murray and al, 1987 |

General advantages and/or disadvantages

- Capacity of representing with extreme accuracy any shape of $M-\phi$ curve;
- Purely empirical \rightarrow range of application limited to joints, the geometrical and mechanical properties of which are similar to those considered when calibrating the formula
- Inability to recognize that, depending on the geometrical and mechanical parameters, the type of connection behaviour as well as the contribution of each component to the overall joint response may change significantly.

B**SIMPLIFIED ANALYTICAL MODELS****Definition**

- Simplified analytical methods to predict the main characteristic values of the $M-\phi$ curves (initial stiffness, design moment resistance, ...); this step requires the knowledge of the mechanical and geometrical properties of the joints.
- Verification of these analytical methods by comparison with test data or results of numerical simulations.
- Description of the $M-\phi$ behaviour by curve fitting using the calculated initial stiffness, plastic and ultimate moment, ... in suitable mathematical expressions.

Example

Jaspart's model :

$$M = \frac{(S_{j,ini} - S_{j,post-limit})\phi}{\left\{ 1 + \left[\frac{(S_{j,ini} - S_{j,post-limit})\phi}{M_{Rd}} \right]^C \right\}^{1/C}} + S_{j,post-limit} \phi \leq M_{u,Rd}$$

with

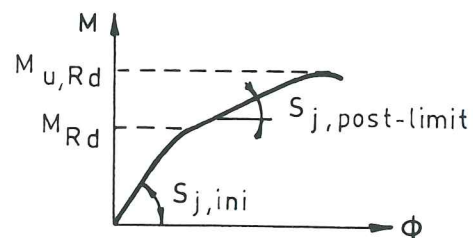
$S_{j,ini}$ = initial stiffness;

$S_{j,post-limit}$ = post-limit stiffness;

M_{Rd} = design resistance;

$M_{u,Rd}$ = ultimate resistance;

C = curve fitting constant



List of existing models

- Lothers, 1951 (double web cleat)
- Johnson and Law, 1981 (flush end-plate)
- Chen and al, 1987/88 (flange and/or web cleat(s))
- Yee and Melchers, 1986 (end-plate)
- Jaspart, 1991 (welded end-plate - flange cleats)

General advantages and/or disadvantages

- Allow to approximate the form of the $M-\phi$ curves without resort to testing;
- Still require empirical curve fitting to generate the full curve (but limited !);
- Special remark :

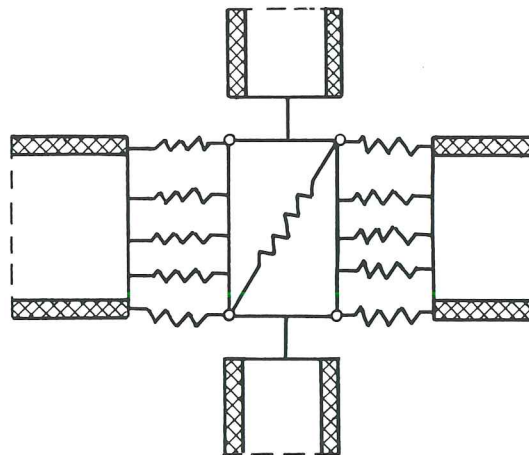
Eurocode 3 method (Annex J) refers basically to this section; it provides an original way to generate the $M-\phi$ curves.

C**MECHANICAL MODELS****Definition**

- Set of rigid and deformable elements representing each the behaviour of specific parts of the joint.
- Non-linearity of the joint response is then accounted for by inelastic constitutive laws adopted for the deformable elements.
- These constitutive laws are obtained from test data, numerical simulations or analytical models.

Example

Tschemmernegg's model :



List of existing model

- Kennedy and Hafez, 1984 (Header plate connections)
- Wales and Rossow, 1983 (Double web cleat connections)
- Richard and al, 1987 (Cleated connections)
- Tschemmerneegg and al, 1988 (Fully welded and end-plate connections)
- Jaspart, 1990 (Composite joints with end-plate and cleated connections - also applicable to similar steel connections)
- Tschemmerneegg, 1995 (Composite joints with contact plates)
- Guisse, Jaspart and Vandegans, 1996 (Column bases)
- Jaspart, 1996 (Steel joints subjected to combined moment, shear and axial forces)

General advantages and/or disadvantages

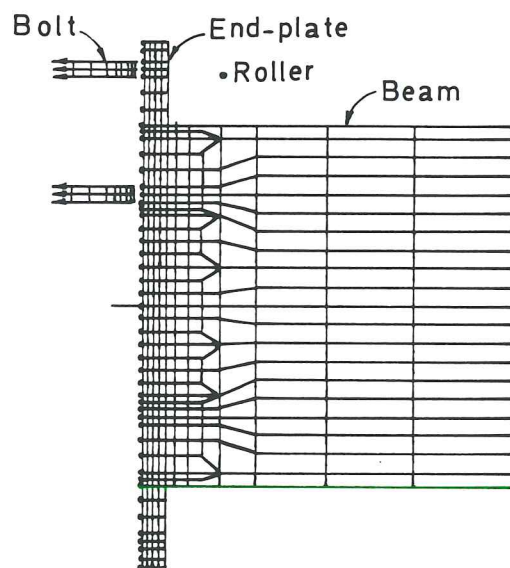
- Really suitable for modelling provided that a knowledge of the load deformation curve of the key components is available.
- May be easily extended to different types of joint configurations and of connections provided the knowledge of the key components is available.
- May require the use of computer programs to generate the curve.

D**FINITE ELEMENT ANALYSIS****Definition**

- Prediction of $M-\phi$ curves by means of a finite element analysis.

Example

Krishnamurthy's analysis :



List of existing models

Welded connections

- Bose and al, 1972
- Patel and Chen, 1984
- Atamaz Sibai, Jaspert, Frey, 1988

Bolted connections

- | | |
|--------------------------------|--|
| • Lipson and Hague, 1978 | (Single angle bolted-welded connections) |
| • Richard and al, 1980 | (Single web plate connections) |
| • Patel and Chen, 1985 | (Fully bolted connections) |
| • Richard and al, 1983 | (Double web cleat connections) |
| • Krishnamurty, 1980 | (End plate connections) |
| • Murray and al, 1987 | (Flush end-plate connections) |
| • Ziomek and al, 1992 | (End plate connections) |
| • Robert and al, 1992 | (End plate connections) |
| • Sherbourne and Bahaari, 1994 | (End plate connections) |
| • Bursi and Jaspert, 1996 | (End plate connections) |

General advantages and/or disadvantages

- Suitable to predict the response of welded joints.
- Sufficient ability to model the non-linear 3-D response of joints with bolted connections and in particular :
 - the actual bolt action;
 - the contact phenomena;
 - the slips;
 - ...

not yet fully attained.

2.2 Principles of the component method

The component method may be presented as the application of the well-known finite element method to the calculation of structural joints.

In the characterization procedures, a joint is generally considered as a whole and is studied accordingly; the originality of the component method is to consider any joint as a set of "individual basic components". In the particular case of Figure 2-1 (joint with an extended end-plate connection subject to bending), the relevant components are the following :

- compression zone :
 - column web in compression;
 - beam flange and web in compression;
- tension zone :
 - column web in tension;
 - column flange in bending;
 - bolts in tension;
 - end-plate in bending;
 - beam web in tension;
- in shear zone :
 - column web panel in shear.

Each of these basic components possesses its own level of strength and stiffness in tension, compression or shear. The coexistence of several components within the same joint element - for instance, the column web which is simultaneously subjected to compression (or tension) and shear - can obviously lead to stress interactions that are likely to decrease the strength and the stiffness of each individual basic component; this interaction affects the shape of the deformability curve of the related components but does not call the principles of the component method in question again.

The application of the component method requires the following steps :

- a) listing of the "activated" components for the studied joint;
- b) evaluation of the stiffness and/or strength characteristics of each individual basic component (specific characteristics - initial stiffness, design strength, ... - or the whole deformability curve);

- c) "assembly" of the components in view of the evaluation of the stiffness and/or strength characteristics of the whole joint (specific characteristics - initial stiffness, design resistance, - or the whole deformability curve).

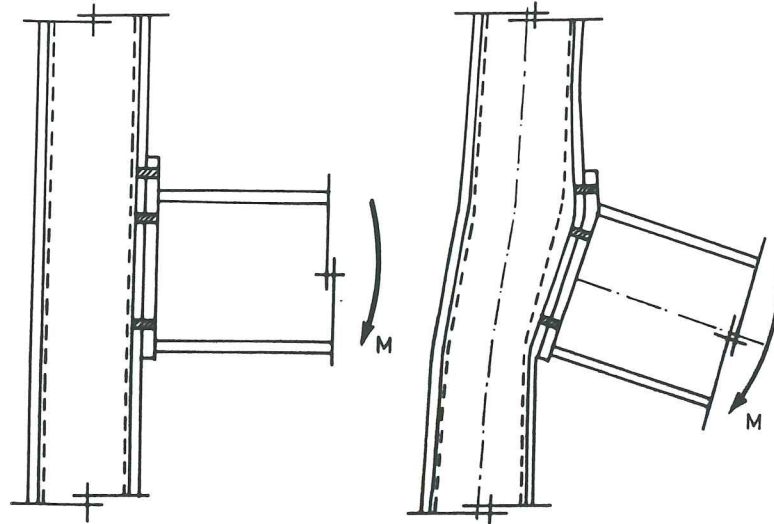


Figure 2-1 Joint in bending with an extended end-plate

These three steps are schematically illustrated in Figure 2-2 in the particular and simple case of a beam-to-column steel joint with a welded connection.

As specified here above, the parallelism with the finite element method is obvious. To "component" and "joint" may then be substituted the words "finite element" and "structure".

The assembly is based on a distribution of the internal forces within the joint. As a matter of fact, the external loads applied to the joint distribute, at each loading step, between the individual components according to the instantaneous stiffness and resistance of each component. Distributions of internal forces may be obtained through different ways as discussed in 2.3.

The application of the component method requires a sufficient knowledge of the behaviour of the basic components. Figure 2-3 gives an overview of the steel components covered by the revised Annex J of Eurocode 3 [E2]. In the recently drafted Annex J of Eurocode 4 [E3], a new component is added : the reinforcement bars in tension; the stiffening and the strengthening of the column web panel in shear and of the column web in compression by means of encased concrete is also made available.

The combination of these components allows to cover a wide range of joint configurations, what should largely be sufficient to satisfy the needs of practitioners as far as beam-to-column joints and beam splices in bending are concerned.

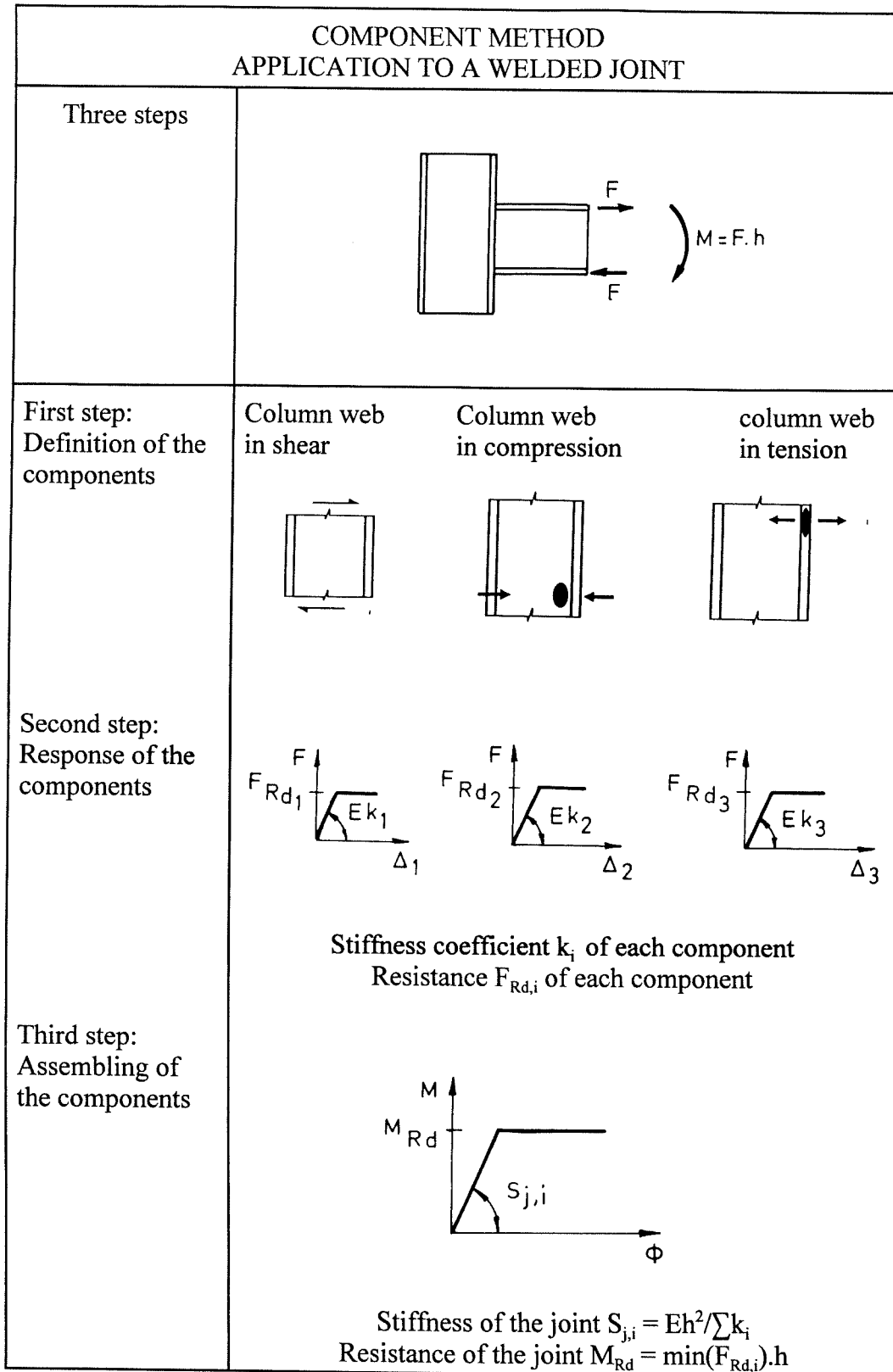
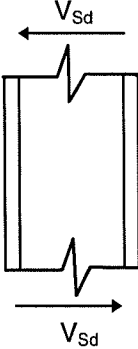
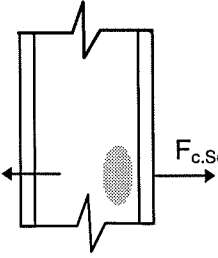
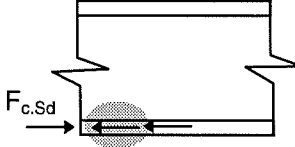
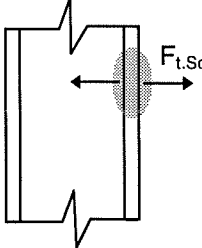
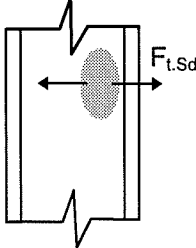


Figure 2-2 Application of the component method to a welded steel joint

N°	Component	
1	Column web panel in shear	
2	Column web in compression	
3	Beam flange and web in compression	
4	Column flange in bending	
5	Column web in tension	

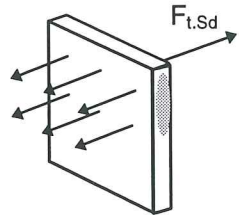
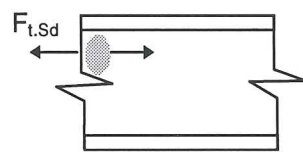
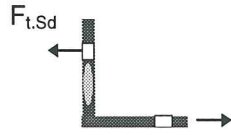
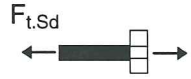

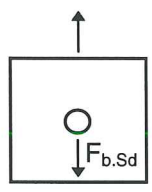
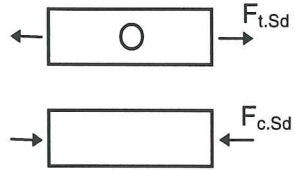
6	End-plate in bending	
7	Beam web in tension	
8	Flange cleat in bending	
9	Bolts in tension	
10	Bolts in shear	
11	Bolts in bearing (on beam flange, column flange, end-plate or cleat)	
12	Plate in tension or compression	

Figure 2-3 Components available in Eurocode 3

Some fields of application are however not yet covered by the codes :

- Weak axis joints where the beam is connected to the web of a H or I column profile are characterized by an out-of-plane deformability of the column web under the tension and compression forces carried over by the beam. The "column web in transverse compression and tension" component still requires specific studies to be performed in view of the development of reliable stiffness and strength characterization tools. Knowledges about this component would directly allow the extension of the component method to joints where tubular columns with rectangular hollow sections are used, as shown in [V1]. As a matter of fact, similar phenomena occur in the face of the hollow section where the beam is connected.
- Joints subject to bending moment (and shear) and axial compression or tension forces have been less studied and, in particular, the way to distribute the internal forces for stiffness and strength calculations, the stiffness and strength component properties remaining unchanged whatever is the type of loading.
- Column bases are subjected to combinations of bending moments and axial forces and possess specific components for which a limited knowledge is available. For instance :
 - concrete block in compression;
 - end-plates with specific geometries;
 - anchorages in tension;
 - contact between soil and foundation;
 - ...
- An improvement of the mechanical properties of the joints may be achieved through the use of beam haunches, end-plate stiffeners or high strength steels. These aspects are not yet covered in the codes.
- In pitch-roof portal frames, connected beams and columns form an angle higher than 90° . This requires specific amendments to be made to the existing characterization procedures.
- When columns with rather slender webs are used, the usual rules for "column web panels in shear" are no more valid because of the apparition of shear buckling and post-critical phenomena. Few recommendations are available in this field.

Research works in Liège have recently allowed to investigate these different aspects; they have brought some answers to these last questions which prevent the general use of the component method to any structural joint.

These developments are discussed in chapter 3.

2.3 Levels of refinement

The framework of the component method is sufficiently general to allow the use of various techniques of component characterization and joint assembly.

In particular, the stiffness and strength characteristics of the components may result from experimentations in laboratory, numerical simulations by means of finite element programs or analytical models based on theory. At Liège, experimentations and numerical simulations have been performed and used as references when developing and validating analytical models. These ones may be developed with different levels of sophistication according to the persons to whom they are devoted :

- expressions as those presented in our Ph.D. Thesis [J1] cover the influence of all the parameters which affect significantly the component behaviour (strain hardening, bolt head and nut dimensions, bolt prestressing, ...) from the beginning of the loading to collapse and fit therefore well with a scientific publication;
- the rules which have been introduced in Annex J of Eurocode 3 [E2] are more simple and are therefore more suitable for hand calculations.
- The SPRINT design sheets presented in chapter 7 constitute an ultimate step in the simplification process; the procedures for stiffness and strength evaluation are reduced to the essentials and allow a quick and nevertheless accurate prediction of the main joint properties.

Similar levels of sophistication exist also for what regards the joint assembly.

3. NEW CONTRIBUTIONS TO THE COMPONENT METHOD

3.1 Contents of the chapter

As explained in Chapter 2, the component method is a quite flexible and powerful tool for joint characterization. Its scope may be extended to any type of joint, any connection type and also to any material (timber, concrete, pre-cast concrete, ...) as recently demonstrated in the frame of the COST C1 activities as soon as :

- the stiffness and/or resistance and/or deformation properties of the constitutive components are known;
- the possible interactions between constitutive components are clearly established;
- the way to assemble the components together is mastered.

All these aspects have been extensively discussed in [J1] for traditional beam-to-column joints with end-plate and flange cleated connections.

In Eurocode 3 Annex J [E2] and in the SPRINT design sheets and tables [S1], simplified procedures for beam-to-column joints with similar connection types and for beam splices with end-plates have also been presented.

In Eurocode 3 Annex J, other components have also been introduced : plates in tension, plates in bearing, bolts in shear. Means of component stiffening and strengthening like backing plates, web plates or transverse and diagonal stiffeners are also proposed.

The combination of all these components already covers a wide range of structural joints but still limits, anyway, possibilities of the practical designer who is often faced, in a specific structure, to quite unusual local joint detailings where the stiffness and resistance properties have to be also determined.

In this context, it has been felt that investigations were still necessary in order to :

- complete the set of available components for strong axis beam-to-column joints and beam splices;
- extend the component method to weak axis joints and composite joints;
- apply the same principles than those developed for structural joints to column bases.

The outcome of these investigations is summarized in Sections 3.2 to 3.5 of the present chapter. Section 3.4 on column bases appears as a quite detailed and scientific investigation in a field where few developments have been performed in comparison to other structural joints. The other sections present mainly design rules of more practical interest which could be taken into consideration in a further revision of Eurocode 3 Annex J.

Section 3.3, on the other hand, briefly refers to the recent drafting efforts to produce Eurocode 4 Annex J on « Joints in composite building frames ».

Lastly, the possibility to extend the component method, and more especially the rules available for components, to high strength steels is discussed in Section 3.6.

3.2 Strong axis beam-to-column joints and beam splices

In Section 3.2.1, the response of new components and the influence of new stiffening or strengthening means are discussed. Design rules are proposed and justified.

The results of complementary investigations on the interactions as they take place in a column web panel subjected to shear, compression and tension forces are then presented in Section 3.2.2. First research works in this field had been extensively discussed in [J1].

Finally, assembly procedures are described in Section 3.2.3. where, in 3.2.3.3, an original procedure for joints under bending, shear and axial compressive or tensile forces is suggested.

3.2.1 Behaviour of new components and additional considerations on existing ones

3.2.1.1 Beam flange and web in compression

Resistance

This component is not a new one; it is available to designers in the revised Annex J of Eurocode 3. The background of the design formula proposed in Annex J for resistance evaluation seems, however, usually not to be clearly understood by the reader; it appears so quite important, as one of the authors of the proposal, to give some words about it.

When a bending moment M is carried over from the beam to the joint, a compression zone develops in the beam, close to the joint; it includes a beam flange and a part of the beam web in compression. The compressive force F_c carried over by the connection may, as indicated in (3-1), be quite higher than the compressive force F in the beam flange resulting from the resolution, at some distance of the joint, of the same bending moment M . In (3-2), the forces F and F_c are applied to the centroid of the beam flange in compression.

This assumption is usually made for sake of simplicity but does not correspond to the reality as the compression zone is not only limited to the beam flange.

The force F_c , quite localized, may lead to the instability of the compressive zone of the beam cross-section and has therefore to be limited to a design value which is defined in Annex J as equal to :

$$F_{c.fb.Rd} = M_{c.Rd} / (h_b - t_{fb}) \quad (3-1)$$

where :

$M_{c.Rd}$ is the design moment resistance of the beam cross-section reduced, when necessary, by the shear forces; $M_{c.Rd}$ takes into consideration by itself the potential risk of instability in the beam flange or web in compression;

h_b is the whole depth of the beam cross-section;

t_{fb} is the thickness of the beam flange.

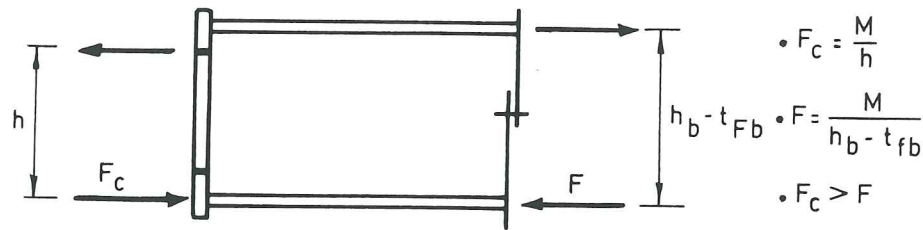


Figure 3-1 Localized compressive force in the beam cross-section located close to the connection

It has to be pointed out that Formula (3-1) limits the maximum force which can be carried over in the compressive zone of the joint because of the risk of loss of resistance or instability in the possibly overloaded compressive zone of the beam located close to the joint. It therefore does not replace at all the classical verification of the resistance of the beam cross-section, except for fully welded joints where both verifications are identical.

It has also to be noted that formula (3-1) applies whatever is the type of connection and the type of loading acting on the joint. For instance, Formula (3-1) is referred to in Eurocode 4 Annex J in the case of composite construction and applies to joints subjected to combined moments and shear and axial compressive or tensile forces.

In the case of a non-symmetrical beam cross-section (built-up members), the formula writes (Figure 3-2) :

$$F_{c.fb.Rd} = M_{c.Rd} / (h_b - 0,5 (t_{fbo} + t_{fbr})) \quad (3-2)$$

where :

t_{fbr} is the thickness of the beam flange in compression being considered;

t_{fbo} is the thickness of the other beam flange.

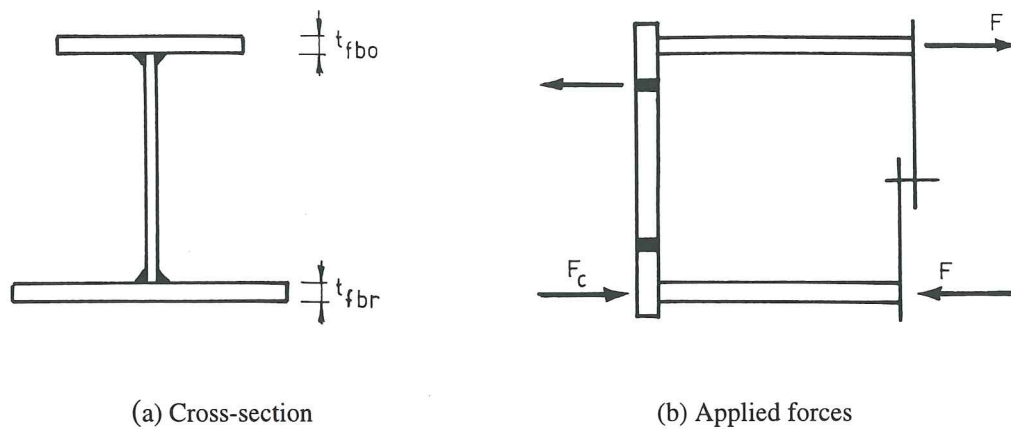


Figure 3-2 Case of a non-symmetrical beam-cross section

The design resistance given by Formula (3-1) has to be compared to the compressive force F_c (see Figure 3-1 and Figure 3-2) which results from the distribution of internal forces in the joint and which is also assumed to be applied at the centroid of the beam flange in compression. It integrates the resistance of the beam flange and of a part of the beam web; it also covers the potential risk of local plate instability in both flange and web.

Stiffness

As explained in Section 3.2.3.2, the deformation of the beam flange and web in compression is assumed not to contribute to the joint flexibility. No stiffness coefficient is therefore needed.

Deformation capacity

To our knowledge, the deformation capacity of the beam flange and web in compression has not yet been studied and no specific rules are therefore available.

In this context, it is wise not to rely on any deformation capacity even if it is thought that, as some experimental tests seem to indicate it, some good deformation capacity may be expected from tests where the beam flange and web fail by plasticity and not by instability.

Should profiles be classified in "Class 1 sections in bending" and "others" for what regards the deformation capacity of the beam flange and web in compression ?

This question should probably be kept in mind for further investigations on this topic.

3.2.1.2 Stiffening and strengthening of the extended part of an end-plate in bending

The stiffening and the strengthening of the extended part of an end-plate may be achieved by the welding of a triangular stiffener as indicated in Figure 3-3.

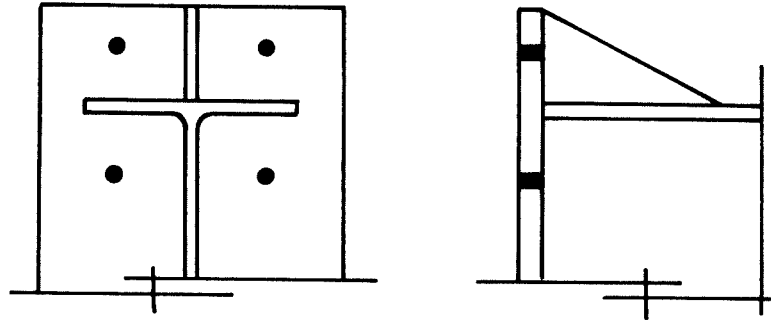


Figure 3-3 Stiffener on an extended end-plate

The stiffness and the strength of the extended part may be evaluated through the concept of T-stub introduced in Appendix 3 to the present thesis and to which it is referred to in Eurocode 3 Annex J for plates subjected to transverse bolt forces.

The use of the formulae presented in Appendix 3 requires the evaluation of effective lengths $l_{eff,cp}$ and $l_{eff,nc}$ for the equivalent T-stub which is substituted to the actual plate in bending.

Resistance

In the case of an unstiffened extended part, the idealized T-stub is defined as indicated in Figure 3-4 and its effective length is derived as explained in Figure 3-5.

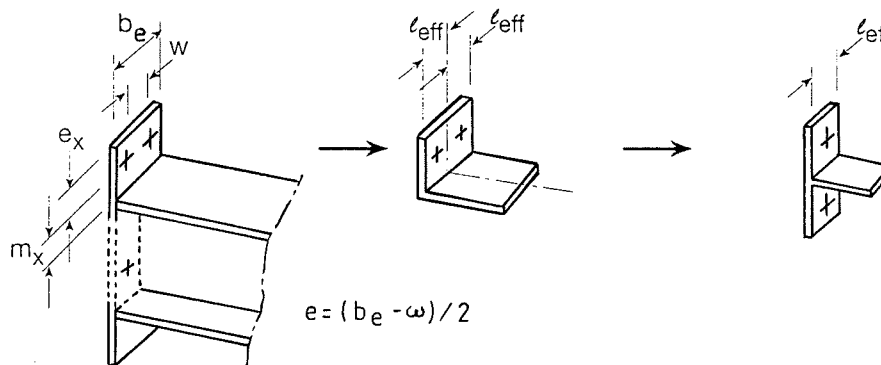
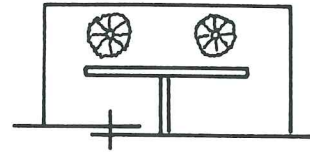
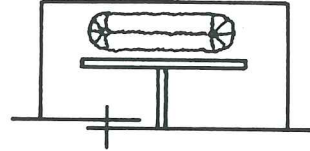


Figure 3-4 T-stub idealization in the case of an unstiffened end-plate (T-stub denoted \perp)

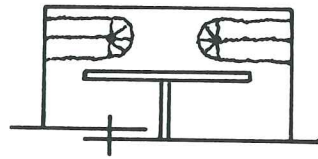
$$l_{eff1} = 2\pi m$$



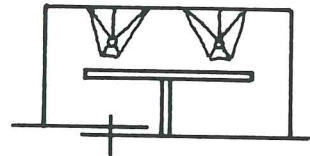
$$l_{eff2} = \pi m_x + \omega$$



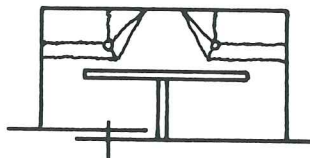
$$l_{eff3} = \pi m_x + 2e$$



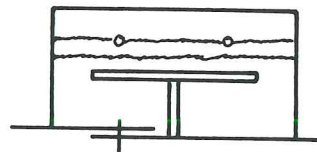
$$l_{eff4} = 4m_x + 1,25e$$



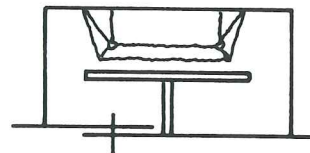
$$l_{eff5} = e + 2m_x + 0,625e_x$$



$$l_{eff6} = 0,5b_e$$



$$l_{eff7} = 0,5\omega + 2m_x + 0,625e_x$$



$$l_{eff,cp,\perp} = \min(l_{eff1}; l_{eff2}; l_{eff3})$$

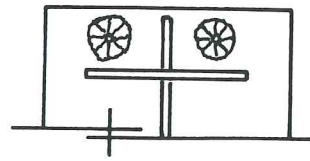
$$l_{eff,nc,\perp} = \min(l_{eff4}; l_{eff5}; l_{eff6}; l_{eff7})$$

Figure 3-5 Evaluation of the effective length.
Case of an unstiffened extended end-plate.

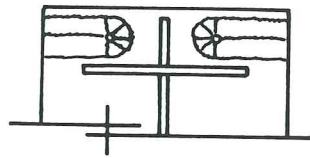
As soon as a stiffener is welded on the extended part of the end-plate, the group mechanisms characterized by effective lengths l_{eff2} , l_{eff6} and l_{eff7} have to be disregarded. So remain four cases and the effective lengths to be considered are obtained from Figure 3-6.

Because of the vicinity of the stiffener, the expressions of l_{eff4} and l_{eff5} has to be slightly changed by substituting, according to Annex J, αm_x to $4m_x + 1,25e_x$ for l_{eff4} and $\alpha m_x - (2m_x + 0,625e_x)$ to $2m_x + 0,625e_x$ for l_{eff5} .

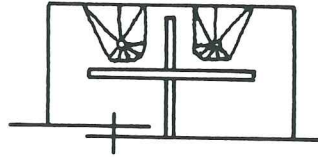
$$l_{eff1} = 2\pi m_x$$



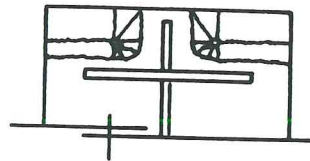
$$l_{eff3} = \pi m_x + 2e$$



$$l_{eff4} = \alpha m_x$$



$$l_{eff5} = \alpha m_x - (2m_x + 0,625e) + e$$



$$l_{eff,cp,\perp} = \min(l_{eff1}; l_{eff3})$$

$$l_{eff,nc,\perp} = \min(l_{eff4}; l_{eff5})$$

Figure 3-6 Evaluation of the effective lengths (\perp)
Case of a stiffened extended end-plate

The so-defined effective lengths are then introduced in the design resistance formulae for Mode 1, Mode 2 and Mode 3 (see Appendix 3) :

$$F_{Rd,1,\perp} = \frac{4M_{pl1,Rd,\perp}}{m_x} \quad (3-3)$$

$$F_{Rd,2,\perp} = \frac{2M_{pl2,Rd,\perp} + 2B_{t,Rd}n_x}{m_x + n_x} \quad (3-4)$$

$$F_{Rd,3} = 2B_{t,Rd} \quad (3-5)$$

where : $M_{pl1,Rd,\perp} = 0,25\ell_{eff,M1,\perp}t_e^2 f_{ye} / \gamma_{M0}$

$M_{pl2,Rd,\perp} = 0,25\ell_{eff,M2,\perp}t_e^2 f_{ye} / \gamma_{M0}$

$n_x = \min(1,25 m_x; e_x)$

In these expressions :

$$\begin{aligned} \ell_{eff,M1,\perp} &= \min(\ell_{eff,nc,\perp}; \ell_{eff,cp,\perp}) \\ &= \min(\ell_{eff1}; \ell_{eff3}; \ell_{eff4}; \ell_{eff5}) \end{aligned} \quad (3-6)$$

$$\begin{aligned} \ell_{eff,M2,\perp} &= \min(\ell_{eff,nc,\perp}) \\ &= \min(\ell_{eff4}; \ell_{eff5}) \end{aligned} \quad (3-7)$$

t_e and f_{ye} are respectively the thickness and the yield stress of the end-plate.

Other yield mechanisms related to another T-stub idealization of the extended part of the plate may also be contemplated. This other T-stub is represented in Figure 3-7.

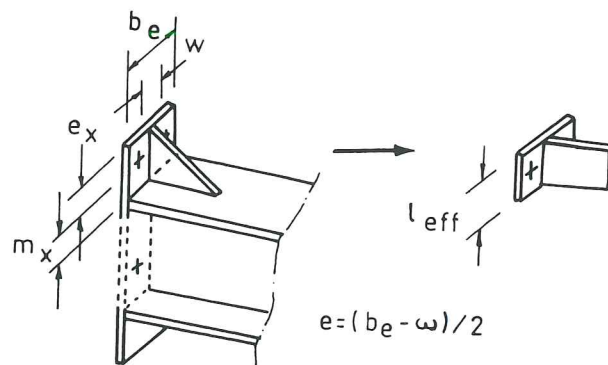
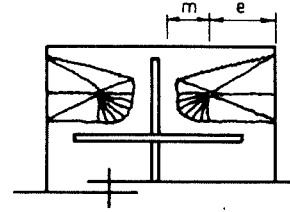


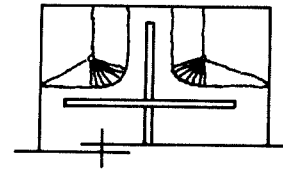
Figure 3-7 Possible other T-stub idealization in the case of a stiffened end-plate (T-stub denoted //)

The new yield mechanisms associated to this second possible T-stub idealization are drawn in Figure 3-8; the values of the associated effective lengths derived according to Eurocode 3 Annex J are indicated in the same figure.

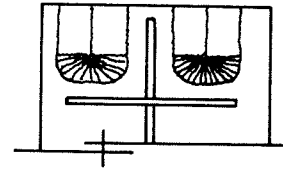
$$l_{eff8} = \alpha m$$



$$l_{eff9} = \alpha m - (2m + 1,25 e) + e_x$$



$$l_{eff10} = \pi m + 2 e_x$$



$$l_{eff,cp, //} = l_{eff10}$$

$$l_{eff,nc, //} = \min(l_{eff8}; l_{eff9})$$

Figure 3-8 Evaluation of the effective length (l_{eff}).
Case of a stiffened extended end-plate.

The design resistances of the T-stub are expressed as follows :

$$F_{Rd,1, //} = \frac{4M_{pl1, Rd, //}}{m} \quad (3-8)$$

$$F_{Rd,2, //} = \frac{2M_{pl2, Rd, //} + 2B_{t, Rd}n}{m + n} \quad (3-9)$$

$$F_{Rd,3} = 2B_{t, Rd} \quad (3-10)$$

with :

$$M_{pl1, Rd, //} = 0,25 l_{eff, M1, //} t_e^2 f_{ye} / \gamma_{M0}$$

$$M_{pl2, Rd, //} = 0,25 l_{eff, M2, //} t_e^2 f_{ye} / \gamma_{M0}$$

$$n = \min(1,25 m; e)$$

where :

$$\begin{aligned} \ell_{eff,M1,//} &= \min(\ell_{eff,nc,//}; \ell_{eff,cp,//}) \\ &= \min(\ell_{eff8}; \ell_{eff9}; \ell_{eff10}) \end{aligned} \quad (3-11)$$

$$\begin{aligned} \ell_{eff,M2,//} &= \min(\ell_{eff,nc,//}) \\ &= \min(\ell_{eff8}; \ell_{eff9}) \end{aligned} \quad (3-12)$$

Finally, the design resistance of the stiffened extended part of the end-plate is defined as :

$$F_{Rd} = \min(F_{Rd,1,\perp}; F_{Rd,2,\perp}; F_{Rd,1,//}; F_{Rd,2,//}; F_{Rd,3}) \quad (3-13)$$

Stiffness

A similar distinction has to be made for stiffness calculation. By referring to Appendix 3 and to the previous paragraphs, the following expression of the stiffness coefficient may be derived in the case where the extended part of the end-plate is stiffened :

$$k_{ip} = \min(k_{ip,\perp}; k_{ip,//}) \quad (3-14)$$

with :

$$k_{ip,\perp} = \frac{0,85l_{eff,\perp}t_e^3}{m_x^3} \quad (3-15)$$

$$k_{ip,\perp} = \frac{0,85l_{eff,//}t_e^3}{m^3} \quad (3-16)$$

where :

$$\ell_{eff,\perp} = \ell_{eff,M1,\perp} \quad (3-17)$$

$$\ell_{eff,//} = \ell_{eff,M1,//} \quad (3-18)$$

Deformation capacity

The deformation capacity of the extended part of the end-plate decreases with the welding of the stiffener while the resistance is increasing. As explained in Section 3.2.3, this is likely to limit the possible redistribution of internal forces within the joint or within the frame. The criteria to check the sufficient deformation capacity, which are similar for plates with or without stiffeners, are described and justified in Appendix 3.

3.2.1.3 Intermediate stiffeners

The stiffening and strengthening of a column flange in bending may be achieved by adding transverse stiffeners in line with the beam flanges. They may be used to improve the properties of the column flange in bending, but also those of the column web in tension or compression. Such so-called intermediate stiffeners are welded there where additional resistance is required at the level of a specific bolt-row, as shown in Figure 3-9. Possibilities exist also to place them on the beam side so as to stiffen and strengthen the end-plate.

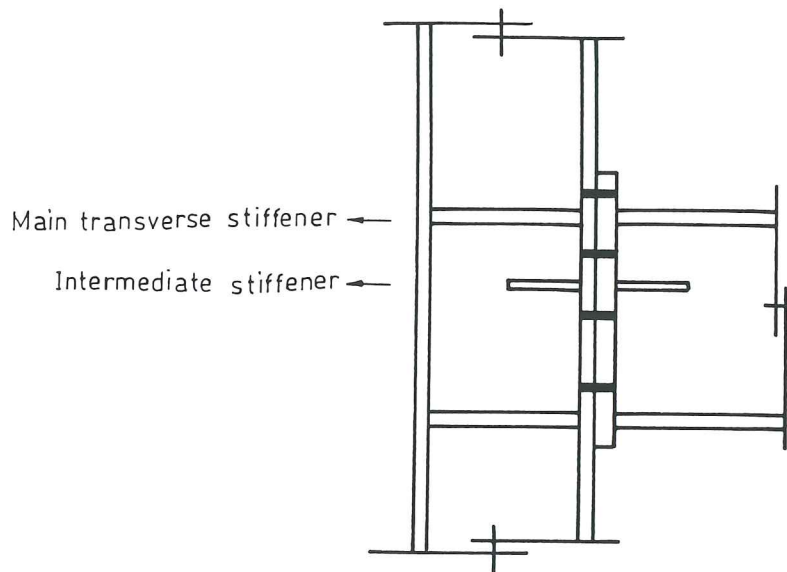


Figure 3-9 Intermediate stiffeners on beam and column sides

Resistance

The concept of the T-stub idealization may again be referred to in this particular situation and this again requires the definition of appropriate effective lengths for the column flange or the end-plate in bending at the level of the bolt-row being considered.

Eurocode 3 Annex J provides the designer with adequate rules for effective lengths as long as two successive stiffeners - usual and/or intermediate ones - are separated by two bolt-rows at least.

When it is not the case, as in Figure 3-10, the effective length may be derived as indicated in Figure 3-11.

The expression appears simply as an extension of the cases covered by Eurocode 3 Annex J.

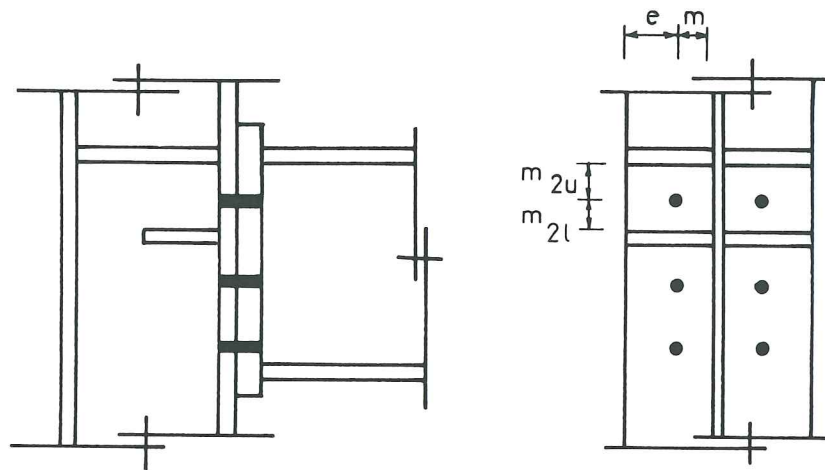


Figure 3-10 Single bolt-row between two stiffeners

$$l_{\text{eff}} = (\alpha_u + \alpha_\ell)m - (4m + 1,25e)$$

where α_u and α_ℓ are evaluated from

Eurocode 3 Annex J on the basis

of m_{2u} and $m_{2\ell}$ respectively.

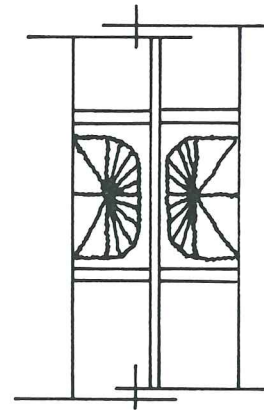


Figure 3-11 Effective length for a single bolt-row located between two stiffeners

Stiffness and deformation capacity

The evaluation of these characteristics is achieved as explained in Appendix 3 for usual plated components. No specific considerations are needed.

3.2.1.4 Haunches

Industrial buildings constituted of portal frames with rather large beam spans are quite common. These buildings represent a significant part of the activity in the field of steel construction.

The large spans lead to rather high bending moments at the supports, there where joints are, and often require a local increase of the beam depth so as to provide a higher inertia to the beam, but also to increase the level arm of the internal forces in the joints.

Two different ways are usually followed to achieve this goal, without increasing the beam depth all along the beam member, what would result in an unjustified and significant increase of the total weight of the structure :

- use of tapered built-up members (Figure 3-12.a);
- welding of haunches on hot-rolled beam profiles or built-up profiles with constant geometrical properties along their length (Figure 3-12.b).

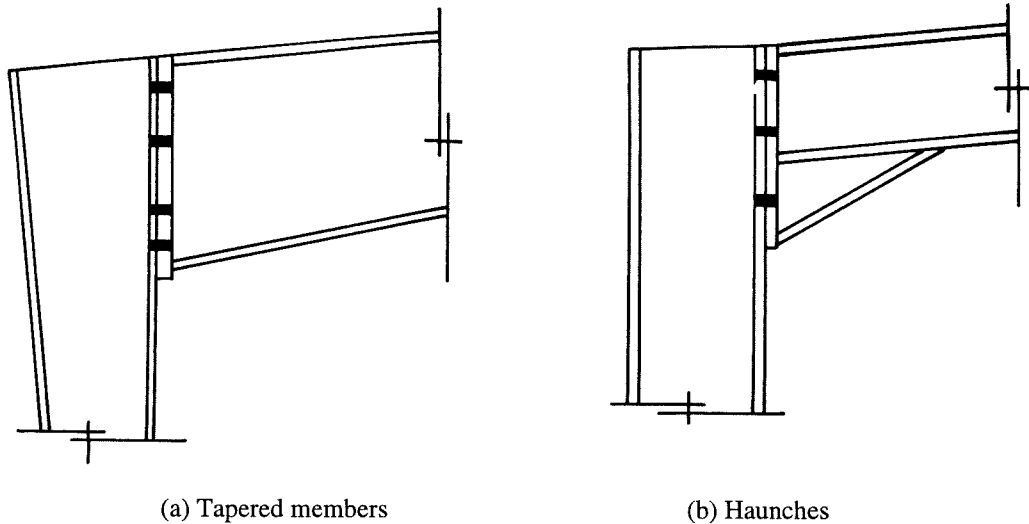


Figure 3-12 Increase of the beam geometrical properties at supports

In this section, haunches are dealt with and their influence on the design process of joints is discussed.

Two types of haunches may be distinguished :

- haunches with a flange (Figure 3-13.a);
- haunches without a flange (Figure 3-13.b).

In the first type, the haunch in itself is usually extracted from a similar profile than the beam one. For the second type, the stability in compression is ensured by the plate alone, which is therefore rather thick. The welding of such a thick plate to the beam and to the end-plate requires often more than one pass, what is expensive, and, as a consequence, this type of haunch is not commonly used in practice.

Recommendations for the design of haunches of both types are given in [Z1] and [Z4].

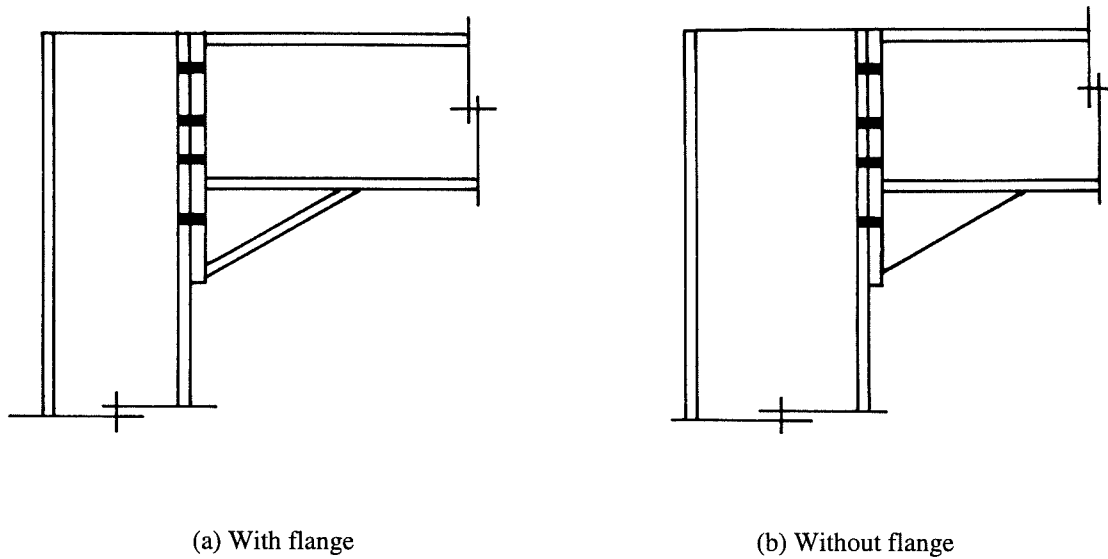


Figure 3-13 Two types of haunches

Because of their bigger practical interest, only haunches with a flange are considered here and as the rules given in [Z1] and [Z4] are no more fully in line with the new existing regulations, updates are suggested in the next paragraphs. These ones have been proposed by D. Vandegans from CRIF and ourselves and have been extensively discussed and finally agreed by the group in charge of the drafting of the ECSC Manual on "Frame Design including Joint Behaviour" in which we ensure, together with Prof. Maquoi from the University of Liège the coordination (see Chapter 6).

Geometrical and mechanical properties of the haunch

The main geometrical characteristics of the haunch are indicated in Figure 3-14.

Others are not reported. These are :

t_{wh} : thickness of the web plate;

b_{fh} : width of the flange.

The yield stress of the flange is denoted f_{yfh} .

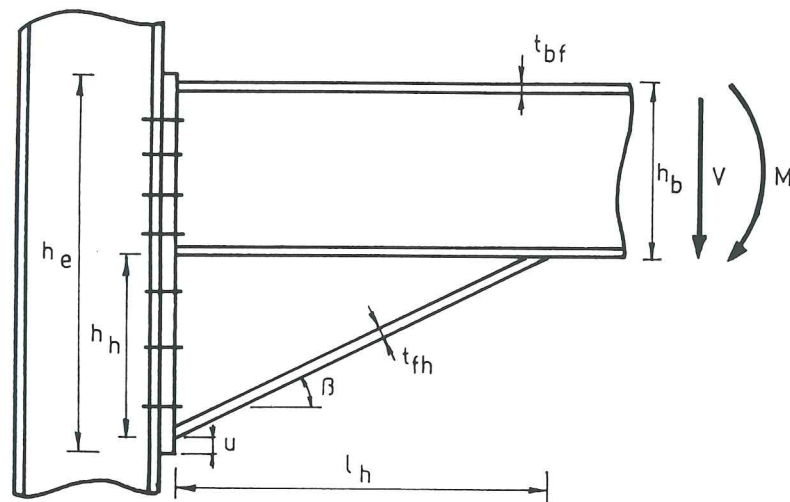


Figure 3-14 Geometrical properties

Resistance of the haunch flange

The bending moment acting on the joint distributes, as shown in 3.2.3, between the constitutive joint components; this is represented in a schematic way at Figure 3-15 where the bending moment is resolved into two statically equivalent forces F_c and F_t acting at a distance z (level arm).

As in joints without beam haunches, the compression force F_c is assumed to act at the centroid of the haunch flange.

The intensity of the F_c and F_t forces and the level arm vary with the joint detailing and the loading (bending and shear, or additional axial forces as shown in 3.2.3.3.).

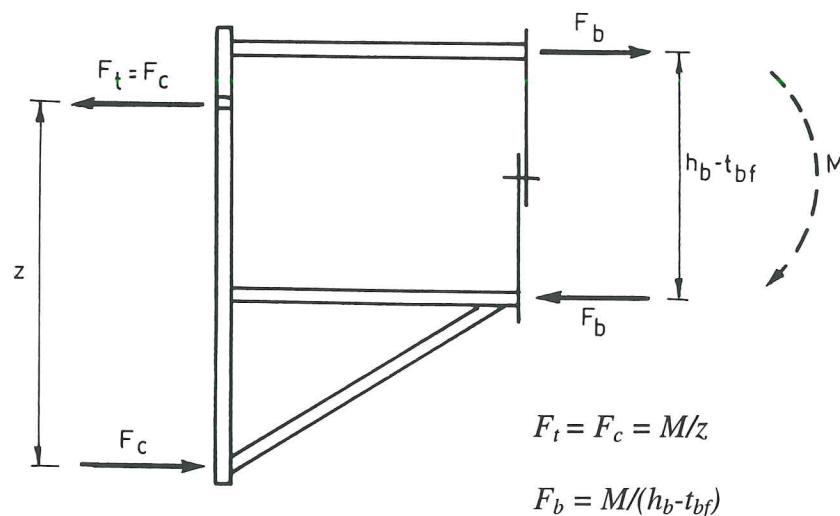


Figure 3-15 Distribution of internal forces in the connection
(Constant moment and a single bolt-row in tension)

Through the resolution of the forces acting on the haunch, the axial forces in the haunch flange and the shear forces transferred to the haunch web may be derived as shown in Figure 3-16 :

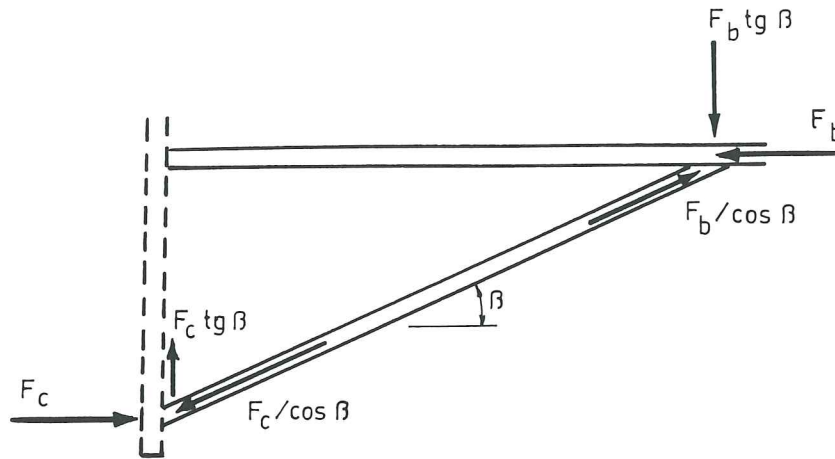
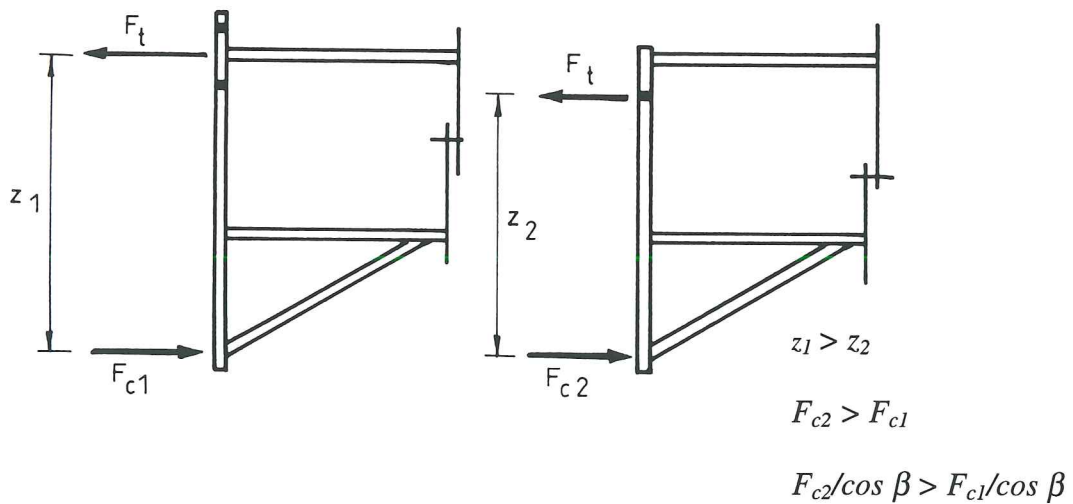
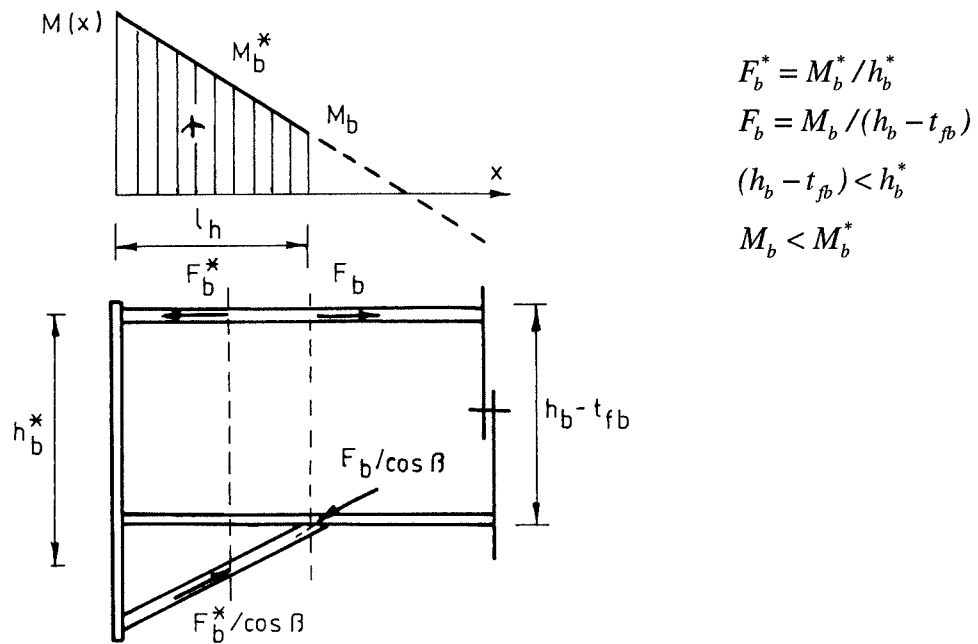


Figure 3-16 Internal forces in the haunch

The axial force in the flange is seen to vary along the haunch. Its value depends on the variation of the beam bending moment in the haunch area and on the joint detailing as explained in Figure 3-17.



(a) Variation with the joint detailing for a constant moment



(b) Variation with the beam bending moment

Figure 3-17 Evolution of the axial force in the haunch flange

The force F_c results from the distribution of internal forces in the joint and is therefore known. On the other hand, the place where the force F_b^* is maximum along the haunch is unknown as it depends on how the "level arm" and "beam bending diagram" effects compensate.

In practical cases, the higher value between $F_c / \cos \beta$ and $F_b^* / \cos \beta$ is selected and compared to the design resistance of the flange defined as :

$$F_{h.Rd} = b_h t_{fh} f_{yfh} / \gamma_{MO} \quad (3-19)$$

where b_h is the effective width of the flange defined as :

$$b_h = \min(b_{hi}; b_{fh}) \quad (3-20)$$

where b_{hi} , defined as follows :

$$b_{hi} = 42 t_{fh} \sqrt{\frac{235}{f_{yfh}}} \quad (3-21)$$

limits, according to Eurocode 3 recommendations, the effective width of the flange because of the potential risk of plate instability.

Resistance of the haunch web

As seen in Figure 3-18, the resolution of the force F_c leads to the application of a shear force $F_c \operatorname{tg} \beta$ to the haunch web. The latter has therefore to be checked accordingly. The beam end section is also subjected to a beam shear force V as illustrated in Figure 3-18.

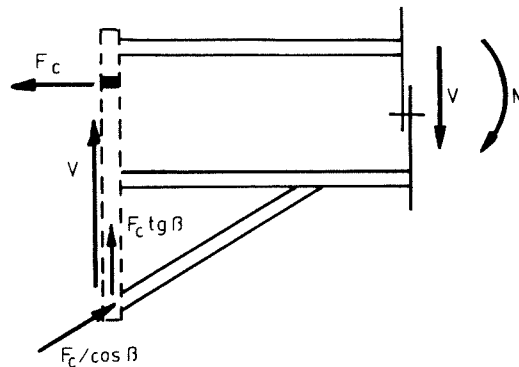


Figure 3-18 Shear forces on the beam end section

The transfer of the shear forces V and $F_c \operatorname{tg} \beta$ may be contemplated in some different ways. For instance :

- the shear force V is carried over to the end-plate by the beam web only (and the corresponding welds) and the force $F_c \operatorname{tg} \beta$ through the web of the haunch (and the corresponding welds);
- the force $F_c \operatorname{tg} \beta$ is transferred at the level of the haunch web (and welds) and V is partly transferred by the web of the beam and the web of the haunch (and the corresponding welds).

For practical applications, the first way is first selected. For high shear values, the second one may appear as more economical.

The loading of the two other sides of the triangular haunch web and of the corresponding welds connecting the web to the beam flange and the haunch flange may be simply derived from equilibrium equations.

Resistance of the column web in compression

The evaluation of the resistance of the column web in compression is performed according to Eurocode 3 Annex J :

$$F_{wc.Rd} = \rho \frac{f_{ywc} \cdot t_{wc} \cdot b_{eff} \cdot k_{wc}}{\gamma_{mo}} \quad \text{if } \bar{\lambda} \leq 0,673 \quad (3-22)$$

with : $k_{wc} = (1,25 - 0,5\sigma_{com.Ed} / f_{ywc}) \leq 1$

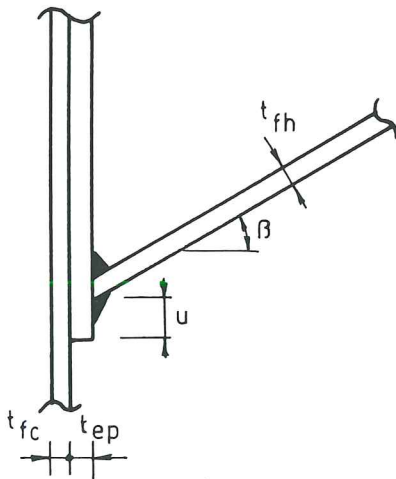
$$F_{wc.Rd} = \rho \frac{f_{ywc} \cdot t_{wc} \cdot b_{eff} \cdot k_{wc}}{\gamma_{mo}} \left[\frac{1}{\bar{\lambda}} \left(1 - \frac{0,22}{\bar{\lambda}} \right) \right] \quad \text{if } \bar{\lambda} > 0,673 \quad (3-23)$$

with : $\bar{\lambda} = 0,93 \sqrt{\frac{b_{eff} d_c f_{ywc}}{E \cdot t_{wc}^2}}$ (3-24)

d_c is the clear depth of the column web and f_{ywc} , the yield stress of the column web.

ρ takes into consideration the possible decrease of the resistance because of high shear stresses in the column web panel. k_{wc} is a reduction factor depending on the value of the longitudinal stresses $\sigma_{com.Ed}$ in the column web.

The effective width b_{eff} results from the diffusion of the compressive force through the end-plate as well as through the flange and the radius of fillet (or the weld) of the column cross-section. It may be expressed as indicated in Figure 3-19 where a_{hc} is the throat thickness of the weld connecting the haunch flange to the end-plate and s is respectively defined as r_c - radius of fillet of the column - in the case of a hot-rolled column profile and $\sqrt{2}a_c$ in the case of a built-up column profile (a_c is the throat thickness of the weld connecting the flanges to the web).

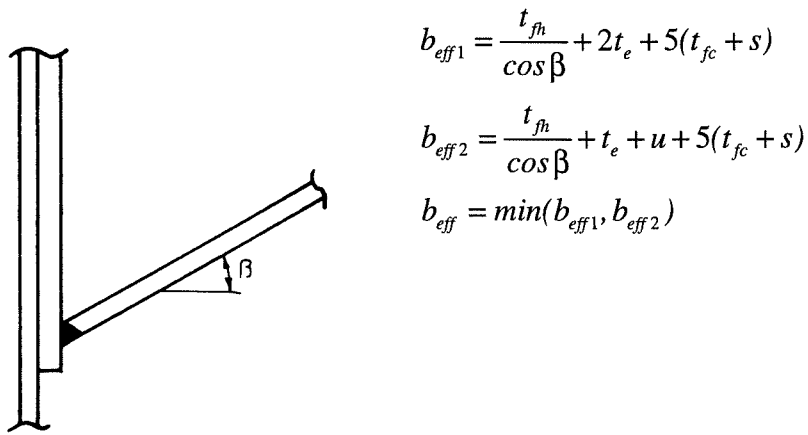


$$b_{eff1} = \frac{t_{fh}}{\cos \beta} + 2\sqrt{2}a_{hc} + 2t_e + 5(t_{fc} + s)$$

$$b_{eff2} = \frac{t_{fh}}{\cos \beta} + \sqrt{2}a_{hc} + t_e + u + 5(t_{fc} + s)$$

$$b_{eff} = \min(b_{eff1}, b_{eff2})$$

(a) Fillet welds



(b) Butt welds

Figure 3-19 Effective width for the column web in compression**Resistance of the beam web in transverse compression**

In Figure 3-16, the beam web is seen to be subjected to a compressive transverse force $F_b \tan \beta$. As for the column web in compression, this force may lead to crushing, crippling or buckling of the beam web.

Traditionally, a web stiffener is welded there so as to avoid any failure, but in most of the cases, this one is not strictly necessary and a substantial economy in fabrication costs may be achieved by simply checking the sufficient resistance of the beam web in compression.

This verification may be performed with similar formulae than those presented in the previous paragraph dealing with column web in compression. No reduction of the resistance because of interactions with high shear stresses has therefore to be usually considered ($\rho = 1,0$).

From a more conceptual point of view, troubles may be avoided in this component by limiting the value of the haunch inclination β . A value of 30° is quite usual and a value of 45° should never be exceeded.

Stiffness

As explained in Section 3.2.3, components such as beam web in compression and haunch web and flange are not contributing to the joint deformability and related stiffness coefficients have not to be evaluated.

For the column web in compression, reference has obviously to be made to Eurocode 3 Annex J recommendations.

Deformation capacity

The deformation capacity of haunch flanges and webs and of beam webs in compression has never been deeply investigated. It has to be said that it is usually considered as good practice to concentrate the failure of the joint in the bolted connection in itself or in the column web panel, but not in the haunch. In such conditions, no specific deformation is obviously required from the haunch components.

We personally agree with this concept which allows to better control the response of the joint, its failure mode and its global ductility.

3.2.1.5 Non-perpendicularly connected elements

General

In building structures, the structural steel frame is usually made of beam and column elements connected perpendicularly so as to constitute what we could call here rectangular frames, such as office buildings.

Most of the experimental, numerical and theoretical research works carried out in the field of structural joints relate to this type of structural configuration and Eurocode 3 Annex J, which appears as the outcome of these research works, is not an exception even if nothing is explicitly said about that.

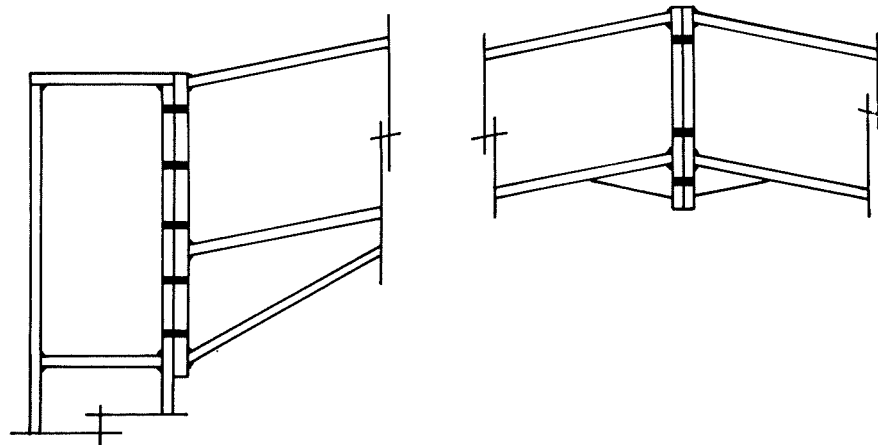
Pitched-roof industrial portal frames where the structural elements are not perpendicularly connected (Figure 3-20) represent however a quite important part of the steel construction activity where high profit of the new concepts introduced in Eurocode 3, and in particular in its Annex J, could be made.

We therefore decided to investigate this topic. In the next paragraphs the slight modifications to be made to the Eurocode 3 rules for joint characterization are presented. We will also come back to the pitched-roof portal frames in Chapters 4 and 5 respectively when the idealization and the classification of « non-rectangular » joints will be discussed.

For what regards joint characterization, three main aspects have to be considered :

- the external loading on the joint;
- the distribution of internal forces in the joint;
- the properties of the constitutive components.

They are successively introduced here below in the case of a beam-to-column joint with an end-plate connection; conclusions drawn are however valid whatever is the joint configuration and connection type (beam splice, haunched beam, ...).



(a) Beam-to-column joint

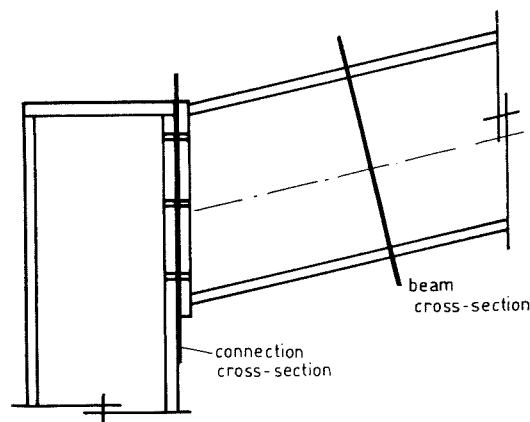
(b) Beam splice

Figure 3-20 Typical joints in a pitched-roof portal frame**Loading**

In rectangular frames, beam-to-column joints and beam splices are mainly subjected to in-plane bending moments and shear forces. Axial forces in the beam remain rather low and are usually disregarded. To know whether it is justified or not to act in such a way is a question which will be raised in Section 3.2.3.3.

In pitched-roof portal frames, the inclination of the rafters induce higher axial forces and a specific attention has, in all the cases, to be paid to their influence on the joint rotational response.

Another aspect is the non-perpendicularity between the beam cross-sections and the connection cross-section, as indicated in Figure 3-21, what is again due to the inclination of the rafters.

**Figure 3-21** Beam and connection cross-sections

As a result, the internal forces M_r , V_r and N_r acting at the rafter extremity and obtained through a frame analysis have to be transformed into a bending moment M , a shear force V and an axial force N acting on the connection cross-section, as shown in Figure 3-22.

These forces are derived as follows :

$$M = M_r \quad (3-25.a)$$

$$V = V_r \cos \alpha + N_r \sin \alpha \quad (3-25.b)$$

$$N = N_r \cos \alpha - V_r \sin \alpha \quad (3-25.c)$$

M , N and V are expressed at the level of the rafter neutral axis.

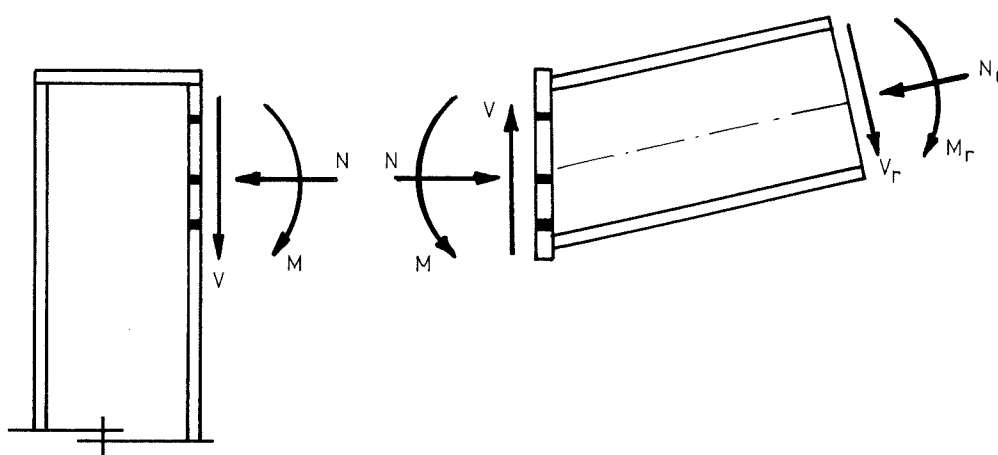


Figure 3-22 External forces acting on the connection

Distribution of internal forces

The distribution of the external forces M , N and V into internal forces within the joint components relates to what is defined in Chapter 2 as the step number three « joint assembly » of the component method. The assembly procedures are discussed in Section 3.2.3 of the present chapter : the general principles are first introduced; the Eurocode 3 procedures for the evaluation of the stiffness and resistance properties of joints in bending and/or shear is then described and, finally, an original assembly procedure for joints subjected to axial forces in addition to bending moments and shear forces is proposed.

All the principles and procedures reported in Section 3.2.3 applies to « rectangular » joints as well as to « non-rectangular » ones.

Component properties

In this paragraph, the capacity of rules included in the Eurocode 3 Annex J for the characterization of the mechanical properties of the basic individual components is contemplated.

In order not to make the text unnecessarily heavy, we consider that it is not worth our while repeating large parts of Eurocode 3 Annex J here; in fact, we prefer to focus on the modifications to be brought to the available rules in the cases where the structural elements are not perpendicularly connected.

Through a quick examination of the components, it appears clearly that :

- some components are affected by the rafter inclination;
- some components are not affected at all;
- some components can no more be used as soon as the rafters are inclined.

In Table 3-1, the component available in Eurocode 3 Annex J are classified according to these three categories. The flange of a haunch being inclined by nature, no additional information to that given in Section 3.2.1.4 is required here.

The influence of the rafter inclination is so restricted to five components. Let us discuss each of them successively.

Column web in compression

From the distribution of internal forces in the joint, the resultant compressive force in the column web is deduced. It is assumed, according to Annex J of Eurocode 3, to diffuse through the end-plate, if any, and then through the column flange and the radius of fillet or the weld. The diffusion width, $b_{eff,c,wc}$, which is evaluated as indicated in Figure 3-23.a, is the key value in the determination of the stiffness and resistance properties of the column web in compression.

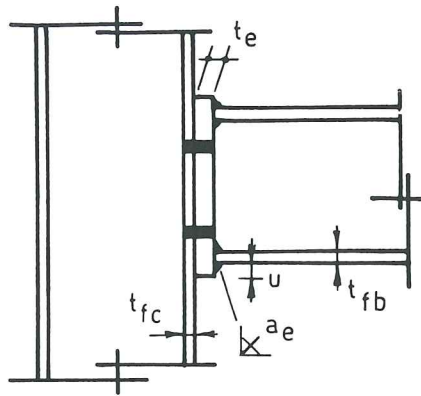
N°	Components	Affected	Not affected	No more available
1	Column web panel in shear		×	
2	Column web in compression	×		
3	Beam flange and web in compression	×		
4	Column flange in bending	×*		
5	Column web in tension	×*		
6	End-plate in bending	×		
7	Beam web in tension		×	
8	Flange cleat in bending			×
9	Bolts in tension		×	
10	Bolts in shear		×	
11	Bolts in bearing			×
12	Plate in tension or compression			×

* For welded connections only

Table 3-1 Influence of rafter inclination on the component properties

A small amendment ($t_{fb} \rightarrow t_{fb} / \cos \alpha$) is simply carried out, as shown in Figure 3-23.b, so as to take into consideration the increase of the diffusion width through the flange of the rafter.

No further change has to be contemplated.

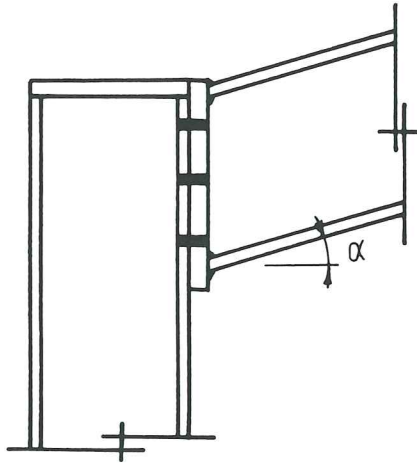


$$b_{eff} = t_{fb} + t_e + \sqrt{2}a_e + 5(t_{fc} + r_c) + s_e$$

with : r_c = column radius of fillet

$$s_e = \min(t_e + \sqrt{2}a_e; u)$$

(a) Joint in a rectangular frame



$$b_{eff,c,wc} = \frac{t_{fb}}{\cos \alpha} + t_e + \sqrt{2}a_e + 5(t_{fc} + r_c) + s_e$$

(b) Joint in a pitched-roof portal frame

Figure 3-23 Evaluation of the effective width
(bolted end-plate connection and hot-rolled column cross-section)

Beam flange and web in compression

As for haunch flanges, the compressive force resulting from the distribution of internal forces within the joints has to be resolved, as shown in Figure 3-24, in order to determine the force applied to the beam flange and web in compression ($F_c / \cos \alpha$). The design resistance in itself remains unchanged in comparison to what has been said in Section 3.2.1.1. Formulae (3-1) and (3-2) therefore still applies.

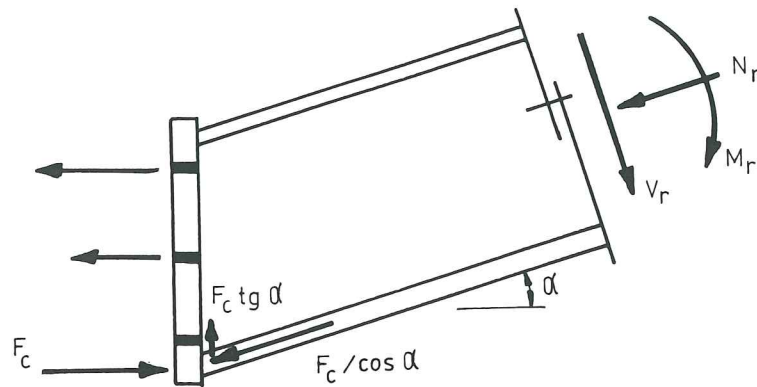


Figure 3-24 Force applied to the beam flange and web in compression

Column flange in bending

In welded beam-to-column joints where the column flanges are unstiffened in the tensile zone, non-uniform stress distribution develops in the beam flanges in tension (Figure 3-25). There where high stresses are reported, i.e. at mid-width of the flange, the brittle failure in the connecting welds in tension has to be avoided.

This is achieved in Eurocode 3 through the definition of an effective width for the beam flange in tension (see Figure 3-25) :

$$b_{eff,fc} = t_{wc} + 2s_c + 7k t_{fc} \quad (3-26)$$

where : t_{wc} = is the thickness of the column web;

$$k = (t_{fc} / t_{fb}) (f_{yfc} / f_{yfb}) \text{ but } k \leq 1$$

f_{yfc} is the yield stress of the column flange

f_{yfb} is the yield stress of the beam flange

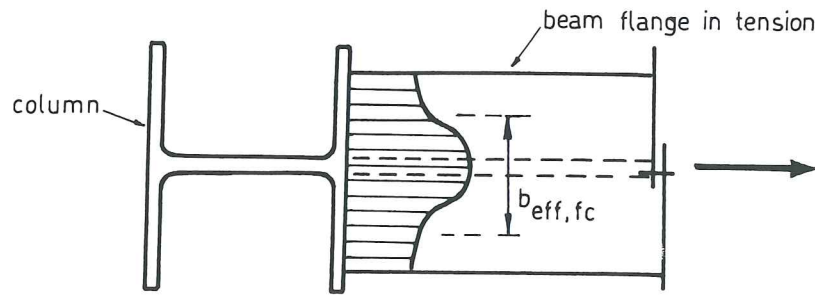


Figure 3-25 Non uniform distribution of stresses in a beam flange in tension

Based on this value, the design resistance of the column flange is derived as :

$$F_{fc,Rd} = b_{eff,fc} t_{fb} f_{y,fb} / \gamma_{M0} \quad (3-27)$$

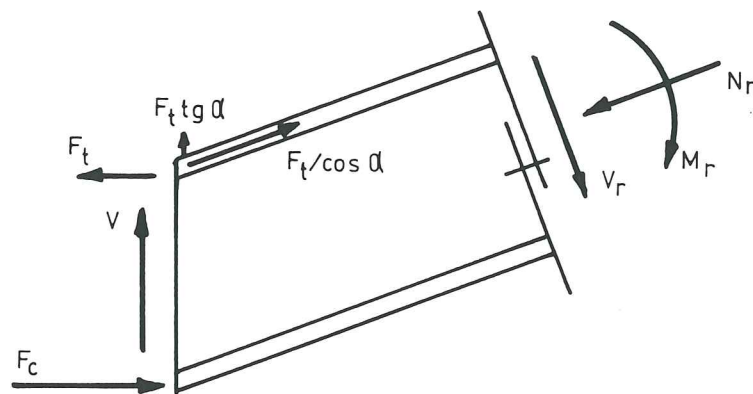


Figure 3-26 Force applied to the beam flange in tension (welded connections)

Formula (3-27) applies as long as $b_{eff,fc}$ is higher than 0,7 times the width of the beam flange in tension. When this condition is not fulfilled, the maximum stress in the weld is too high and this can lead to a brittle failure. In this case, it is so recommended to weld transverse stiffeners on the column web and flanges in the prolongation of the beam web. This makes the distribution of stresses in the beam flange uniform and avoids stress concentrations.

The extension of the formula to beam-to-column welded joints belonging to pitched-roof portal frames requires two modifications :

- The value $t_{fb}/\cos\alpha$ is substituted to t_{fb} in formulae (3-26) and (3-27);
- The tensile force to which $F_{fc,Rd}$ is compared is $F_t/\cos\alpha$ (see Figure 3-26).

In the case of joints with bolted connections, the tensile force is applied to the column by bolts in tension; no amendment to the formula expressing the design resistance of the column flange in bending has therefore to be contemplated.

Column web in tension

As for column webs in compression, the key parameter for the evaluation of the stiffness and resistance properties of column webs in tension is the effective width $b_{eff,t,wc}$. In the case of bolted connections, $b_{eff,t,wc}$ is taken as equal to the effective length (see Appendix 3) of the column flange in bending. The response of the latter being not affected by the inclination of the rafters, no modification has to be brought to $b_{eff,t,wc}$ in comparison to what is explained in Annex J.

In welded connections, the value of $b_{eff,t,wc}$ is evaluated in a similar way than what is described in Figure 3-23 for the compressive zone. Only the diffusion of the tensile force in the beam flange is therefore affected ($t_{fb}/\cos\alpha$ instead of t_{fb}).

End-plate

When evaluating the effective length of the equivalent T-stubs (see Appendix 3), $t_{fb}/\cos\alpha$ has again to be substituted to t_{fb} . This is the only slight modification to be taken into consideration because of the inclination of the rafters.

3.2.1.6 Slender column web panels

Context

The yielding of unstiffened column web panels in shear is a common type of failure in single-sided joint configurations with welded or end-plate connections or in double-sided joint configurations, with similar connections, subjected to unbalanced loading.

Recommendations for the calculation of column web panels in shear have therefore been included in the first version of Eurocode 3 Annex J and these ones have been kept in the revised Annex J, but with some amendments reflecting results of more recent researches that we had been carried out in the meantime (see [J1] and [J2]).

In the next paragraphs, we will first describe briefly the actual recommendations included in revised Annex J, as well as their field of application.

In a second step, we will reflect recent research works aimed at extending the Eurocode 3 rules to slender web panels - not presently covered by Annex J - and we will present some results relative to an original model for slender stiffened panels which is now in development at the Department MSM of the University of Liège.

The development of this model started last year in the frame of the diploma work of F. Cerfontaine who is now assistant at the Department MSM. These works proceed under our guidance. A collaboration with the Commercial Intertech (Astron) company in Diekirch has also been set-up; it results from the particular interest of ASTRON for

industrial portal frames made of rather slender built-up profiles where shear of the column web panel is a predominant criterion for joint design.

In order to allow F. Cerfontaine to possibly valorize the results of his work in a forthcoming Ph.D. Thesis, we will deliberately restrict the contents of the present section to generalities allowing the reader to understand the way followed in the research, the results already available and the perspective for further developments.

For detailed information, it is recommended to refer to [C4] or preferably to a forthcoming research report now in preparation in Liège.

Recommendations of Eurocode 3 Annex J

As for all the other individual components, three different aspects are covered as far as column web panels in shear are concerned : stiffness, resistance and deformation capacity.

Resistance

It has been demonstrated in the past, through different approaches - numerical and experimental - , that the distribution of shear forces in column web panels is rather uniform as long as no shear buckling occurs. Based on this, the resistance formula included in Annex J is strictly limited to non-slender panels and writes :

$$V_{n,Rd} = \frac{0,9A_{vc}f_{ywc}}{\sqrt{3}\gamma_{M0}} \quad (3-28)$$

where : A_{vc} is the shear area of the column cross-section;

f_{ywc} is the yield stress of the column web.

Non-slender columns means that the slenderness ratio d_c/t_{wc} is limited to :

$$\frac{d_c}{t_{wc}} \leq 69\varepsilon \quad (3-29)$$

where : $\varepsilon = \sqrt{235/f_{ywc}}$ (f_{ywc} expressed in Mpa)

d_c is the clear depth of the column web

Formula (3-28) is seen to limit the stress τ in the shear area to $0,9f_{ywc}/\sqrt{3}$ and not to $f_{ywc}/\sqrt{3}$ as stated in the other codes or reference books. But we have shown in [J1] and [J2] that longitudinal stresses σ_n in the column were reducing the shear resistance of the column web panels from about 5 to 12 % according to the level of the longitudinal stresses. The reduction factor 0,9 has been selected as a constant value in Eurocode so as

to avoid, by taking explicitly the σ_n - τ interaction into consideration, an iterative evaluation procedure of the shear resistance.

In the case of transversally stiffened panels (Figure 3-27), an additional shear resistance is provided by the frame constituted by the column flanges and the transverse stiffeners.

According to [J1], Eurocode 3 Annex recommends to evaluate the shear resistance of a transversally stiffened panel as follows :

$$V_{n,Rd} = \frac{0,9A_{vc}f_{ywc}}{\sqrt{3}\gamma_{M0}} + \frac{4M_{pl,fc,Rd}}{d_s} \quad (3-30)$$

where : d_s is the distance between the centrelines of the stiffeners;

$M_{pl,fc,Rd}$ is the design plastic moment resistance of the column flange.

When diagonal web stiffeners are used to increase the shear resistance of a column web, they should be designed to resist the forces to which they are subjected.

For design purposes, the design shear resistance of the panel is compared to the applied shear force V_n which may be expressed, through equilibrium equations, as a function of the bending moments and shear forces acting on the panel (see formulae (1.1) and (1.2) given in Chapter 1).

Stiffness

The contribution of the individual basic components to the rotational deformability of a joint is expressed in Annex J through the definition of so-called stiffness coefficients. That relative to unstiffened column web panels in shear writes as follows :

$$k_{i,swc} = \frac{0,38A_{vc}}{\beta z}$$

where : z is the level arm of internal forces derived as explained later in Section 3.2.3.2

β is the transformation factor introduced in Chapter 1 (Section 1.3.4).

No significant effect of the transverse stiffeners on the elastic stiffness of the column web panels is assumed, as demonstrated in [J1].

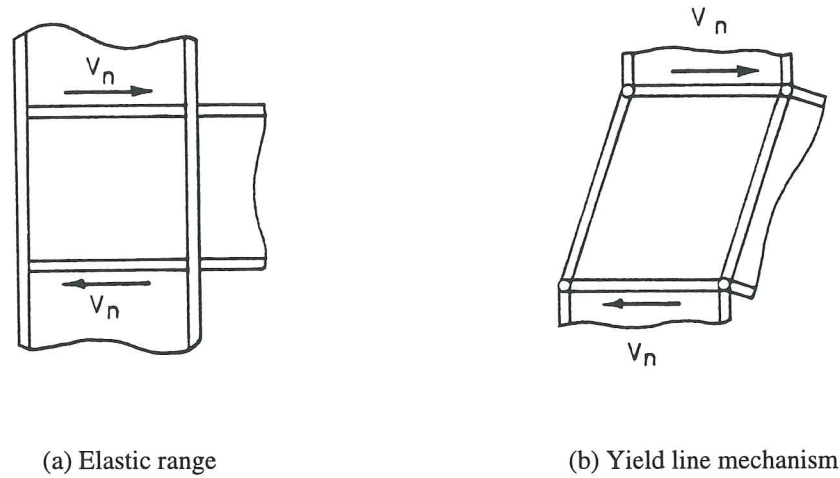


Figure 3-27 Frame effect

Deformation capacity

Web panel in shear possess an important deformation capacity, quite large enough to allow full redistribution of internal forces in the structural frame.

This fact is recognized by Annex J.

Design approaches for slender panels

Existing material

When the slenderness ratio of the column web panel exceeds a limit, the value of which is taken as equal to 69ϵ (see Formula (3-29), buckling occurs for a shear critical resistance termed V_{cr} . Beyond this value, the uniform distribution of shear stresses (Figure 3-28.b) is replaced by a non-uniform one (Figure 3-28.c) where a well-known diagonal tension field develops. Finally, failure under ultimate shear forces is preceded by the apparition of a yield line mechanism where hinges form in the surrounding column flanges and stiffeners which are usually present because of the significant risk of premature failure by column web buckling in compression (load-introduction effect).

This idealization of the panel response which consists in isolating three contributions and summing them up to derive the ultimate resistance of the panel has been first applied to beam in bending and shear - let us remember the well-known Cardiff model [E5] - before being applied years later to column web panels in shear by Pasternak [V2] and others [S3, S4] in Braunschweig.

$$\text{So :} \quad V_{n,Ru} = V_{cr} + V_{tf} + V_m \quad (3-31)$$

where : V_{cr} is the critical shear resistance of the panel;

- V_{if} is the shear resistance associated to the diagonal tension field;
- V_m is the shear resistance associated to the yield line mechanism in the surrounding plates.

Analytical expressions are provided by Pasternak for each of these three contributions to the ultimate shear resistance. For design purposes, it could probably be considered that only the two first contributions have to be taken into consideration. From comparisons with experimental test results [C4], the reasonable accuracy of the model may be shown.

No indication is provided on how to derive the shear stiffness of the panel in the elastic range as well as in the non-elastic one.

In [C4], Cerfontaine tries to bring justification to the model, the background of which seems not yet fully available. He also discusses the assumptions on which the model is based as well as the inconsistencies on which the application of the model is leading. The outcome of this work is summarized here below where criticisms are sometimes addressed to the Pasternak's model; but more often, interrogations resulting from the lack of background information are raised.

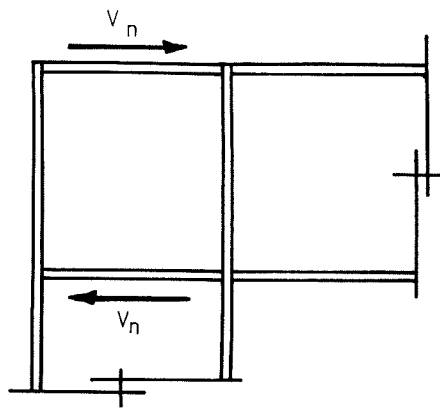
Pasternak's model

- In the Pasternak's model, the critical shear resistance is assessed by assuming that the web is simply supported on the surrounding plates (flanges and stiffeners). This is a safe assumption which is not confirmed by experiments and by numerical simulations of the whole panel response as demonstrated by Taquet in [T1]. The rotational restraint provided by the surrounding plates depends on their dimensions and on their own support conditions.
- The effective width of the tension field is known to be highly dependent on the flexural stiffness of the surrounding plates along the web edges. In the Pasternak's model, the tension field extends over more than half-a-panel and the width g of the tension field is seen to be independent on the connexion type, welded or bolted (see Figure 3-29).

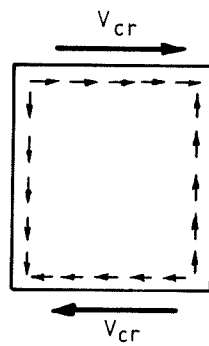
These assumptions appear as quite questionable.

In [T1], Taquet shows, by means of numerical simulations, that the zone of high tensile stresses is much narrow than that selected by Pasternak. On the other hand, in some bolted connections, the level of connection between the end-plate and the column flange is limited to the zones located close to the beam flanges (Figure 3-29.b). The flexural stiffness of the column flange between the two internal bolt-rows is rather limited, and certainly lower than what it is in a welded connection where the column flange is stiffened by the beam web to which it is welded (Figure 3-29.a).

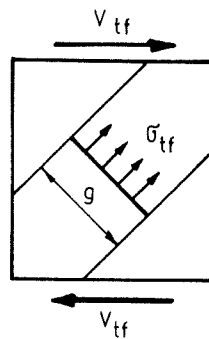
In other words, the quite different support conditions of the column web panel in welded and bolted connections respectively leads to consider different anchorages for the tension field and therefore different effective widths.



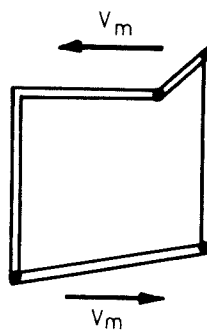
(a) Beam-to-column joint



(b) Critical contribution



(c) Tension field contribution



(d) Yield mechanism contribution

Figure 3-28 Contribution to the shear resistance of slender column web panels

- Similar conclusions apply also to the location of the plastic hinges in the yield line mechanism associated to the shear resistance V_m (Figure 3-30 shows one of the two mechanisms suggested by Pasternak, that leading to the lower resistance being selected). Some kinematic incompatibilities as that highlighted in Figure 3-30.b - there where the additional triangular stiffener is welded to the upper web transverse stiffener - are also likely to occur as long as the actual distribution of stiffness all around the panel is disregarded.

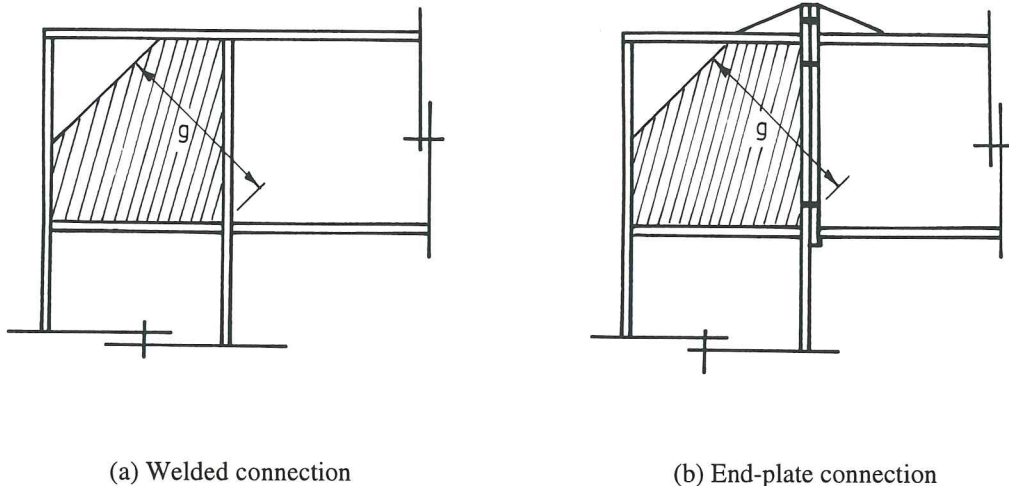


Figure 3-29 Typical tension field according to Pasternak

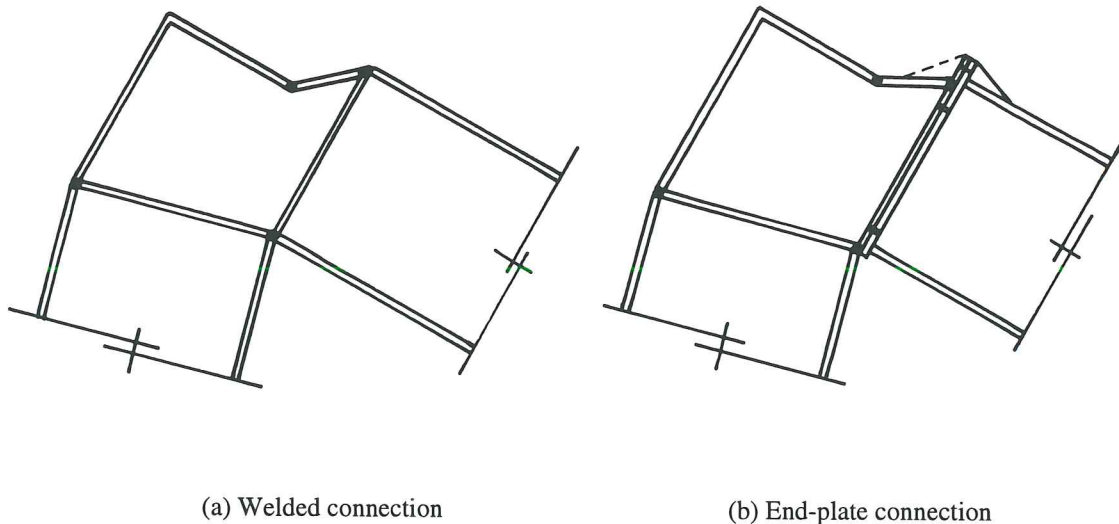


Figure 3-30 Yield line mechanism according to Pasternak

- The only apparent way to re-derive the expression of the shear resistance V_{tf} proposed by Pasternak, and to respect at the same time all the equilibrium equations of the panel, is to assume that the resultant of the forces in the tension field acts along the

diagonal of the panel, what seems in contradiction with Figure 3-29 where the tension field is not centred on the diagonal.

- The reduced slenderness $\bar{\lambda}_\omega$ of the column web panel is defined as $\sqrt{f_{ywc}/(\sqrt{3}\tau_{cr})}$ where τ_{cr} is the elastic critical shear stress.

Figure 3-31 illustrates the evaluation of the design resistance $V_{n,Rd}$ proposed by Pasternak ($V_{cr} + V_{tf}$) versus the reduced slenderness of the web. The variation of $\bar{\lambda}_\omega$ is obtained through the modification of one of the dimensions of the panel. For low values of $\bar{\lambda}_\omega$, $V_{n,Rd}$ is equal to the plastic shear resistance of the panel defined as equal to $A_{vc}f_{ywc}/(\sqrt{3}\gamma_{M0})$ by Pasternak. For progressively increasing values of $\bar{\lambda}_\omega$, an increase of the shear resistance is first obtained before a more logical behaviour occurs, characterized by a decrease of $V_{n,Rd}$ with increasing values of $\bar{\lambda}_\omega$.

The model of Pasternak is therefore seen to present imperfections, and some of them appear as quite unacceptable as, for instance, the respect or not, according to the circumstances, of the basic assumptions on which the model is initially based, when deriving the resistance evaluation formulae.

Present developments in Liège

On the basis of this preliminary work and of the conclusions drawn, the criteria that a "good model" for slender web panel would have to satisfy have been listed :

- Better reflect the relative importance of the critical and tension field contributions to the shear resistance;
- Use a consistent set of assumptions throughout the whole development process of the model;
- To be in accordance with present Annex J rules when the slenderness ratio of the panel decreases beyond 69 ε.
- To differentiate the behaviour of web panels being part of joints with welded and bolted joints respectively.

This work has started and first proposals for amendments have already been brought. In particular, Cerfontaine has suggested in [C4] an original procedure to take into consideration the restraints at the web edges as well as a new definition of the tension field width and yield mechanisms to be considered in the case of bolted and welded joints respectively.

A preliminary stiffness model has also been established. All these developments should go on in the next months; experimental tests are planned, in collaboration with Commercial Intertech and it is thought that numerical finite element simulations should help in deriving reliable models based on a deep understanding of the web panel response in terms of stiffness and resistance.

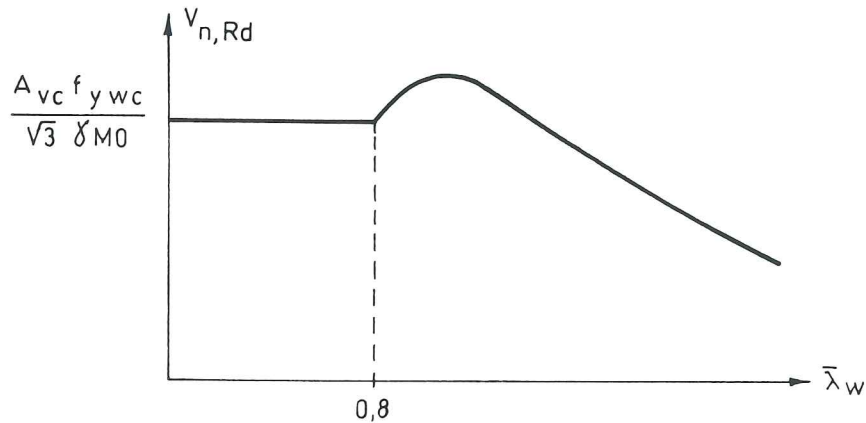


Figure 3-31 Variation of $V_{n,Rd}$ with $\bar{\lambda}_w$

3.2.2 Interaction between components

3.2.2.1 Generalities

It is well-known that the joint behaviour has a major influence on the frame response. On the opposite side, it is much less known that the interaction between the forces acting in the connected members influences, generally in a negative way, the joint design resistance.

The elastic stiffness of the components is obviously not influenced by such stress interactions. The components which are likely to be influenced are the column web panel in compression, the column web panel in tension, the column web panel in shear and the column flange in bending.

In the old Annex J, some limited interactions in the column flange in bending were taken into consideration through appropriate reduction factors. These ones have been kept when drafting the new revised Annex J, without any further investigations.

During this revision, and on the basis of the theoretical and numerical studies performed in Liège and reported in our Ph.D. Thesis [J1], new reduction factors have been introduced so as to avoid the unconservative character of some of the old formulae.

At present, revised Annex J includes therefore some different reduction factors which can be classified in two categories :

- those which were already included in the old Annex J, the background of which is quite limited (these coefficients have been kept in the revised Annex J because no other work confirming the validity or recommending to modify them or to cancel them was available);

- those which have been included in revised Annex J on the basis of the theoretical and numerical works reported in [J1].

This situation led us quickly to the conclusion that experimentation was needed in order to check the validity of the reduction factors against test results and possibly improve their expression or field of application. This has been made possible through the European COST C1 project funded by the Walloon Region of Belgium.

In this chapter, the different reduction factors are first introduced. The main conclusions that can be drawn from the comparisons with the recent numerical simulations and experimental tests are then described.

3.2.2.2 Physical descriptions of the interactions

Interactions in the column web panel

In a strong axis joint between H or I sections, the failure of the column web panel can result from two different modes: shear yielding or local yielding under the tensile or compressive forces carried over from the beam to the column by the connection (also called *load-introduction*). For slender webs, a third mode (web buckling or crippling) can also be observed in the compressive zone.

For a given joint, the failure mode of the web panel depends on its external loading; this is illustrated in Figure 3-32.a where the ratio η between the left and right loads, P_l and P_r , varies from 0 to 1. Figure 3-32 corresponds to a joint where the column web has a low slenderness and is therefore not affected by buckling.

The ratio η is the one between the two bending moments in the beams on each side of the column. When it is close to *zero*, the web panel is subjected to high shear forces what leads usually to a shear failure. A ratio close to *one* means that the joint is symmetrically loaded; in this case, the collapse can only result from load-introduction yielding (web buckling or crippling is also possible for more slender webs)

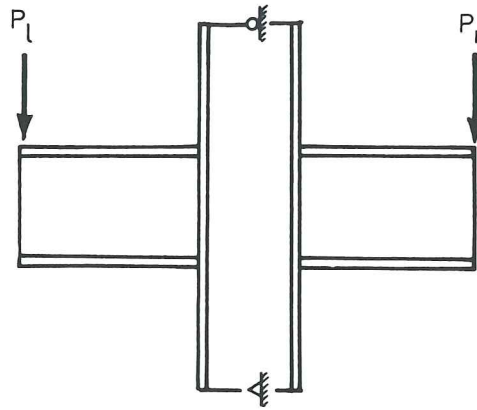
In the column web panel, three kinds of stresses are acting together :

- shear stresses τ ,
- longitudinal stresses σ_n due to normal force and bending moment in the column;
- transverse stresses σ_t due to load-introduction.

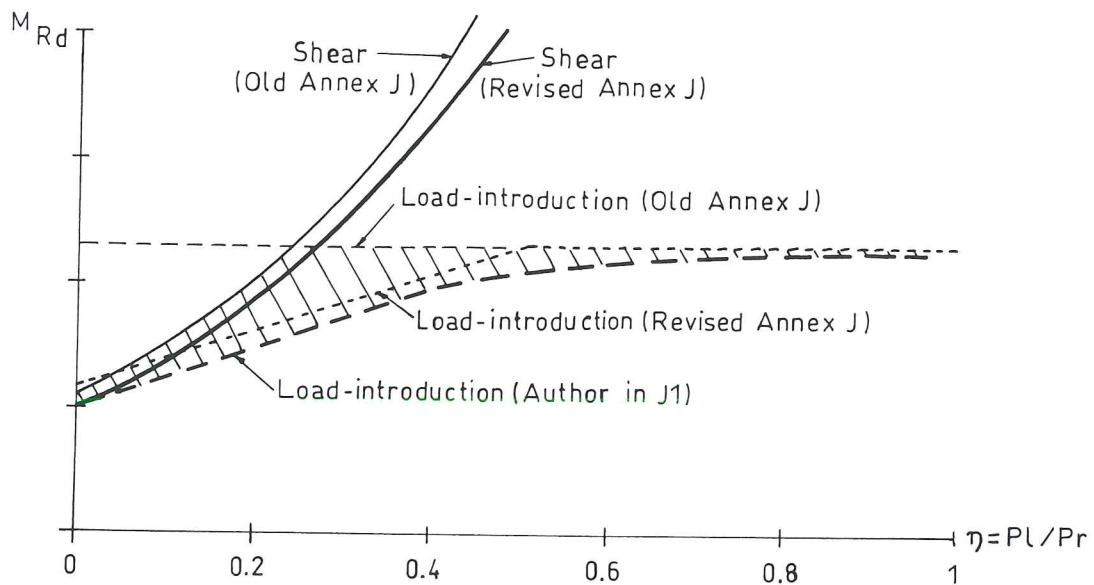
The interactions between these stresses affect the joint resistance :

- longitudinal stresses σ_n decrease the shear resistance;
- shear stresses τ decrease the load-introduction resistance;
- longitudinal stresses σ_n may decrease the load-introduction resistance (compression zone).

The possible influence of σ_n stresses on the load-introduction resistance in the compression zone is known for several years; the two other types of interaction, on the one hand, were not taken into consideration in the old version of Eurocode 3 Annex J. In our thesis [J1], we investigated deeply these interactions and, as a result, we suggested expressions for reduction factors, in full agreement with available test results and numerical simulations. The unsafe character of the previous Annex J, compared to our model, is represented by the hachured zone in Figure 3-32.



(a) External loading



(b) Resistance

Figure 3-32 Variation of web panel resistance according to the external loading

But Annex J has been recently revised and the rules for the design of web panels have been modified according to our proposals. The first modification concerns the shear

resistance, $V_{n,Rd}$. The influence of the longitudinal stresses σ_n has been simply taken into account with a constant reduction factor equal to 0,9:

$$V_{n,Rd} = 0,9 \frac{A_{v,c} \cdot f_{ywc}}{\gamma_{m0} \cdot \sqrt{3}} \quad (3-32)$$

$A_{v,c}$ is the shear area of the profile, f_{ywc} the yield stress and γ_{m0} the partial safety factor.

Formula (3-32) applies to web panels that have a web of sufficient thickness to ensure that shear buckling is not a design criterion, i.e. $d_c/t_{wc} \leq 69\varepsilon$ (see Eurocode 3, where d_c is the clear depth of the column and $\varepsilon = \sqrt{235/f_{ywc}}$ with f_{ywc} expressed in MPa.

The second modification consists in a possible reduction of the design resistance $F_{wc,Rd}$ of the column web in tension or compression with the shear stresses, by means of a reduction factor ρ :

$$F_{wc,Rd} = \rho \frac{f_{ywc} \cdot t_{wc} \cdot b_{eff}}{\gamma_{m0}} \quad (3-33.a)$$

$$\text{with : } \rho = \rho_1 = \frac{1}{\sqrt{1 + 1,3 \cdot \left(\frac{b_{eff} \cdot t_{wc}}{A_{v,c}} \right)^2}} \quad \text{if } \eta = 0 \quad (3-33.b)$$

$$= \rho_1 + (1 - \rho_1) \cdot 2 \cdot \eta \quad \text{if } 0 < \eta < 0.5 \quad (3-33.c)$$

$$= 1 \quad \text{if } 0.5 \leq \eta \leq 1 \quad (3-33.d)$$

t_{wc} is the web thickness and b_{eff} is the effective width, the value of which is given in the code according to the connection detailing. Equation 3-33, represented by two lines, is a simplification of the initial proposal we made. The difference between the two approaches is illustrated in Figure 3-32.

The effect of the longitudinal stresses σ_n on the resistance of the column web in compression is taken into account by means of an other reduction factor, k_{wc} , that was already existing in the old Annex J [Z5] :

$$k_{wc} = 1,25 - 0,5 \frac{\sigma_{n,Ed}}{f_{ywc}} \leq 1 \quad (3-34)$$

$\sigma_{n,Ed}$ is the normal stress in the column web, at the root of the fillet or of the weld, due to longitudinal force and bending moment in the column. The minimum value of k_{wc} is 0,75 (when $\sigma_{n,Ed}$ is equal to f_{ywc}). k_{wc} covers the possible buckling of the web panel under the combined action of the σ_i and σ_n compressive stresses.

Finally, the last modification introduced in Annex J for the web panel is the extension of the design rules for load-introduction to slender webs ($\bar{\lambda} > 0.673$) [A1] by limiting the design resistance of the web given in Equation (3-33) to its buckling or crippling resistance:

$$F_{wc,Rd} = \rho \frac{k_{wc} f_{ywc} \cdot t_{wc} \cdot b_{eff}}{\gamma_{m0}} \quad \text{if } \bar{\lambda} \leq 0.673 \quad (3-35.a)$$

$$F_{wc,Rd} = \rho \frac{k_{wc} f_{ywc} \cdot t_{wc} \cdot b_{eff}}{\gamma_{m0}} \left[\frac{1}{\bar{\lambda}} \cdot \left(1 - \frac{0,22}{\bar{\lambda}} \right) \right] \quad \text{if } \bar{\lambda} > 0.673 \quad (3-35.b)$$

with :

$$\bar{\lambda} = 0,93 \sqrt{\frac{b_{eff} \cdot d_c \cdot f_{ywc}}{E \cdot t_{wc}^2}}$$

d_c is the clear depth of the column web, E the Young modulus and the other parameters are defined here above.

Equations (3-32) to (3-35) are discussed in the present Chapter on the basis of comparisons with numerical simulations (Section 3.2.2.3) and experimental tests (Section 3.2.2.4).

Interaction in the column flange for bolted connections

In bolted joints (with flush or extended end-plates, flange cleats), the column flange is subjected to transverse forces. The design resistance of this component according to Annex J of Eurocode 3 (see Appendix 3) may be reduced because of possible high longitudinal stresses $\sigma_{com,Ed}$ (> 180 MPa) in the column flange by means of a reduction factor k_{fc} equal to [Z5] :

$$k_{fc} = \frac{2 f_{yfc} - 180 - \sigma_{com,Ed}}{2 f_{yfc} - 360} \leq 1 \quad (3-36)$$

f_{yfc} is the yield stress of the column flange.

The validity of this reduction factor is discussed in Section 3.2.2.4.

3.2.2.3 Numerical investigations

Test specimens

A large set of numerical simulations have been performed with the non-linear finite element program FINELG [F1]. This software is developed in Liège since several years. It simulates the behaviour of structures until collapse and takes into account various phenomena such as non-linear mechanical properties for steel, second order effects, residual stresses, initial imperfections.

Welded joints have been modeled with shell elements (Figure 3-33). These numerical 3D simulations, based on the geometry of experimental tests performed some years ago in Innsbruck [K1], provide very interesting information such as strains and stresses anywhere in the joint, or global behaviour curves which allow direct comparisons with the theoretical models described in our Ph.D. Thesis [J1] and in the revised Annex J of Eurocode 3.

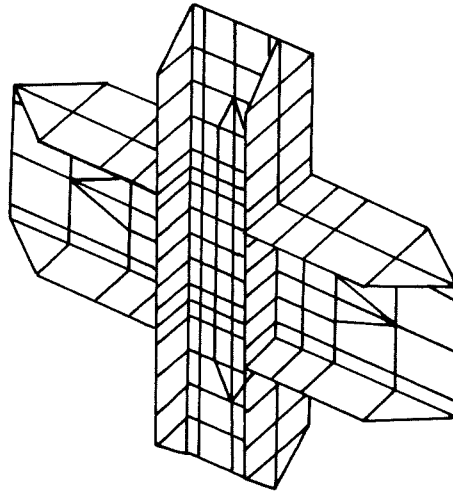


Figure 3-33 Discretization of welded joints

In [J1], the results of a quite large number of such numerical simulations are reported. They had been performed in order to investigate the effect of parameters such as :

- the type of loading;
- the steel grade;
- the strain hardening;
- the initial imperfection of the column web.

As an outcome of these simulations, the validity of formulae (3-32) and (3-35) had been demonstrated in the case of symmetrically loaded double-sided joint configurations ($\eta = 1$) and single-sided joint configurations ($\eta = 0$).

In this section, the results of recent extra simulations performed in collaboration with S. Guisse and C. Briquet from the MSM Department are discussed.

The two main studied parameters are here :

- the load factor η (see Figure 3-32);
- the load factor β defined as the ratio between the axial compressive force in the column and its squash load $N_{p,c}$ (see Figure 3-34).

The configurations considered are those described in Figure 3-34 and Table 3-2. The reader interested in their geometrical and mechanical properties is begged to refer to [C3].

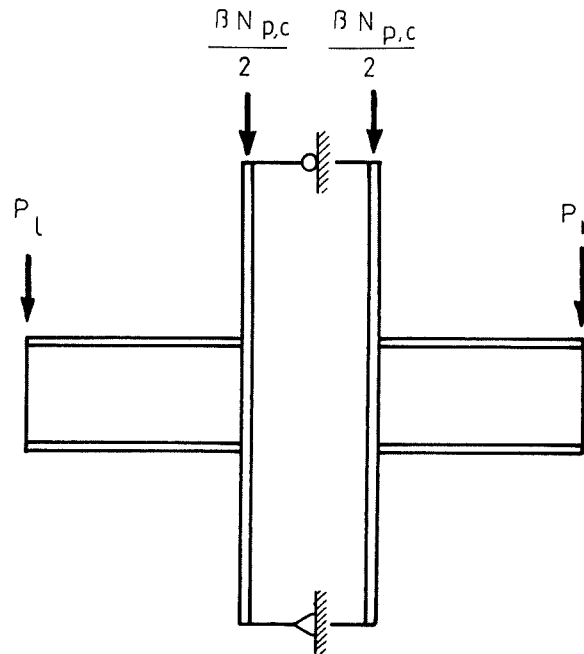


Figure 3-34 Joint configuration and loading for numerical simulations

Analysis of the results

Influence of η

Figure 3-35 shows how the $M-\phi$ characteristic of the configuration A is affected by the modification of the η loading parameter. For low values of η , the pseudo-plastic resistance (see Appendix 1) is reached by shear of the column web panel. The curve exhibits then a rather significant post-limit stiffness resulting from the development of strain-hardening; the available rotation capacity of the joint is quite important. For increasing values of η , shear becomes less predominant and failure occurs by load-introduction, so leading to the instability of the column web panel in compression. The strain-hardening range vanishes progressively and the ultimate resistance of the joint identifies itself to the pseudo-plastic one for the value of the loading parameter η equal to 1,0. No plastic rotation capacity of the joint is then available. For intermediate values of η (for instance, $\eta = 0,6$ in Figure 3-35), the resistance of the joint is seen to be higher than for $\eta = 1,0$.

	Configuration A Column : HE160B Beam : IPE300		Configuration B Column : HE300B Beam : HE500B	
	η	β	η	β
Influence of η	0,0	0,0	0,0	0,0
	0,2	0,0	0,2	0,0
	0,4	0,0	0,4	0,0
	0,6	0,0	0,6	0,0
	0,8	0,0	0,8	0,0
	1,0	0,0	1,0	0,0
Influence of β	1,0	0	1,0	0,0
	1,0	0,4	1,0	0,4
	1,0	0,5	1,0	0,5
	1,0	0,6	1,0	0,6
	1,0	0,7	1,0	0,7
	1,0	0,8		
	0,0	0,0	0,0	0,0
	0,0	0,4	0,0	0,4
	0,0	0,5	0,0	0,5
	0,0	0,6	0,0	0,6
	0,0	0,7	0,0	0,7
	0,0		0,0	

Table 3-2 Considered parameters for numerical simulations

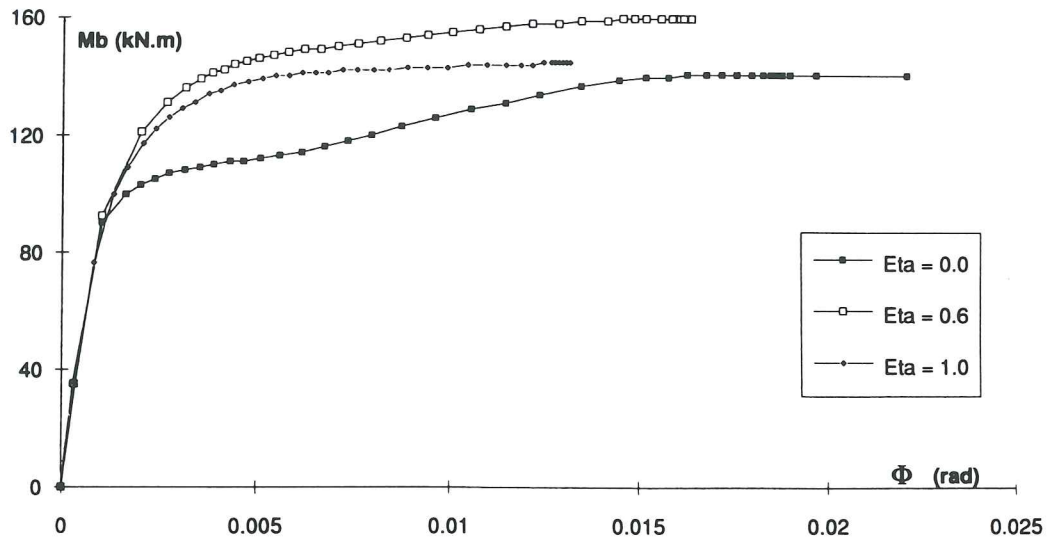


Figure 3-35 Evolution of the $M-\phi$ characteristic with η .
Configuration A with $\beta = 0$

This is also apparent in Figure 3-36 and in Figure 3-37 where the pseudo-plastic moment resistances of the joints A and B are reported versus loading parameter η .

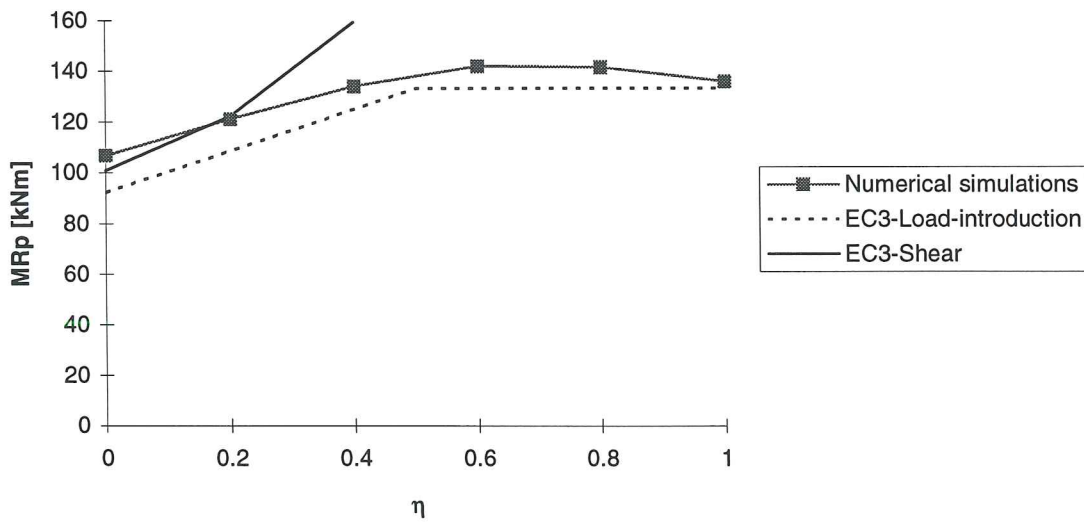


Figure 3-36 Comparison between Eurocode 3 and numerical simulations.
Influence of η on the pseudo-plastic resistance of the joint.
Configuration A with $\beta = 0$.

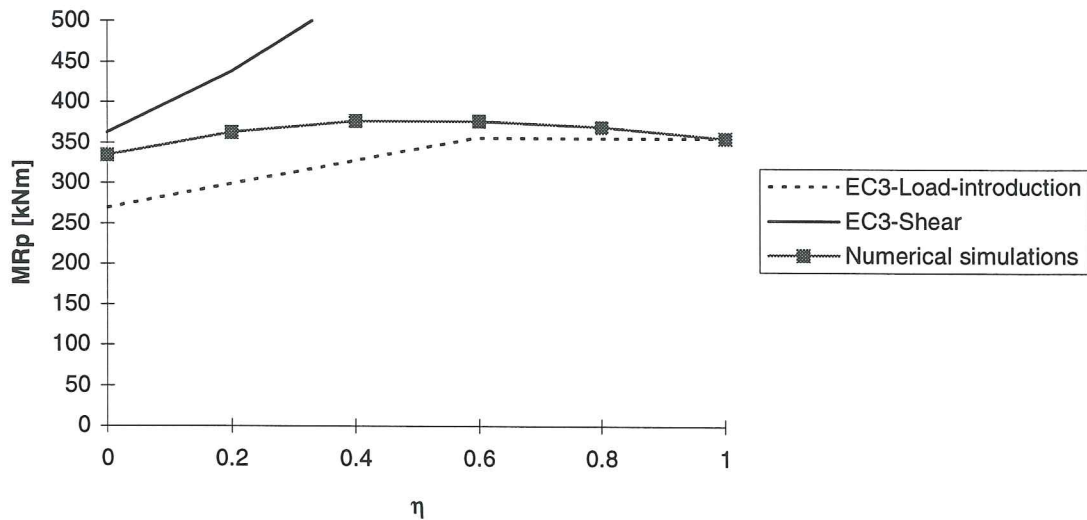


Figure 3-37 Comparison between Eurocode 3 and numerical simulations.
Influence of η on the pseudo-plastic resistance of the joint.
Configuration B with $\beta = 0$.

This evolution of the design resistance may be explained by referring to Figure 3-38 where the " $\eta = 1$ " situation is illustrated. At the beginning of the loading, the column web response is elastic and the edges may be considered as rigidly connected to the flanges (Figure 3-38.a). The buckling load of the web rigidly connected to the flanges is much higher than the actual buckling load. In fact, the buckling of the web is preceded by the yielding of the web at the beam-to-flange intersections, what modifies the support conditions of the panel (Figure 3-38.b) : it may be assumed that the web is then simply supported. For HEA, HEB and even DIL profiles - slenderness usually lower than 0,67 (see Formula (3-35)-, we have shown in [J1] that the pseudo-plastic resistance of the web - which is linked to yielding - is a lower bound of the actual buckling length. In other words, as soon as the pseudo-plastic resistance of the web is reached, the support conditions of the web change, the web is no more restrained, and the instability may develop.

In cases where $\eta < 1$, the pseudo-plastic resistance is reached on one side first while the web is still restrained on the other side; the instability load is therefore higher.

To summarize, the risk of instability becomes greater with increasing values of η while the crushing resistance increases (less interaction with shear stresses).

By referring to the diagrams given in Figure 3-36 and Figure 3-37, we can conclude that the stress interaction is governing the failure for low and moderate values of η . For higher values of η , instability predominates, what results in a decrease of the pseudo-plastic resistance of the joint.

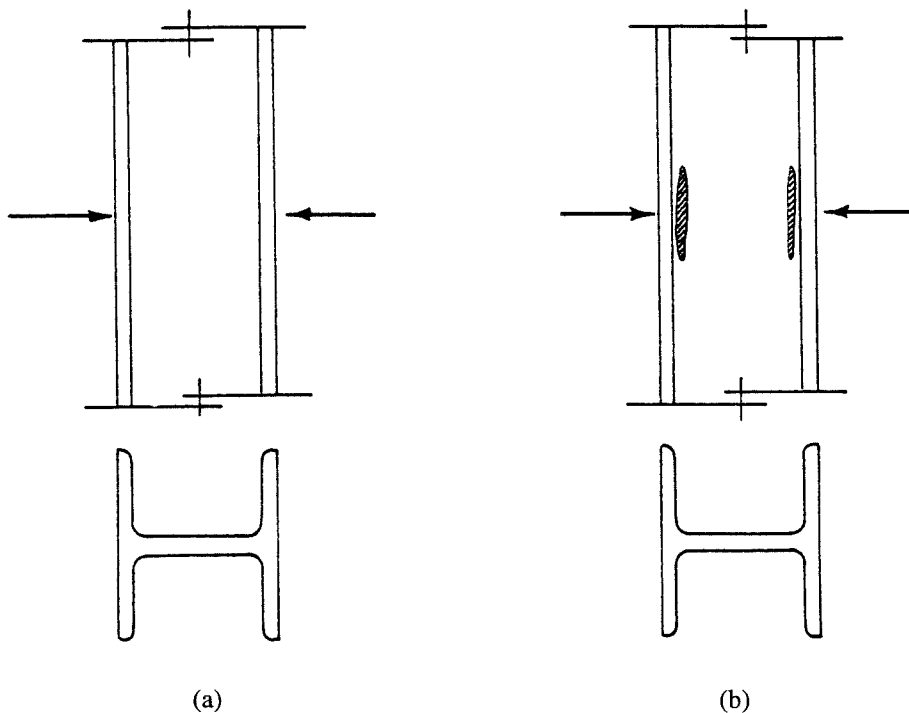


Figure 3-38 Support conditions of the column web

A refined model to follow accurately this kind of evolution diagrams has been developed by Guisse in [C1, C2 and C5]. In Eurocode 3 Annex J, Formulae (3-32) and (3-35) are recommended and the agreement with the results of the numerical simulations is seen to be quite good.

Influence of β on the symmetrically loaded configurations ($\eta = 1$)

The evolution of the $M-\phi$ characteristics are shown in Figure 3-39 and Figure 3-40 for increasing values of the β parameter.

The main conclusions are as follows :

- the elastic initial stiffness is not affected by β ;
- the ultimate resistance is quite similar to the pseudo-plastic one and decreases with increasing values of β . In the simulations of the A configuration with $\beta = 0,8$ and of the B configuration with $\beta = 0,7$, failure occurs by buckling of the column in compression; these curves have therefore to be disregarded;
- the maximum drop of the resistance amounts 30 % for the A configuration and 25 % for the B one.

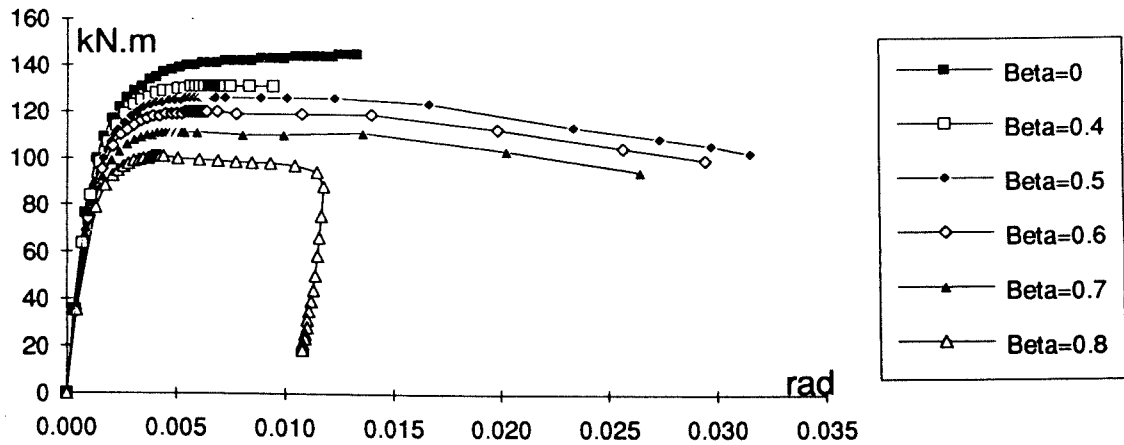


Figure 3-39 Evolution of the $M-\phi$ characteristic with β .
Configuration A with $\eta = 1,0$

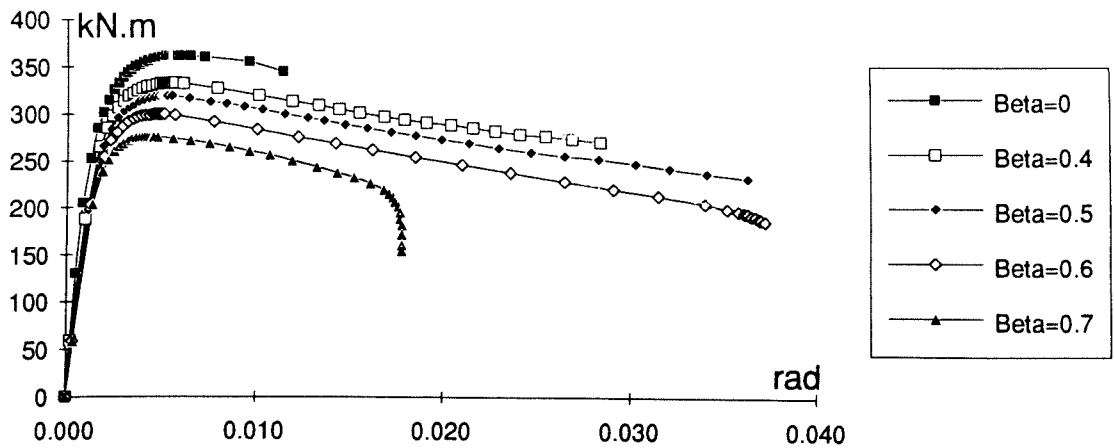


Figure 3-40 Evolution of the $M-\phi$ characteristic with β .
Configuration B with $\eta = 1,0$.

In Figure 3-41 and Figure 3-42, comparisons between Eurocode 3 Formula (3-35) and results of numerical simulations are presented. How to derive the pseudo-plastic resistance of the joints (see Appendix 1) from the $M-\phi$ curves is explained in Section 3.2.2.4. under the heading "Definition of the experimental pseudo-plastic moment resistance". The agreement is seen to be quite good. It has to be noted again that the results obtained for $\beta = 0,8$ in Figure 3-41 and $\beta = 0,7$ in Figure 3-42 should ideally be

ignored as they correspond to a flexural buckling of the column in compression and not to the local buckling of the column web in compression.

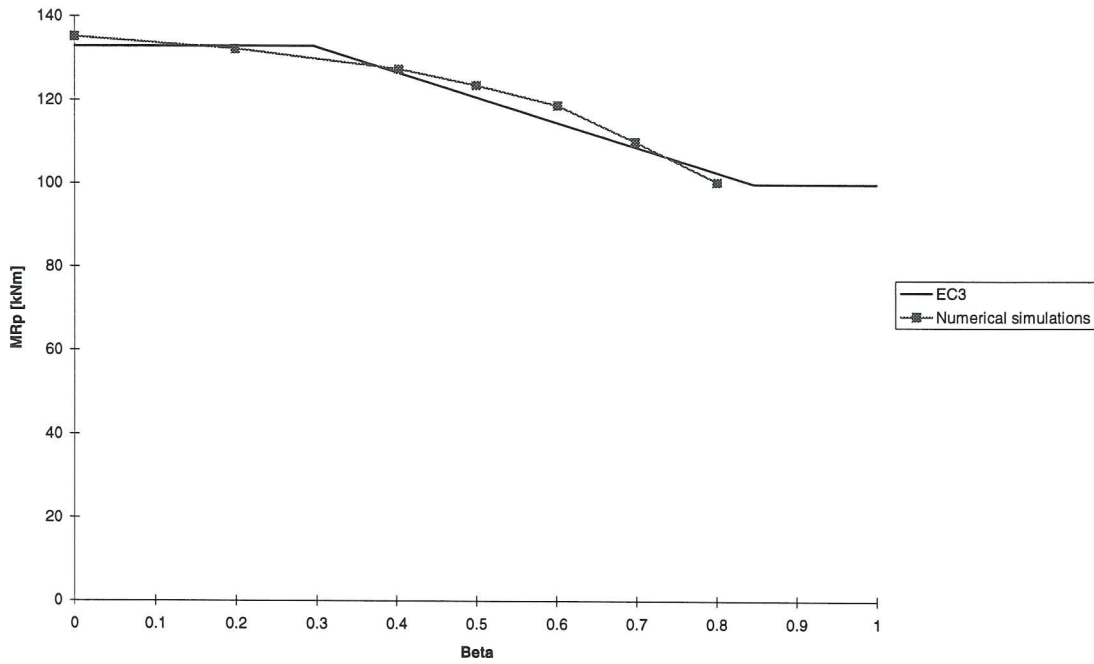


Figure 3-41 Comparison between Eurocode 3 and numerical simulations. Influence of β on the pseudo-plastic resistance of the column web in compression. Configuration A with $\eta = 1,0$.

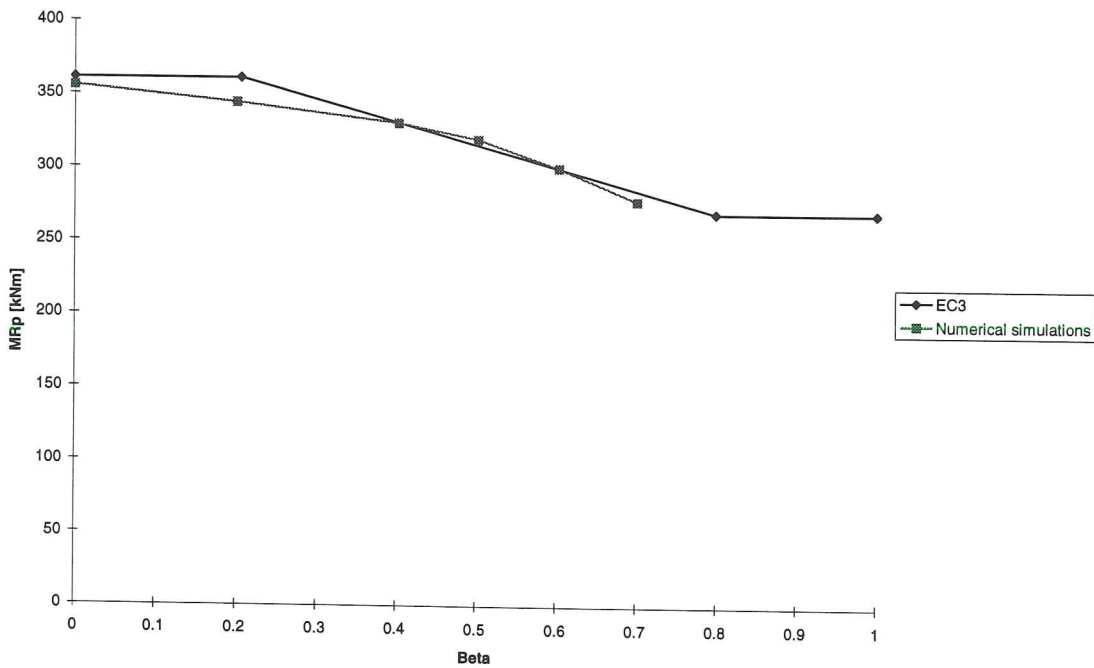


Figure 3-42 Comparison between Eurocode 3 and numerical simulations. Influence of β on the pseudo-plastic resistance of the column web in compression. Configuration B with $\eta = 1,0$.

Influence of β on the single-sided configuration ($\eta = 0$)

In single-sided joint configurations, the longitudinal stresses in the column result not only from the applied compressive force $\beta N_{p,c}$, but also from the bending of the column itself. The value of $\sigma_{n,Ed}$ to consider in Formula (3-34) is therefore significant, at joint collapse, even for low values of the β coefficient.

In Figure 3-43 and Figure 3-44, the V_n - γ and M - ϕ characteristics of the web panel in shear and load-introduction respectively (see Chapter 1) are reported for the A configuration.

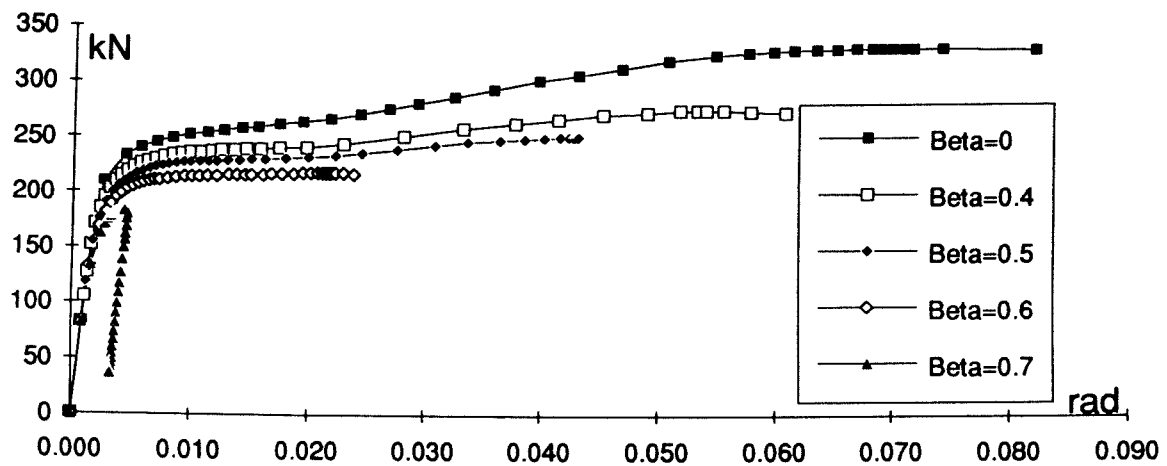


Figure 3-43 Evolution of the V_n - γ characteristic with β .
Configuration A with $\eta = 0$

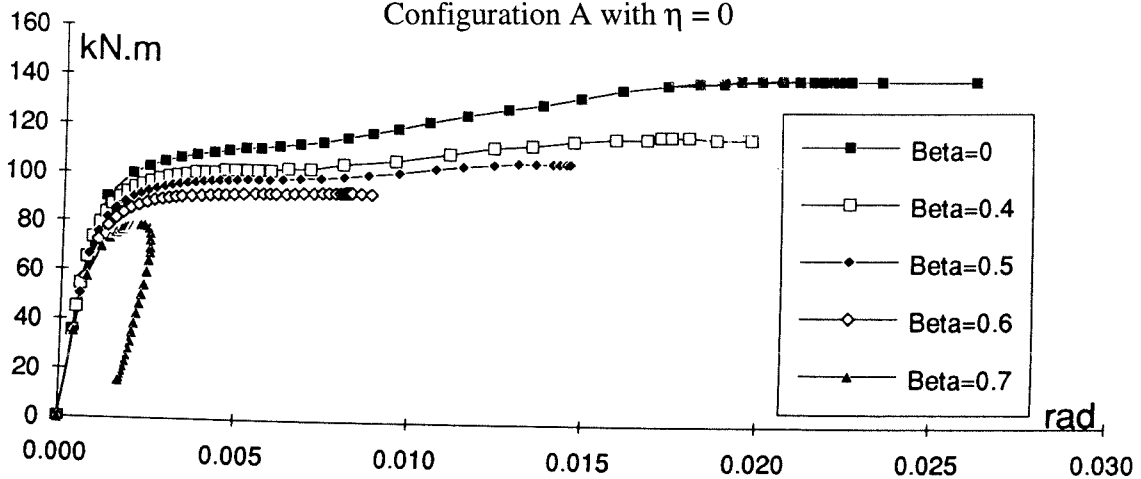


Figure 3-44 Evolution of the M - ϕ characteristic with β .
Configuration A with $\eta = 0$

Failure occurs by excessive yielding of the column web panel in shear for a zero β value, while load-introduction is predominant even for moderate values of β . This is clearly apparent from Figure 3-44 : for $\beta = 0$, the M - ϕ curve exhibits a significant post-limit stiffness corresponding to the development of strain-hardening; for higher values of β , load-introduction leads more and more quickly to instability phenomena in the column web in compression and the importance of the post-limit effects reduce, together with the

rotation capacity. For high values of β , the flexural buckling of the column occurs under axial forces and moments ($\beta = 0,7$).

Similar conclusions may be drawn from Figure 3-45 and Figure 3-46 relative to the B configuration; the only difference is that load-introduction predominates also for a zero β value.

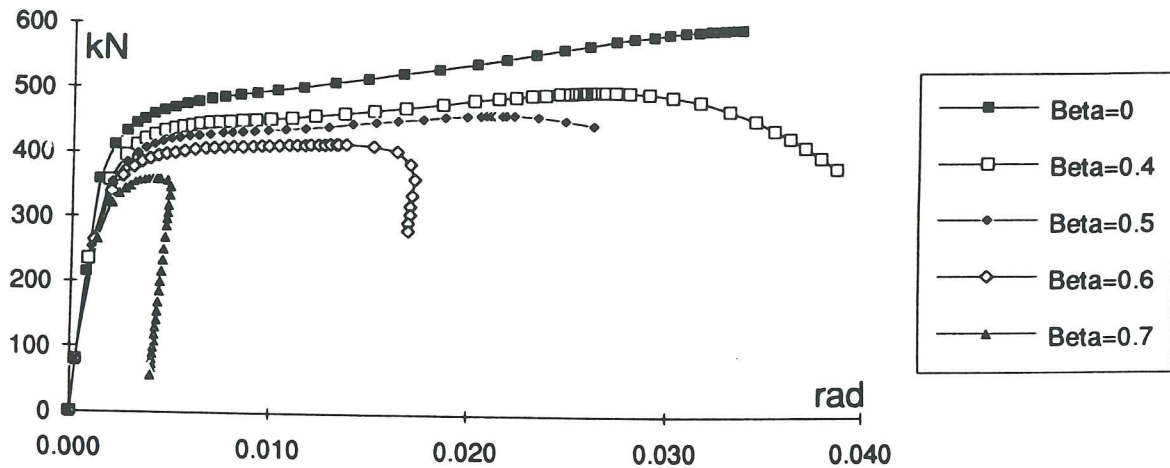


Figure 3-45 Evolution of the V_n - γ characteristic with β .
Configuration B with $\eta = 0$.

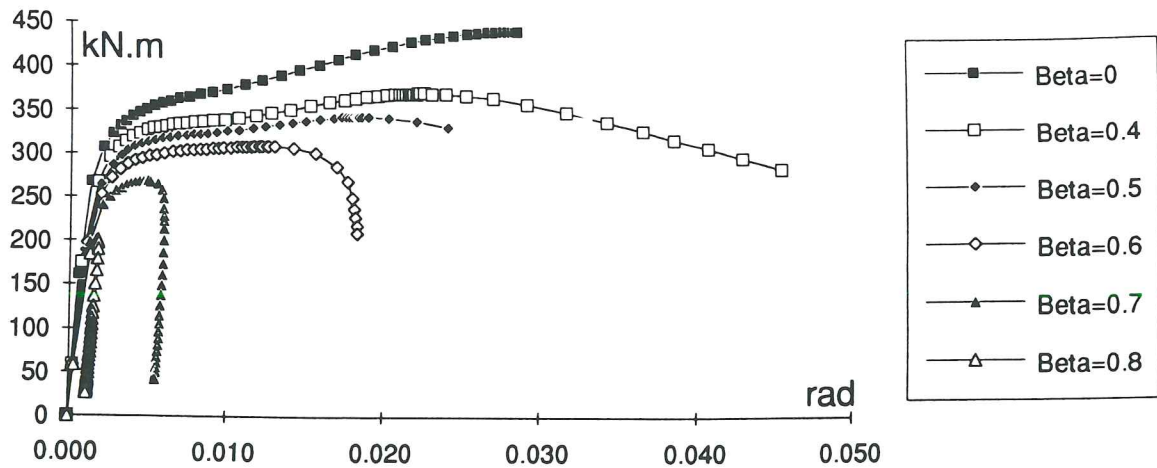


Figure 3-46 Evolution of the M - ϕ characteristic with β .
Configuration B with $\eta = 0$.

In Figure 3-47 and Figure 3-48, the pseudo-plastic resistances obtained numerically are compared to the corresponding shear and load-introduction resistances provided by Eurocode 3 Annex J. Again the rather good agreement may be pointed out. Results corresponding to $\beta = 0,7$ have to be disregarded for above-mentioned reasons.

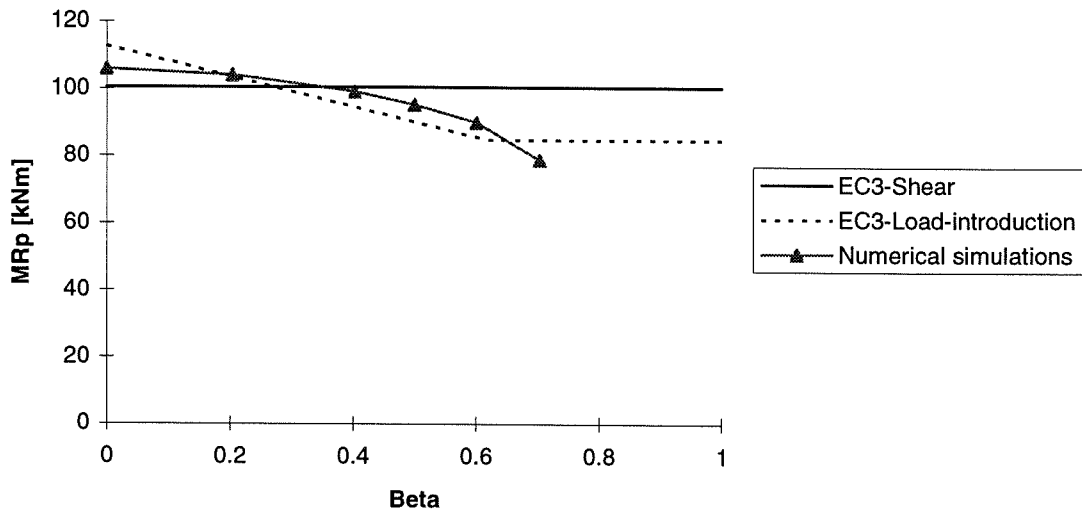


Figure 3-47 Comparisons between Eurocode 3 and numerical simulations.
 Influence of β on the pseudo-plastic resistance of the joint.
 Configuration A with $\eta = 0,0$

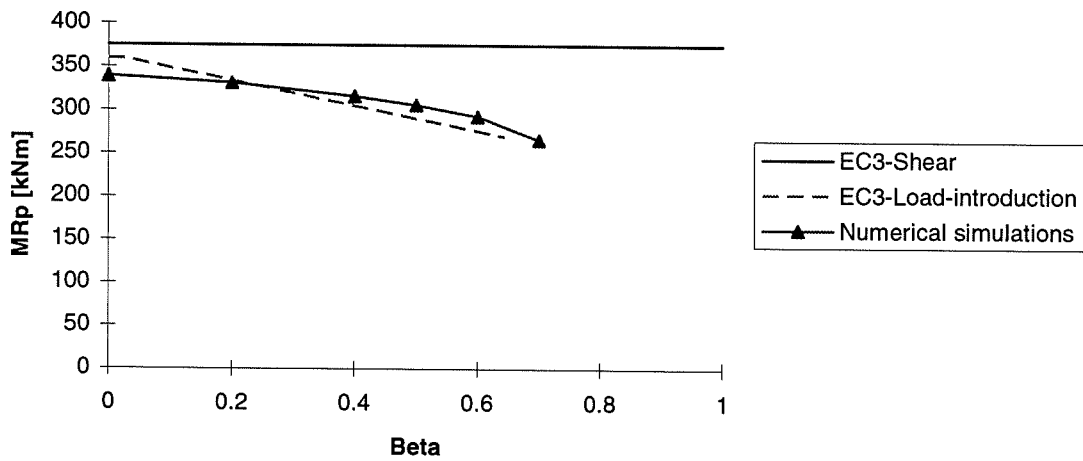


Figure 3-48 Comparisons between Eurocode 3 and numerical simulations.
 Influence of β on the pseudo-plastic resistance of the joint.
 Configuration B with $\eta = 0,0$.

3.2.2.4 Experimental investigations

Test specimens

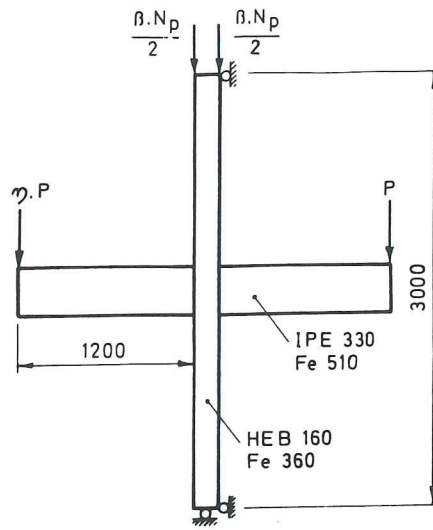
Twenty-four experimental tests on joints have been performed in the laboratory of the MSM Department. Sixteen of them were welded joints while the others were bolted ones with flush end-plates. Three different joint configurations, illustrated in Figure 3-49 respectively named WS, WN and EPN have been tested (8 tests for each configuration).

Tests WS are dedicated to the study of the load-introduction and shear stress interactions in the column web panels. "W" means "Welded" and "S" is the first letter of "Shear". The main parameter is the ratio η between the forces applied on the left and right beams. η varies from $\eta = 0$ in test WS0 to 1,0 in test WS10. In tests WS0C and WS10C, the effect of the longitudinal stresses in the column, respectively for $\eta = 0$ and $\eta = 1,0$, is investigated (« C » means « compression in the column »).

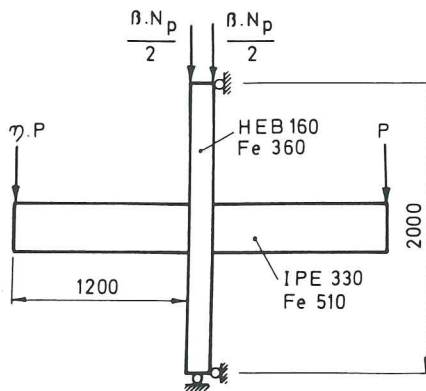
Tests WN are aimed at studying the effect of the axial compressive force N in the column. In the four first tests (WN0 to WN6), the ratio β between the constant applied load N and the squash load of the column varies from 0 to 0,6 and $\eta = 0$; this corresponds to single-sided joint configurations. In the four last ones (WN0S to WN7S), β varies from 0 to 0,7 and η is fixed equal to one, what corresponds to Symmetrically loaded double-sided joint configurations.

Tests EPN are all carried out on symmetrically loaded double-sided joint configurations ($\eta = 1,0$). They are aimed at pointing out the influence of the force N in the column on the resistance of the End-Plate, and more especially on the resistance of the column flange in bending. β varies between 0 and 0,8. Two series of tests have been performed, respectively with S235 (tests EPN235) and S355 (test EPN355) steel columns. In tests EPN235, 10.9 bolts are used while 8.8 ones connect the beams to the column in EPN355 tests.

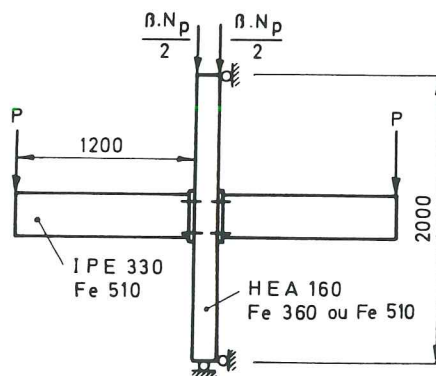
The actual geometrical characteristics of all the tests specimens as well as the mechanical properties of the constitutive steels are reported in [C5]. This report also includes all the details concerning the instrumentation used and the way how the measurements have been combined so as to obtain reliable moment-rotation characteristic curves for each test.



(a) WS tests



(b) WN tests



(c) EPN tests

Figure 3-49 Test configurations

Test number	Steel grade of the column	Values of η	Values of β
WS0	S235	0,0	0,0
WS2	S235	0,2	0,0
WS4	S235	0,4	0,0
WS6	S235	0,6	0,0
WS8	S235	0,8	0,0
WS10	S235	1,0	0,0
WS0C	S235	0,0	0,5
WS10C	S235	1,0	0,6
WN0	S235	0,0	0,0
WN3	S235	0,0	0,3
WN5	S235	0,0	0,5
WN6	S235	0,0	0,6
WN0S	S235	1,0	0,0
WN3S	S235	1,0	0,3
WN5S	S235	1,0	0,5
WN7S	S235	1,0	0,7
EPN235C0	S235	1,0	0,0
EPN235C5	S235	1,0	0,5
EPN235C7	S235	1,0	0,7
EPN235C8	S235	1,0	0,8
EPN355C0	S355	1,0	0,0
EPN355C5	S355	1,0	0,5
EPN355C7	S355	1,0	0,7
EPN355C8	S355	1,0	0,8

Table 3-3 Test numbers and parameters

Definition of the experimental pseudo-plastic moment resistance

As specified in Appendix 1, the pseudo-plastic moment resistance of a joint differs significantly from the ultimate one. While the latter can be identified as the peak resistance of the moment-rotation curve, the pseudo-plastic one is much more difficult to determine precisely. The procedure followed in this section - amongst those presented in

[J1] - is that where the pseudo-plastic resistance is identified as the intersection point between the actual moment-rotation curve and the a straight line passing through the origin of the axes and the slope of which is equal to the third of the experimental initial stiffness of the curve, according to the definition of the secant stiffness given in Eurocode 3 Annex J.

The accuracy of this procedure depends on the ability to define a precise value of the initial stiffness. This is the case in the present experimental programme where "unloading-reloading" cycles have been systematically carried out during the tests so allowing to determine an estimation of the initial stiffness to be considered as independent of the unavoidable lacks of fit occurring during the first loading.

The same procedure has been used for the results of the numerical simulations presented in Section 3.2.2.3.

The procedure is illustrated in Figure 3-50 where tests WS0 to WS10 are reported. The consistency between the six curves in the elastic range - from a theoretical point of view, the initial stiffnesses of the six curves should be exactly the same - has to be noted.

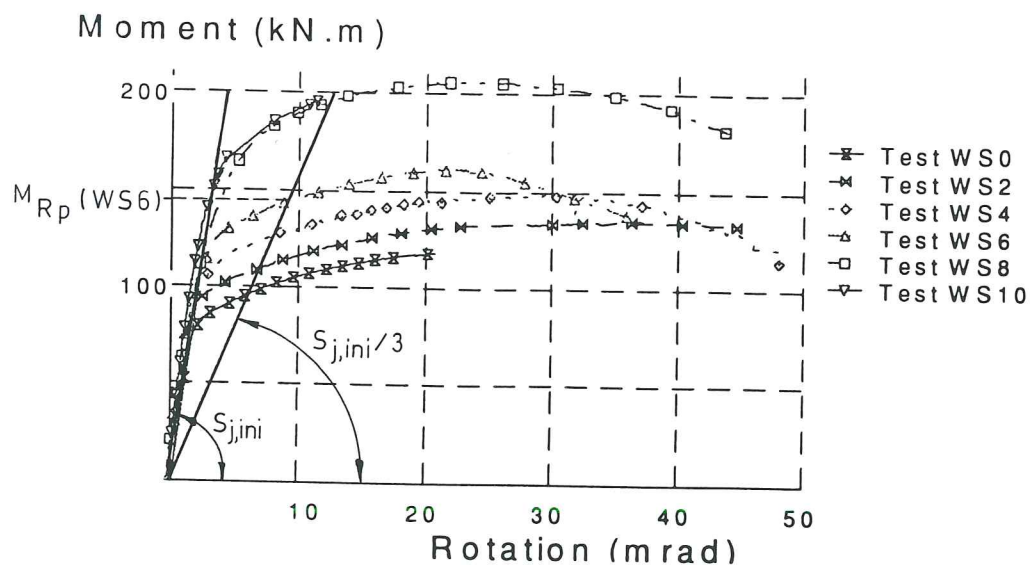


Figure 3-50 Definition of the pseudo-plastic moment resistance

Analysis of the WS test results

The $M-\phi$ curves of the six WS tests with $\beta = 0$ are reported in Figure 3-51 where the significant influence of the loading parameter η is again clearly seen. Tests WS8 and WS10 appear however much stronger than the four others. This difference can not only be explained by the influence of the η parameter. It seems, in contrary to what was certified by the fabricator, that all the columns were not from the same rolling. The

profiles had been evacuated from the laboratory when we realized this difference, so preventing us from performed coupon tensile tests on WS8 and WS10 specimens.

The pseudo-plastic resistances of the six tests are compared in Figure 3-52 to the values predicted by Eurocode 3 revised Annex J. The discontinuity of the two tests WS8 and WS10 is apparent. For the four first tests, the agreement is seen to be rather good even if Eurocode 3 overestimates a bit the resistance for low and moderate values of η ; for these ones, the ultimate resistance of the joints is much higher than the pseudo-plastic one and the ductility is quite significant, so limiting the impact of this overestimation on the structural design and analysis process.

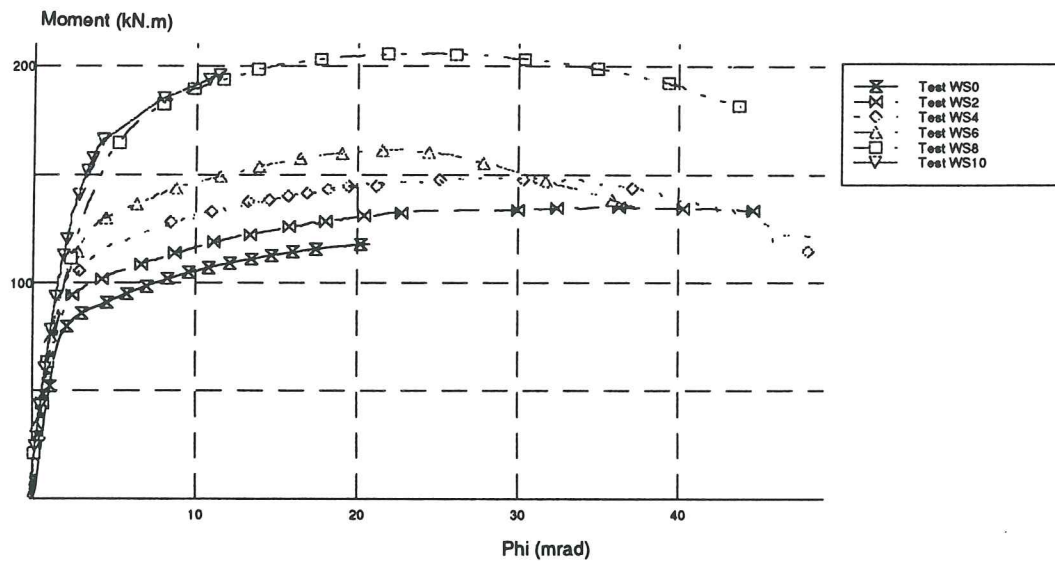


Figure 3-51 Comparison of the $M-\phi$ curves for WS tests

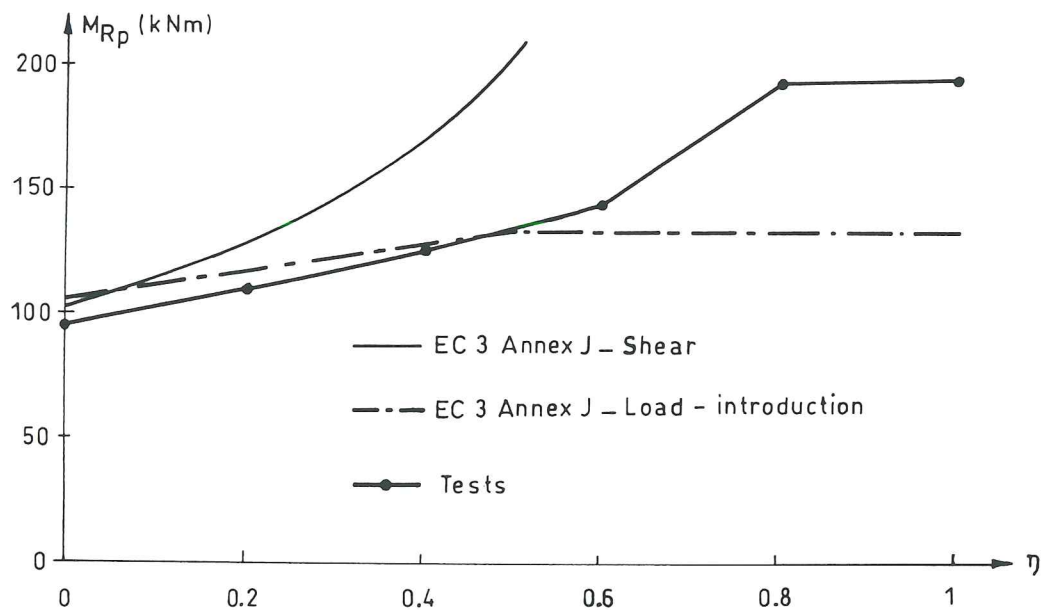


Figure 3-52 Comparison between Eurocode 3 and experimental test results. Influence of η on the pseudo-plastic resistance of the joints. Tests WS

Analysis of the WN test results

Figure 3-53 and Figure 3-54 show the experimental $M-\phi$ curves got from tests WN ($\eta = 0,0$) and WNS ($\eta = 1,0$) respectively.

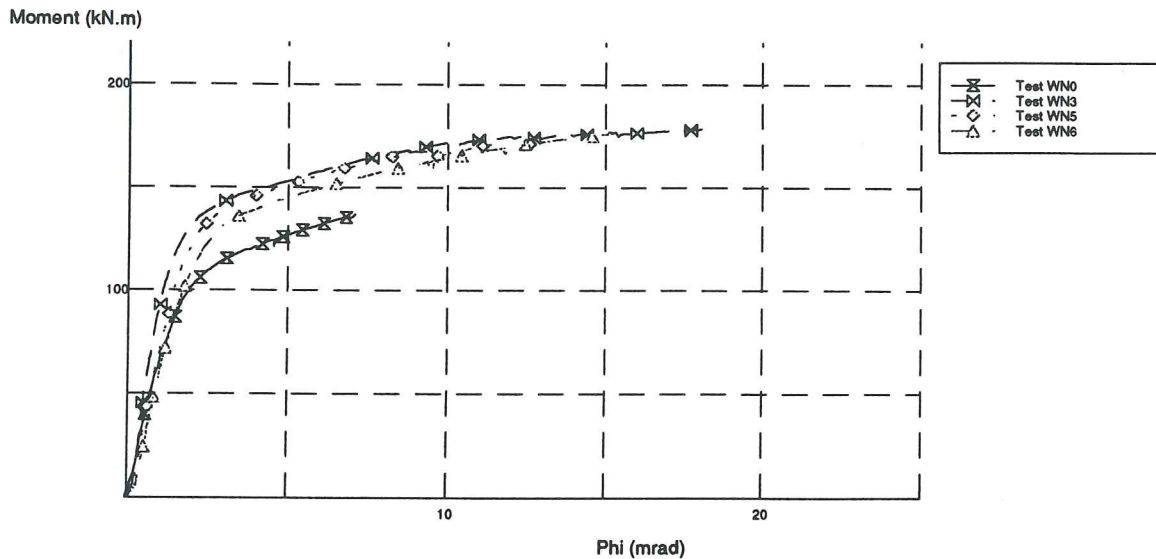


Figure 3-53 Comparison of the $M-\phi$ curves for tests WN ($\eta = 0,0$).

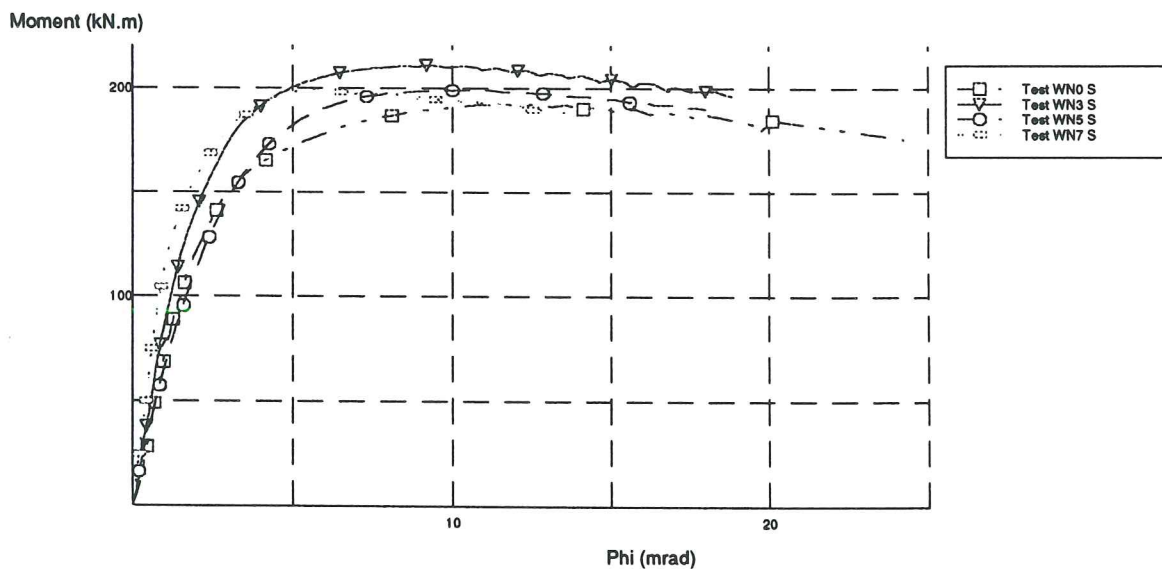


Figure 3-54 Comparison of the $M-\phi$ curves for tests WNS ($\eta = 1,0$)

Test WN0 has to be disregarded because of technical problems during experimentation. From the other tests, it may be concluded that the evolution of the moment-rotation curve, and in particular of the pseudo-plastic resistance (see Figure 3-55) is not enough

significant to be taken into consideration. The level of the longitudinal stresses in the column is however rather high but is anyway limited to β values where no, or very limited, reduction of the pseudo-resistance is recommended by Eurocode ($\approx 0,45$ for unsymmetrical joints, $\approx 0,6$ for symmetrical ones in Figure 3-55) because of the risk of flexural buckling of the column in the plane of the test specimens - the out-of-plane buckling of the column was prevented during the tests -. The actual values of β differ from the nominal ones reported in Table 3-3 because of the difference between measured and nominal values of the yield stresses.

It may be concluded, from these comparisons, that the values of the longitudinal stresses are often limited, in practical cases, because of the risk of flexural buckling of the column, and that the use of the reduction factor given by Formula (3-34) is rarely affecting the pseudo-plastic resistance of the joints.

It has to be noted that high values of β have been obtained in the numerical simulations presented in Section 3.2.2.3. through the use of short column stubs.

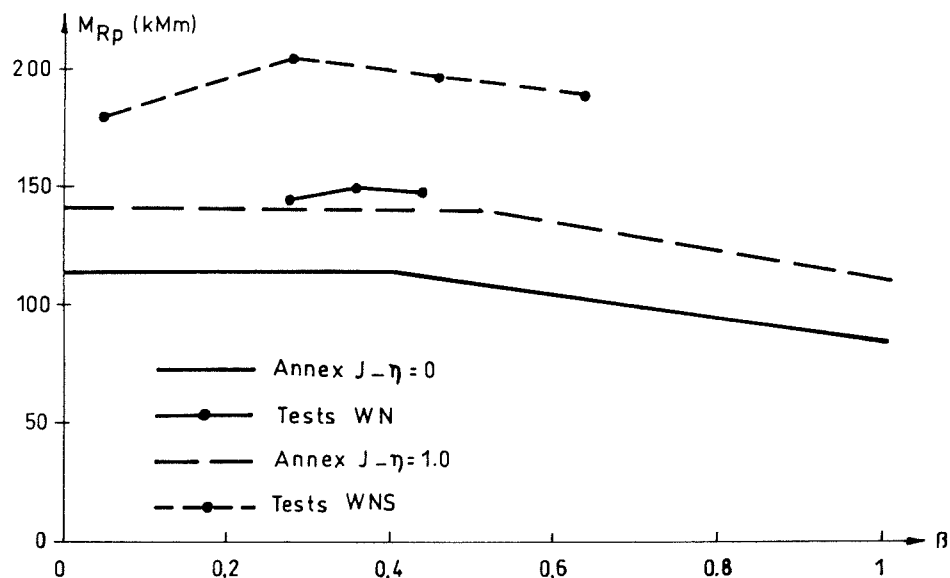


Figure 3-55 Comparison between Eurocode 3 and experimental test results.
Influence of β on the pseudo-plastic resistance of the joints.
Tests WN and WNS.

Analysis of the EPN test results

The $M-\phi$ characteristics of the EPN 235 and EPN 355 tests are compared in Figure 3-56 and Figure 3-57. Test EPN 235C8 is not reported because of technical troubles during experimentation.

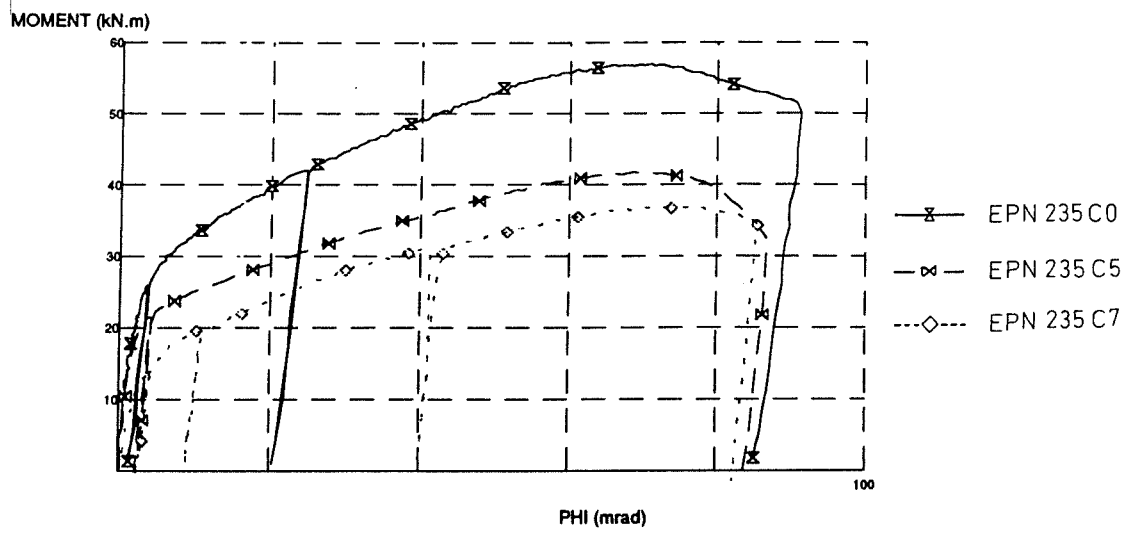


Figure 3-56 Comparisons of the connection $M-\phi$ curves for tests EPN235

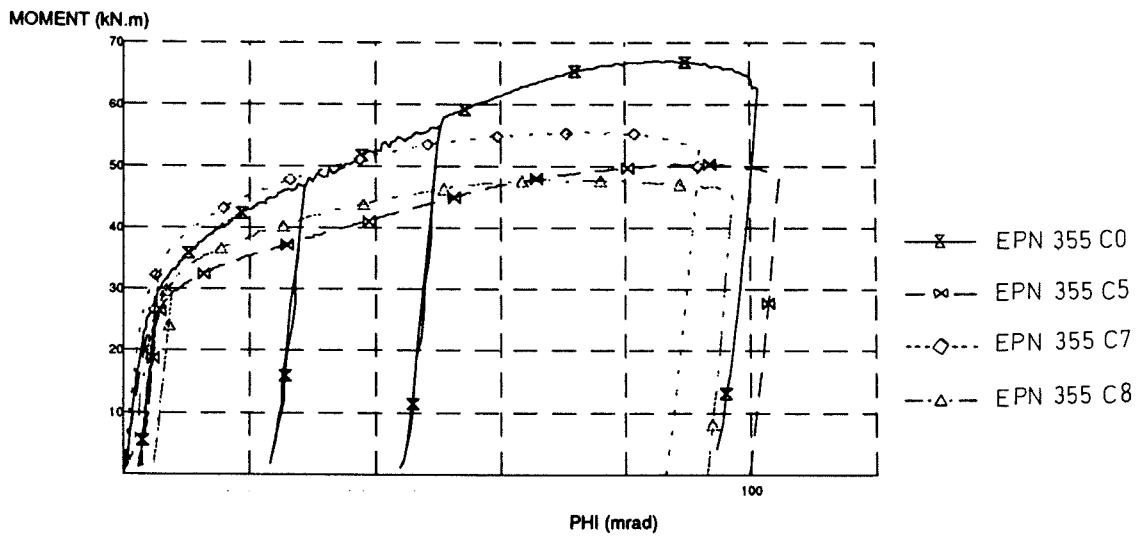


Figure 3-57 Comparisons of the connection $M-\phi$ curves for tests EPN355

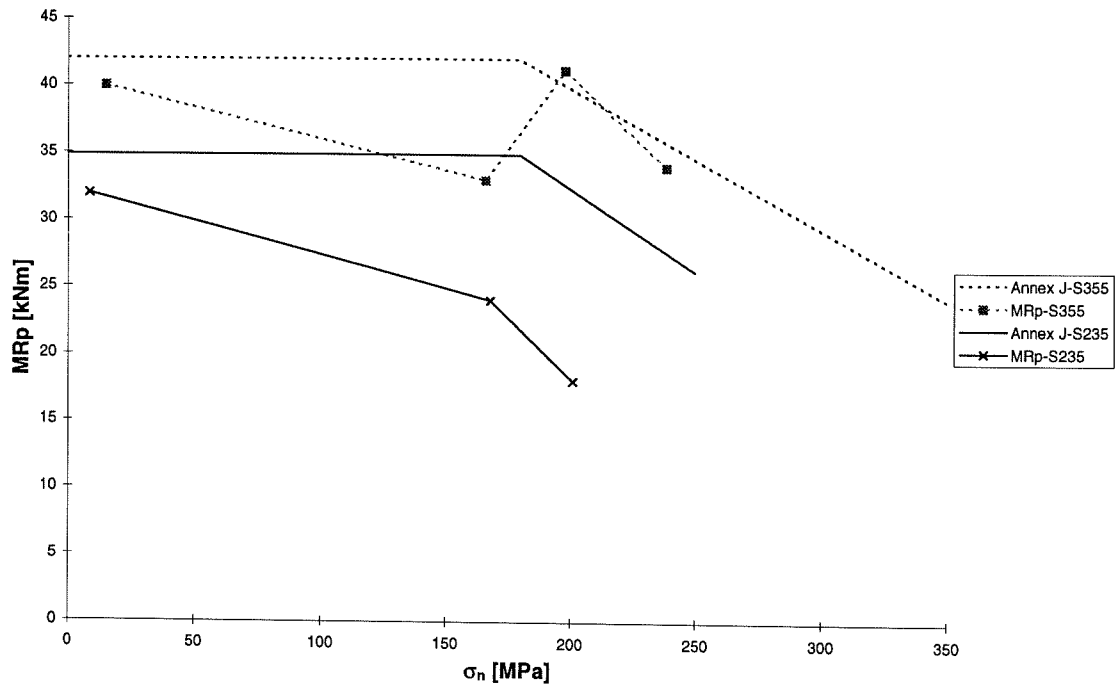


Figure 3-58 Comparison between Eurocode 3 and experimental test results. Influence of σ_n stresses on the pseudo-plastic resistance of the joints. Tests EPN.

In Figure 3-58, comparisons are made between the experimental and predicted pseudo-plastic resistances of the beam flange in bending where yielding first occurs.

From these diagrams, the significant influence of the longitudinal stresses in the column flange is seen. The unconservative character of the reduction factor given by Formula (3-36) is also apparent.

A rather good agreement between tests and models is obtained for $\sigma_n = 0$ but the decrease of the resistance with σ_n is higher in the tests than it is predicted by the code.

The argument which would consist in expressing that the level of stresses in the flange is limited by the risk of flexural instability of the whole column in bending seems less pertinent here than in the case of the column webs in compression and that is why we would recommend to investigate more deeply this aspect in the future through appropriate further experimental investigations and possibly numerical ones, as reliable models for the finite element simulations of bolted connections should be soon available for parametrical studies [B2, B3].

3.2.2.5 Conclusions

According to the component method described in Chapter 2, a joint is constituted of so-called individual basic components. This does not prevent some of these components to interact. These interactions may lead to substantial decreases of the resistance of the joint as a whole, what justifies the need to take them carefully into consideration.

On the basis of available studies, recent and older reduction factors have been introduced in Eurocode 3 Annex J so as to cover the influence of these interactions :

- the reduction factor ρ possibly limits the load-introduction resistance of the column web in tension and compression when high shear stresses are simultaneously acting in the column web panel;
- the reduction factor k_{wc} may decrease the buckling resistance of the column web in compression in the case of high longitudinal stresses in the column;
- the reduction factor k_{fc} reduces the resistance of column flanges in bending subjected to high longitudinal stresses resulting from axial forces and bending moments in the column.

In order to confirm the accuracy of these reduction factors (ρ) and to justify their need (k_{wc} and k_{fc} for which a quite limited background was available), numerical simulations and experimental tests have been performed in the frame of the COST C1 project funded by the Walloon Region of Belgium.

The conclusions of the study are as follows :

- the reduction factor ρ is quite justified and its degree of accuracy has been confirmed;
- the reduction factor k_{wc} , despite its quite simple expression, seems to cover rather well the possible interactions with longitudinal stresses in the column higher than $0,5 f_{yfc}$ where f_{yfc} is the yield stress of the column flange in bending.

In practical situations, the level of the stresses remains however limited because of the risk of flexural buckling of the column; no interaction is therefore usually taking place.

That is why it may be recommended not to take this reduction factor into consideration in the first design steps and only check the suitability of the assumption made by checking, in a later step, that the longitudinal stresses are lower than $0,5 f_{yfc}$, what should happen in most of the cases.

- the reduction factor k_{fc} seems, from available tests, to underestimate the level of interaction with longitudinal stresses in the column flange in bending; further studies appear to be quite necessary to confirm these first conclusions and possibly suggest another expression more in line with the experimental evidence.

3.2.3 Assembly of the components

3.2.3.1 Introduction

The assembly of the components constitutes the third and last step of the component method. As its name indicates, it consists in assembling the individual components all together so as to derive the mechanical properties of the whole joint. The relationship between component properties and joint properties is based on what is commonly called the "distribution of internal forces in the joint". The latter consists in determining, for a

given set of external forces acting on the joint, the way these forces distribute between all the constitutive components, the force to which every component is subjected being termed "internal force".

All this not only applies to structural joints. In any cross-section of beams and columns, this distribution is commonly carried out so as to determine its flexural rigidity or its level of resistance in bending, shear, torsion and/or axial compression or tension. That is why, in the next paragraphs, the word "cross-section" covers as much beam and column sections as joint sections.

The distribution of internal forces has to be carried out in a rational way, and has, from a theoretical point of view, to fulfil the following requirements :

- the internal forces - which result from the distribution - have to be in equilibrium with the external forces acting on the cross-section;
- the compatibility of the displacements between the constitutive parts of the cross-section - namely components in the case of a joint - has to be respected;
- each part of the cross-section has to be able to transfer the internal force to which it is subjected;
- the maximum deformation capacity of each part of the cross-section has never to be exceeded.

In the case of a beam or column H or I cross-section subjected to bending moment, the distribution of internal forces - read stresses in this particular case - in the elastic range follows the Navier rule (Figure 3-59).

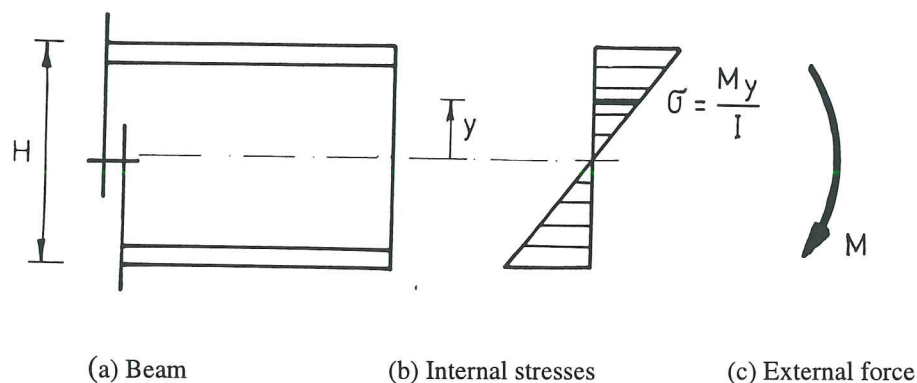


Figure 3-59 Elastic distribution of internal forces - stresses here - in a beam profile in bending ($I =$ second moment of inertia)

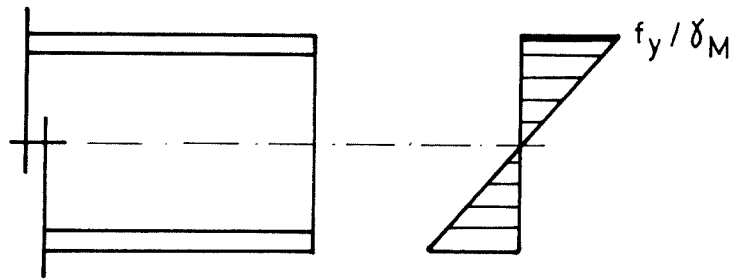


Figure 3-60 Internal forces - stresses here - corresponding to the maximum elastic design moment resistance of the cross-section

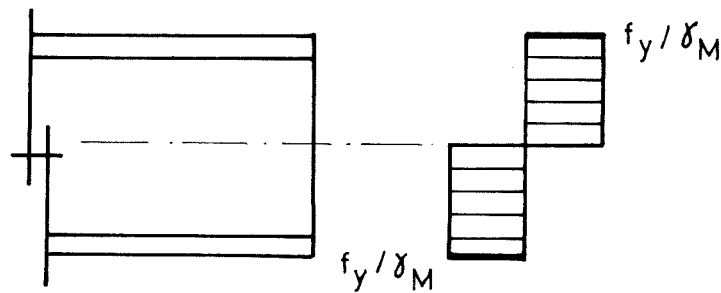


Figure 3-61 Internal forces - stresses here - corresponding to the plastic moment resistance of the cross-section

When the maximum internal stresses reach (in $y = \pm H/2$) the value of the yield stress f_y of the constitute steel divided by a partial safety factor γ_M , the maximum elastic moment resistance of the cross-section is obtained (Figure 3-60). The design moment resistance is expressed as :

$$M_{Rd} = \frac{I}{H/2} \frac{f_y}{\gamma_M} = W f_y / \gamma_M \quad (3-37)$$

where W is the elastic modulus of the cross-section in bending.

To profit from the plastic extra resistance of the cross-section, reference has therefore to be made to the distribution represented at Figure 3-61. The design resistance amounts then :

$$M_{Rd} = Z f_y / \gamma_M \quad (3-38)$$

where Z designates the plastic modulus of the cross-section in bending.

In these distributions, the Bernoulli's assumption has been considered so expressing a compatibility between the elongation - or shortening - of all the constitutive fibers of the cross-section. Both elastic and plastic distributions illustrated in Figure 3-60 and Figure 3-61 are in equilibrium with the applied external forces and respect the plasticity criterion ($\sigma \leq f_y/\gamma_M$). Therefore, they satisfy three of the four criteria expressed here above and to that any distribution of internal forces should fulfil.

To reach the elastic or plastic moment resistance, the constitutive fibers of the section have to possess a sufficient deformation capacity so as to reach the yield stress - in the case of the elastic distribution - or to reach the yield stress and to allow a plastic redistribution of the stresses between the adjacent fibers - in the case of the plastic distribution. This means that no premature local buckling of one of the section walls in compression and that no rupture of the material in tension has to occur so limiting the moment capacity of the section. Specific criteria are provided in the codes so as to prevent the user from overestimating the resistance when such limitations apply. In these conditions, the fourth criterion on ductility is also fulfilled.

In a H or I profile, it is also common to reduce the bending moment applied to the cross-section to a couple of forces located at the level of the axes of the beam flanges. The intensity of the forces is limited to the design resistance of the flanges in tension and compression, due attention being paid to the possible local buckling of the flange in compression. The web, the bending resistance of which is neglected, is usually devoted to the transfer of shear forces. Amongst the four above-mentioned criteria, three are therefore satisfied. As a matter of fact, no condition is fixed for what regards the compatibility of the displacements within the section. This so-called static approach is known to lead to a safe estimation of the design resistance of the section and is usually followed for sake of simplicity.

The procedure to distribute internal forces within structural joints is quite similar to that described in the foregoing paragraphs for beam and column cross-sections. That is what we intend to demonstrate in the remainder of this chapter. In 3.2.3.2, the procedure followed by Eurocode 3 Annex J is described; it applies to steel beam-to-column joints and beam splices where the beam(s) is (are) subject to bending moments and shear forces. For sake of simplicity and to allow for a hand calculation, two separate distribution procedures are detailed, one for the evaluation of the elastic initial stiffness and another one for the assessment of the design resistance of the joint.

In 3.2.3.3, a more general procedure is presented, that allows to follow the behaviour of the studied joint from the first beginning to collapse. It also applies to steel beam-to-column joints and beam splices but its particularity is to allow for axial tensile or compressive forces to be applied to the joint(s) in addition to bending moments and shear forces.

3.2.3.2 Joint under bending and shear forces

In the next pages, the Eurocode 3 Annex J procedures for distribution of internal forces in the elastic range and at collapse are presented.

It has to be pointed out that the initial elastic stiffness and the design resistance are considered by Eurocode 3 as the two main parameters characterizing the response of a joint in bending. Based on these two values, a full $M-\phi$ curve can then be derived as shown in Figure 3-62.

Provided that the non-linear $M-\phi$ curve of revised Annex J is not limited by the rotational capacity (ϕ_{Cd}), this curve consists of three parts. Up to a level of $2/3$ of the design moment resistance M_{Rd} , the curve is assumed to be linear elastic. The corresponding stiffness is the so-called initial stiffness $S_{j,ini}$. Between $2/3 M_{Rd}$ and M_{Rd} , the curve is non-linear. After the moment in the joint reaches M_{Rd} a yield plateau develops.

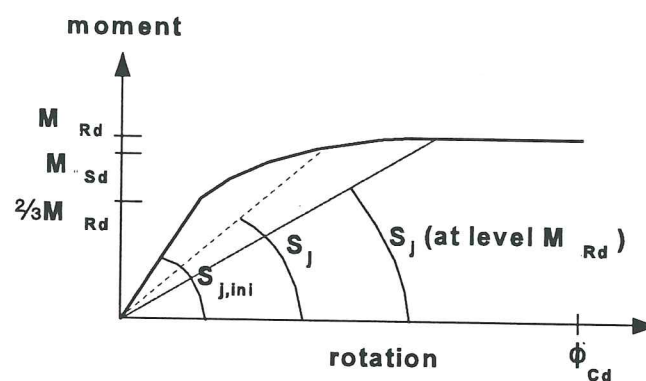


Figure 3-62 Non-linear $M-\phi$ curve according to Annex J

The model assumes a fixed ratio between the initial stiffness $S_{j,ini}$ and the secant stiffness at the intersection between the non-linear part and the yield plateau (S_j at level M_{Rd}). For end-plated and welded joints, this ratio is equal to 3. For flange cleated joints, this ratio is 3,5. These values are approximated values; they result from studies and test observations reported in our Ph.D. thesis [J1].

The shape of the non-linear part between $2/3 M_{Rd}$ and M_{Rd} is given by the following interpolation formula :

$$S_j = \frac{S_{j,ini}}{\left(\frac{1,5M_{Sd}}{M_{Rd}} \right)^\psi} \quad (3-39)$$

where $\psi = 2,7$ for end-plated and welded joints and 3,1 for flange cleated joints.

In this interpolation formula, the value of S_j is dependent on M_{Sd} .

Stiffness assembly

As revised Annex J refers to the so-called component method, the rotational response of a joint is determined based on the mechanical properties of its different constitutive components. The advantage is that an engineer is able to calculate the mechanical properties of any joint by decomposing the joint into relevant components. Annex J gives direct guidance for end-plated, welded and flange cleated joints for this decomposition. Table 3-4 shows an overview of components to be taken into account when calculating the initial stiffness for these types of joints.

Component	Number	End-plated	Welded	Flange cleated
Column web panel in shear	1	x	x	x
Column web in compression	2	x	x	x
Column flange in bending	3	x		x
Column web in tension	4	x	x	x
End-plate in bending	5	x		
Flange cleat in bending	6			x
Bolts in tension	7	x		x
Bolts in shear	8			x
Bolts in bearing	9			x

Table 3-4 Overview of components for different joints

In the model, it is assumed that the deformations of the following components : a) beam flange and web in compression, b) beam web in tension and c) plate in tension or compression are included in the deformations of the beam in bending. Consequently they are not assumed to contribute to the flexibility of the joint. Haunches, when present, fall also in this category.

The initial stiffness $S_{j,ini}$ is derived from the elastic stiffnesses of the components. The elastic behaviour of each component is represented by an extensional spring. The force-deformation relationship of this spring is given by :

$$F_i = k_i \cdot E \cdot \Delta_i \quad (3-40)$$

where F_i is the force in the spring i ;
 k_i is the stiffness coefficient of the component i ;
 E is the Young modulus;
 Δ_i is the deformation of the spring i .

The spring components in a joint are combined into a spring model. Figure 3-63 shows for example the spring model for an unstiffened welded beam-to-column joint.

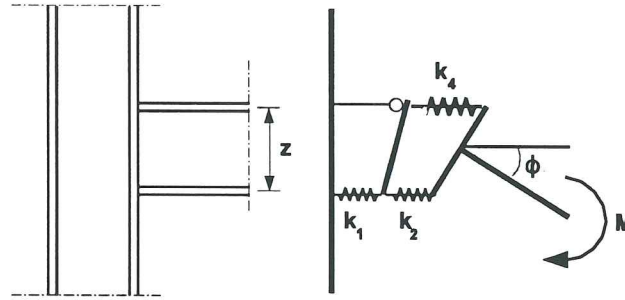


Figure 3-63 Spring model for an unstiffened welded joint

The force in each spring is equal to F . The moment M acting on the spring model is equal to $F \cdot z$, where z is distance between the centre of tension (for welded joints, located in the centre of the upper beam flange) and the centre of compression (for welded joints, located in the centre of the lower beam flange). The rotation ϕ in the joint is equal to $(\Delta_1 + \Delta_2 + \Delta_4) / z$. In other words:

$$S_{j,ini} = \frac{M}{\phi} = \frac{F_z}{\frac{\sum \Delta_i}{z}} = \frac{Fz^2}{E \sum \frac{1}{k_i}} = \frac{Ez^2}{\sum \frac{1}{k_i}} \quad (3-41)$$

The same formula applies for an end-plated joint with a single bolt-row in tension and for a flange cleated joint. However, components to be taken into account are different, see Table 3-2.

Figure 3-64.a shows the spring model adopted for end-plated joints with two or more bolt-rows in tension. It is assumed that the bolt-row deformations for all rows are proportional to the distance to the point of compression, but that the elastic forces in each row are dependent on the stiffness of the components. Figure 3-64.b shows how the deformations $k_{i,r}$ of components 3, 4, 5 and 7 are added to an effective spring per bolt-row, with an effective stiffness coefficient $k_{eff,r}$ (r is the index of the row number). In Figure 3-64.c is indicated how these effective springs per bolt-row are replaced by an equivalent spring acting at a lever arm z . The stiffness coefficient of this effective spring is k_{eq} . The effective stiffness coefficient k_{eq} can directly be applied in Formula 3-41. The formulae to determine $k_{eff,r} z$ and k_{eq} are as follows :

$$k_{eff,r} = \frac{1}{\sum_i \frac{1}{k_{i,r}}} \quad (3-42)$$

$$z = \frac{\sum_r k_{eff,r} h_r^2}{\sum_r k_{eff,r} h_r} \quad (3-43)$$

$$k_{equ} = \frac{\sum_r h_{eff,r} h_r}{z} \quad (3-44)$$

They can be derived from the sketches of Figure 3-64. The bases for these formulae is that the moment-rotation behaviour of each of the systems in Figure 3-64.a to 3-64.c is equal. An additional condition is that the compressive force in the lower rigid bar is equal in each of these systems.

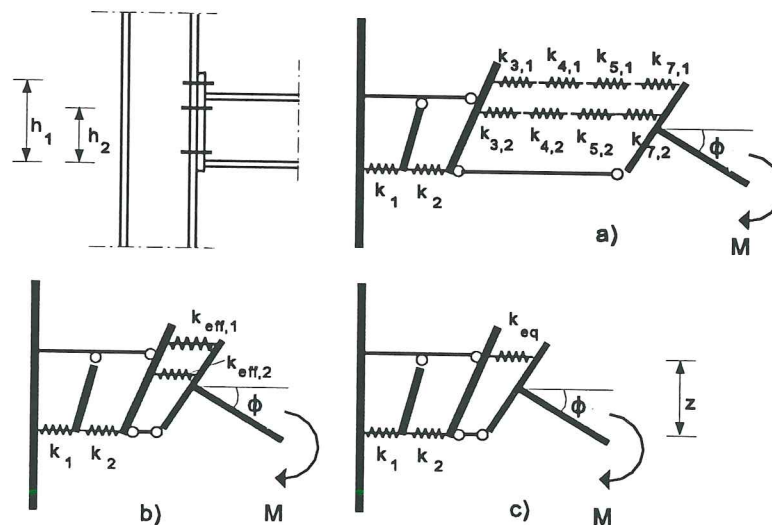


Figure 3-64 Spring model for a beam-to-column end-plated joint with more than one bolt-row in tension

In this stiffness model :

- the internal forces are in equilibrium with the bending moment;
- the compatibility of the displacements is ensured through the assumption of an infinitely rigid transverse stiffness of the beam cross-section;

- the plasticity criterion is fulfilled as long as the elastic resistance of the springs is not reached;
- no ductility requirement is likely to limit the deformation capacity of the springs in the elastic range of behaviour as long as Eurocode 3 Annex J components are of concern.

The solution provided by Eurocode 3 Annex J for initial stiffness prediction fulfils the four main requirements to which any distribution of internal forces should satisfy, from a theoretical point of view, and can therefore be considered as an « exact » one.

Strength assembly

The procedure for strength assembly as suggested in Eurocode 3 revised Annex J is aimed at deriving the value of the so-called design resistance of the joint (see Appendix 1). By sake of clarity, it is not presented here in a general way but is illustrated in the particular case of beam splices with flush end-plates.

For the connection represented in Figure 3-65, the distribution of internal forces is quite easy to obtain : the compressive force is transferred at the centroid of the beam flange, the tension force, at the level of the upper bolt-row. The resistance possibly associated to the lower bolt-row is usually neglected as it contributes in a quite modest way to the transfer of bending moment in the joint (small level arm).

The design resistance of the joint M_{Rd} is associated to the design resistance F_{Rd} of the weakest joint component, either the beam flange and web in compression, the beam web in tension or the plate in bending and bolts in tension. For the two last components (plate and bolts), reference is made to the concept of "idealized T-stub" introduced in Appendix 3. So :

$$M_{Rd} = F_{Rd} \cdot z \quad (3-45)$$

where z is the level arm.

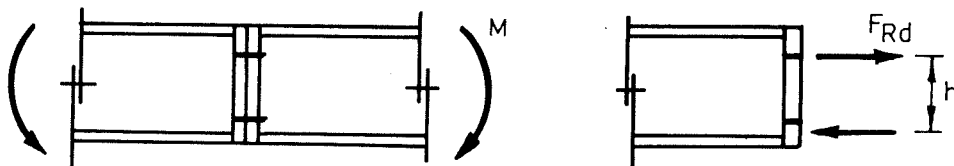


Figure 3-65 Joint with one bolt-row in tension

When more than one bolt-row are to be considered in the tension zone (Figure 3-66), the distribution of internal forces is more complex.

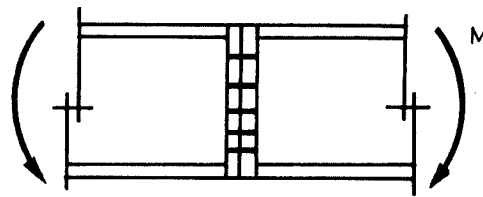


Figure 3-66 Joint with more than one bolt-row in tension

Let us assume, in a first time, that the design of the joint leads to adopt a particularly thick end-plate in comparison to the bolt diameter (Figure 3-67). The distribution of internal forces between the different bolt-rows is linear according to the distance from the centre of compression. The compression force F_c which equilibrates the tension forces acts at the level of the centroid of the lower beam flange. For sake of clarity, it is only represented in Figure 3-67 and not in the following ones.

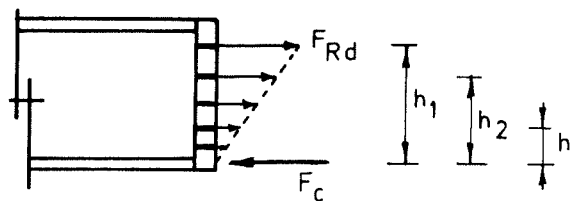


Figure 3-67 Joint with a thick end-plate

The design resistance M_{Rd} of the joint is reached as soon as the bolt-row subjected to the highest stresses - in reality, that which is located the farthest from the centre of compression - reaches its design resistance in tension $2B_{t,Rd}$.

As a matter of fact, the quite limited deformation capacity of the bolts in tension does not allow any redistribution of forces to take place between bolt-rows.

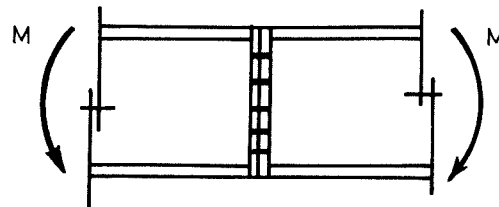
It is here assumed that the design resistance of the beam flange and web in compression is sufficient to transfer the compression F_c force. The tensile resistance of the beam web is also assumed not to limit the design resistance of the joint. M_{Rd} is so expressed as (Figure 3-67) :

$$M_{Rd} = \frac{F_{Rd}}{h_1} \sum h_i^2 \quad (3-46)$$

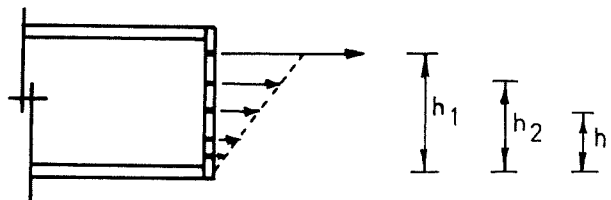
For thinner end-plates, the distribution of internal forces requires much more attention. When the first loads are applied to the joint, the forces distribute between the bolt-rows according to the relative stiffnesses of the latter. This stiffness is namely associated to that of the part of the end-plate adjacent to the considered bolt-row. In the particular case

of Figure 3-68 , the upper bolt-row is characterized by a higher stiffness because of the presence there of the beam flange and web welded to the end-plate.

Because of the higher stiffness, the upper bolt-row transfers proportionally a higher load than the lower ones (Figure 3-68.b)



(a) Configuration



(b) Distribution of the internal forces at the beginning of the loading

Figure 3-68 Joint with a thin end-plate

In Eurocode 3 Annex J, it is assumed that the upper bolt-row will reach first its design resistance. This assumption is probably quite justified in the particular case being considered but is probably less justified for other connection types such as for end-plate connections with an extended part in the tension zone where it is usual that the second bolt-row reaches first its design resistance - that located just beneath the beam flange in tension-.

The design resistance of the upper bolt-row may be associated to that of the bolts only (Mode 3 in Appendix 3), of the end-plate only (Mode 1), of the bolt-end-plate assembly (Mode 2) or to that of the beam web in tension. If its failure mode is ductile, a redistribution between the bolt-rows can take place : as soon as the upper bolt-row reaches its design resistance, the supplementary bending moments applied to the joint are carried over by the lower bolt-rows (the second, then the third, etc.) which, each one in their turn, reach their own design resistance.

The failure may occur in three different ways :

- i. The plastic redistribution of the internal forces extends to all bolt-rows because of their sufficient deformation capacity. The redistribution is said "complete" and the resulting distribution of internal forces is called "plastic".

The design moment resistance M_{Rd} is expressed as (Figure 3-69) :

$$M_{Rd} = \sum_i F_{Rd,i} h_i \quad (3-47)$$

The plastic forces $F_{Rd,i}$ vary from one bolt-row to another according to the failure modes (bolts, plate, bolt-plate assembly, beam web, ...).

Eurocode 3 considers that a bolt-row possesses a sufficient deformation capacity to allow a plastic redistribution of internal force to take place when :

- $F_{rd,i}$ is associated to the failure of the beam web in tension or;
- $F_{Rd,i}$ is associated to the failure of the bolt-plate assembly (including failure of the bolts alone or of the plate alone) and :

$$F_{Rd,i} \leq 1,9 B_{t,Rd}$$

The background of the « $1,9 B_{t,Rd}$ » criterion is given in the Appendix 3 of the present thesis.

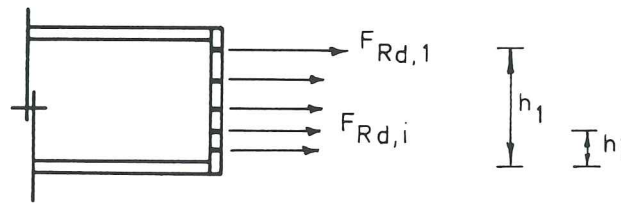


Figure 3-69 Plastic distribution of forces

- ii. The plastic redistribution of forces is interrupted because of the lack of deformation capacity in the last bolt-row which has reached its design resistance ($F_{Rd,k} > 1,9 B_{t,Rd}$ and linked to the failure of the bolts or of the bolt-plate assembly).

In the bolt-rows located lower than bolt-row k , the forces are then linearly distributed according to their distance to the point of compression (Figure 3-70).

The design moment resistance equals :

$$M_{Rd} = \sum_{i=1,k} F_{Rd,i} + \frac{F_{Rd,k}}{h_k} \sum_{j=k+1,n} h_j^2 \quad (3-48)$$

where : n is the total number of bolt-rows;

k is the number of the bolt-row, the deformation capacity of which is not sufficient.

In this case, the distribution is said "elasto-plastic".

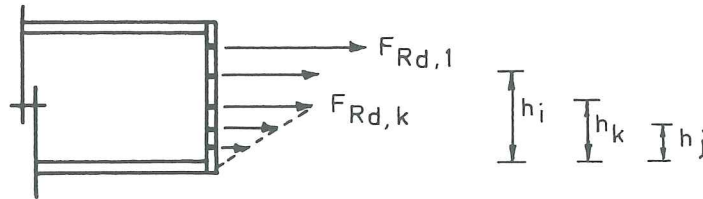


Figure 3-70 Elasto-plastic distribution of internal forces

iii. The plastic or elasto-plastic distribution of internal forces is interrupted because the compression force F_ℓ identifies itself to the design resistance of the beam flange and web in compression. The moment resistance M_{Rd} is evaluated with similar formulae than (3-47) and (3-48) in which, obviously, only a limited number of bolt-rows are taken into consideration. These bolts rows are such that :

$$\sum_{\ell=1,n} F_\ell = F_{c.Rd}$$

where : m is the number of the last bolt-row transferring a tensile force;

F_ℓ is the tensile force in bolt-row number ℓ ;

$F_{c.Rd}$ is the design resistance of the beam flange and web in compression

The application of the here above-described principles to beam-to-column joints is quite similar. The design resistance associated to each of the bolt-rows is possibly limited in this specific situation not only by the resistance of :

- the end-plate in bending,
- the bolts in tension,
- the beam web in tension,

but also by that of :

- the column web in tension,
- the column flange in bending.

The design moment resistance M_{Rd} is, as for the beam splices, likely to be limited by the resistance of :

- the column web in compression;

but also by that of :

- the column web panel in shear.

In Eurocode 3 Annex J, evaluation formulae are provided for each of these components. Annex J also presents a full example showing how to distribute the internal forces in a beam-to-column joint with a "multi-bolt-rows" end-plate connection.

This example also highlights the concept of individual and group yield mechanisms. When adjacent bolt-rows are subjected to tension forces, various yield mechanisms are likely to form in the connected plates (end-plate or column flange).

- individual mechanisms (see Figure 3-71.a) which develop when the distance between the bolt-rows are sufficiently large;
- group mechanisms (see Figure 3-71.b) including more than one adjacent bolt rows.

To these mechanisms are associated equivalent lengths (see Figure 3-71) and, through specific formulae, design resistances (see Appendix 3 of the present thesis).

When distributing the internal forces, Eurocode 3 recommends never to transfer in a bolt-row :

- a higher load than that which can be carried out if it is assumed that the considered bolt-row is the only one able to transfer tensile forces (individual resistance);
- a load such that the resistance of the whole group to which the bolt-row belongs is exceeded.

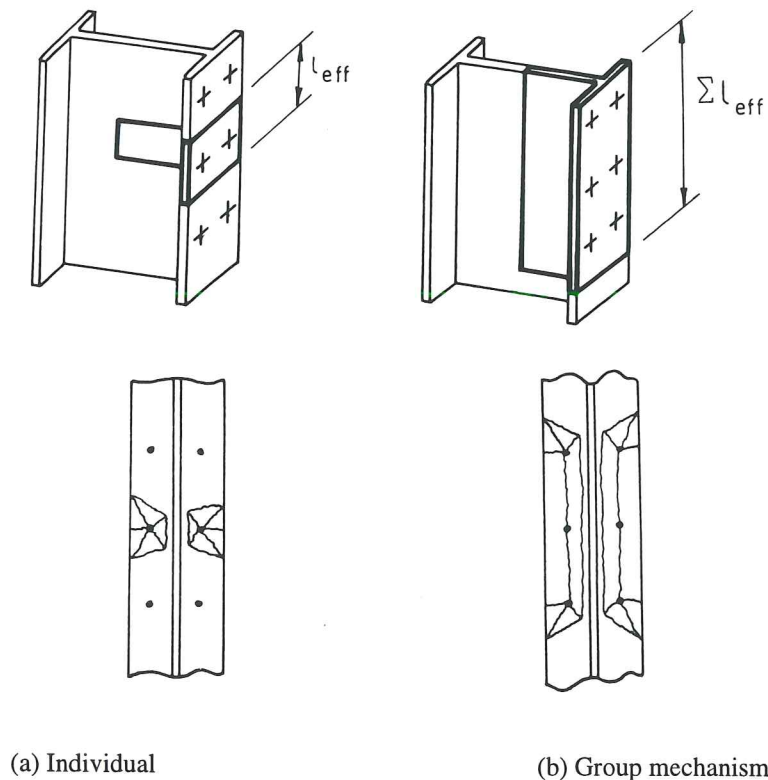
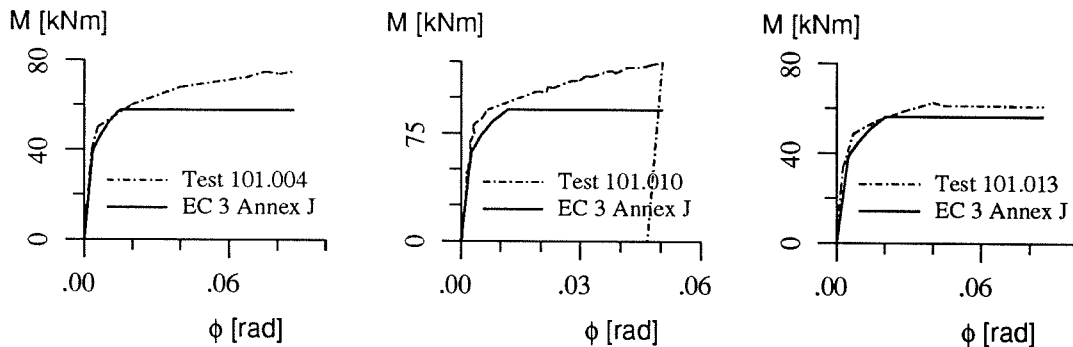


Figure 3-71 Plastic mechanisms

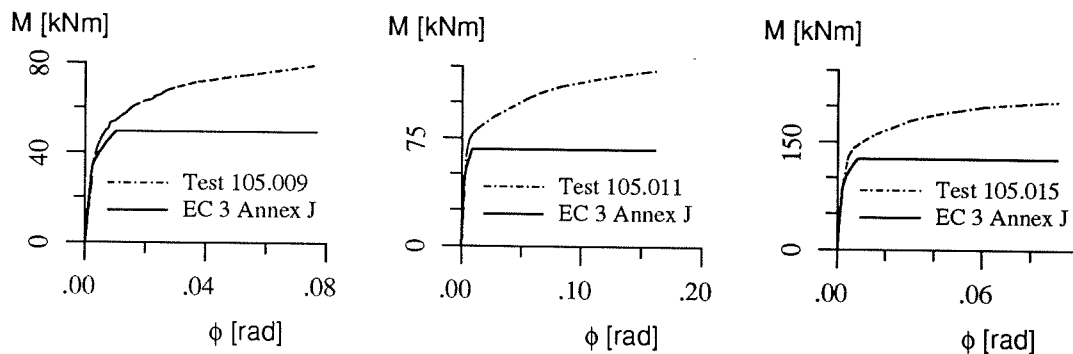
Validation through comparisons with test results

This section presents comparisons between the stiffness and resistance models of Eurocode 3 and test results. The test data are taken from the databank SERICON [S2]. The comparisons, which are extracted from a common publication with K.Weynand (RWTH Aachen) and M. Steenhuis (TNO Delft) [W1], are made on full non-linear moment-rotation curves so as to show the general accuracy of the model as a whole.

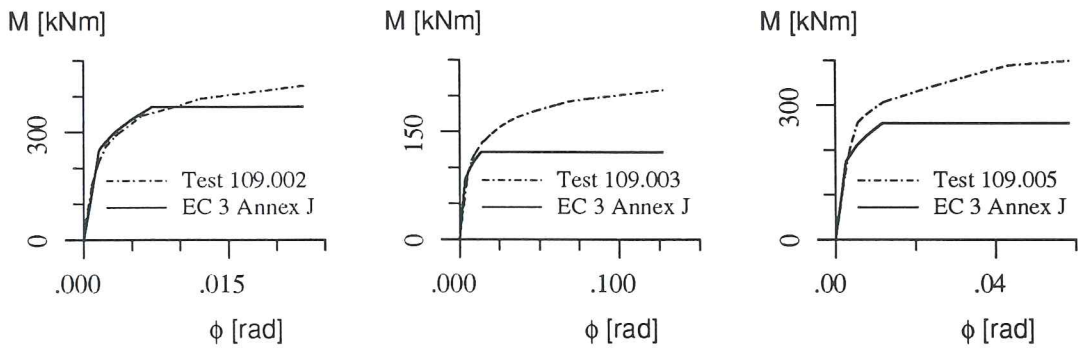
For the determination of the joint properties, i.e. initial stiffness and resistance, measured material and geometrical data obtained from tests are used. The value of the moment resistance M_{Rd} is calculated with safety factors $\gamma=1,0$. The moment resistance is determined according to the most accurate model of Annex J, e.g. the alternative method to determine the resistance of the T-stub is used for joints with bolted connections. Both the rotational stiffness and the moment resistance are calculated by taking into account the actual forces in the shear panel of the column web through exact values of the β -coefficient.



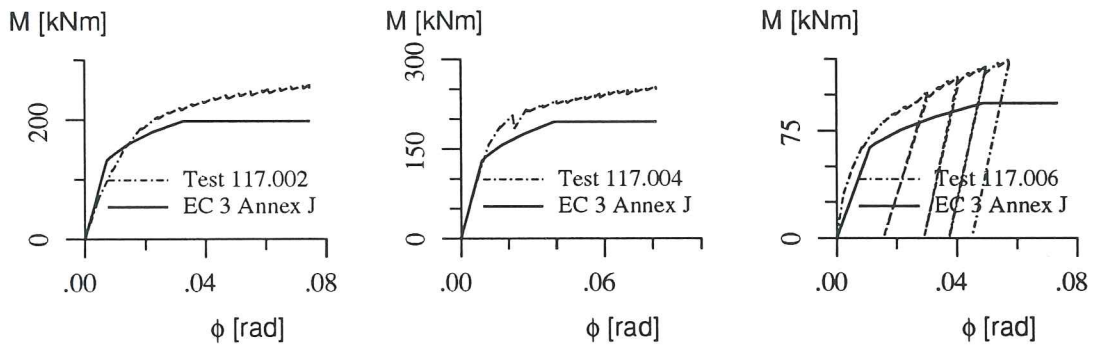
(a) Liège, single-sided, end-plated joints



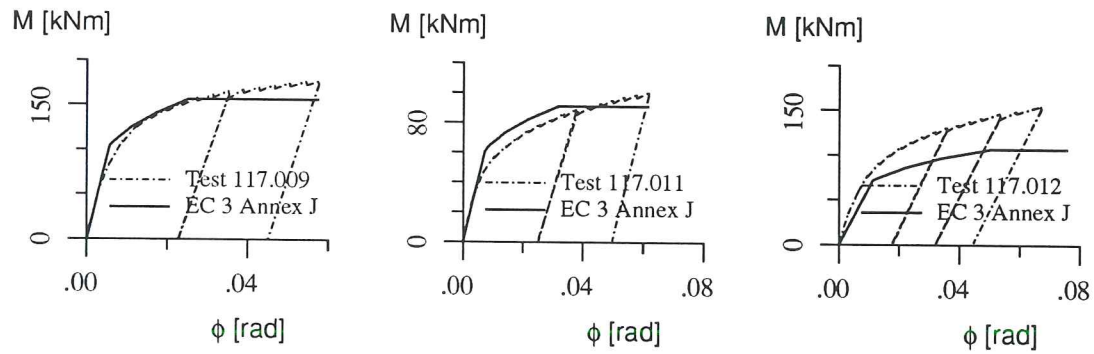
(b) Innsbruck, single-sided, welded joints



(c) Innsbruck, double single-sided, end-plated joints



(d) Leipzig/Aachen, single-sided, end-plated joints



(e) Leipzig/Aachen, double-sided, end-plated joints

Figure 3-72 Comparison with test results

It can be seen from Figure 3-72 that the prediction of the joint stiffness and resistance is in good agreement with the actual behaviour. The differences in the resistance are due to strain hardening and membrane effects which are not taken into account in the design rules of Annex J. This point is discussed in Appendix 2. In the stiffness model, it is assumed that a joint remains elastic up to a level of 2/3 of M_{Rd} . This assumption is confirmed by the curves.

3.2.3.3 Joint under bending, shear and axial compressive or tensile forces

Introduction

In most of the cases, beam-to-column joints and beam splices are also subjected to axial compressive or tensile forces in addition to in-plane bending moments and shear forces.

These forces affect the joint response in terms of stiffness, resistance and rotation capacity. They can therefore not be disregarded.

In revised Annex J of Eurocode 3, this reality has been recognized and a range of validity has been defined where it is assumed that the axial forces are not influencing significantly the joint response and where it is therefore recommended to evaluate the joint properties under bending moments and shear forces only. The related criterion writes :

$$\left| \frac{N}{N_{p,b}} \right| \leq 0,1 \quad (3-49)$$

where : N is the axial force in the beam;

$N_{p,b}$ is the design resistance of the beam in compression.

It has to be immediately said that no background exists to justify this so-called "10 % rule" and that it has been included in Annex J despite the opinion of the three authors of the document - and we were amongst them - who, convinced of the necessity to specify the field of application of the Eurocode 3 stiffness and resistance evaluation procedures for joints, were suggesting a "5 % rule", so following the French Recommendations [].

The criterion (3-49) is not often restrictive as long as beam-to-column joints and beam splices are concerned. It however becomes quickly limitative if the latter - then respectively called knee and ridge joints - belong to pitched-roof portal frames where the inclination of the rafters induce significant axial forces in the joints.

For column splices and column bases, the axial compressive force in the column element is predominant; these joints fall outside the range of application defined by Formula (3-49).

For joints which would not fulfil the "10 % rule", Eurocode 3 gives no recommendations. In fact, the designer may still refer to the component method to evaluate the joint properties - the individual response of the basic components being not dependent on the external loading of the joint, except for what regards interactions - but has to determine by himself the procedure to assemble the components together in an appropriate way. In other words, the responsibility of the joint design is in the hands of the designer.

This does not result from a wish, but clearly from a lack of information on how to introduce the influence of axial forces in the available design procedures for joints.

In order to deepen the knowledge in this field, we have carried out research works that we reflect in the following sections.

Similarities and specificities comparatively to joints under bending and shear

As already said, the component properties remain unchanged whatever the external loading applied to the joint. On the other hand, the definition of the activated components and the assembly procedures raise specific problems. Let us first comment on these similarities and specificities, sometimes by referring to particular cases, for clarity.

Similarities

- As for any other joint, the distribution of internal forces has to be such that the four basic conditions listed in Section 3.2.3.1 are fulfilled; these are briefly recalled here :
 - equilibrium between internal and external forces;
 - compatibility of the internal displacements;
 - limitation of the internal forces to their design values;
 - limitation of the deformation of the components to its maximum value.

Safe estimations of the resistance properties may be obtained by fulfilling the first, third and four conditions and disregarding the second one. A so-called static approach is then followed.

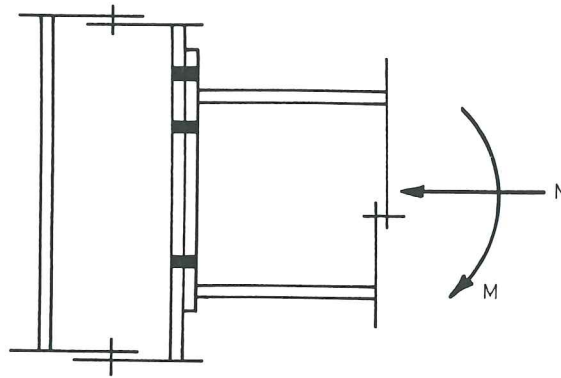
- The procedures for component characterization remain unchanged and no other interactions between components than those discussed in Section 3.2.2 have to be contemplated.

Specificities

- The joint drawn in Figure 3-73.a is subjected to bending moments and axial forces. Two possible distributions of internal forces in the joint are reported in Figure 3-73.b and in Figure 3-73.c. They correspond to two different ratios between M and N .

For a rather high value of M/N , compressive forces are carried over in the vicinity of the lower beam of flange and tensile forces are transferred in the bolt-rows in tension.

For decreasing values of M/N , the axial force slowly predominates and the upper part of the connection tends to transfer compressive forces as illustrated in 3.73.c; the bolts are no more activated in tension and the same applies to the end-plate in bending, the beam web in tension, the column flange in bending and the column web in tension.



(a) Joint in bending and compression

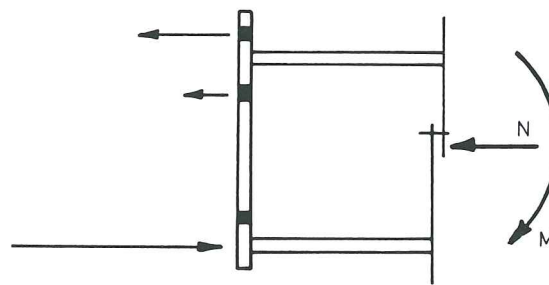
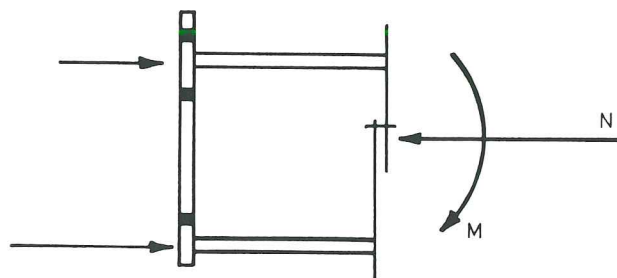
(b) High M/N ratio(c) Low M/N ratio

Figure 3-73 Activation of the components according to the external joint loading

In contrast to what happens for joints in bending, the activation of the components is seen here to depend on the joint loading and the definition of the activated components in advance of the calculation may therefore not be contemplated.

- In the two identical sub-structures illustrated in Figure 3-74 where the beam is respectively subjected to bending and bending and axial compression, the shear forces in the column web panels are equal. The tensile and compressive load-introduction forces in the panel are identical in the first sub-structure while they differ in the second one. The level of interaction between load-introduction forces and shear forces differs therefore, in the second sub-structure, in the tensile and compressive zones, what does not occur in joints subjected to bending only. This specific aspect has also to be carefully taken into consideration.

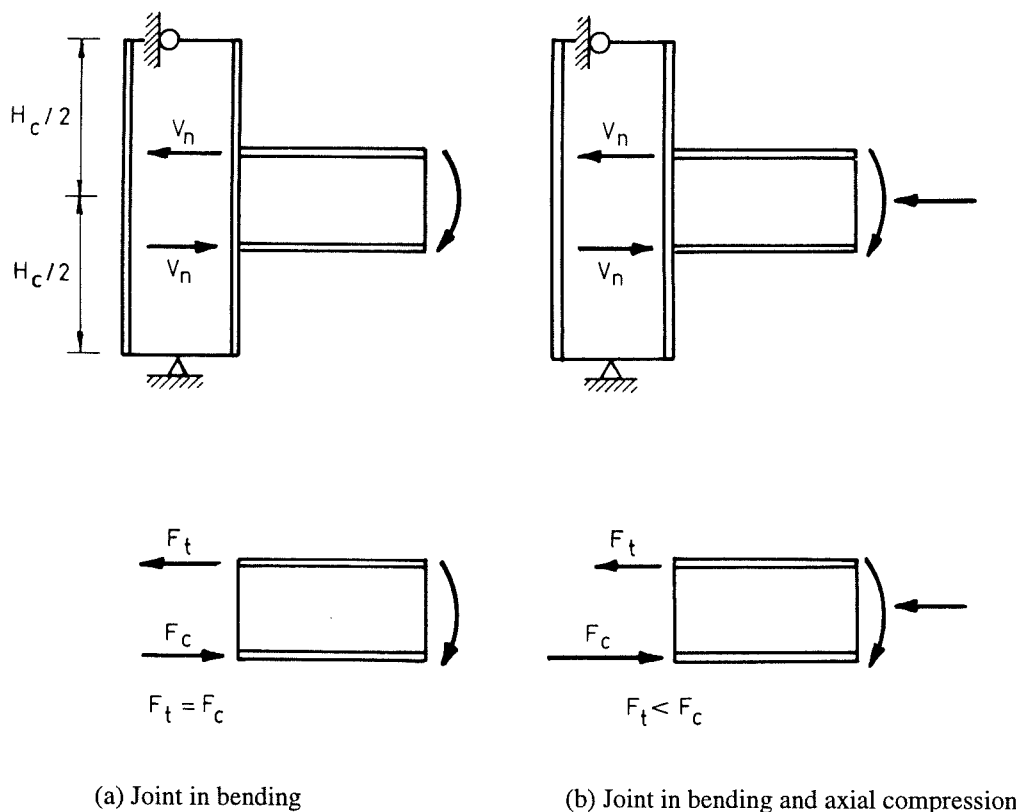


Figure 3-74 Particular sub-structures with different load-introduction forces and identical shear forces in the column web panel

Recent works on joint assembly

Different research works aimed at deriving a procedure for distribution of internal forces in joints subjected to combined bending and axial forces have been carried out in the last years. In the next sections, we reflect these ones in a chronological order before reporting on our recent developments.

To introduce these three contributions, let us consider, for clarity, the particular case of a major axis single-sided beam-to-column joint with an end-plate connection (Figure 3-75).

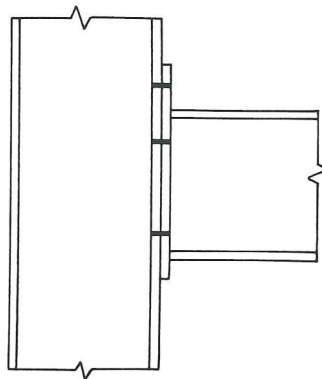


Figure 3-75 End-plated joint

Contribution of Hoffmann [H1]

The objective of Hoffmann is to derive a hand calculation procedure for the evaluation of the design resistance of joints subjected to bending and compression (or tension). The determination of the stiffness joint properties is not contemplated.

To achieve this goal, Hoffmann develops an approach, the steps of which are described hereunder.

Step 1 : All the possibly activated components in the joint are first identified and their design resistance is assessed according Eurocode 3 Annex J. The way the internal forces distribute within the joint being unknown, two resistances have in fact to be considered for each component.

To clarify this point, let us consider the diagrams presented in Figure 3-76, and more particularly the extended part of the plate. When M is predominant, the extended part of the plate is subjected to transverse bolt forces and a risk of yielding in the plate has to be contemplated. On the other hand, when N is predominant, the extended part of the plate is in a compression zone and do not contribute to the transfer of forces between the connected members. A "zero" resistance is then associated to this non-activated component. A similar conclusion may be drawn for the column flange in bending. For the column web panel in shear, two "non-zero" design resistances have to be evaluated according to the sense in which shear is applied. The beam flange in compression is only activated when located in the compression zone, as seen in Figure 3-76.a and b.

Finally, the column web in compression is activated only there where a transverse compressive force is applied by a beam flange. When the beam flange is in the tensile zone, a "zero" resistance is given to the component, and another component called "beam web in tension" is activated.

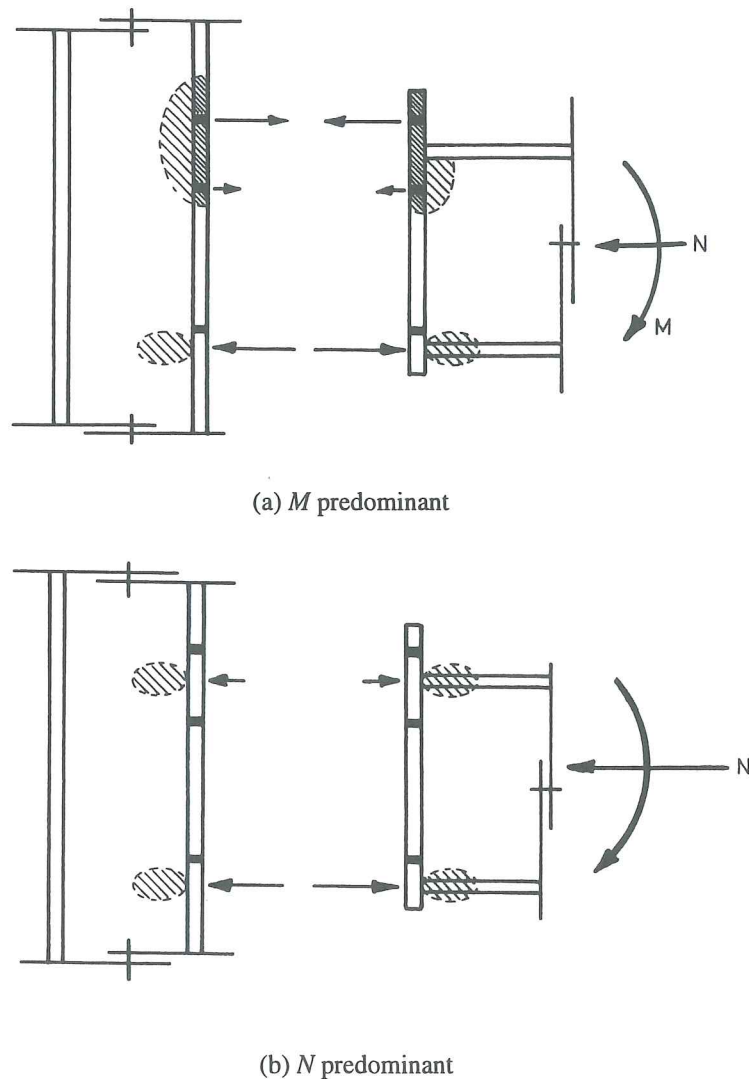


Figure 3-76 Design resistances of the constitutive components

Step 2 : Unknown forces are applied to all the components.

Step 3 : The equilibrium between the applied forces and the unknown internal forces is expressed through appropriate equations.

Step 4 : By a sort of trials and error process, sets of internal forces are selected.

These sets have :

- to fulfil the equilibrium equations;
- not to exceed the design resistance of the individual components;
- to form a logical pattern, e.g. to activate a column web in compression between two bolt-rows in tension is unacceptable.

The procedure applies as follows :

- a value of the applied external axial force is chosen;
- sets of internal forces equilibrating these axial forces are selected on the basis of the here above-mentioned criteria; plastic distributions of internal forces are considered as quite acceptable;
- the bending moment associated to these sets of internal forces is evaluated;
- the set of forces leading to the maximum moment resistance is selected; it is considered as the design moment resistance of the joint under combined loading.

Step 5 : The sufficient deformation capacity of the components, the design resistance of which has been reached, is checked in accordance with the rules of Eurocode 3 revised Annex J.

If one of these components does not satisfy the criteria on deformation capacity, the design resistance of the joint in terms of bending moment and axial force is considered to be equal to $2/3$ of the first calculated value obtained in step 4.

This procedure is nothing else than an application of the static approach where internal forces are selected so as to fulfil equilibrium equations and not to exceed the resistance of the components. The safe character of the process has been pointed out, what justifies the wish to maximize the solution in terms of joint design resistance.

The sufficient deformation capacity of the yielded components has obviously to be ensured, but the sequence in which the components yield is unknown, what obliged Hoffmann to limit the design resistance of the joint to its maximum elastic value as soon as a component is seen not to possess sufficient deformation capacity. Such a safe approach may be obviously considered as rather uneconomical in cases where the non-ductile component is the last one to yield and is therefore not limiting the design resistance of the joint.

In conclusion, the study of Hoffmann shows that a solution satisfying all the basic requirements for joint design may be obtained through a static approach. The procedure is long and tedious to apply by hand and is therefore clearly not suitable for practical applications.

Contribution of Steenhuis [S5]

The approach followed by Steenhuis is quite similar than that suggested by Hoffmann. His work goes however beyond what has been described in the previous paragraphs, in the sense than he proposes a more consistent way to solve the problem and maximize the solution through the use of linear programming.

As a matter of fact, Steenhuis identifies similarities between the problem of plastic distribution of internal forces in the joints and the analysis of a frame by means of a first-order rigid-plastic theory where the objective is to maximize the external load acting on the frame with the following constraints :

- the internal forces in the frame have to be in equilibrium with the external ones;
- the internal forces should not exceed the plastic capacity of the members.

The similarities between the two problems being obvious, Steenhuis therefore suggests to use for joints the same tools than those traditionally used for frames and, in particular, linear programming.

The use of a computer has obviously to be contemplated, what has been clearly understood by Steenhuis who introduced this procedure in the CASTA connections software developed in the Netherlands.

In this approach, it is implicitly assumed that the deformation capacity of all the constitutive components is unlimited as full plastic redistribution of internal forces in the joints is allowed. No guideline is given in [S5] on how to proceed when this basic criterion is not fulfilled.

Contribution of Finet [F2] and the author

On the basis of the work performed by Hoffmann and Steenhuis, we arrived to the conclusion that it was quite premature nowadays to investigate further the possibility to derive a hand calculation procedure to derive the resistance properties of joints in bending and compression or tension. We therefore decided to revise our initial work planning by trying first to develop a software approach in which :

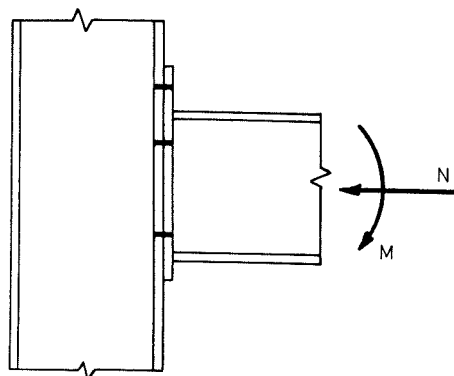
- the component method would be referred to;
- the response of the joint would be followed from the first loading steps to failure;
- the aspects of stiffness, resistance and deformation capacity of the components would be all taken into consideration.

In a second step, this tool, aimed at reflecting as closely as possible the actual response of the joint throughout its loading, could then be used in the frame of parametrical studies to better understand how the joints behave, and could constitute a sort of reference when

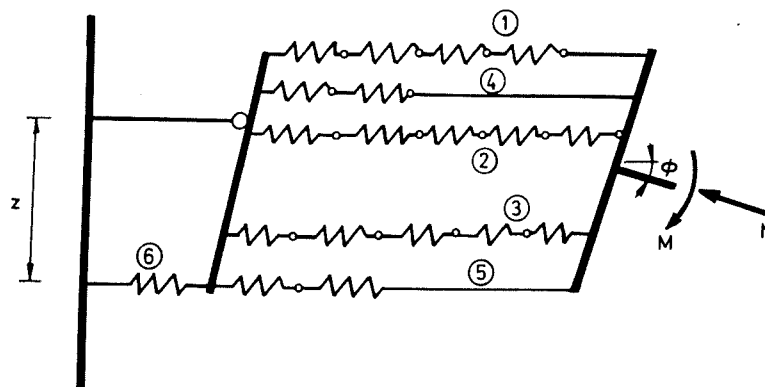
validating, in the final steps, simplified hand calculation procedures that would be based on the knowledge acquired in the previous research steps. In the following pages, we will report on the first step of this work planning.

The work started in 1994 in the frame of the diploma work of Finet. We suggested him to develop a so-called mechanical model, similar to those presented in Chapter 2 (Section 2.1), in which (see Figure 3-77) :

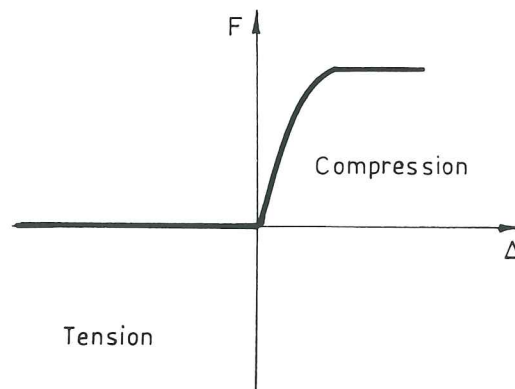
- the response of each component would be simulated by an extensional spring (Figure 3-77.b);
- the non-linear behaviour law of each component would be that predicted by Eurocode 3 revised Annex J;
- the two possible senses of application of the loading would be considered (Figure 3-77.c);
- the four basic requirements expressed in Section 3.2.3.1. and that any distribution of internal forces should fulfil would be satisfied.



(a) Joint detailing



(b) Mechanical model



(c) Behaviour law for components (particular case of the column web in compression)

Figure 3-77 Development of a mechanical model

The selected model is shown in Figure 3-77.b; it exhibits the following main behavioural features :

- At the level of the bolt-rows (levels 1, 2 and 3 in Figure 3-77.b), tensile forces are likely to be transferred by four or five springs in series corresponding respectively to :
 - the beam web in tension;
 - the beam flange in bending;
 - the bolts in tension;
 - the end-plate in bending;
 - the beam web in tension (except in the extended part of the plate);

All these components exhibit a zero stiffness in compression.

- At the level of the beam flanges (levels 4 and 5 in Figure 3-77.b), compression is transferred through two springs, those of the beam flange in compression and column web in compression respectively. They also carry no forces when located in a tensile zone.
- Components like beam web in tension or column flange in compression do not contribute, as already said, to the joint flexibility and are therefore characterized by an infinite stiffness in tension and compression respectively. However they are likely to limit the moment resistance.
- The beam end-section is assumed to be infinitely rigid under transverse in-plane bending; the way how the compatibility of the displacements is expressed is based on this assumption.

- The shear deformability of the column web panel is covered by the spring denoted 6 in Figure 3-77.b. The level arm z of the internal forces in the connection is derived from the study of the "connection" part of the model, similarly to what has been said in Section 3.2.3.2. (stiffness assembly), and used further when characterizing the response of the column web panel in shear.

The deformability curves ($M-\phi_I$, $N-\phi_I$, ...) characterizing the response of the whole system are built progressively by applying successive increments of loads and evaluating then the resulting deformability of the system and its constitutive components.

As the components exhibit a non-linear behaviour, the solution may only be found through an iterative procedure. At each iteration, the tangential stiffness of each component is evaluated so as to reflect the actual contribution of the latter to the stiffness of the whole system.

A similar approach is used in Section 3.4 for column bases and detailed information is given there on how to establish the system of equations characterizing the model and how to solve it in an appropriate way. The interested reader is therefore begged to refer to this section for more details.

The first steps in the software developments have been performed by Finet in [F2]; at the end of his diploma work, most of the components included in the revised Annex J of Eurocode 3 were available and the software was running for joints with end-plated joints where only a single bolt-row was activated in tension close to the beam flanges.

Recently we extended the scope of the software to connections with more than one bolt-row and solved the rather difficult problem which consisted in controlling the possible apparition of group yield line mechanisms in the column flange in bending, the end-plate in bending, the beam web in tension and the column web in tension. The complexity of the problem is linked to the apparent incompatibility of group yield mechanisms and the use of individual rows of springs (as the 1, 2 and 3 ones in Figure 3-77.b) in which the forces evolves independently (the only link is achieved through the criterion of displacement compatibility).

As these developments have been carried out in the frame of a bilateral collaboration with the COMMERCIAL INTERTECH-ASTRON company, all the details that the reader would require to make his own opinion on the pertinence of the works we carried out are not reported in this thesis but will in fact constitute the background for forthcoming publications in international journals or conferences.

Application of the software and conclusions

The procedure to compute the deformability curve of the joints allows to control the displacement and the level of plasticity in each of the components at any loading step. The progressive redistribution of internal forces between the components may be observed and the deformation capacity of the components may be checked.

The maximum resistance of the joints may be reached by full plastic redistribution of internal forces or by excess of deformation in one or more of the constitutive components in which an instability or brittle failure is expected to occur.

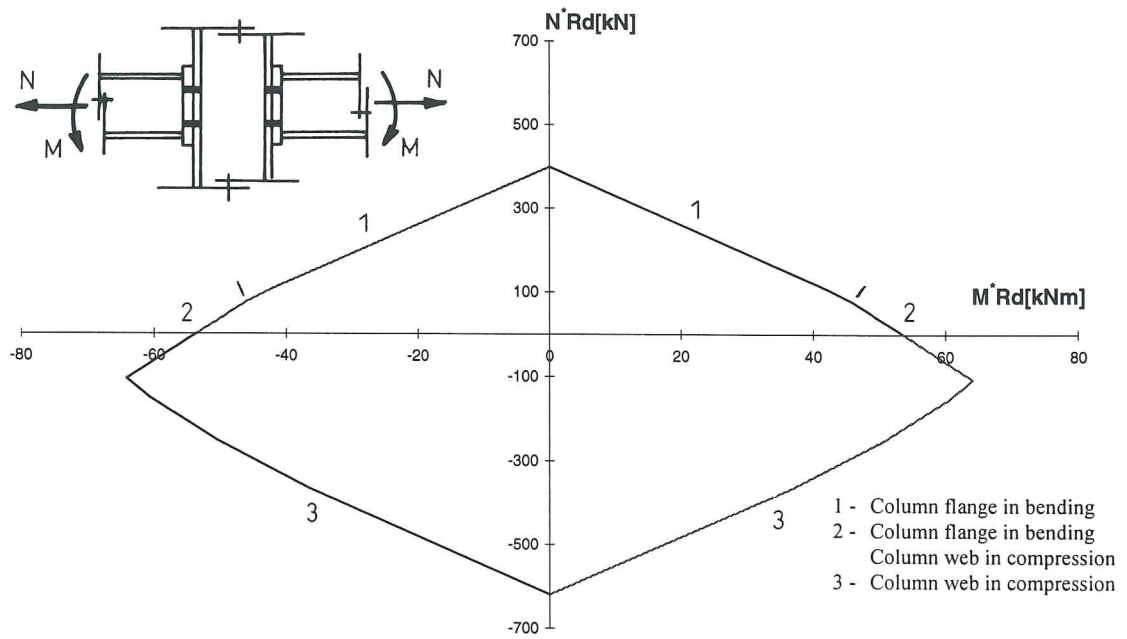
This makes of the software a rather good tool for further investigations in the field of structural joints, for instance, through parametrical studies aimed at pointing out the influence of specific parameters.

As already said, the software may also be used as a reference when deriving simplified calculation procedures more in line with designer's expectations.

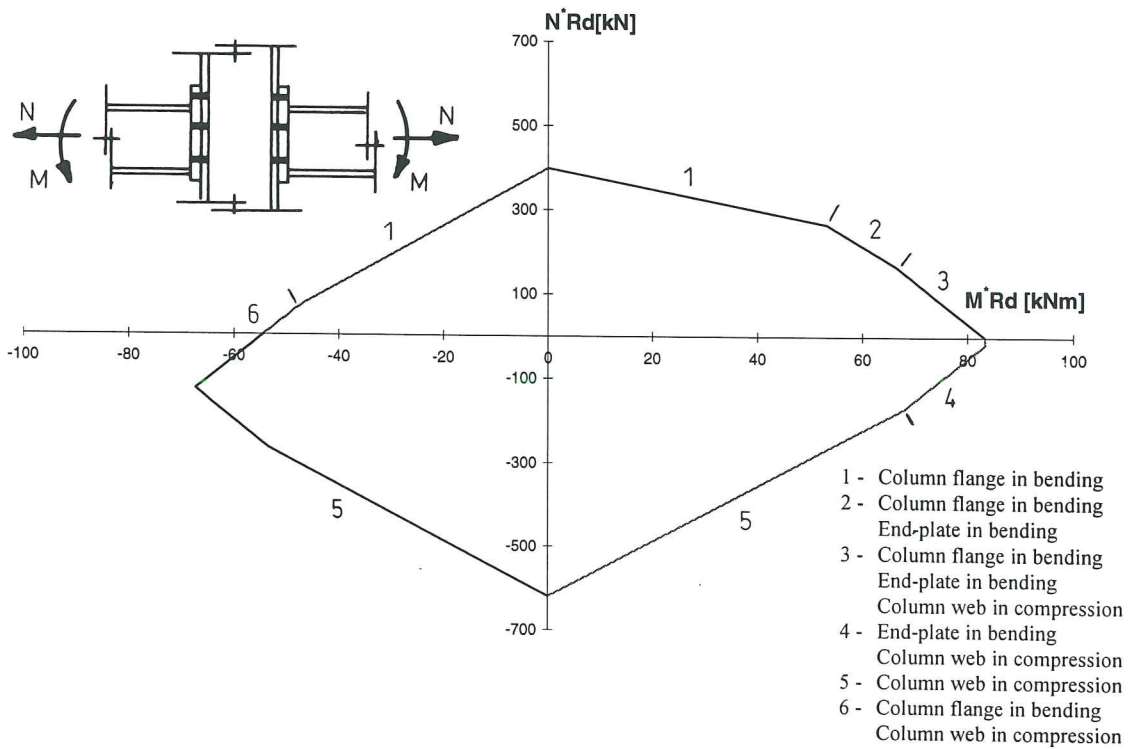
This work is presently in progress and should also be reflected in forthcoming publications.

In this section, we will illustrate its use through two applications on beam-to-column double-sided joint configurations, with a flush and an extended end-plate respectively. The results are presented in Figure 3-78.a and 78.b in the form of $M_{Rd}^* - N_{Rd}^*$ diagrams where $M_{Rd}^* - N_{Rd}^*$ are the design resistances of the joints subjected simultaneously to moments and axial forces. The positive sign of the applied forces is indicated in the sketches illustrating the joint configuration. The failure mode are indicated on the diagrams. They allow to understand why the axial force is sometimes increasing and sometimes decreasing the design resistance of the joint in bending only. The symmetry and dissymmetry of the diagrams reflect those of the joints themselves.

From these diagrams, it appears also clearly that the Eurocode 3 Annex J criterion (3-49) which specifies the range of validity of the assembly procedures for joints in bending only is far from being satisfactory. For an axial force $N/N_{p,b}$ in the beam equal to 0,1 , i.e. 115 kN, substantial decreases of design moment capacity of the joints may be observed, sometimes whatever is the sense of the axial force in the beam.



(a) Flush end-plate connection



(b) Extended end-plate connection

Figure 3-78 *M-N* interactions in end-plated joints

3.3 Minor axis beam-to-column joints

3.3.3 Introduction

Figure 3-79 shows some common types of beam-to-column minor-axis joints where the beam is directly connected to the column web without any stiffening. The connection may be welded or bolted by means of web cleats, flange cleats, flush end-plates or extended end-plates.

Revised Annex J of Eurocode 3 provides design rules for the evaluation of the resistance of most of the possible constitutive components (end-plates, cleats, bolts) but does not cover the main component, the column web under transverse forces, which contributes quite significantly to the overall joint deformability and where yielding occurs first in most of the cases.

The minor axis joints have been much less studied in the past than major axis ones. Their rotational behaviour is traditionally idealized as pinned; no bending moment is so transferred to the column, what is usually considered as quite beneficial as far as column flexural buckling is concerned.

In reality, minor axis joints exhibit a significant semi-rigid behaviour, what is likely to lead to a better balance between the end and mid-span moments in the secondary beams and to bring some restraint at the column ends; the effect of the end moments on the column stability being more than compensated by the decrease of the buckling length, as highlighted by different authors [J1], the use of semi-rigid minor axis joints is therefore likely to increase, but never to decrease, the carrying capacity of the columns.

Experimental studies have been carried out in Liège these last years so as to investigate the rotational response of welded and bolted minor axis joints with flush end-plates, flange cleats and web cleats.

The two first experimental studies were funded by the research centre CRIF in Liège, and the last one by the Walloon Region of Belgium in the frame of the COST C1 European Project. More details about the tests may be found in [J3], [G4] and [C6].

Besides experimentation, theoretical and numerical investigations aimed at developing analytical expressions for the prediction of the main web properties started in Liège in the frame of the preparation of Ph.D. thesis of F. Gomes who stayed for some years at the Department MSM. Gomes focused more in his works on the resistance evaluation than on the stiffness prediction. Some publications that we co-signed with Gomes resulted from this work. The Ph.D. thesis of Gomes being not yet presented [G3], we will briefly summarize this work in the next sections without presenting all the details and comparisons with tests that the interested reader should find in the forthcoming Gomes thesis.

More recently, a colleague of Gomes, L. Neves proposed a stiffness model for web panels in minor axis joints [N2, N3]. During a three-months stay in Liège, Neves had the

opportunity to validate its model with the new available COST C1 tests as well as numerical simulations carried out in Liège with the finite element program FINELG [C6].

Let us now come back to the resistance model. The pseudo-plastic resistance of the web results from its yielding and from the progressive apparition of plastic yield line mechanisms; it can be emphasized that the same kind of mechanisms can be observed in the case of connections between a I beam and a rectangular hollow section (RHS) column (Figure 3-80). These failure mechanisms are divided into two main groups: *local* and *global* mechanisms. A local mechanism means that the yield line pattern is localized only in the compressive zone or in the tensile zone of the joint, Figure 3-81, while in the global failure the yield line pattern involves both compressive and tensile zones, Figure 3-82.

The moment carried out by the beam to the column web may be resolved in a couple of forces F acting in the compressive and tensile zones. Two different loading cases are analysed:

- *Loading case 1*: the load F acts on a rigid rectangle with the dimensions $b \times c$, Figure 3-83, as in the case of a welded connection where these dimensions are defined by the perimeter of the welds around the beam flange;
- *Loading case 2*: the load F is transferred by one or more rows of bolts, as in the tensile zone of bolted connections, see Figure 3-84 and 3-86.

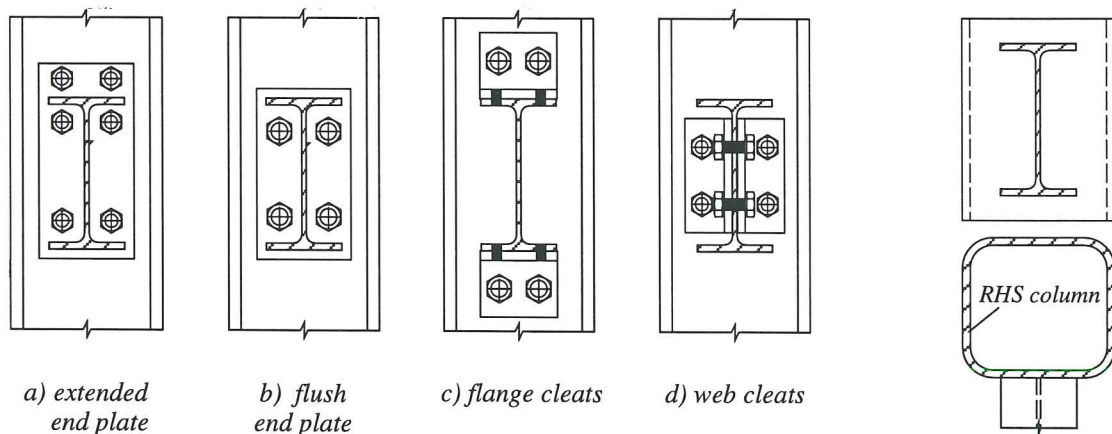


Figure 3-79 Beam-to-I section column minor axis joints

Figure 3-80 Beam-to-RHS column joint

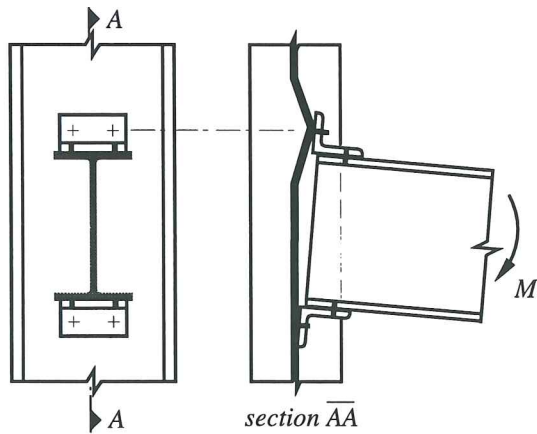


Figure 3-81 Local mechanism

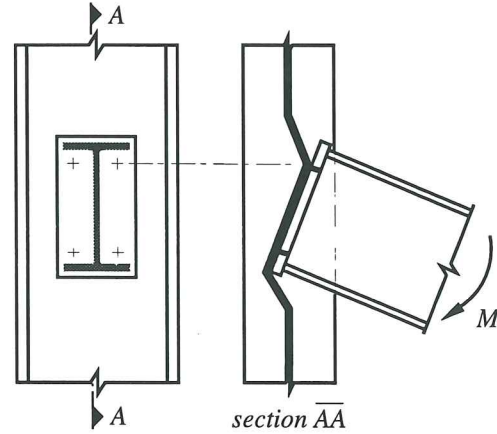


Figure 3-82 Global mechanism

3.3.4 Local failure

3.3.4.3 Flexural mechanisms

Basic failure mechanisms are obtained by the Johansen yield line method, using log-spiral fans in order to optimize the yield line pattern. The plastic moment per unit length of yield line is given by :

$$m_{pl,Rd} = 0,25t_w^2 f_y / \gamma_{M0}$$

(f_y = yield stress; t_w = thickness of the column web).

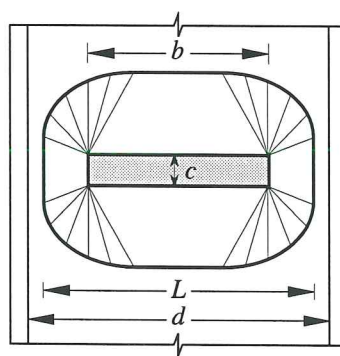


Figure 3-83 Yield line pattern (Local mechanism)

In the flexural mechanisms, it is assumed till now that the plastic moment is not reduced by the presence of shear forces perpendicular to the plane of the web; this reduction is taken into account in Section 3.3.2.3. The plastic failure load associated to the optimized

mechanism given in Figure 3-83 - for F acting on a rectangle $b \times c$ (*loading case 1*) - is given by :

$$F_{pl} = 4\pi m_{pl,Rd} \left(1 + \frac{4}{\pi} \cot \theta + \cot^2 \theta + \frac{2c}{\pi(L-b)} \right) \quad (3-50)$$

where θ is the solution of the equation $\frac{b}{L-b} = 2e^{\frac{\pi}{2} \cot \theta}$ and $L = d - 1,5r$.

For practical design purposes it is desirable to make use of a simplified formula, explicit in F_{pl} , which may be given by the approximate solution :

$$F_{pl} = \frac{4\pi m_{pl,Rd}}{1 - \frac{b}{L}} \left(\sqrt{1 - \frac{b}{L}} + \frac{2c}{\pi L} \right) \quad (3-51)$$

For the *loading case 2* (e.g. Figure 3-84), the mean diameter of the bolt head, Figure 3-85, is defined as :

$$d_m = \frac{d_1 + d_2}{2} \quad (3-52)$$

The yield line mechanism of Figure 3-84 leads to the plastic load :

$$F_{pl} = \frac{4\pi m_{pl,Rd}}{1 - \frac{a^*}{L-b_1}} \left(1 + \frac{4}{\pi} \cot \theta + \cot^2 \theta \right) \quad (3-53)$$

where : $a^* = d_m e^{-\frac{\pi}{2} \cot \theta}$

$$b_1 = b_0 + d_m \left(1 - e^{-\frac{\pi}{2} \cot \theta} \right)$$

and θ is the solution of the equation :

$$\frac{b_1}{L-b_1} = 2e^{\frac{\pi}{2} \cot \theta} \cot \theta$$

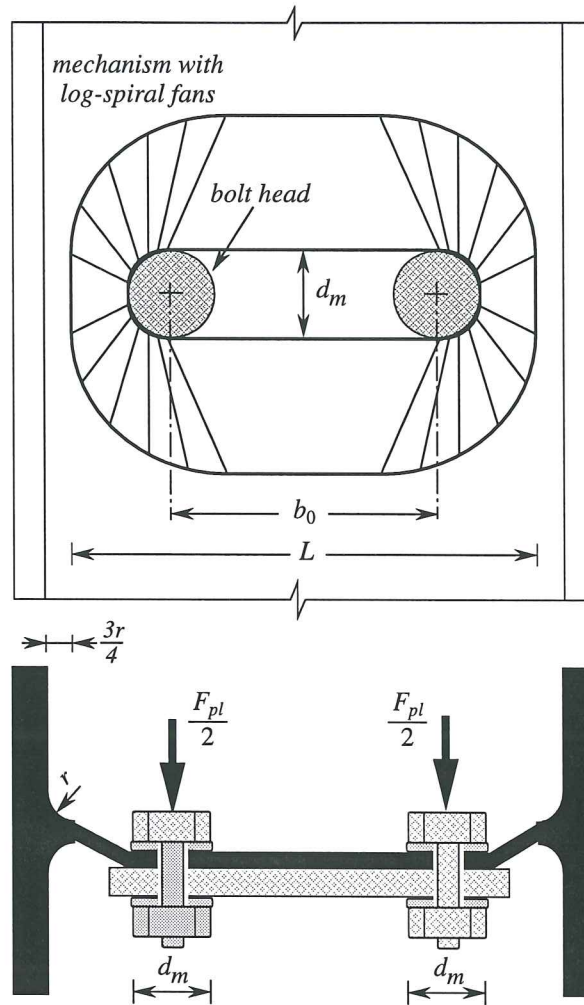


Figure 3-84 Failure mechanism for a bolted connection

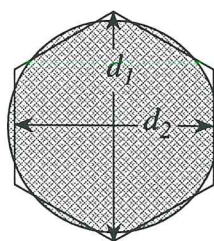


Figure 3-85 Bolt head (or nut)

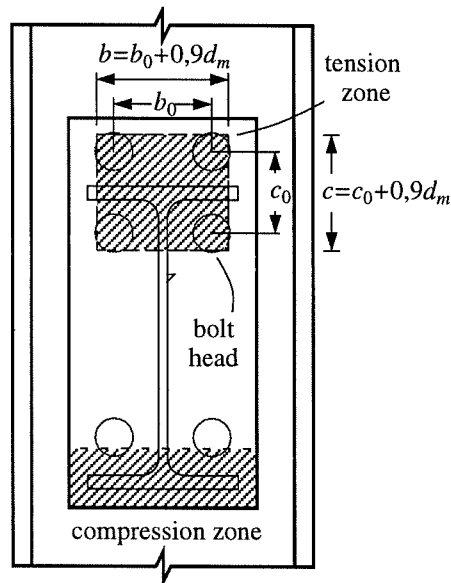


Figure 3-86 Bolted connection

Instead of this complex system of equations, the simplified Formula (3-51) may also be used for the evaluation of the failure load in the tensile zone, Figure 3-86, if this zone is replaced by an equivalent rectangle with the dimensions:

$$\begin{cases} b = b_0 + 0,9d_m \\ c = c_0 + 0,9d_m \end{cases} \quad (3-54)$$

The same Formula (3-51) may therefore be used for the two loading cases.

3.3.4.4 Punching shear mechanisms

For the *loading case 1* the punching perimeter is a rectangle with the dimensions $b \times c$. The punching load is then given by :

$$F_{punch} = 2(b+c)v_{pl,Rd} \quad \text{where} \quad v_{pl,Rd} = t_w f_y / \sqrt{3} \gamma_{M0} \quad (3-55)$$

For the *loading case 2* the punching of the column web around each bolt head must be checked. If there are n bolts in the tensile zone, the punching load is given by :

$$F_{punch} = n \pi d_m v_{pl,Rd} \quad (3-56)$$

3.3.4.5 Combined flexural and punching shear mechanisms

A combined flexural and punching shear mechanism presents not only flexural yield lines (thick lines in Figure 3-87) but also punching shear yield lines (dotted lines in Figure 3-87). Packer *et al* [P1] proposed similar combined failure modes using straight lines or circular fans, instead of the optimized mechanism of Figure 3-87 that uses log-spiral fans.

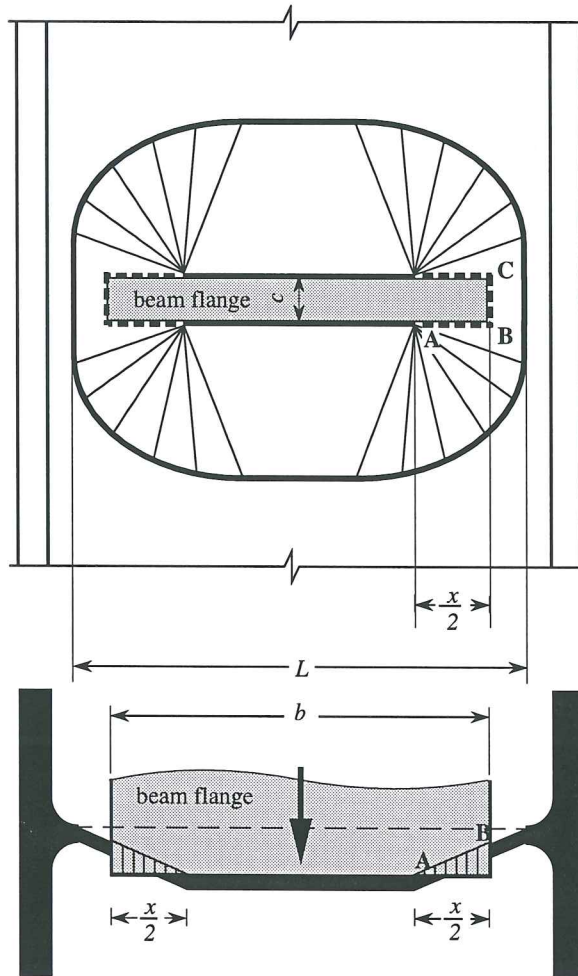


Figure 3-87 Combined flexural and punching shear failure

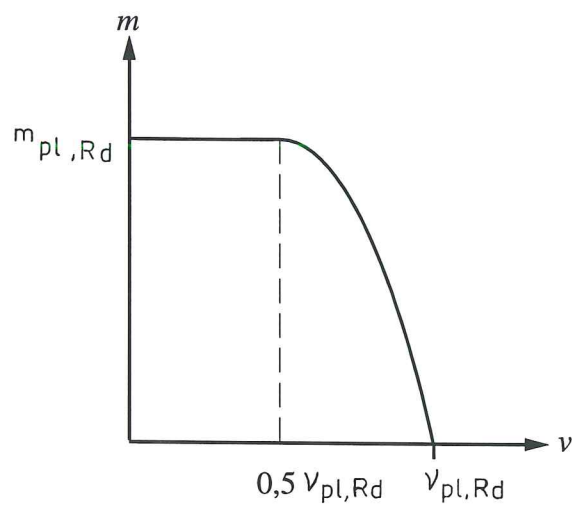


Figure 3-88 Interaction between m (moment) and v (shear force)

The present solution also takes into account that the plastic moment per unit length of yield line is reduced by the presence of shear when v (the shear force per unit length) exceeds 50% of $v_{pl,Rd}$ according to the interaction diagram of Figure 3-88. This provides a refinement of the previous solution proposed in [G2]. Despite this refinement, the expression for the plastic load is presented in a simpler form (avoiding the iterative procedure of the previous solution):

$$F_{Q2} = 4m_{pl,Rd} \left[\frac{\pi\sqrt{L(a+x)} + 2c}{a+x} + \frac{1,5cx + x^2}{\sqrt{3}t_w(a+x)} \right] \quad (3-57)$$

where: $a = L - b$

$$\begin{cases} x = 0 & \text{if } b \leq b_m \\ x = -a + \sqrt{a^2 - 1,5ac + \frac{\sqrt{3}t_w}{2} \left[\pi\sqrt{L(a+x_0)} + 4c \right]} & \text{if } b \geq b_m \end{cases}$$

$$x_0 = L \left[\left(\frac{t}{L} \right)^{\frac{2}{3}} + 0,23 \frac{c}{L} \left(\frac{t}{L} \right)^{\frac{1}{3}} \right] \left(\frac{b - b_m}{L - b_m} \right)$$

and

$$b_m = L \left[1 - 0,82 \frac{t_w^2}{c^2} \left(1 + \sqrt{1 + 2,8 \frac{c^2}{t_w L}} \right)^2 \right], \text{ but } b_m \geq 0,$$

Equation (3-57) provides an additional advantage with respect to the previous solution [G2]: it may be applied in the full range $0 \leq b \leq L$; in [G2], the application of the formula was limited to $b \leq 0,8L$.

For the *loading case 2* (bolted connections) the equivalent rectangle, defined by equation (3-54), may be used.

3.3.4.6 Correction to take into account the difference between Johansen and Von Mises yield criteria

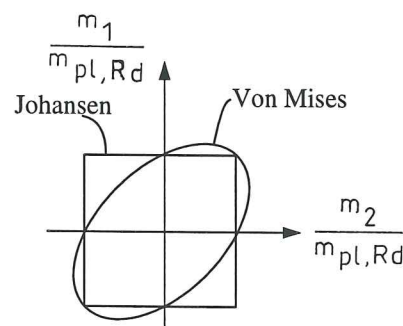


Figure 3-89 Yield criteria for plates (m_1 , m_2 - principal moments)

The plastic failure loads obtained by the yield line method differ from the exact solutions based on the Von Mises yield criterion. It was shown [G5] that if $(b+c)/L \geq 0,5$ the optimized yield line mechanisms provide an accurate solution. However, if $(b+c)/L < 0,5$, the yield line method overestimates the plastic load. The influence of the yield criteria on the plastic load was evaluated by numerical simulations performed with the finite element program FINELG that uses the Von Mises yield criterion, instead of the square yield criterion (Figure 3-89) used in the Johansen yield line method.

Final expressions for flexural mechanism as well as for combined mechanism should then include a correction factor k that multiplies Eq. (3-51) or Eq.(3-57) in order to obtain an accurate plastic load. The correction factor k may be evaluated as [G5]:

$$k = \begin{cases} 1 & \text{if } (b+c)/L \geq 0,5 \\ 0,7 + 0,6(b+c)/L & \text{if } (b+c)/L \leq 0,5 \end{cases} \quad (3-58)$$

3.3.4.7 Comparison between the three modes of local failure

It is obvious that equations (3-57) and (3-51) are identical when $x = 0$ (no punching), what means that the combined mechanism is transformed into the pure flexural mechanism. This occurs when $b \leq b_m$, where b_m is the particular value of b that determines the boundary between the two mechanisms. When $b > b_m$, equation (3-57) gives a plastic load always smaller than equation (3-51), which means that equation (3-51) is useless.

The local failure mechanism is the mechanism associated to the lowest plastic load which is then given by :

$$F_{local} = \min(F_{punch}; kF_{Q2}) \quad (3-59)$$

The three modes of local failure are compared in Figure 3-90 for a bolted connection with two bolts in the tensile zone, like that of Figure 3-84. The bolted diameter is fixed to $d_m = 0,1L$, and from equation (3-54) the equivalent rectangle is defined by $b = b_0 + 0,09L$ and $c = 0,09L$. Figure 3-90 shows the variation of the failure load (thick line) as a function of b , representing the three modes of failure.

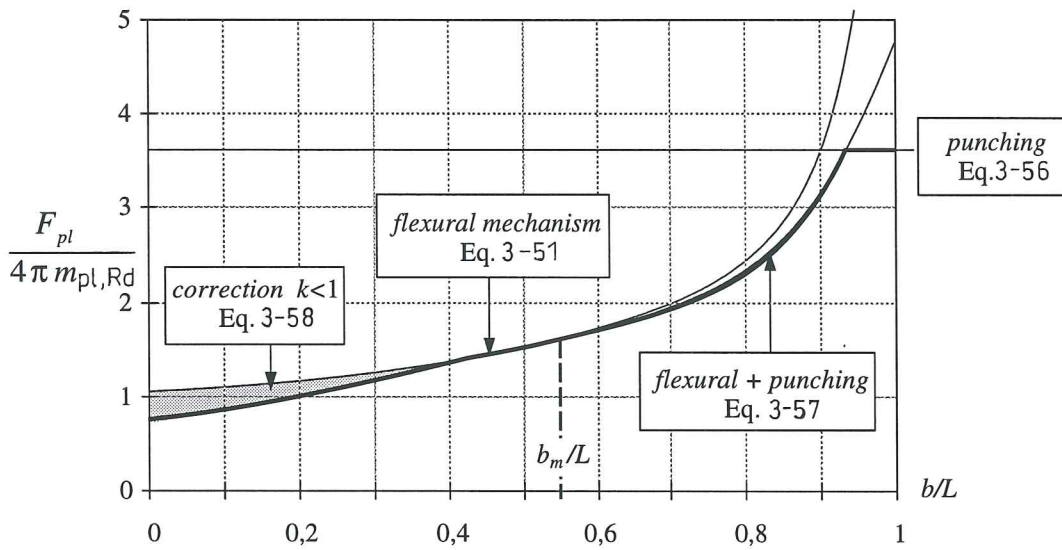


Figure 3-90 Comparison between the three modes of local failure

3.3.5 Global failure

The global failure load, for flexural mechanisms or for combined flexural and punching mechanisms, may be evaluated as :

$$F_{global} = \frac{kF_{Q2}}{2} + m_{pl,Rd} \left(\frac{2b}{h} + \pi + 2\rho \right) \quad (3-60)$$

where F_{Q2} and k are given by equations (3-57) and (3-58), h is the distance between centres of compressive and tensile zones, and ρ is given by :

$$\begin{cases} \rho = 1 & \text{if } 0,7 \leq \frac{h}{L-b} \leq 1 \\ \rho = \frac{h}{L-b} & \text{if } 1 \leq \frac{h}{L-b} \leq 10 \end{cases}$$

Outside the range $0,7 \leq \frac{h}{L-b} \leq 1$ equation (3-60) is no more valid. However it underestimates the plastic load if the following values of ρ are assumed:

$$\begin{cases} \rho = 1 & \text{for } \frac{h}{L-b} < 0,7 \\ \rho = 10 & \text{for } \frac{h}{L-b} > 10 \end{cases}$$

Global failure mechanisms involve both compressive and tensile zones (Figure 3-82). These mechanisms are assumed to be symmetrical with respect to a horizontal and to a vertical axis in the plane of the column web. The horizontal symmetry is not an exact

assumption when the dimensions $b \times c$ of the compressive zone are different from those of the tensile zone, e.g. Figure 3-86. In this case equation (3-60) should be applied separately for each zone, leading to two different loads, and the failure load will be an intermediate value. However the two zones are often assumed to be equal and then equation (3-60) will be applied only once.

3.3.6 Design resistance

The design resistance of the web in transverse compression or tension is finally defined as :

$$F_{Rd} = \min(F_{local}; F_{local}) \quad (3-61)$$

3.3.7 Conclusions

The evaluation of the moment capacity of minor-axis joints is a complex task due to the large number of failure modes of the column web. The proposed method, however, predicts these failure modes with simple expressions, easy to use by designers. Comparisons of theoretical predictions with 12 experimental tests [G5] and with a large number of numerical simulations [N3] confirm the accuracy of the analytical method. Details on the background of this method may be found in [G3].

3.4 Column bases

3.4.1 Introduction

Column bases constitute the link between frame and foundation and so represent quite important structural elements. Those considered in this Section are constituted of concrete blocks embedded in the foundation on which the column steel profile is connected by means of a base plate welded at the column end and maintained on the concrete block by two or four anchor bolts.

In this Section, only the rotational behaviour of the column-to-concrete major axis connections under uniaxial bending is investigated. The study of the concrete-to-soil connection requires the collaboration of experts in structures and geotechnics and is now the object of researchers performed in the frame of the new European Project COST C6.

The Section reflects the common activities of the Department MSM of the University of Liège and the Steel Department of CRIF during these last years in the field of column bases and more especially the collaboration between S. Guisse and J.P. Jaspert (University of Liège) and D.Vandegans (CRIF) which recently opened on a CRIF report [G6] ; it includes three main parts :

- The results of 12 experimental tests on column bases with two and four anchor bolts and the discussion of their main behavioural features.
- The proposal of a simple analytical model for resistance evaluation.
- The development of a rather sophisticated mechanical model allowing to follow step by step the loading of the column bases until collapse is reached through a detailed study of the evolution of the displacements and stresses in the different components.

The validity of the proposed models is then shown through comparisons with the experimental results.

Both models refer to the so-called component method. For column bases however, specific components are activated, such as "anchor bolts in tension" or "concrete in compression", and the loading is different from that presently covered by Eurocodes 3 and 4 as high axial forces have to be transferred to the foundation in addition to bending moments and shear forces.

These aspects are discussed and original solutions are proposed.

3.4.2 Experimental tests

3.4.2.1 Test set-up and general configuration of the specimens

Twelve experimental tests on column bases have been recently carried out in Liège. The general configuration shown in Figure 3-91 is identical for all the tests. For technical reasons the tests were carried out with a compressive force F_1 in the column acting horizontally whereas the force F_2 generating bending moment was acting vertically.

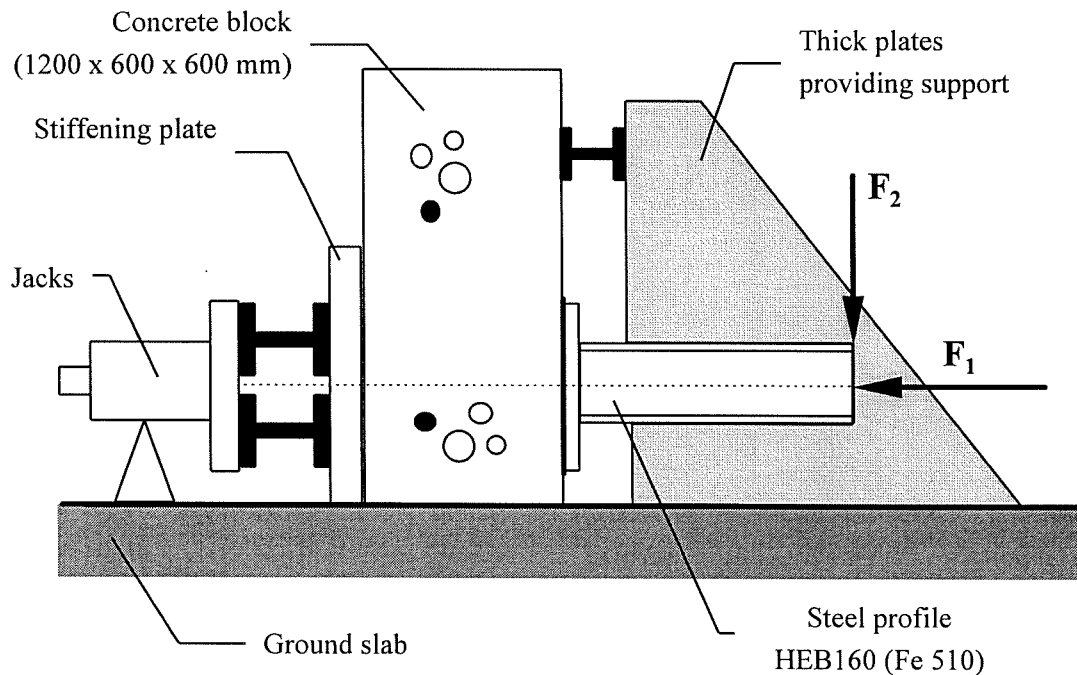


Figure 3-91 Test set-up

The compressive force F_1 is applied by means of two jacks acting on the rear face of the concrete block. Thanks to the extremely thick stiffening plate (10 centimetres), the distribution of the stresses inside the concrete block may be considered to be the same as it would be if the block was placed directly on the ground.

Similar concrete blocks are used for all the tests : 1200 mm high for a 600 x 600 mm square base. All the blocks were concreted at the same time in order to ensure that their mechanical behaviour is as homogeneous as possible.

To prevent any movement of the block, an efficient support against the moment created by force F_2 was formed by two large thick steel plates placed on each side of the column profile (see Figure 3-91). In order to be able to resist applied stresses, the concrete block has been slightly reinforced. The reinforcements, however, are placed so as not to prevent the possible formation of cracks under the action of the compressive force, as it could happen in practical situations.

A thin layer of grout has been placed between the base-plate and the concrete block so as to ensure a good contact. Two types of test configurations were envisaged, with four (Figure 3-92) or two (Figure 3-93) anchor bolts. In the first case, the column base is nearly rigid, while in the second it is usually considered as pinned.

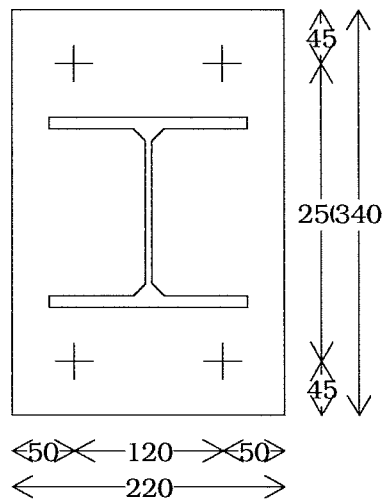


Figure 3-92 Plate with four anchor bolts

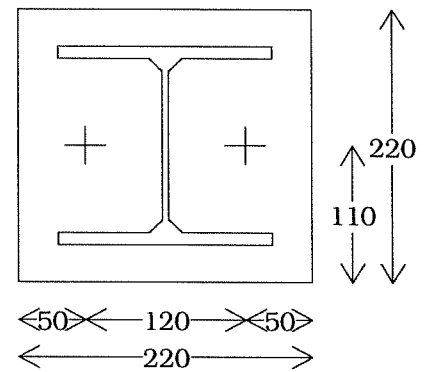


Figure 3-93 Plate with two anchor bolts

Only one steel column profile was considered in the test series : HE160B. Its steel grade is S355.

The base-plates are welded to the column; the throat radius is 6 mm. Two different thicknesses are used for base-plates: 15 mm and 30 mm. The steel grade is also S235.

Anchor bolts M20 10.9 are used. They are made from steel rods curved as shown in Figure 3-94

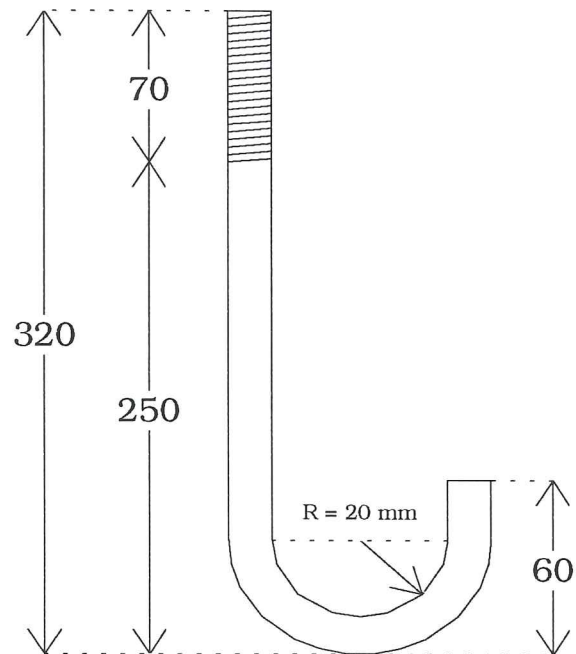


Figure 3-94 Anchor bolts

The same loading history is applied to all the tests (Figure 3-95) : preliminary application of the full compressive force on the column (F_1), which remains then constant, followed by a progressive application of the force F_2 until collapse.

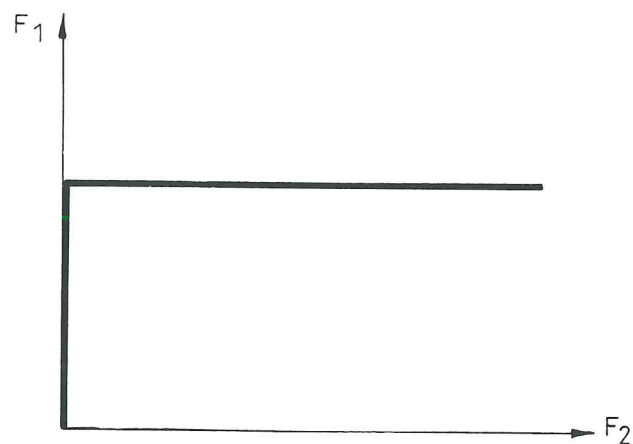


Figure 3-95 Loading history

Table 3-5 gives the nomenclature of the tests and the value of the parameters which differentiate the test specimens. The designations given to the tests consist of the initial letters "PC", followed by three numbers: the first indicates the number of anchor bolts (2

or 4), the second relates to the thickness of the plate (15 mm or 30 mm) while the last gives the value of the axial load applied to the column, in kN. The initials PC mean « Pied de Colonne », what means nothing else than « column bases » in French.

Name	Anchor Bolts	Plate thickness	Normal force
	-	mm	kN
<i>PC2.15.100</i>	2	15	100
<i>PC2.15.600</i>	2	15	600
<i>PC2.15.1000</i>	2	15	1000
<i>PC2.30.100</i>	2	30	100
<i>PC2.30.600</i>	2	30	600
<i>PC2.30.1000</i>	2	30	1000
<i>PC4.15.100</i>	4	15	100
<i>PC4.15.400</i>	4	15	400
<i>PC4.15.1000</i>	4	15	1000
<i>PC4.30.100</i>	4	30	100
<i>PC4.30.400</i>	4	30	400
<i>PC4.30.1000</i>	4	30	1000

Table 3-5 Nomenclature of the tests

All of the data relative to the dimensions, geometrical and mechanical characteristics of the different components of the test specimens are outlined in the following section.

3.4.2.2 Measured geometrical and mechanical characteristics

One of the main components in column bases is, of course, the concrete. To determine its mechanical properties, six tests on cubes were cast at the same time than the foundation blocks. They were also tested few days after the column bases, i.e. about two months after the concreting.

The results of the compression tests on the cubes are given in Table 3-6. All the cubes were 158 x 158 x 158 mm ones (cross-section of 24964 mm²). The very low scatter of the results and the high quality of the concrete have to be noted.

Cube No.	Ultimate load <i>kN</i>	Strength <i>MPa</i>	Young's Modulus <i>MPa</i>
1	1135	44.6	34200
2	1150	45.19	35100
3	1185	46.57	36700
4	1120	44.01	33600
5	1150	45.19	34500
6	1175	46.17	35900
Mean value		45.29	35000

Table 3-6 Actual mechanical characteristics of the concrete

The nominal dimensions of the steel bases-plates are shown in Figure 3-92 and Figure 3-93. For what regards their strength, tensile tests carried out in the laboratory revealed that their yield stress amounts 280 MPa while their ultimate strength is about 412 MPa, both for the 15 mm and the 30 mm plates.

The dimensions of the steel profile were measured on different specimens. As it has been asked to the manufacturer, all the beams were from the same rolling pass, so exhibiting a very low scatter for what regards geometrical and mechanical properties. For each test, the following values were therefore adopted as mean actual dimensions:

- total depth of the section.....164.7 mm
- width of the flanges160.35 mm
- web thickness 8.3 mm
- thickness of the flanges13.35 mm
- fillet radius 15 mm

The mechanical characteristics were also measured in laboratory:

- yield stress464 MPa
- ultimate stress.....580 MPa

High-strength steel was used for column profiles so as to prevent yielding of the column cross-section as far as possible and so as to concentrate the deformability and the failure mode in the column base. This was achieved, except in the last test, PC4.30.1000, where high stresses were obtained in the column.

From the measured characteristics of the steel profile, the following geometrical quantities, which will be useful later, can be derived :

- Moment of inertia (major axis)..... 2801.9 cm⁴
- Area 56.2 cm²
- Reduced area (shear force)..... 11.4 cm²

The anchor bolts exhibit a quite special behaviour. In fact, although their base metal is of very good quality (ultimate strength of about 1000 MPa but with good ductility), various phenomena tend to reduce the strength which can be expected:

- the shaping, carried out in the laboratory, consisted in bending a rod at 180 degrees (see Figure 3-94). To prevent microcracks from occurring in the curved zone, the metal was heated considerably, thereby reducing the strength of the material.
- in the concrete, the anchor bolts are fixed to bars embedded in the block. Unfortunately, for some tests, an initial unbending of the curved rod was observed before the ultimate resistance of the rod in tension is reached.

Consequently, even if a tensile test on a straight anchor bolt yields a strength of 250 kN, specific tests carried out on bolts fixed in the concrete block revealed a lower strength, i.e. 187 kN.

3.4.2.3 Instrumentation

Three types of measurement devices were used:

- the displacement transducers D_1 to D_7 ;
- the rotational transducers ROT_1 and ROT_2 (direct measurement of the absolute rotations);
- the bolt strain gauges, placed in the anchor bolts, J_1 and J_2 .

Figure 3-96 and Figure 3-97 show the positions of the various transducers used for the tests with four anchor bolts. A similar arrangement is used for configurations with two anchor bolts. The only difference is the position of the D_2 and D_4 transducers, which are located closer to the column flanges.

Transducers D_6 and D_7 are just there to detect any overall rotation of the concrete block under the action of force F_2 . In fact, the supports used were so rigid that this movement proved to be completely negligible.

Transducers D_2 to D_5 give a rather good picture on how the base-plate deforms relatively to the concrete block. Transducer D_1 is the most important one as it measures the transverse displacement of the steel column in the direction of the force F_2 .

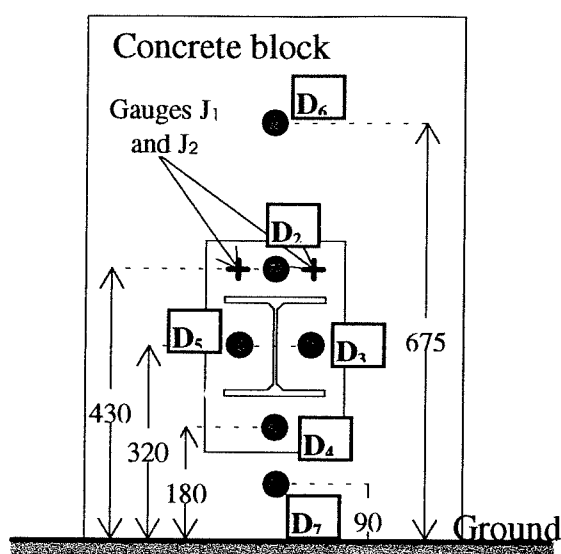


Figure 3-96 Instrumentation (front view)

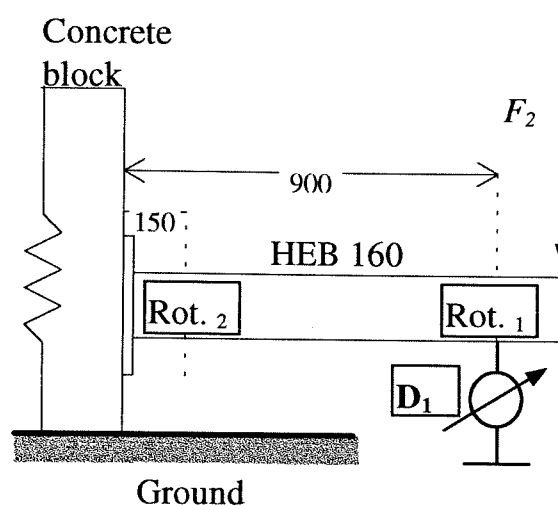


Figure 3-97 Instrumentation (side view)

Rotational transducers ROT_1 and ROT_2 (Figure 3-97) give a direct measurement of absolute rotations along the column. These instruments are of great accuracy. They represent an excellent mean to obtain reliable moment-rotation curves.

Finally, cylindrical gauges J_1 and J_2 are glued in a hole drilled in the centre of the two anchor bolts where tension is likely to occur. They measure the strain at the centre of the shank of the bolt, at a place where the stresses can be considered as uniform. In practice, the top of the gauge was placed at least two centimetres beneath the bottom face of the nut.

3.4.2.4 Moment-rotation curves

Derivation of the curves

Introduction

Through the measurements outlined in the previous paragraphs, the moment-rotation curve of the column bases may be derived. How to combined rough measurements carried out during the tests to get moment and rotation at each loading step requires few explanations. This is the subject of the following paragraphs.

Expression of the bending moment in the column base

Because of the considerable amount of deformability and the high magnitude of the normal forces in the column, second order effects cannot be ignored. In fact, Figure 3-98 shows that the bending moment in the column base, although mainly due to the force F_2 , is influenced by the compressive force F_1 in the column. The latter acts along a direction represented by the dotted line in Figure 3-98; this direction changes during the test. It may

therefore be resolved into two components: a horizontal and a vertical one. The first one creates an additional moment due to its eccentricity (measured at the level of the base-plate). The second component acts along the same direction than F_2 but tends to reduce the bending moment.

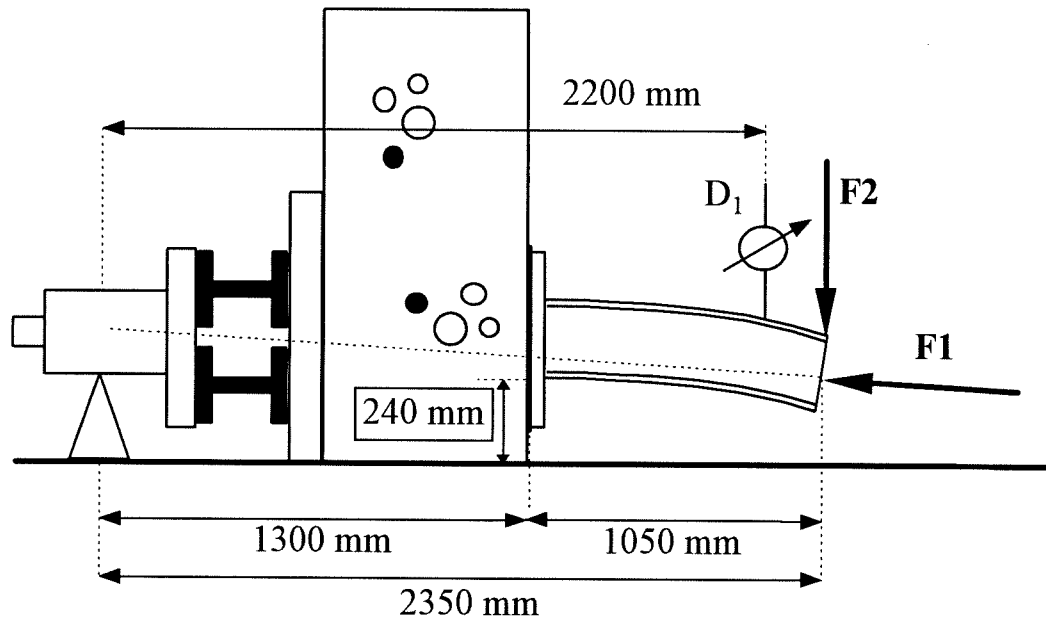


Figure 3-98 Determination of the bending moment in a column base

The action line of the force F_1 has an inclination termed α . The α value is:

$$\alpha \approx \text{tg} \alpha = \frac{D_1 \text{ (en m)}}{2,2} \quad (3-62)$$

The moment on the column base writes:

$$M = (F_2 - F_1 \cdot \sin \alpha) \cdot 1,05 + F_1 \cdot \cos \alpha \cdot (\text{tg} \alpha \cdot 1,3) \quad (3-63)$$

In equation (3-63), F_1 and F_2 are expressed in meters, while the bending moment is in kNm. By replacing α by its expression (3-62) and by considering that the angle α is rather small, the following definition of M is obtained :

$$\begin{aligned} M &= (F_2 - F_1 \cdot \sin \frac{D_1}{2,2}) \cdot 1,05 + F_1 \cdot \cos \frac{D_1}{2,2} \cdot (D_1 \cdot \frac{1,3}{2,2}) \\ &= (F_2 - F_1 \cdot \frac{D_1}{2,2}) \cdot 1,05 + F_1 \cdot (\approx 1) \cdot D_1 \cdot 0,591 \\ &= 1,05 \cdot F_2 + 0,114 \cdot F_1 \cdot D_1 \end{aligned} \quad (3-64)$$

In this expression, the first term relates to the first order, whereas the second term represents the additional moment produced by the second order effects. D , F and M quantities in equation (3-64) are expressed respectively in m, kN and kNm.

Figure 3-99 shows the comparison between the first and second order curves $M-D_1$ for the test where the difference is the largest - test PC2.30.1000. For the tests with a small compression load, the difference is usually rather limited.

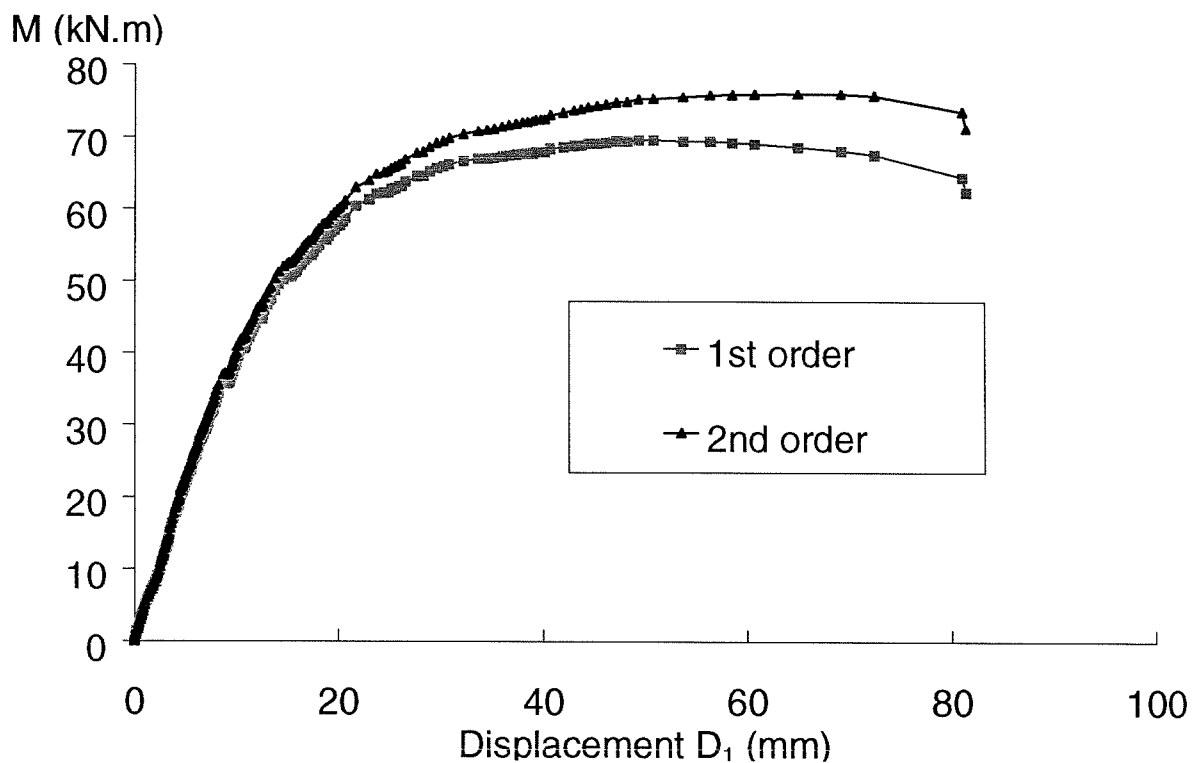


Figure 3-99 Comparison between the first and second order $M-D_1$ curves (test PC2.30.1000)

Evaluation of the relative rotation

The most reliable way to evaluate the rotation of the column base is to derive it from the three measurements carried out on the steel profile, i.e. the two rotational transducers ROT_1 and ROT_2 and the displacement transducer D_j . It is obvious that, in addition to the deformation of the column base, these measurements also include the elastic deformation of the column in bending and shear (except for test PC4.30.1000 where the column stub experiences severe yielding; this problem will be discussed later). Figure 3-100 illustrates the deformation of the column stub subject to a transverse concentrated force P .

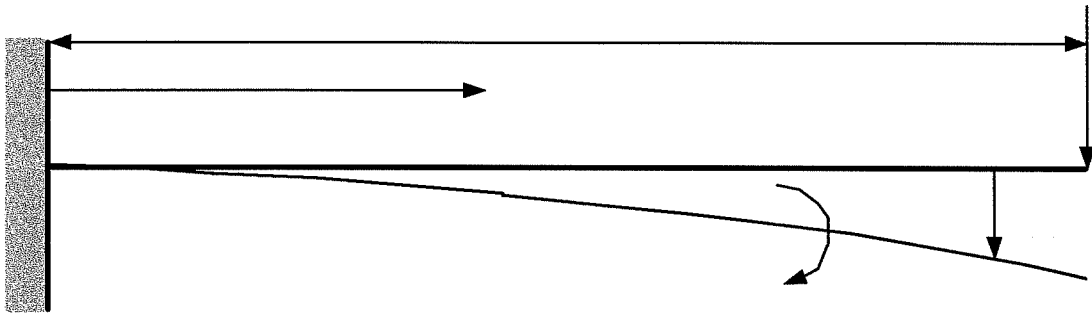


Figure 3-100 Deformation of the steel column

The shear deformation of the column stub cannot be ignored because of its limited length and the following expressions are therefore obtained:

$$\begin{aligned}
 M(x) &= P \cdot (L - x) \\
 \theta(x) &= \frac{P}{E \cdot I} \left(L \cdot x - \frac{x^2}{2} \right) \\
 v(x) &= \frac{P}{E \cdot I} \left(\frac{L \cdot x^2}{2} - \frac{x^3}{6} \right) + \frac{P}{G \cdot A'}
 \end{aligned} \tag{3-65}$$

where P is the applied force (Figure 3-100)

L is the length of the element (Figure 3-100)

E is the Young's modulus

G is the Coulomb modulus (modulus of transverse elasticity)

I is the moment of inertia

A' is the Reduced area

$v(x)$ is the deflection at one point

$\theta(x)$ is the absolute rotation at one point

The positive sign of $v(x)$ and $\theta(x)$ is indicated by the arrows in Figure 3-100.

On the basis of A' and I characteristics obtained from the actual geometrical properties measured in the laboratory, it is possible to calculate the deflection and the theoretical rotation at any point of the column, and in particular, there where the rotational transducers ROT_1 and ROT_2 , as well as the D_1 deflection transducer, are located (Figure 3-97) :

$$v(x=0,9 \text{ m})=0,063 \cdot P \text{ mm} \tag{3-66}$$

$$\theta(x=0,9 \text{ m})=0,094 \cdot P \text{ mrad} \tag{3-67}$$

$$\theta(x=0,15 \text{ m})=0,025.P \text{ mrad} \quad (3-68)$$

It should be remembered that equations (3-66) to (3-68) are only valid when the column is totally elastic, what is true for all the tests (except for PC.4.30.100 where yielding occurs, at a very advanced stage of loading).

The rotation ϕ of the column base can be now expressed. The rotational transducers constitute the simplest method in the sense that they directly give the desired rotation, provided that the deformation of the steel profile is subtracted. Two different estimations of the same rotation ϕ may therefore be obtained as follows :

$$\varphi_a = ROT_2 - 0,025.F_2 \text{ (en kN)} \quad (3-69)$$

$$\varphi_b = ROT_1 - 0,094.F_2 \text{ (en kN)} \quad (3-70)$$

These expressions have been derived by substituting P by F_2 in Formulae (3-67) and (3-68), so neglecting the second order effects. In fact, it has been demonstrated that these effects alter in a non significant way the rotations φ_a and φ_b ; for sake of simplicity, it has therefore been decided not to report the "exact" expression of φ_a and φ_b here.

A third estimation may also be calculated from transducer D_1 :

$$\varphi_c = \frac{D_1 - 0,063.F_2}{0,9.10^3} \quad (3-71)$$

Equations (3-69) to (3-72) have been compared for the twelve tests. The similarity is so excellent that it is often impossible to distinguish between the three curves. Thus, in order not to burden the present part of the thesis unnecessarily, only the curves which have been calculated on the basis of equation (3-69) are included in the next sections.

Before discussing the test results, it is quite important to point out, again, that the $M-\phi$ curves reported below include the deformation of the column base itself and the possible plastic contribution to the rotational deformation of the column profile close to the base plate.

Comparison of the curves

Figure 3-101 shows a comparison between the moment-rotation curves for the three tests PC2.15. It has to be noted that the higher the force in the column, the higher the bending moment resistance of the column base.

The initial stiffness of the curves is quite similar for the three tests, as far as the very first loading steps are considered. In fact, the stiffness changes significantly as soon as a separation is observed between the plate and the concrete in the tensile zone. Obviously, the lower the initial compression force the more quickly this phenomenon occurs.

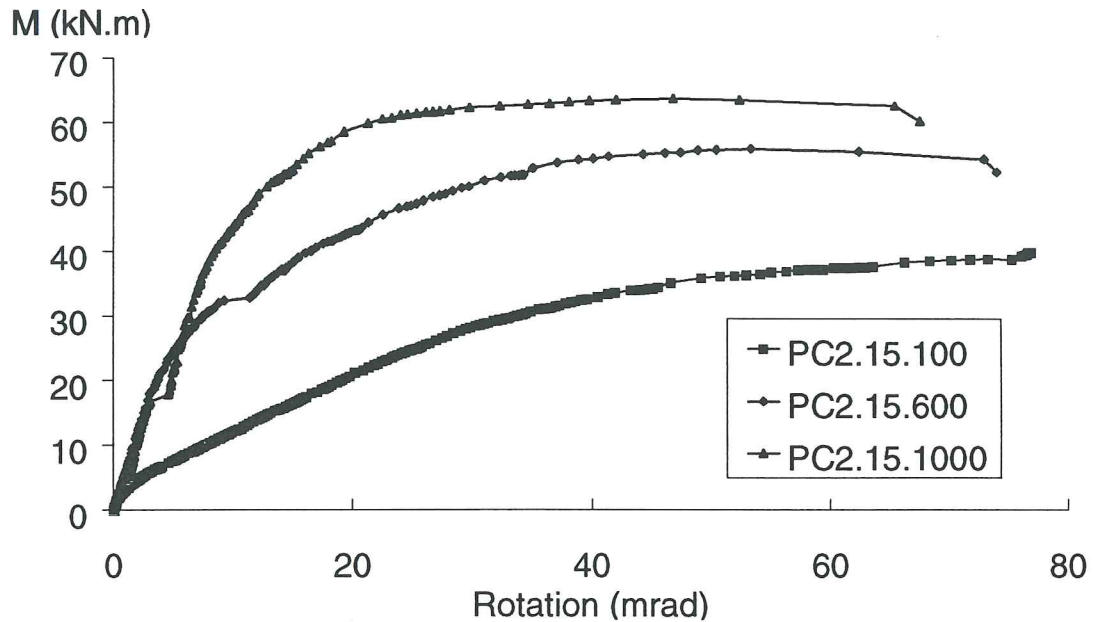


Figure 3-101 M- ϕ curves for tests PC2.15

Figure 3-102 relates to tests PC2.30. Unlike the previous figure, it shows that the initial stiffness of test PC2.30.100 is much lower than that of the other two tests PC2.30. This might be explained as follows: when the blocks were concreted, the anchor bolts embedded in the concrete were held by a plywood board located at the level of the top face of the block and supported by the lateral shuttering. The fresh concrete just arrived at the level of the lower surface of the boards and the concrete was less vibrated than elsewhere, because of the limited accessibility. When it hardened, it proved to be of inferior quality, containing numerous air bubbles. The introduction of a compression force into the column had the effect of homogenizing the concrete located under the plate by reducing its porosity. The higher the compression force, the lower the default in the concrete, and the steeper the moment-rotation curve. This could explain the significant difference observed between the curves relating to test PC2.30.100 and the two other tests PC2.30.600 and PC2.30.1000.

By examining Figure 3-101 and Figure 3-102, the particularly high value of the ultimate strength of these column bases, traditionally considered as nominally pinned, can be noted.

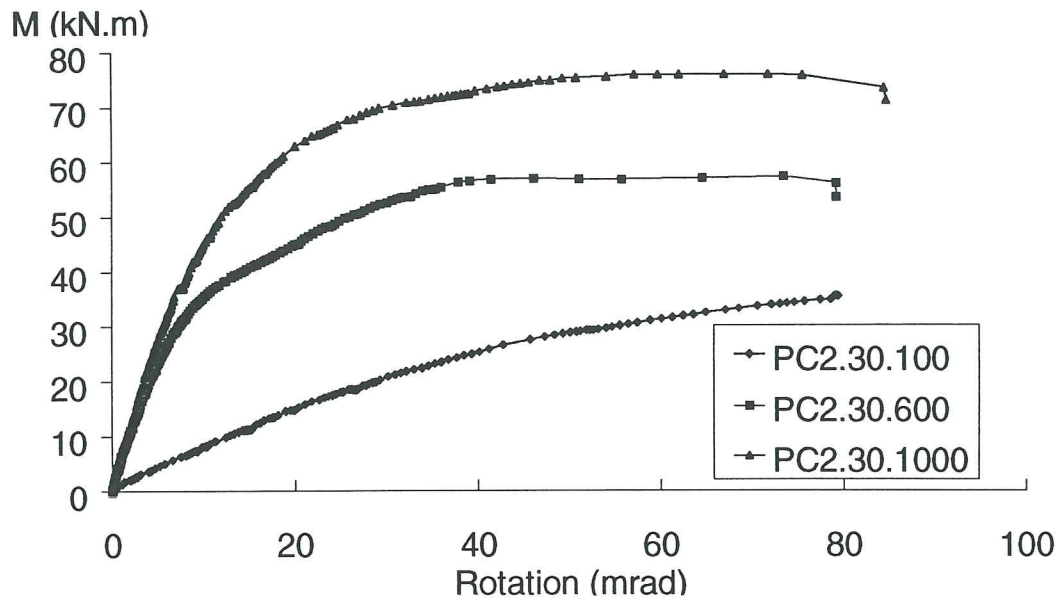


Figure 3-102 M- ϕ curves for tests PC2.30

Figure 3-103 shows the three curves for tests PC4.15. Test PC4.15.400 is the only one which has been subjected to an unloading/reloading cycle.

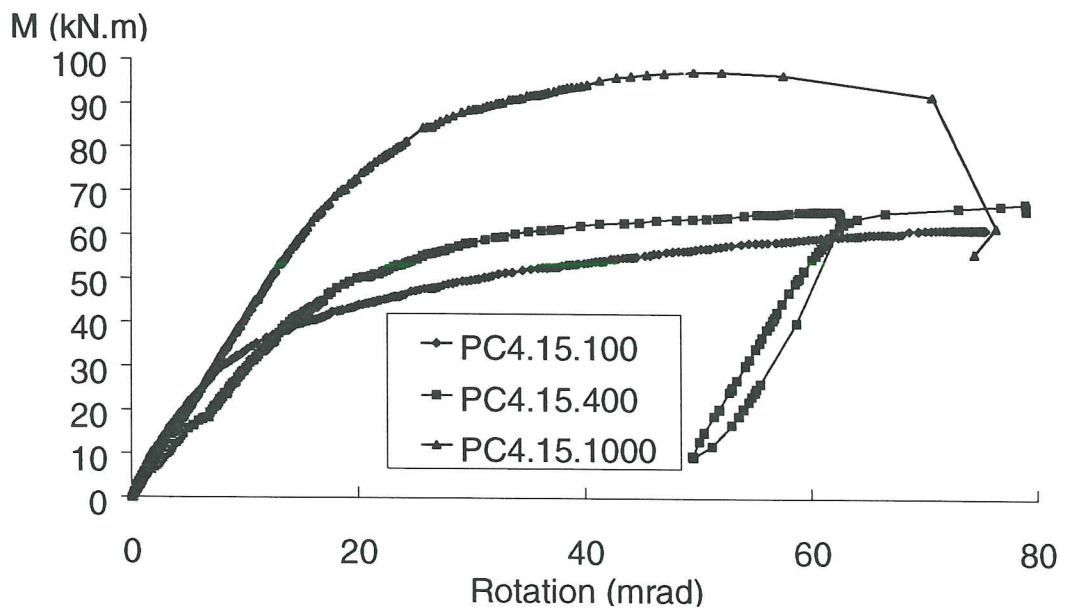


Figure 3-103 M- ϕ curves for tests PC4.15

The very marked difference in strength between test PC.415.1000 and the other two tests PC4.15 has to be pointed out. This is readily explained by the fact that the anchor bolts in tension are activated much later when the compression force in the column is high.

Finally, Figure 3-104 shows the curves of to the four last tests, PC4.30. These are, a priori, the most rigid and the strongest, what is confirmed by their moment-rotation curves. Unlike the three previous figures it will be noted that test PC4.30.1000 does not reveal a greater strength than test PC4.30.400. In fact, this is due to the yielding of the end section of the steel profile HE160B, as explained later.

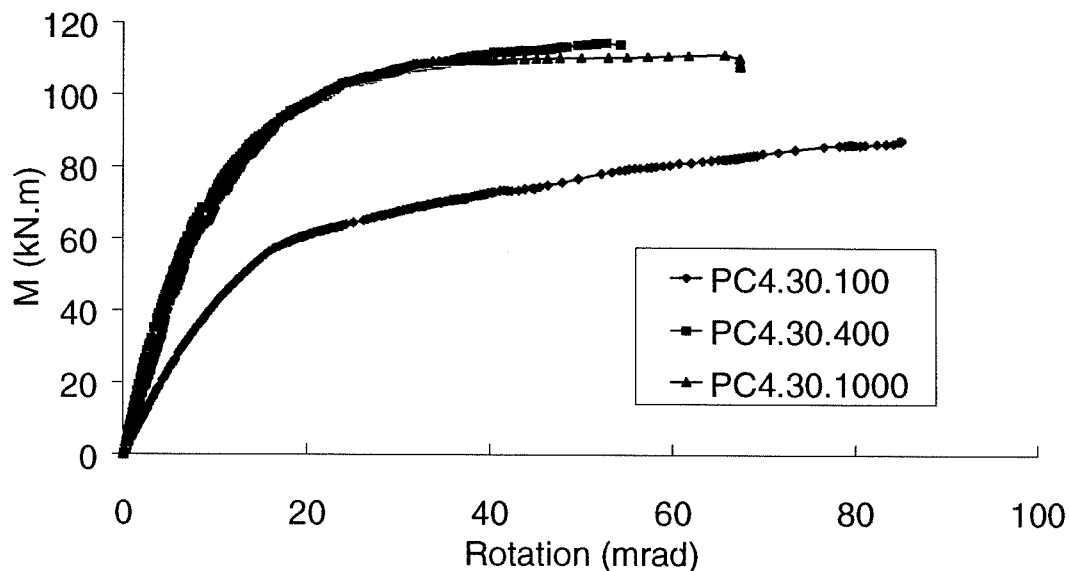


Figure 3-104 M- ϕ curves for tests PC4.30

Main characteristic values of the curves

Some characteristic values can be derived from the curves shown in Figure 3-101 to Figure 3-104. These will allow comparisons to be made with the theoretical models described later. These quantities are:

- the initial stiffness (slope of the initial part of the curve);
- the ultimate strength: peak value of the M - ϕ curve;
- the failure mode of the column base.

Table 3-7 presents the measured values of these quantities for each of the twelve experimental tests. $S_{j,ini}$ designates the initial stiffness and $M_{Ru,test}$ the ultimate strength.

The value of the pseudo-plastic resistance is not given here because the shape of the curves varies from one test to another. It is very difficult to measure it objectively.

Name	$S_{j,ini}$	$M_{Ru,test}$	Collapse mode
	kN.m/mrad	kN.m	-
PC2.15.100	0.9	40	Failure of anchor bolts
PC2.15.600	5.5	56	Failure of anchor bolts
PC2.15.1000	7	63	Crushing of the concrete
PC2.30.100	0.75	35	Failure of anchor bolts
PC2.30.600	4.6	57	Failure of anchor bolts
PC2.30.1000	5.2	75	Failure of anchor bolts
PC4.15.100	3.5	62	Yielding of the plate
PC4.15.400	4	68	Collapse of the plate and of anchor bolts
PC4.15.1000	4	97	Yielding of the plate
PC4.30.100	4.5	86	Tearing of the anchor bolts
PC4.30.400	11	117	Tearing of the anchor bolts
PC4.30.1000	8	110	Yielding and local buckling of HEB160

Table 3-7 Characteristic quantities of the experimental tests

Analysis of Table 3-7 confirms the conclusions previously drawn: the most rigid and resistant tests, for a given configuration, are those for which the compressive force in the column is high. The only exception is test PC4.30.1000 for which considerable yielding of the column cross-section is observed at failure.

Test PC2.30.100 differs from the other twelve tests by a particularly low stiffness and strength. This point has been discussed here above.

3.4.3 ANALYTICAL MODEL

In this Section, an analytical model for the prediction of the ultimate and design resistance of column bases with two or four anchor bolts is presented. It is partly based on the revised Annex J [E2] and Annex L [E6] of Eurocode 3 for what regards the resistance of the components. Despite its simplicity, this model is seen to be in a rather good agreement with the available test results.

The possibility to develop such a model for the evaluation of the initial stiffness is then discussed.

3.4.3.1 Evaluation of the resistance

Introduction

In the following sections, the carrying capacity of the constitutive components is first given. The assembly procedure is then discussed. Finally, comparisons with test results are shown.

Carrying capacity of the concrete block

In the case of axial compression

It is relatively simple to calculate the strength of the concrete block under axial compression if the recommendations of Annex L of Eurocode 3 [E6] are followed.

The first step consists in calculating a "concentration ratio", k_j , which is dependent on the geometrical dimensions of the block (Figure 3-105) :

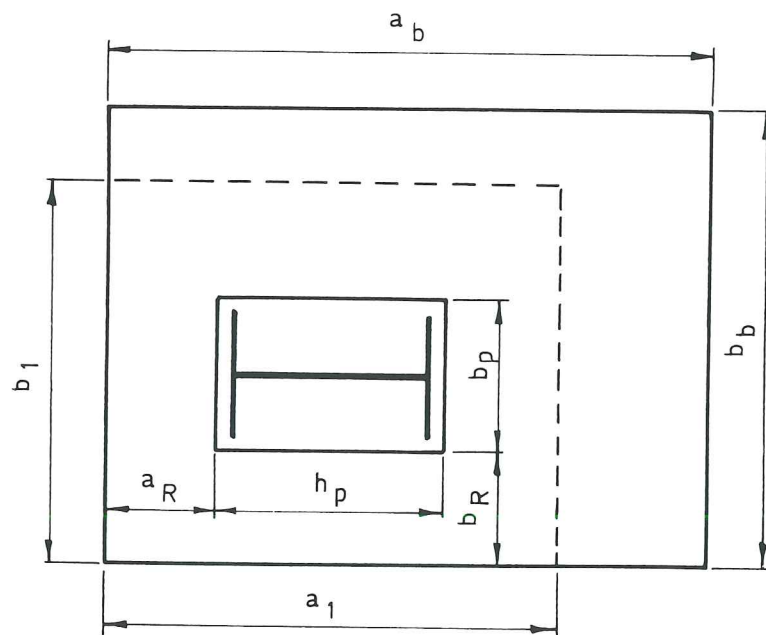


Figure 3-105 Actual and effective dimensions of the concrete block

$$k_j = \sqrt{\frac{a_1 \cdot b_1}{h_p \cdot b_p}} \quad (3-72)$$

where: h_p is the length of the base plate;

b_p is the width of the base plate;

- b_p is the width of the base plate;
 a_l is the effective length of the concrete block;
 b_l is the effective width of the concrete block.

The effective dimensions of the concrete block, a_l and b_l , are calculated using the following equations:

$$a_l = \min(h_p + 2a_R; 5h_p; h_p + h_{block}; 5b_l) \geq h_p \quad (3-73.a)$$

$$b_l = \min(b_p + 2b_R; 5b_p; b_p + h_{block}; 5a_l) \geq b_p \quad (3-73.b)$$

where: a_R and b_R are given in Figure 3-105.

h_{block} is the height of the concrete block.

The maximum stress that the concrete can resist, f_j , is then evaluated by means of the following equation :

$$f_j = \beta_j \cdot k_j \cdot \frac{f_{ck}}{\gamma_c} \quad (3-74)$$

where: $\beta_j = 2/3$ (1)

f_{ck} is the characteristic strength of the concrete in compression

γ_c is the partial safety factor for the concrete.

Finally, to take into account the flexibility of the base plate, an equivalent rigid plate (Figure 3-106) is defined, through parameter c given by :

$$c = t_p \cdot \sqrt{\frac{f_{yp}}{3 \cdot f_j \cdot \gamma_{M0}}} \quad (3-75)$$

where: t_p is the thickness of the base plate;

f_{yp} is the yield strength of the base plate;

γ_{M0} is the partial safety factor for steel.

Obviously, the dimensions of the equivalent rigid plate have not to exceed those of the actual base plate.

¹ To apply this value, two requirements on the grout layer (between the plate and the concrete) have to be satisfied, what occurs in most of the usual cases.

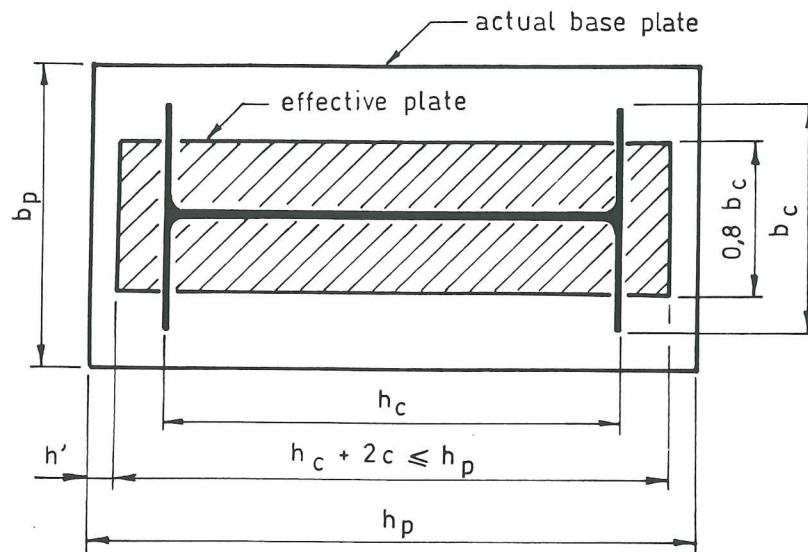


Figure 3-106 Dimensions of the equivalent rigid plate

Finally the maximum resistance of the concrete block under axial compression is expressed :

$$N_{c,Rd} = f_j \cdot A_{eff} \quad (3-76)$$

where A_{eff} is the effective area of the equivalent rigid plate defined in Figure 3-106.

In the case of non-axial compression

It is obvious that all the developments described in the foregoing paragraph may be used to calculate the carrying capacity of the concrete block under non-axial compression; this is done by considering the effective area defined in Figure 3-106 as being independent on the eccentricity of the applied compressive force.

Strength of the anchor bolts in tension and the base plate in bending

The strength of the whole "plate and anchor bolts" assembly, as a whole, can be determined on the basis of the recommendations given in the Annex J of Eurocode 3 [E2]. The calculation is based on the "equivalent T-stub" approach where the actual plate - here the base plate - is replaced by symmetric T-stubs of effective length ℓ_{eff} . The reader is begged to refer to Appendix 3 for more details about the T-stub approach.

The design resistance $F_{t,Rd}$ of the equivalent stub is the smallest of the resistances obtained by the three following equations :

Mode 1 : plastic yield mechanism in the base plate

$$F_{t,Rd} = \frac{(8.n - 2.e_w) \cdot \ell_{eff,1} \cdot m_{pl,Rd}}{2.m.n - e_w(m+n)} \quad (3-77)$$

Mode 2 : mixed failure involving yield lines - but no mechanism - in the plate and exhaustion of the strength of the anchor bolts

$$F_{t,Rd} = \frac{2 \cdot \ell_{eff,2} \cdot m_{pl,Rd} + n \cdot \sum B_{t,Rd}}{m+n} \quad (3-78)$$

Mode 3 : failure of the anchor bolts in tension

$$F_{t,Rd} = \sum B_{t,Rd} \quad (3-79)$$

with : $e_w = d_w/4$ (d_w is the diameter of the washer or the nut if there is no washer);

$$m_{pl,Rd} = \frac{t_p^2 \cdot f_{yp}}{4 \cdot \gamma_{M0}} \quad (3-80.a)$$

where: $m_{pl,Rd}$ is the plastic moment of the base plate per unit length;

t_p is the thickness of the base plate;

f_{yp} is the yield strength of the base plate;

γ_{M0} is the partial safety factor;

$\ell_{eff,1}$ and $\ell_{eff,2}$ are effective lengths (see below);

$$B_{t,Rd} = 0,9 \frac{A_s \cdot f_{ub}}{\gamma_{mb}} \quad (3-80.b)$$

where: $B_{t,Rd}$ is the design resistance of an anchor bolt in tension;

A_s is the stress area of the anchor bolts in tension;

f_{ub} is the ultimate strength of the anchor bolts;

γ_{mb} : is the partial safety factor for the anchor bolts;

$$n = e \leq 1.25 m$$

m and e are defined in Figure 3-107.

$\sum B_{t,Rd}$ is the sum of the design resistances in tension of all the anchor bolts belonging to the T-stub being considered.

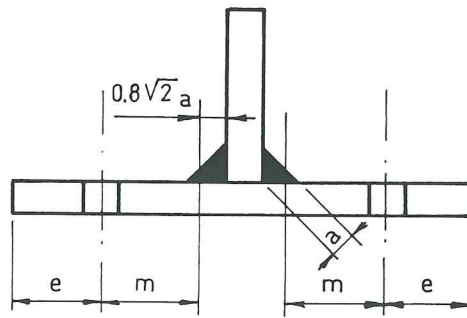


Figure 3-107 Geometrical characteristics of an equivalent welded T-stub

Two effective lengths $\ell_{eff,1}$ and $\ell_{eff,2}$ are defined for each equivalent T-stub. The first one applies for Mode 1 failure; the second for Mode 2 failure. In fact, according to Eurocode 3, two types of plastic yield mechanisms may occur in plated components, like base plates, subject to transverse forces : circular and non-circular ones. Circular yield line patterns form is the plate without developing any prying effects between the plate and the foundation. The possible failure modes are therefore limited to Mode 1 and Mode 3. In the case of circular patterns, Mode 1, 2 or 3 failures may occur.

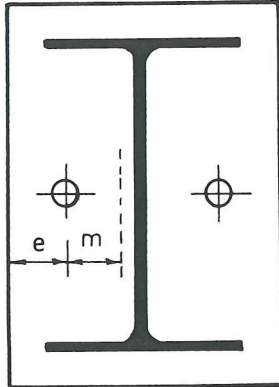
As a consequence, $\ell_{eff,1}$ and $\ell_{eff,2}$ are defined as follows :

$$\ell_{eff,1} = \min(\ell_{eff,cp}; \ell_{eff,nc}) \quad (3-81.a)$$

$$\ell_{eff,2} = \ell_{eff,nc} \quad (3-81.b)$$

where $\ell_{eff,cp}$ and $\ell_{eff,nc}$ are the minimum values of the effective lengths associated to all the yield lines patterns, respectively circular and non-circular, which are likely to develop in the plated component being considered.

For the practical applications, the calculation of the effective lengths is derived from the following formulations:

Anchor bolts located between the column flanges

Assuming that bolt-row is located at mid-distance between the column flanges, l_{eff} is determined by the following formula:

$$l_1 = 2\alpha m - (4m + 1,25e)$$

$$l_2 = 2\pi m$$

$$l_{eff,1} = \min(l_1; l_2)$$

$$l_{eff,2} = l_1$$

where m , n are shown in Figure 3-108 and α is defined in EC 3 Annex J.

Figure 3-108 Anchor bolts located between the column flanges

Anchor bolts located in the extended part of the plate

In this case the effective length is evaluated as follows :

$$l_1 = 4 \cdot m_x + 1,25 e_x$$

$$l_2 = 2\pi m_x$$

$$l_3 = 0,5 \cdot b_p$$

$$l_4 = 0,5 \cdot w + 2 \cdot m_x + 0,625 \cdot e_x$$

$$l_5 = e + 2 \cdot m_x + 0,625 \cdot e_x$$

$$l_6 = \pi m_x + 2e$$

$$l_{eff,1} = \min(l_1; l_2; l_3; l_4; l_5; l_6)$$

$$l_{eff,2} = \min(l_1; l_3; l_4; l_5)$$

where b_p , m , e , m_x , e_x and w are given in Figure 3-109.

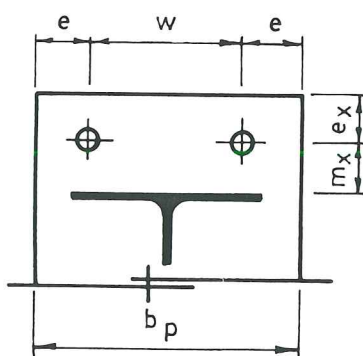


Figure 3-109 Anchor bolts located in the extended part of the plate

It has to be noted that these formulae for ℓ_{eff} only apply to base plates where the anchor bolts are not located outside the beam flanges, as indicated in Figure 3-110.

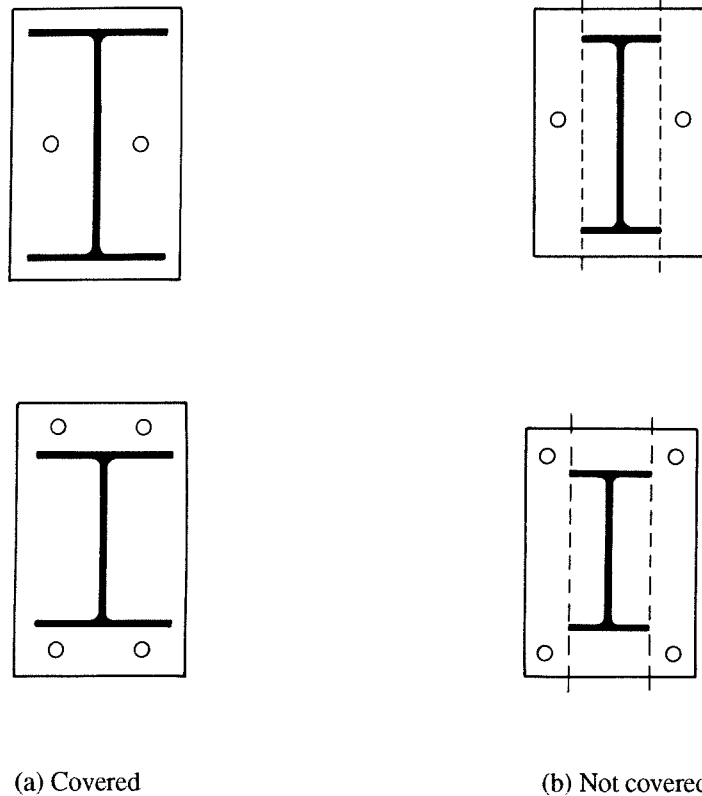


Figure 3-110 Limits of validity for Formulae (3-77) and (3-78)

The application of the T-stub approach - as recommended in Eurocode 3 Annex J - to column bases possibly requires some adaptations ; these are discussed in section 4.2.2.

Resistance of the steel profile

The steel column is subjected to combined bending and compression. In the case of HE sections of classes 1 and 2, bent about the strong axis, the bending resistance of the cross-section is expressed by the following equation extracted from Eurocode 3 [E1] :

$$M_{Rd}^* = 1,11 M_{pl,Rd} \left(1 - \frac{N_{Rd}^*}{N_{pl,Rd}}\right) \not\geq M_{pl,Rd} \quad (3-82)$$

where: $M_{pl,Rd}$ is the design moment resistance of the cross-section in bending

$N_{pl,Rd}$ is the design squash load of the cross-section

M_{Rd}^* and N_{Rd}^* is the design values of the bending moment and compressive force simultaneously applied to the column base.

Assembly of the components

In order to draw the interaction curve between the maximum axial compressive force and bending moment which can be simultaneously applied to column base, a static assembly of the components described above is considered. For column bases with four anchor bolts, the bolts located at the compression side are assumed never to be activated.

Depending on the eccentricity of the axial force in the column - the eccentricity is defined as the ratio between the applied bending moment and axial compressive force - two possible cases may occur. They are described hereafter.

Case 1. No anchor bolt is activated

This case will occur when the axis of the anchor bolts is located there where concrete is in compression, i.e. when the compression force acts only with a slight eccentricity (Figure 3-111). In order to verify the overall rotational equilibrium of the column base, the applied forces and the resistant loads must of course be aligned.

By expressing equilibrium along the column axis (Figure 3-111), it is so possible to write:

$$N_{Rd}^* = 0,8 \cdot b_c \cdot h_{cpr} \cdot f_j = 0,8 \cdot b_c (h_{eff} + h' - 2 \cdot e) \cdot f_j \quad (3-83)$$

where b_c , h_{cpr} , h_{eff} and e are given in Figure 3-111 while f_j designates the strength of the concrete beneath the plate as given by equation (3-74), defined as equal to $(h - h_{eff})/2$, is shown in Figure 3-106.

This makes it possible to express the eccentricity e as a function of the axial force:

$$e = \frac{1}{2} \left[h_{eff} + h' - \frac{N_{Rd}^*}{0,8 \cdot b_c \cdot f_j} \right] \quad (3-84)$$

By introducing (3-84) in (3-83), the value of N_{Rd}^* can be derived. The maximum bending moment which may be applied to the column base together with the compression force N_{Rd}^* is simply obtained by multiplying equation (3-84) by N_{Rd}^* . This approach is valid as long as :

$$h_{cpr} \geq h_{eff} + h' - d$$

where d is the distance between the edge of the plate in the tensile zone and the axis of the anchor bolts.

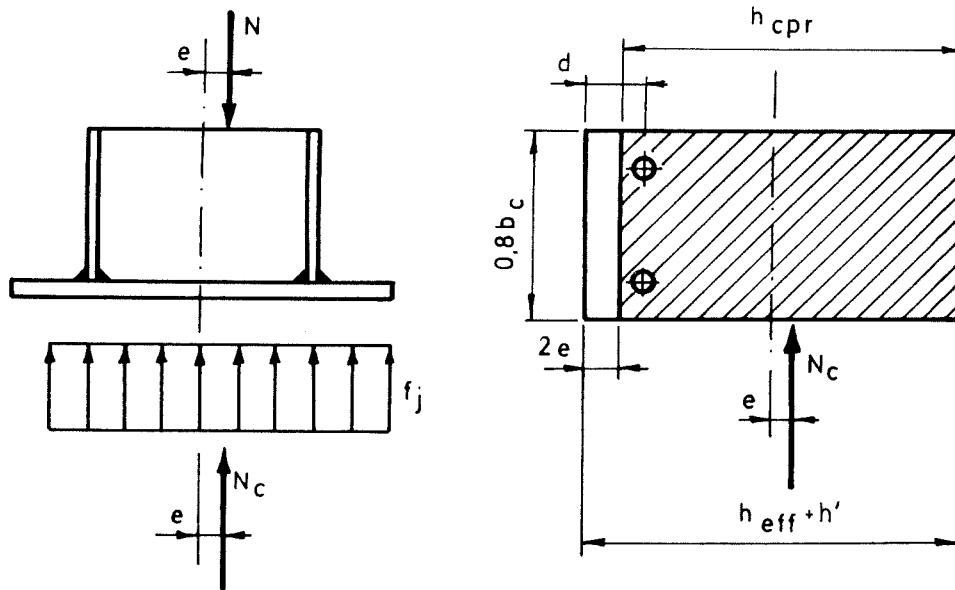


Figure 3-111 Case 1: Bolts not activated in tension

Case 2. Anchor bolts are activated in tension

As explained in the foregoing paragraph, the anchor bolts are not activated in tension as long as $h_{cpr} \geq (h_{eff} + h' - d)$.

For increasing eccentricities, the value of h_{cpr} decreases, what results in a progressive activation of anchor bolts in tension (force F_b in Figure 3-113).

For a specific value of h_{cpr} , defined as equal to $\zeta(h_{eff} + h' - d)$ hereafter, F_b reaches the tensile resistance $2 B_{t,Rd}$ of the row of anchor bolts. For lower values of h_{cpr} , F_b remains than equal to $2 B_{t,Rd}$.

The variation law of F_b versus h_{cpr} has been selected as linear on a totally empirical basis. It is represented by equation 3-85 and illustrated in Figure 3-112.

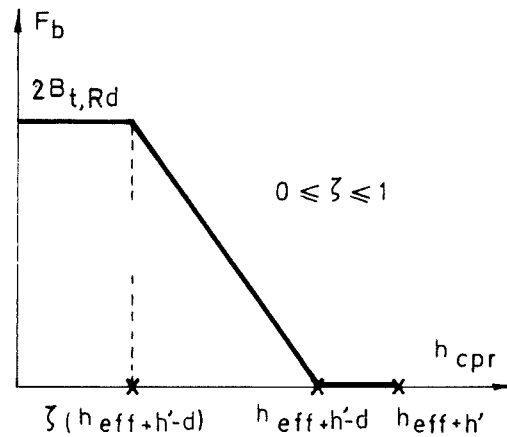


Figure 3-112 Variation law of F_b

$$F_b = \begin{cases} 0 & \text{si } h_{cpr} \geq h_{eff} + h' - d \text{ (case 1)} \\ 2B_{t,Rd} \cdot \frac{(h_{eff} + h' - d) - h_{cpr}}{(1 - \zeta) \cdot (h_{eff} + h' - d)} \neq 2B_{t,Rd} & \text{si } h_{cpr} < h_{eff} + h' - d \text{ (case 2)} \end{cases} \quad (3-85)$$

where: h_{eff} is the effective height of the plate

h_{cpr} is the height of the compressive zone

d is the distance between the edge of the plate (tension side) and the axis of the anchor bolts

ζ is the parameter varying between 0 and 1. Fixed later.

Thanks to this simplifying assumption, the problem reduces now to the evaluation of h_{cpr} which would result in a distribution of internal forces able to counterbalance the compression force; the maximum eccentricity associated to this force may be deduced.

In fact, from the vertical equilibrium (Figure 3-113) :

$$N_{Rd}^* = 0,8 \cdot b_c \cdot h_{cpr} \cdot f_j - 2B_{t,Rd} \frac{(h_{eff} + h' - d) - h_{cpr}}{(1 - \zeta)(h_{eff} + h' - d)} \quad (3-86)$$

$$h_{cpr} = \frac{N_{Rd}^* + 2B_{t,Rd} \frac{1}{1 - \zeta}}{0,8 \cdot b_c \cdot f_j + 2B_{t,Rd} \cdot \frac{1}{(1 - \zeta) \cdot (h_{eff} + h' - d)}} \quad (3-87)$$

Equation (3-87) is valid only if:

$$\zeta \cdot (h_{eff} + h' - d) \leq h_{cpr} \leq (h_{eff} + h' - d) \quad (3.88)$$

If condition (3-88) is not satisfied and if the conditions relating to case 1 are not fulfilled, then equation (3-87) may be simplified as follows:

$$h_{cpr} = \frac{N_{Rd}^* + 2B_{t,Rd}}{0,8 \cdot b_c \cdot f_j} \quad (3.89)$$

Once the height of the compressive zone, h_{cpr} , is known, the force to which the anchor bolts are subjected is calculated using equation (3-85). Finally, the maximum moment that the column base is able to transfer is calculated by expressing the rotational equilibrium about the neutral axis of the column (Figure 3-113):

$$M_{Rd}^* = N_{Rd}^* \cdot e = 0,8 \cdot b_c \cdot h_{cpr} \cdot f_j \cdot \frac{h_{eff} - h_{cpr}}{2} + F_b \cdot \left(\frac{h_{eff} + h'}{2} - d \right) \quad (3.90)$$

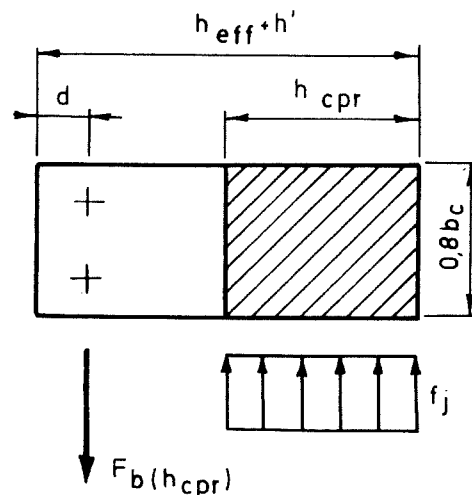
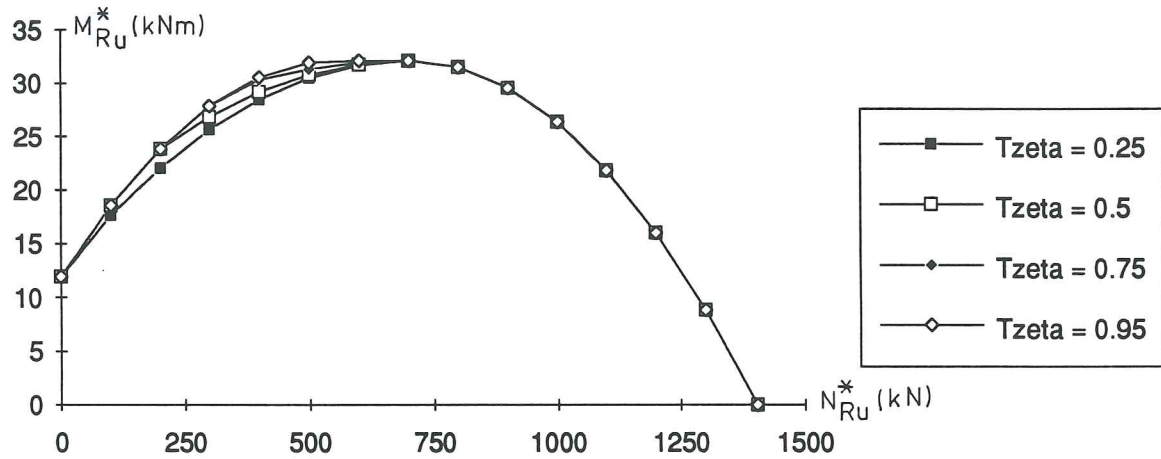


Figure 3-113 Distribution of internal forces (case 2)

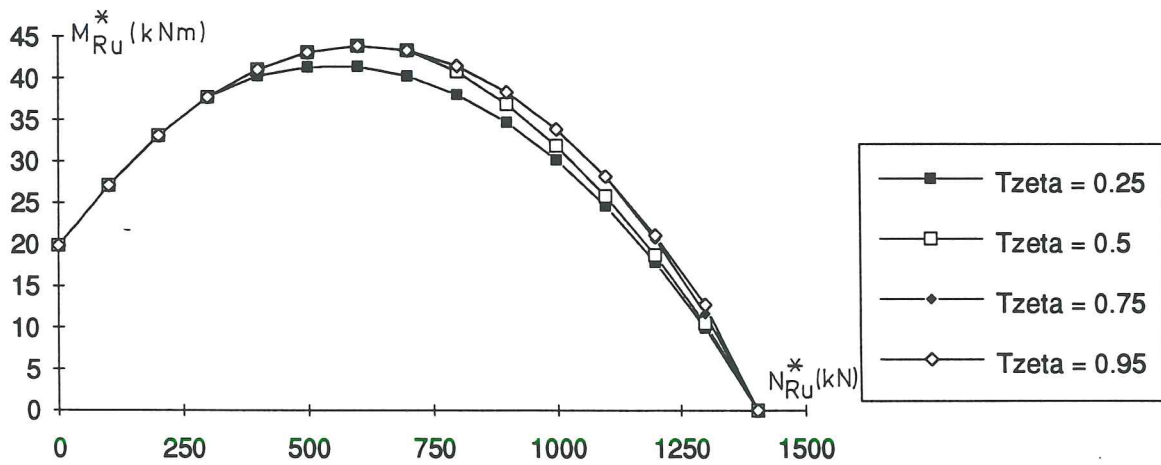
It should be noted that equation (3-90) is also valid when a tensile force is applied to the column, a situation which can occur with light structures subject to strong wind. In the case of column bases with four anchor bolts ("rigid" type), however, it is sometimes necessary to activate the two rows of anchor bolts. For sake of clarity, this situation is not covered here.

The last remaining unknown of the problem is the numerical value to adopt for the parameter ζ . In reality, this one depends on the mechanical characteristics of the bolts and concrete and, more precisely, on the magnitude of their respective deformations. It is clear that a theoretical evaluation of ζ is quite complex. Thus, for simplicity, its value is fixed empirically. Figures Figure 3-114.a and Figure 3-114.b illustrate the influence of ζ on the

ultimate values N_{Ru}^* and M_{Ru}^* of the applied forces in configurations with to 2 and 4 anchor bolts respectively. This influence is seen negligible and a value of 0,5 is therefore selected for ζ .



(a) Configuration with 2 anchor bolts



(b) Configuration with 4 anchor bolts

Figure 3-114 Influence of ζ on the ultimate resistance

Comparison with the experimental tests

Figure 3-115 to Figure 3-118 present a comparison between the analytical model presented in the foregoing paragraphs and the experimental results reported in Table 3-7. The strengths quoted are ultimate ones. It should be remembered that the ultimate resistance of a column base is calculated by taking into account the ultimate actual

strengths of each component (steel, concrete, column cross-section, etc.) and the partial safety factors taken as being equal to unity.

In each of the Figure 3-115 to Figure 3-118, three curves are reported. The first one corresponds to the ultimate resistance of the column base, without any consideration of the possible yielding of the HE160B cross-section (equations 3-83 to 3-90). The second series of points gives the experimental ultimate strengths reported in Table 3-7. Finally, the last curve covers the carrying capacity of the steel column cross-section considered on its own (equation 3-82).

Tests PC2.15 are reported in Figure 3-115. It is clear that there is an excellent agreement between theory and experimentation. It has also to be noted that the column cross-section is far from experiencing yielding when the collapse of the column base occurs.

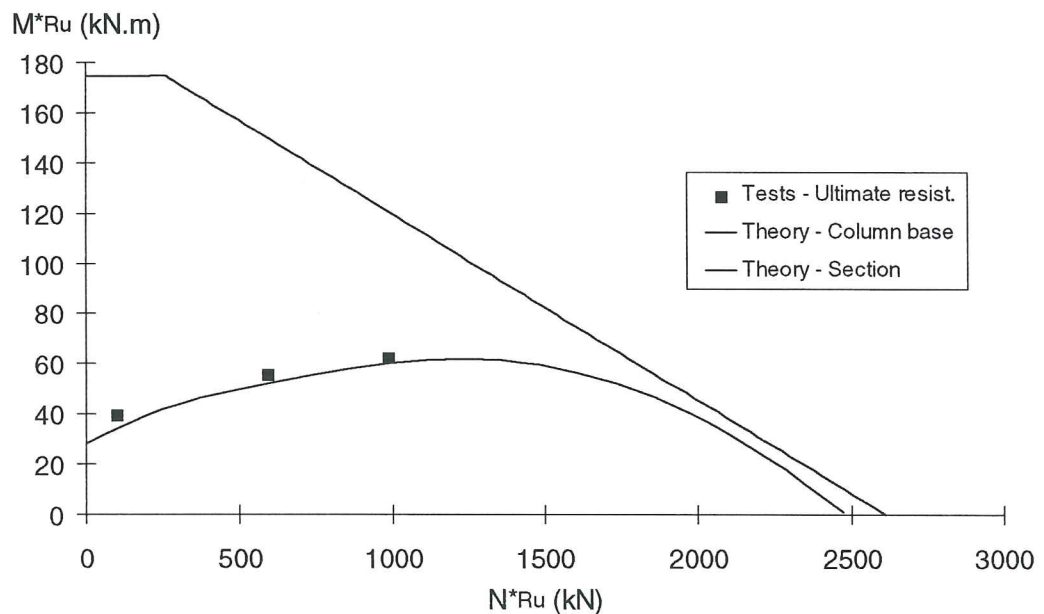


Figure 3-115 Comparison between tests and model-tests PC2.15

In Figure 3-116, the agreement appears also as satisfactory, even if it is a bit less than in Figure 3-115. The experimental resistance of test PC2.30.100, for instance, is lower than the theoretical prediction. This is due to the fact that the ultimate moment has not been reached during the test which has been interrupted because of high deformations (Figure 3-101).

Nevertheless, bearing in mind the simplicity of the model, the agreement may be considered as quite acceptable.

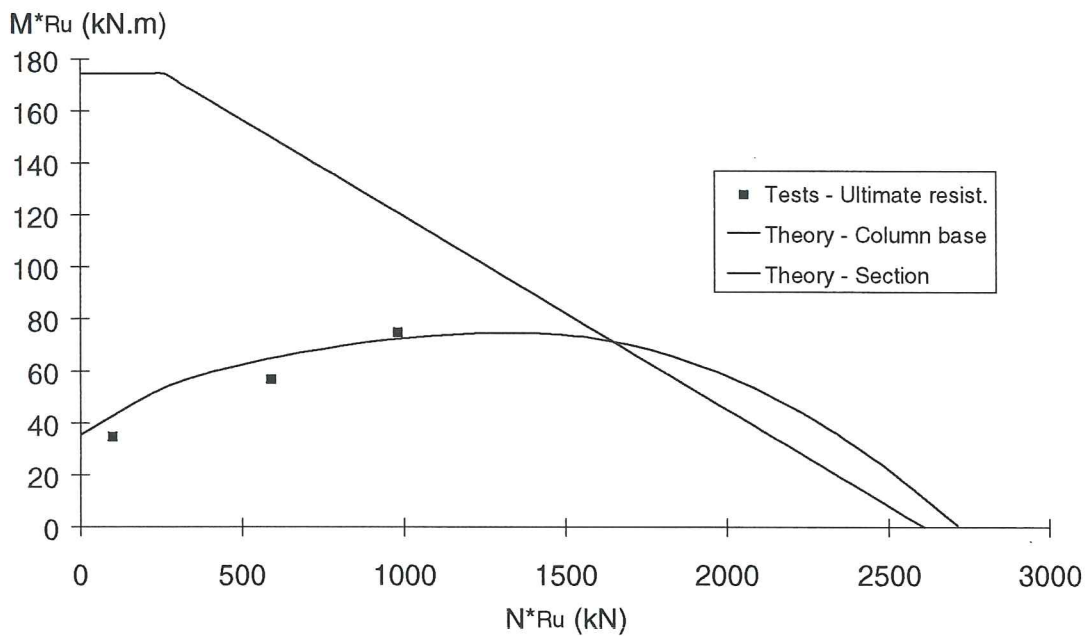


Figure 3-116 Comparison between tests and model-tests PC2.30

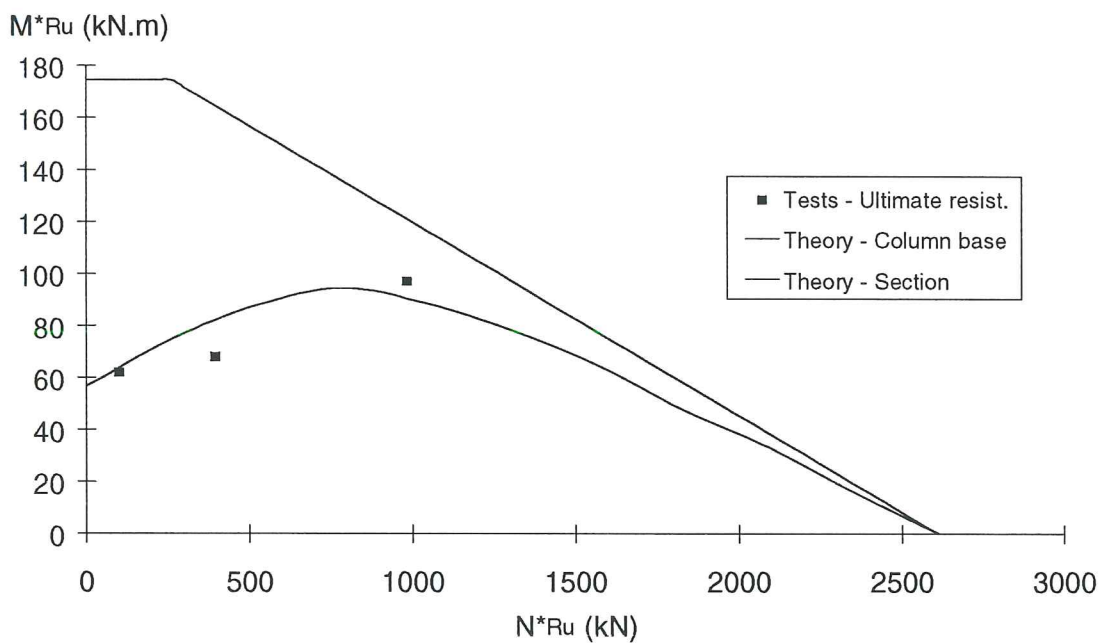


Figure 3-117 Comparison between tests and model-tests PC4.15

The results for tests PC4.15 are plotted in Figure 3-117. Here again, a rather good agreement between theory and experiment may be seen, except for test PC4.15.400

where, because of its considerable deformability, the peak of the curve has not been reached during the test.

The last series of tests is presented in Figure 3-118. The agreement between theory and experimentation is again quite acceptable. Test PC4.30.1000 is the only one which fails by lack of resistance of the column cross-section, what is quite in line with what was observed in the laboratory. A slight over-estimation of the strength is noted. That is explained by the local buckling occurring at the end of the test in the column flange in compression. This failure load is not taken into consideration as far as now in the model.

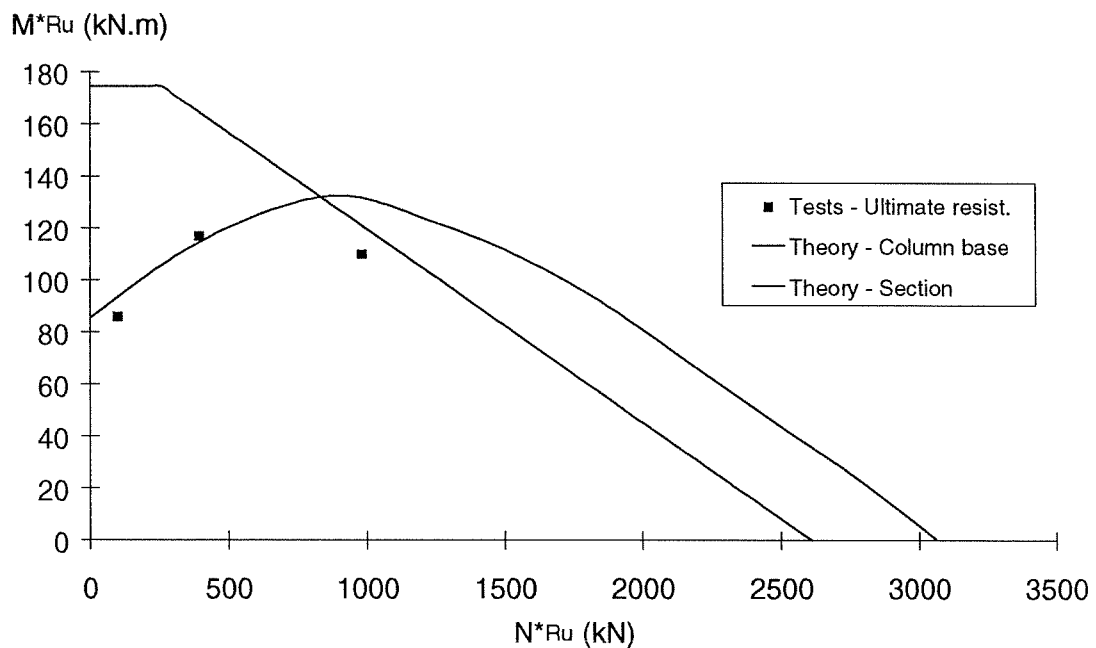


Figure 3-118 Comparison between tests and model-tests PC4.30

In conclusion, it can be stated that the analytical model, despite its simplicity, is particularly suitable for the prediction of the failure load of column bases.

3.4.3.2 Evaluation of the initial stiffness

The initial stiffness, i.e. the slope of the moment-rotation curve at the origin, is another main mechanical property of the column bases.

By contrast with the beam-to-column joints or beam splices, the initial stiffness of the column bases is difficult to evaluate. The effect of the axial force in the column and the plate-to-concrete contact which involves separation effects, activation or non-activation of the anchor bolts, etc., have to be considered to explain the particular behaviour of column bases. For the test configurations for which the axial applied force is low, a highly premature separation of the plate is observed, what modifies the distribution of internal forces and therefore the global stiffness of the column base. Consequently, by contrast

with conventional joints which exhibit an elastic linear initial behaviour, the column bases may experience very quick changes of stiffness. In this context, the need for the theoretical prediction of the initial stiffness becomes questionable.

This is why it has been decided in Liège not to go further with investigations on initial stiffness but to develop a kinematic (mechanical) model allowing to follow the behaviour of the column bases all along their loading history. Such an approach appears as the most suitable one to understand deeply the complex phenomena to which the scientist is faced when studying column bases. We are so following the approach initiated some years ago by Penserini [P2], whose works constituted a quite valuable reference all along our developments.

It should be mentioned, however, that the team of F. Wald, in Prague, is actively working on the development of a simple model which should enable the stiffness and strength of column-bases to be evaluated by hand [W2].

The combination of these two complementary works in the future could probably help in deriving simple guidelines for practitioners, to be possibly included in a new issue of Eurocode 3 Annex J and Annex L.

3.4.4 Mechanical model

3.4.4.1 Background of the model

The main objective is to develop a model based on the component method and able to follow the behaviour of the column bases all along their whole range of loading.

To ensure the suitability of the models with the expectations, it appears quite important to take good note of the following observations made during the tests in laboratory :

- The unilateral contact between the plate and the concrete is a complex phenomenon which needs to be described in very refined way.
- The bond between the anchor bolts in tension and the concrete which surrounds them is broken very prematurely, as soon as the anchor bolts are subjected to tension. It is therefore allowed to consider that the bolts are free to elongate over their whole length L_b , as measured from the origin of the curved part up to the mid-thickness of the nut, i.e. approx. 250 mm (see Figure 3-94).
- Under the column flange(s) in compression, the plate undergoes substantial deformations. The pressure under the plate is therefore far from being uniform, even under pure compression. As a consequence, it is absolutely essential to keep the concept of equivalent rigid plate in the model.
- In the compressive zone, the extended part of the steel plate has an essential role as it prevents premature crushing into the concrete. The formation of a yield line in the extended part of the plate all along the column flange can also be noted. This requires substantial deformation energy which ought therefore to be modelled.

- The steel column cross-section experiences yielding which, in some cases, produces significant deformations. To compare the mechanical model with the experimental moment-rotation curves defined in Section 3.4.2 - where the plastic deformations of the cross-section are included - it is absolutely essential to consider these deformations in the model.
- The distribution of the internal forces in a column base changes considerably during its loading. In particular, the contact zone, and therefore the lever arm of the internal forces, are in constant evolution. Furthermore, the individual response of each component (concrete, anchor bolts, plate, section, etc.) is highly non-linear. Therefore only an iterative approach can efficiently describe the behaviour of the column bases throughout the whole loading.

In the light of the above statements and after several trials, which are not described here, a mechanical model has been finally selected ; it is illustrated in Figure 3-119.

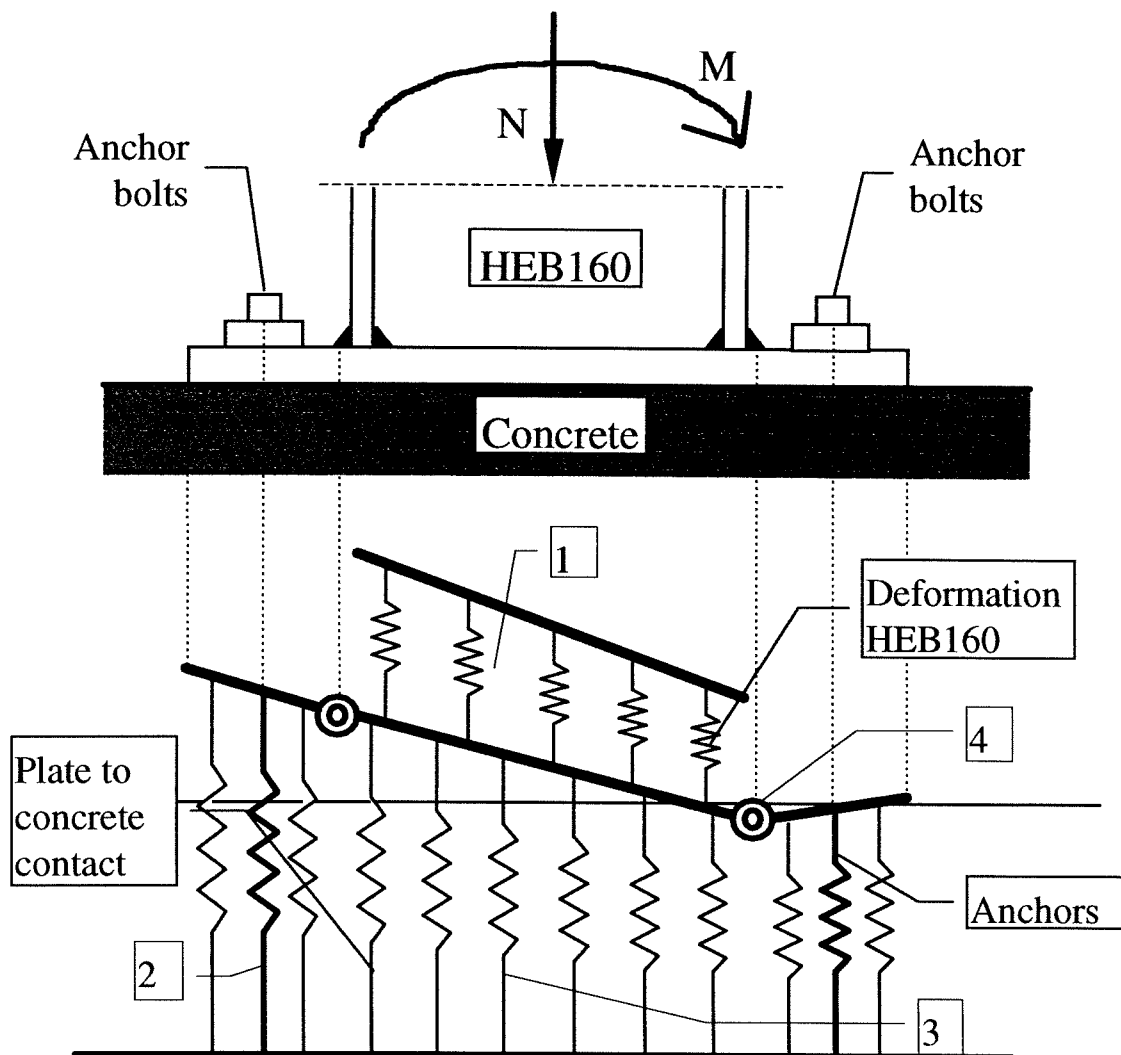


Figure 3-119 Mechanical model for column bases

In this figure, the following components may be identified:

- Extensional springs to simulate *the deformation of the column cross-section (1)*. These springs work both in tension and compression.
- Extensional springs to simulate *the deformation of the "anchor bolts and base plate" component (2)*. They work only in tension. A single spring is used to model a row of anchor bolts and the corresponding part of the plate.
- Extensional springs to simulate *the concrete under the plate (3)*. They work only in compression.
- Rotational springs used to model the plastic deformation associated to the possible development of a yield line in the extended part of the plate in the compressive zone (4). These springs are not activated when the extended part of the plate is in the

tensile zone and is therefore no longer in contact with the concrete as the deformability of the plate is already taken into account in the extensional springs (2) aimed at modelling the anchor bolts and plate assembly in the tensile zone.

In the next sections, details about the laws governing the behaviour of these components and the method used to assemble the components together so as to derive the overall response of the whole column base are presented.

3.4.4.2 Response of the individual components

Concrete in compression

The plate-to-concrete contact is a particularly complex phenomenon because of the modification of the contact zone with the eccentricity of the compressive force and with the flexibility of the plate, which is directly related to its thickness.

First of all, so as to avoid to take explicitly into account the actual flexibility of the plate, the concept of the equivalent rigid plate, already discussed in Section 3.4.3.1, is used. However, contrary to the static model developed in Section 3.4.3, the purpose of which was to calculate the strength of the column base, the whole loading range, characterized by a substantial variation of the eccentricity of the axial force, is considered here. Thus the choice of a rectangular equivalent rigid plate was no longer suitable at all for describing some ranges of eccentricity. Therefore, the idealization of the plate illustrated in Figure 3-120 is adopted. It is quite close to that recommended in Annex L of Eurocode 3 [E6].

The parameter "c" is the one calculated by Formula (3-75). As previously mentioned, yield line(s) are likely to occur in the extended part of the plate. They are located close to the weld, at a distance $0.8 \cdot \sqrt{2} \cdot a_f$ of the column flange, where a_f designates the throat radius of the weld between the column flange and the base plate.

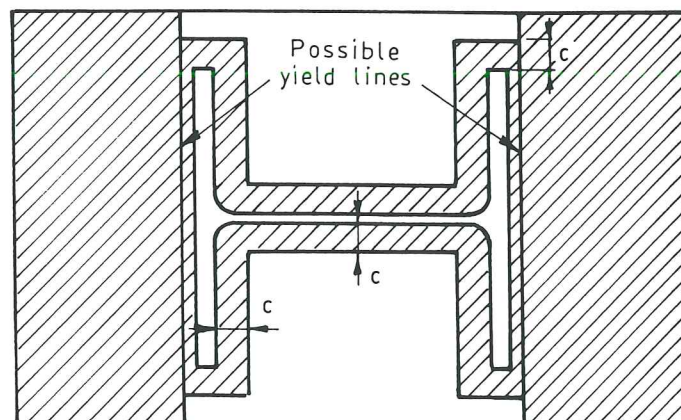


Figure 3-120 Definition of the equivalent rigid plate for the mechanical model

The law σ - ε adopted for concrete in the model is a conventional parabola-rectangle one, as illustrated in Figure 3-121. It is characterized by an almost straight parabolic part. In fact, this is understandable because the strength f_j (see Formula 3-74) of the concrete takes into account the beneficial effects of the confinement and is therefore much higher than that measured on cubes. This does not apply to the Young's modulus E_b of the material. In fact, it may be assumed that the confinement only appears when the deformations are significant.

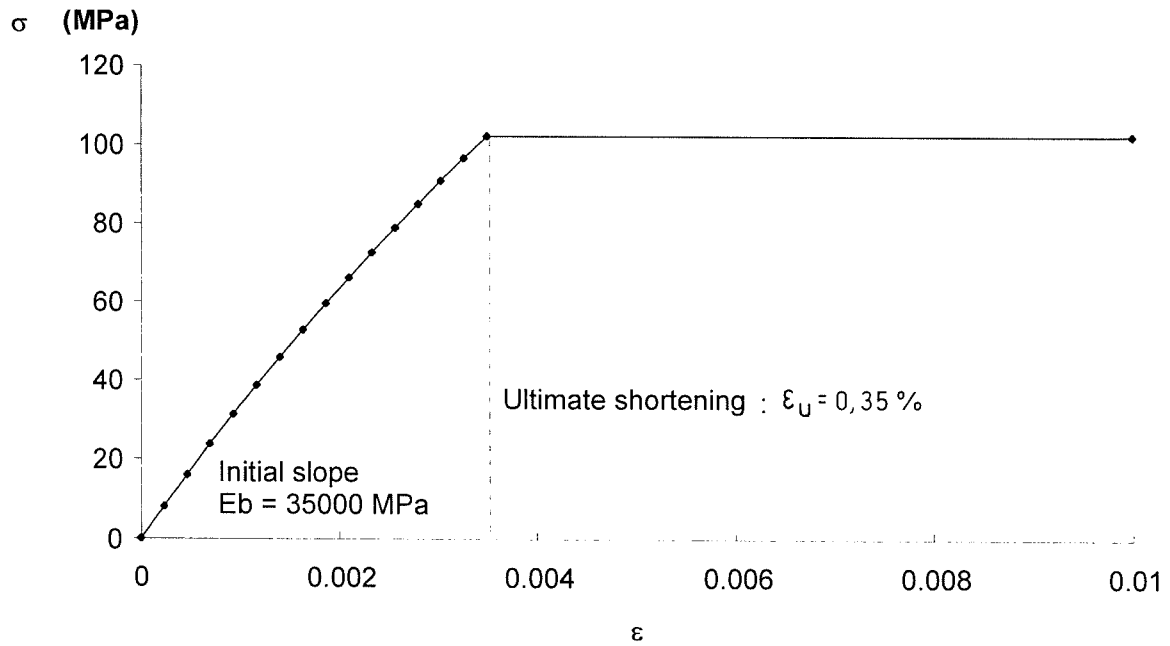


Figure 3-121 σ - ε law for concrete in compression

Equation (3-91) gives the mathematical expression of the law illustrated in Figure 3-121. The curve passes through the origin, with an initial slope equal to the Young's modulus, and passes through the point (ε_u, f_j) .

$$\sigma(\varepsilon) = \frac{f_j - E_b \cdot \varepsilon_u}{\varepsilon_u^2} \cdot \varepsilon^2 + E_b \cdot \varepsilon \quad (3-91)$$

The concrete-to-plate contact is discretized through the use of a finite number of springs, each covering a small part of the contact zone. A number of preliminary tests have shown that about hundred springs provide sufficient accuracy for discretization. To establish the $F_i - \Delta_i$ law of a particular spring, it is sufficient to comply with the two following equations:

$$\begin{aligned} F_i &= \sigma \cdot \Omega_i \\ \Delta_i &= \varepsilon \cdot h_{block} \end{aligned} \quad (3-92)$$

where F_i is the force in the spring i , Ω_i the concrete area it represents, Δ_i its elongation; h_{block} is the depth of the concrete block. By combining equations (3-91) and (3-92), the $F_i - \Delta_i$ relationship is derived as follows :

$$F_i(\Delta_i) = \Omega_i \cdot \left[\frac{f_j - E_b \cdot \epsilon_u}{\epsilon_u^2} \cdot \left(\frac{\Delta_i}{h_{block}} \right)^2 + E_b \cdot \left(\frac{\Delta_i}{h_{block}} \right) \right] \quad (3-93)$$

Equation (3-93) is based on the assumption that the deformation at a point of the plate-to-concrete contact zone is constant over the depth of the block, what is just, of course, a simplification. However, for reasonable dimensions of the block, what is the case for the tests considered here, this idealization gives similar results than those supplied by more complex models, as the Penserini one [P2].

Anchor bolts in tension and base plate in bending

Contrary to the behaviour of the concrete which is identical for each of the twelve tests, the curve relating to the "anchor bolts in tension and plate in bending" assembly depends (a) on the thickness of the plate and (b) on the position of the row: between the flanges or outside the flanges.

The pseudo-plastic and ultimate resistances of the "anchor bolts-base plate" assembly, respectively termed $F_{Rp,model}$ and $F_{Ru,model}$ (see Appendix 1), are given in Table 3-8. They have been basically derived through the use of the formulae given in section 3.4.3.1 (strength of the anchor bolts in tension and the base plate in bending) but sometimes amended as explained in the next paragraphs. As mentioned previously, the ultimate tensile resistance of the anchor bolts has not been reached, in the tests presented in Section 3.4.2, by failure in the cross-section, but by unbending of the curved part. The associated ultimate value measured in laboratory is also reported in Table 3-8 where the italic and bold characters are used for values exceeding $2B_{t,Ru}$.

	PC2.15	PC2.30	PC4.15	PC4.30
$F_{Rp,model}$ (kN)	327	1306	91	363
$F_{Ru,model}$ (kN)	480	1922	264 (PC4.15.100) 133 (others)	447 (PC4.30.100) 534 (others)
$2 B_{t,Ru}$ (kN)	375			

Table 3-8 Strengths of the anchor bolts and plate in tension

During the tests, the anchor bolts elongate usually in a significant way, and more particularly, in comparison with the deformation of the base plate. As a consequence,

prying effects may not develop as they would do in usual end-plate connections. Such a behaviour has been systematically noted in the first loading steps, i.e. there where the response of the column base is approximately elastic. This explains why the elastic stiffness of the "anchor bolts - base plate" assembly is evaluated below on the basis of a "no prying" situation. For what regards the pseudo-plastic resistance of the "bolt-plate" assembly, a distinction has to be made between column bases with two and four anchor bolts respectively.

In column bases with two anchor bolts, no prying forces develop all along the loading. Mode 2 failure in the base plate is therefore not contemplated and only circular patterns are likely to contribute to Mode 1 (see Section 3.4.3.1).

In column bases with four anchor bolts, a similar response is reported for tests PC4.15.100 and PC4.30.100. For the other tests (PC4.15.400 and 1000 and PC4.30.400 and 1000) no prying develops until the pseudo-plastic resistance of the base plate is reached. But because of the high axial compression force acting in the column, the displacements remain limited in the tension zone and a contact progressively develop between the plate and the concrete when the loading is increased beyond the pseudo-plastic resistance of the column base. Formulae (3-77) to (3-79) are therefore used at ultimate state.

This justifies the different values reported in Table 3-8 according to the test numbers.

For the mechanical model, the whole deformability curve of the "anchor bolts-plate" assembly must be determined. First, the elastic stiffness of the different components is evaluated according to Eurocode 3 Annex J where the force -displacement relationship for each component in the elastic range, is expressed as follows :

$$F = E k \Delta \quad (3-94a)$$

or
$$F = K . \Delta \quad (3-94b)$$

with : k is the stiffness coefficient of the component

K is the stiffness of the component

For a row with two anchor bolts, the stiffness coefficient is as follows :

$$k_b = \frac{2 \cdot A_s \cdot E}{L_b} \quad (3-95)$$

where A_s represents the stress area of the anchor bolt, E the Young's modulus for steel and L_b the free length of the bolts. The value to give to L_b has been defined in Section 4.1.

The deformability resulting from the bending of the base plate has to be added to that of the anchor bolts. The elastic stiffness of the base plate is given by :

$$k_p = \frac{E \cdot \ell_{eff} \cdot t_p^3}{2 \cdot m^3} \quad \text{for configurations with 2 anchor bolts} \quad (3-96.a)$$

$$k_p = \frac{E \cdot \ell_{eff} \cdot t_p^3}{2 \cdot m_x^3} \quad \text{for configurations with 4 anchor bolts} \quad (3-96.b)$$

where ℓ_{eff} , m and m_x are given in Section 3.4.3.1; t_p is the thickness of the plate. Formulae (3-95) and (3-96) differ from those recommended in revised Annex J because of the absence of prying forces.

When the elastic stiffness and the resistance of the two components are known, deformability curves for anchor bolts and plate can then be built. Let us start with the anchor bolts in tension. Their behaviour is modelled in accordance with the law illustrated in Figure 3-122. The format of this law is similar to that used in EC3 Annex J but it is referred here, for what regards the peak value of the curve, to the ultimate resistance of the anchor bolts and not to the design resistance as it should be according to Annex J. This freedom has been taken after that the suitability of the proposed law had been checked through comparisons with results of laboratory tests on anchor bolts in tension.

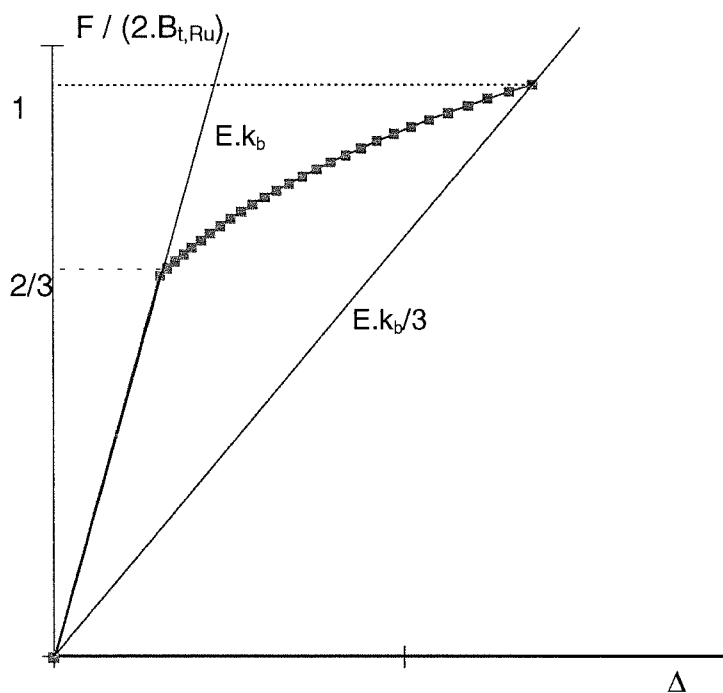


Figure 3-122 Behaviour law for anchor bolts in tension

The equation of the curve plotted in Figure 3-122 can be expressed as follows:

$$\begin{cases} F = E \cdot k_b \cdot \Delta & \text{for } F \leq \frac{2}{3} \cdot 2 B_{t,Ru} \\ F = E \cdot k_b \left(1,5 \cdot \frac{F}{2 B_{t,Ru}} \right)^{-2,7} \cdot \Delta & \text{for } \frac{2}{3} \cdot 2 B_{t,Ru} < F < 2 B_{t,Ru} \end{cases} \quad (3-97)$$

where $2 B_{t,Ru}$ designates the ultimate resistance of an anchor bolt-row and k_b its elastic stiffness coefficient as given by equation (3-95).

The plate behaviour in bending is modelled in a more complex manner than that of the bolts. Use is made in fact of a model we proposed in [J1]; this one is much more suitable for the modelling of a steel component such as the plate. The F - Δ relationship is given by the equation (3-98) :

$$F = \frac{E \cdot (k_p - k_{p,post-limit}) \cdot \delta}{\left[1 + \left[\frac{E \cdot (k_p - k_{p,post-limit}) \cdot \delta}{F_{Rp}} \right]^c \right]^{\frac{1}{c}}} + E \cdot k_{p,post-limit} \cdot \Delta \leq F_{Ru} \quad (3-98)$$

where k_p is the initial stiffness coefficient (equation 3-96) and $k_{p,post-limit}$, the post-limit stiffness coefficient. According to [J1], $k_{p,post-limit}$ may be taken equal to 1/40 times the initial stiffness coefficient k_p in the case of column bases with two anchor bolts, and to 1/20 times k_p in the case of column bases with four anchor bolts where the extended part of the base plate experiences larger deformations resulting in the development of membrane effects. F_{Rp} is the pseudo-plastic resistance of the "bolt-plate" assembly and F_{Ru} its ultimate resistance (see Appendix 1). Parameter c is a shape factor which has been chosen equal to 1.5 on the basis of comparisons with the experimental data. This value is nothing else than that which is recommended in [J1] for most current types of steel beam-to-column joints.

The "anchor bolts + plate" behaviour curve is finally obtained by adding the two "anchor bolts" and "plate" curves (equations 3-97 and 3-98). Figure 3-123 to Figure 3-126 present the resultant curves obtained for the four test configurations described in Section 3.4.2.

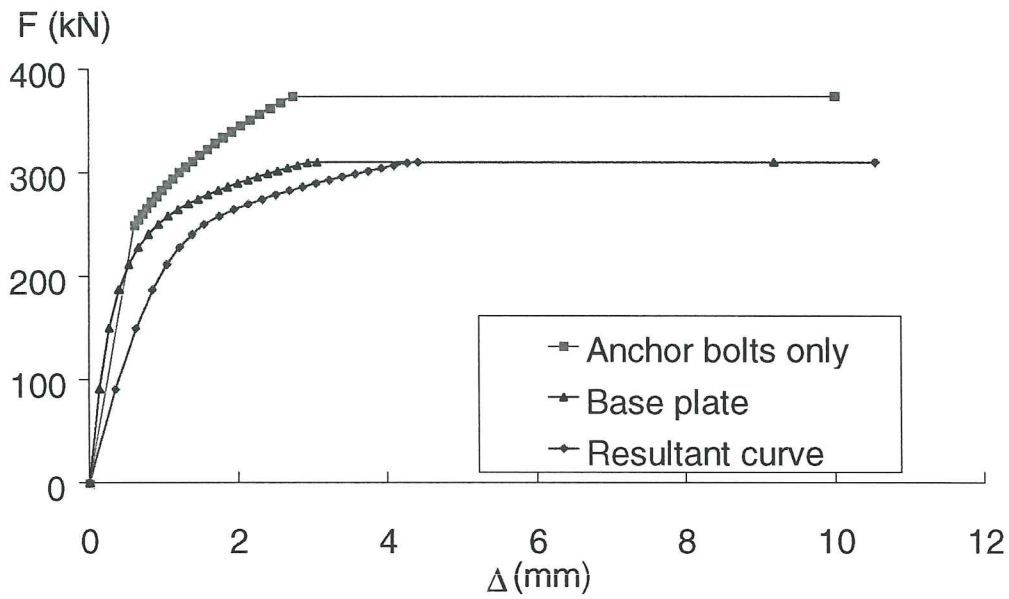


Figure 3-123 Behaviour law for the "anchor bolts + plate" component. Tests PC2.15

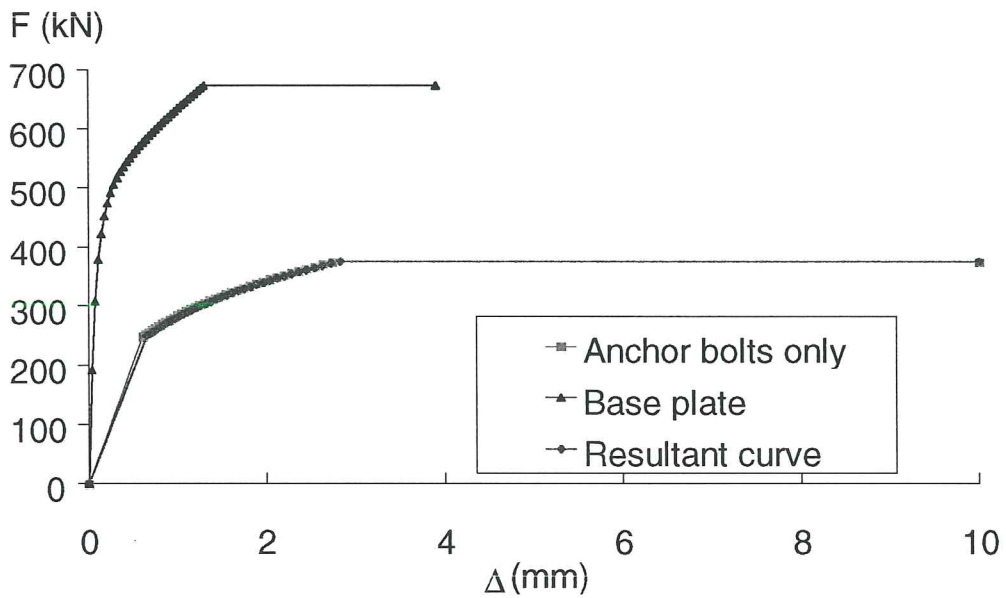


Figure 3-124 Behaviour law for the "anchor bolts + plate" component. Tests PC2.30

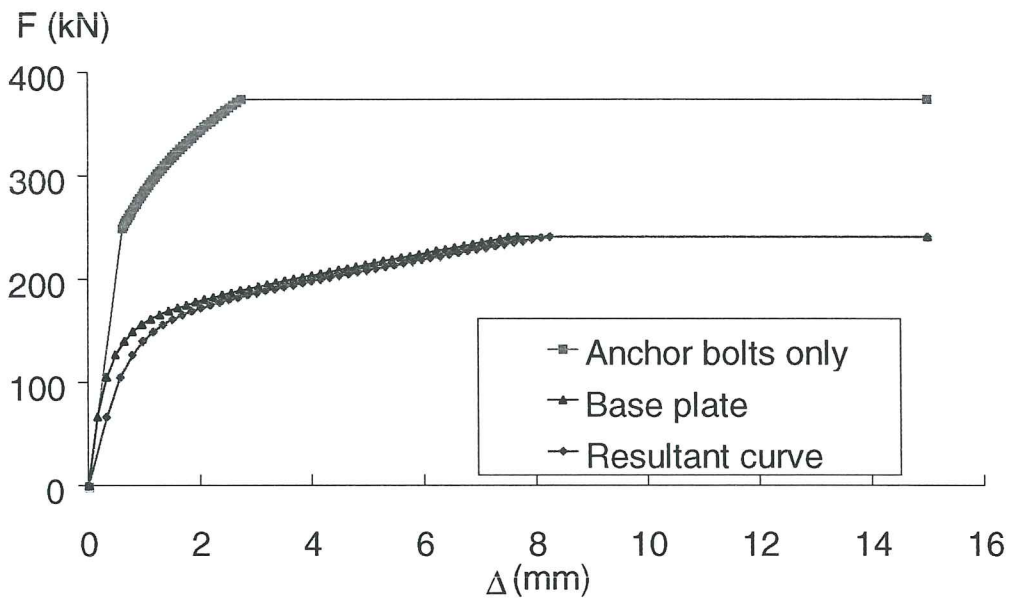


Figure 3-125 Behaviour law for the "anchor bolts + plate" component. Test PC4.15.100

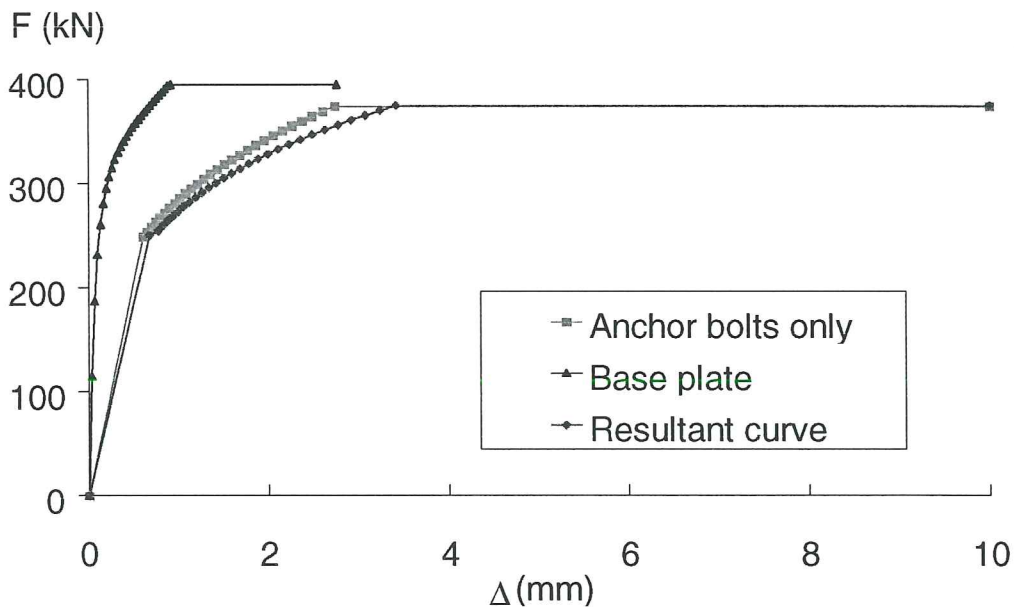


Figure 3-126 Behaviour law for the "anchor bolts + plate" component. Test PC4.30.100

In addition to the "anchor bolts + plate" deformability in the tensile zone, the plate is also likely to deform in the compressive zone in the case of column bases with four anchor bolts (see Section 3.4.4.1). The tests have shown that this deformation is very localized and may be concentrated in a plastic hinge. Thus, in the mechanical model, this

deformability is accounted for by means of a rotational spring characterized by an elastic-perfectly plastic law. In the tensile zone, the deformability of the plate is already considered through the above-described "anchor bolts + plate" spring. The stiffness of the rotational spring is therefore taken as infinite in the tensile zone ($K_t = \infty$). Figure 3-127 illustrates the behaviour law finally adopted.

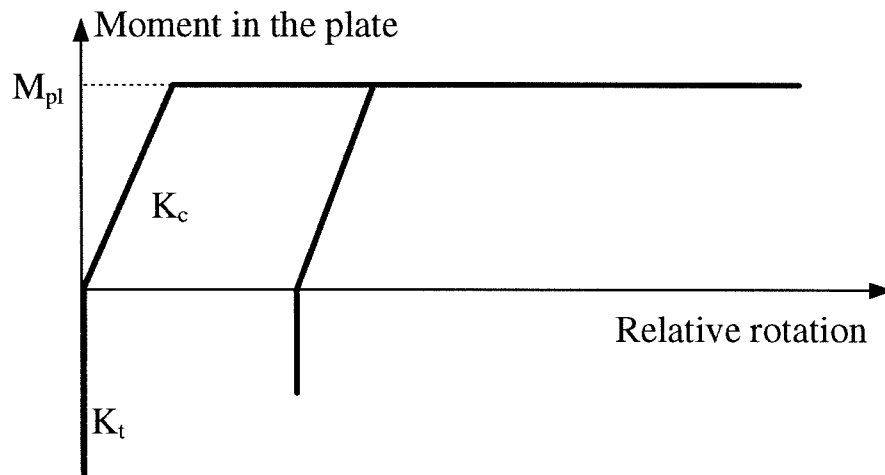


Figure 3-127 Behaviour law for the plate rotational spring (configuration with four anchor bolts)

The characteristics of the spring, i.e. M_{pl} and K_c , should be evaluated as follows:

$$K_c = \frac{E \cdot b_p \cdot t_p^3}{12} \cdot \frac{1}{t_p} = \frac{E \cdot b_p \cdot t_p^2}{12} \quad (3-99)$$

$$M_{pl} = \frac{b_p \cdot f_{yp} \cdot t_p^2}{4} \quad (3-100)$$

where b_p is the total width of the plate, f_{yp} its yield strength, and t_p its thickness. The calculation of the rotational stiffness (3-99) is based on the assumption that the deformation zone extends over a length equal to the thickness of the plate. However, application of the model to tests has shown that equations (3-99) and (3-100) overestimate the deformation energy of the plate. In fact, the best agreement has been obtained by giving to K_c and M_{pl} zero values, i.e. the characteristics of a perfect hinge. This assumption has therefore been selected.

Steel profile

In Section 3.4.2, it has been explained that the column steel profiles HE160B experiences, in some cases, high stresses, what leads to partial yielding of the cross-section. For test PC4.30.1000, a plastic hinge forms, causing the full yielding of the column cross-section.

In order to take this into account in terms of both strength and deformability, the steel cross-section is represented by means of a number of extensional springs, what makes it possible to simulate the development of yielding in the section with increasing values of the bending moment and compressive force.

Figure 3-128 illustrates the way in which the cross-section has been discretized in the mechanical model.

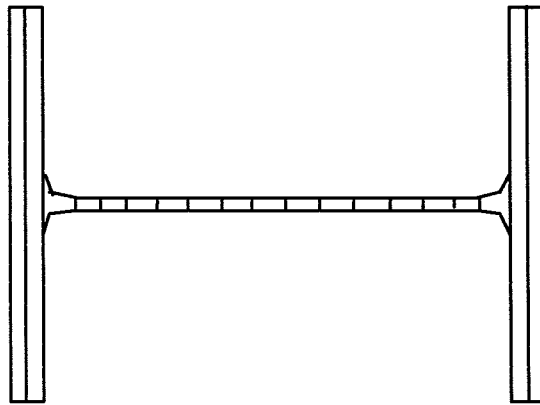


Figure 3-128 Discretization of the column cross-section for the mechanical model

To each of the small discretized parts of the section represented in Figure 3-128 is associated an extensional spring, the stiffness and strength of which are proportional to the area of this zone. The behaviour law for the constitutive steel is elastic - perfectly plastic. The length of the springs is taken equal to the distance between the end-plate and the location of the rotational transducer ROT_2 used in laboratory (see Section 3.4.2.3), so as to allow a direct comparison between test and model. An inconsistency is however likely to occur as the elastic contribution to the rotational deformation of the column close to the column base has been withdrawn from the experimental $M-\phi$ curve. As this contribution is seen to be quite negligible, the comparisons may be anyway considered as valid.

3.4.4.3 Assembly procedure

The characterization of the individual behaviour for all the components is followed by the assembly; this one is performed in accordance with the model illustrated in Figure 3-119 where it is assumed, conventionally, that all the vertical forces and moments are positive if they act upward and in the anti-clockwise direction respectively. The same rule applies also to the displacements.

A schematic representation of the model is given in Figure 3-129.

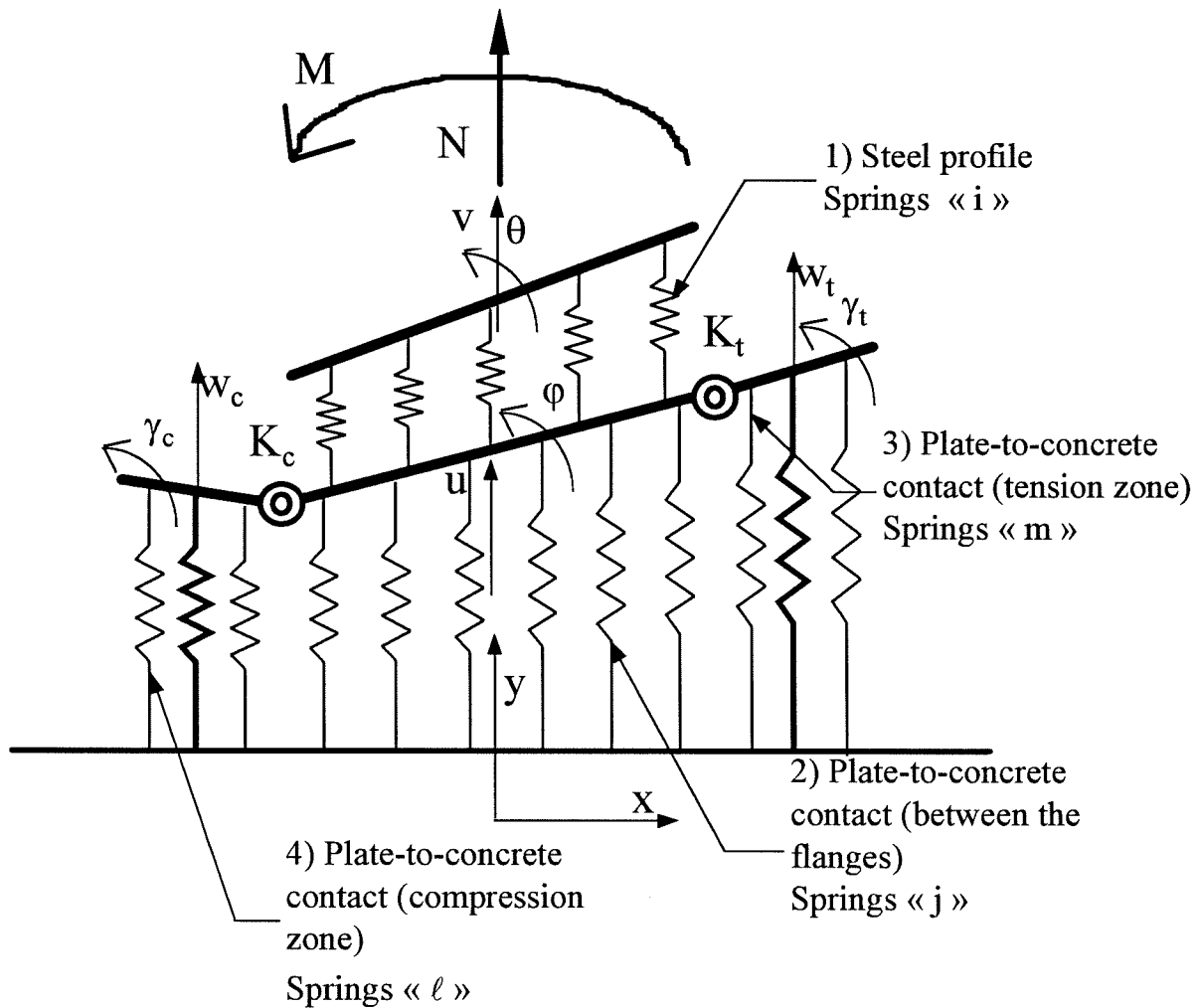


Figure 3-129 Schematic representation of the mechanical model

The origin of the abscissas (x) is placed on the column axis; the displacement field of the model may be so expressed as follows (see Figure 3-129):

$$\begin{aligned}
 u(x) &= u + \varphi \cdot x && \text{zone 1} \\
 v(x) &= v + \theta \cdot x && \text{zone 2} \\
 w_t(x) &= u + \lim_t \cdot \varphi + (x - \lim_t) \cdot \gamma_t && \text{zone 3} \\
 w_c(x) &= u + \lim_c \cdot \varphi + (x - \lim_c) \cdot \gamma_c && \text{zone 4}
 \end{aligned}
 \tag{3-101}$$

where \lim_t and \lim_c designate the abscissas of the flexural springs in the tensile (K_t) and compressive (K_c) zones respectively. The quantities u , v , θ , φ , γ_t and γ_c are defined in Figure 3-129. The numbering of the zones (1 to 4) is also shown in Figure 3-129.

Equation (3-100) shows that the deformed state of the system is fully defined by six parameters: u , v , φ , θ , γ_c , γ_t . The determination of these values under loads M and N loads requires six linearly independent equations. These equations are obtained by expressing the vertical and rotational equilibrium of the different zones of the model. First of all, the equilibrium of zone 1, i.e. the upper part of the model representing the steel profile, is expressed. Equation (3-102) relates to the vertical equilibrium and equation (3-103) represents the rotational equilibrium expressed at the origin of the axes :

$$N + \sum_i F_i = 0 \quad (3-102)$$

$$M + \sum_i F_i \cdot x_i = 0 \quad (3-103)$$

where F_i designates the axial force in the "zone 1" spring i .

In equations (3-102) and (3-103), the summation applies to all the springs of the zone 1 which represents the column profile subject to combined bending and compressive or tensile forces. The force in a spring may be calculated from the displacements as follows:

$$F_i = K_i \cdot (v_i - u_i) = K_i \cdot [(v - u) + x_i \cdot (\theta - \varphi)] \quad (3-104)$$

K_i corresponds to the stiffness of the spring " i ".

By substituting equation (3-104) in (3-102) and (3-103), we obtain:

$$N + \sum_i K_i (v - u) + \sum_i K_i \cdot x_i (\theta - \varphi) = 0 \quad (3-105)$$

$$M + \sum_i K_i \cdot x_i (v - u) + \sum_i K_i \cdot x_i^2 (\theta - \varphi) = 0 \quad (3-106)$$

The vertical equilibrium of the whole lower part of the model, namely zones 2 to 4 writes

$$-\sum_i F_i + \sum_j F_j + \sum_\ell F_\ell + \sum_m F_m = 0 \quad (3-107)$$

The forces in the springs " j ", " ℓ " and " m " (see Figure 3-129) can be expressed as follows:

$$F_j = K_j \cdot u_j = K_j \cdot (u + x_j \cdot \varphi) \quad (3-108)$$

$$F_m = K_m \cdot w_t = K_m \cdot [u + \lim_t \cdot \varphi + (x_m - \lim_t) \cdot \gamma_t] \quad (3-109)$$

$$F_\ell = K_\ell \cdot w_c = K_\ell \cdot [u + \lim_c \cdot \varphi + (x_\ell - \lim_c) \cdot \gamma_c] \quad (3-110)$$

By combining equations (3-108) to (3-110) and (3-104) with equation (3-107), the third equation of equilibrium is obtained :

$$\begin{aligned}
& \left[\sum_i K_i + \sum_j K_j + \sum_\ell K_\ell + \sum_m K_m \right] \cdot u - \sum_i K_i \cdot v + \\
& \left[\sum_i K_i \cdot x_i + \sum_j K_j \cdot x_j + \lim_c \cdot \sum_\ell K_\ell + \lim_t \cdot \sum_m K_m \right] \cdot \varphi - \sum_i K_i \cdot x_i \cdot \theta \quad (3-111) \\
& + \left[\sum_\ell K_\ell \cdot x_\ell - \lim_c \cdot \sum_\ell K_\ell \right] \cdot \gamma_c + \left[\sum_m K_m \cdot x_m - \lim_t \cdot \sum_m K_m \right] \cdot \gamma_t = 0
\end{aligned}$$

The three last equations needed to solve the system are obtained by expressing the individual rotational equilibrium of each of the zones 2, 3 and 4. The moments acting in the end-plate rotational springs can be expressed as follows:

$$M_c = K_c \cdot (\varphi - \gamma_c) \geq 0 \quad (3-112)$$

$$M_t = K_t \cdot (\gamma_t - \varphi) \geq 0 \quad (3-113)$$

As previously explained the stiffnesses K_c and K_t depend on the direction of the bending moment applied to the extended parts of the plate (Figure 3-127). The rotational equilibrium of the interior part of the plate writes :

$$\begin{aligned}
& \left[\sum_i K_i \cdot x_i + \sum_j K_j \cdot x_j + \lim_c \cdot \sum_\ell K_\ell + \lim_t \cdot \sum_m K_m \right] \cdot u - \sum_i K_i x_i \cdot v + \\
& \left[\sum_i K_i \cdot x_i^2 + \sum_j K_j \cdot x_j^2 - K_t - K_c + \lim_c^2 \cdot \sum_\ell K_\ell + \lim_t^2 \cdot \sum_m K_m \right] \cdot \varphi - \sum_i K_i \cdot x_i^2 \cdot \theta \quad (3-114) \\
& + \left[\lim_c \cdot \sum_\ell K_\ell \cdot (x_\ell - \lim_c) + K_c \right] \cdot \gamma_c + \left[\lim_t \cdot \sum_m K_m \cdot (x_m - \lim_t) + K_t \right] \cdot \gamma_t = 0
\end{aligned}$$

Equations (3-115) and (3-116) express the rotational equilibrium of the extended parts under tensile and compressive loads.

$$\begin{aligned}
& \left[\sum_\ell K_\ell \cdot (x_\ell - \lim_c) \right] \cdot u + \left[\sum_\ell K_\ell (x_\ell - \lim_c) \cdot \lim_c + K_c \right] \cdot \varphi \\
& + \left[\sum_\ell K_\ell \cdot (x_\ell - \lim_c)^2 - K_c \right] \cdot \gamma_c = 0 \quad (3-115)
\end{aligned}$$

$$\begin{aligned}
& \left[\sum_m K_m \cdot (x_m - \lim_t) \right] \cdot u + \left[\sum_m K_m (x_m - \lim_t) \cdot \lim_t - K_t \right] \cdot \varphi \\
& + \left[\sum_m K_m \cdot (x_m - \lim_t)^2 + K_t \right] \cdot \gamma_t = 0 \quad (3-116)
\end{aligned}$$

At this stage the six linearly independent equilibrium equations are available. These can be expressed in the form of a matrix. It is here quite important to note that the stiffnesses K of each spring are tangential ones and are deduced from the component non-linear curves;

they vary then with the level of loading applied to the column base. As a consequence, the moment-rotation curve of the column base has to be built step by step by applying successively load increments to the mechanical model and by evaluating the corresponding deformations. This requires, at each loading step, to solve the system of non-linear equations expressed in an incremental format. As the position of all the springs is fixed, the incremental expression of the equilibrium equation is simply achieved (see equation 3-117) by replacing, in the six equations, the displacements u , v , φ , θ , γ_c , γ_t and the external forces applied M and N by their increments.

The springs simulating the anchor bolts belong either to zone 2 in the case of column bases with two anchor bolts- index "j" - or to zones 3 and 4 in the case of column bases with four anchor bolts - indices "m" and "l" -.

$$[K_i] \begin{Bmatrix} \Delta v \\ \Delta \theta \\ \Delta u \\ \Delta \varphi \\ \Delta \gamma_c \\ \Delta \gamma_t \end{Bmatrix} = \begin{Bmatrix} -\Delta N \\ -\Delta M \\ 0 \\ 0 \\ 0 \\ 0 \end{Bmatrix} \quad (3-117)$$

with $[K_i] =$

$$\begin{bmatrix} \sum K_i & \sum K_i \cdot x_i & -\sum K_i & -\sum K_i \cdot x_i & 0 & 0 \\ \sum K_i \cdot x_i^2 & -\sum K_i \cdot x_i & -\sum K_i \cdot x_i^2 & 0 & 0 \\ \sum K_i + \sum K_j & \sum K_i \cdot x_i + \sum K_j \cdot x_j & \sum K_i \cdot x_i^2 + \sum K_j \cdot x_j^2 - K_t - K_c & \sum K_i \cdot x_i & \sum K_m \cdot x_m \\ + \sum K_m + \sum K_l & + \lim_i \sum K_m + \lim_c \sum K_l & + \lim_i^2 \sum K_m + \lim_c^2 \sum K_l & - \lim_c \sum K_l & - \lim_i \sum K_m \\ \lim_c \sum K_l \cdot x_l & \lim_i \sum K_m \cdot x_m & \sum K_l \cdot (x_l - \lim_c)^2 - K_c & 0 \\ - \lim_c^2 \sum K_l + K_c & - \lim_i^2 \sum K_m + K_t & \sum K_m \cdot (x_m - \lim_i)^2 - K_t \\ \text{sym.} & & & & \sum K_m \cdot (x_m - \lim_i)^2 - K_t \end{bmatrix}$$

The different steps of the iterative procedure which leads to build progressively the deformability curve of the column base are detailed hereunder.

- Let us consider the system in equilibrium under applied forces M_i and N_i . The displacements u_i , v_i , φ_i , θ_i , γ_{ci} , γ_{ti} are associated to these forces. At the beginning of the process, all these quantities are equal to zero.

- As the deformation of the system is known, it is possible to calculate the individual deformation of each spring. From this deformation, the tangential stiffness of the springs may be derived from their $F-\Delta$ law (Formulae 3-93, 3-97 and 3-98).
- At the beginning of the iterative process, no information is available on the behaviour of the system; it is therefore assumed a priori that all the springs are activated and that their stiffness is taken equal to the elastic one.
- Load increments ΔN_{i+1} , ΔM_{i+1} , are applied to the system. On the basis of the tangential stiffnesses calculated above, equation (3-117) is solved to obtain the six increments of displacement Δu_{i+1} , Δv_{i+1} , $\Delta \varphi_{i+1}$, $\Delta \theta_{i+1}$, $\Delta \gamma_{ii+1}$, $\Delta \gamma_{ci+1}$ which are then added to the values already calculated.
- For this new deformed state, the forces acting in the different springs are evaluated. Because of the linearization of the equilibrium equations, the resultant of these forces does not counterbalance perfectly the moment and axial load applied. The difference between these two quantities is termed "out-of-equilibrium forces".
- To compensate for this lack of accuracy, equation (3-117) is solved again by replacing ΔN_{i+1} and ΔM_{i+1} respectively by the values of the out-of-equilibrium axial force and the out-of-equilibrium moment. New increments of displacement are obtained which are again added to the previous values, and this iterative procedure is applied until the out-of-equilibrium forces are small enough to be ignored. At this moment, the deformed state of the system under the $N_i + \Delta N_{i+1}$ and $M_i + \Delta M_{i+1}$ loads is finally known.
- A new increment of forces is then applied, and the iterative process described here-above is reactivated until failure is reached, i.e. when:
 - the system of equations have singularities, what only occurs when the resistance of all the springs of zone 1 or all the springs of zones 2 to 4 is exhausted;
 - the system of equations diverges or requires too many iterations to converge, thereby signifying that the resistance of a large number of springs is exhausted and that the equilibrium is practically impossible to satisfy;
 - the displacements observed become too large, thus falling outside the scope of the model (excess of deformation capacity in some components).

In the next section, comparisons between the mechanical model and the experimental results described in Section 3.4.2 are presented.

In these applications, the failure of the column base is reached for the first above-described two reasons; the concrete crushes or the anchor bolts breaks in tension (in most of the tests) or the steel profile yields (test PC4.30.1000).

3.4.4.4 Comparison with the experiments

Figure 3-130 to Figure 3-141 present comparisons between the mechanical model described in the foregoing paragraphs and the twelve experimental tests results.

The curves presented in these figures are the moment-rotation curves of the column bases. With regard to the mechanical model, the graph shows the variation of M as a function of θ , i.e. the rotation measured at the base of the steel profile, with due account being taken of the yielding phenomena occurring in the latter.

For the configurations with two anchor bolts the theoretical curves obtained using the Penserini method [P2] have also been plotted. It is clear that the agreement between the latter and the experimental tests is far from convincing (Figure 3-130 to Figure 3-135). This is simply because the tests carried out in Liège are largely outside the scope of the Penserini model.

Examination of Figure 3-130 to Figure 3-132 presenting tests PC.15 (two bolts - 15 mm plate) reveals an excellent agreement between the mechanical model and experimentation. The initial stiffness of the moment-rotation curve is accurately predicted by the model; the progressive yielding of the column base is perfectly predicted by the theory. On the other hand, the agreement is less satisfactory for the ultimate load; it remains however quite acceptable (scatter of 5 to 10% maximum). This is due to the great complexity of behaviour when the different components of the column base are close to collapse:

- concrete is a material whose mechanical properties can vary considerably according to the quality of the compaction. Furthermore, the crushing of the concrete under local forces is not an easy phenomenon to model;
- the anchorage of the bolts in the concrete is aleatory. In fact, contrary to what was expected, the anchorage of the bolts by the concrete was not sufficient enough to prevent a relative overall movement between the bolt and its support. Fortunately, these movements only occurred in the case of very high tension forces at the end of the test, and thus only altered the ultimate load.
- the displacements at the end of the test become quite significant, what leads to geometry changes which are not correctly taken into account in the mechanical model.

Despite this, and considering the curves as a whole, the general agreement between the mechanical model and the tests can be regarded as being quite good.

A similar conclusion could be drawn at Figure 3-133 to Figure 3-135 relating to tests PC2.30, except for test PC2.30.100 (Figure 3-133).

Some investigations have shown, however, that the only way to come to a better agreement for tests PC2.30.100, with the model, was to reduce the stiffness of the concrete without modifying its ultimate strength.

In other words, the lack of stiffness in the concrete block appears as the main reason to explain the rather poor agreement obtained in this case. And, in fact, that is what happened in test PC2.15.100 as explained in Section 3.4.2.4.

Figure 3-136 and Figure 3-138 relate to PC4.15 tests. Again, the agreement is seen quite acceptable.

Finally, Figure 3-139 to Figure 3-141 show a moderate agreement between theory and experimentation. While test PC4.30.400 (Figure 3-140) gives excellent results, test PC4.30.100 seems to suffer from the same problem than test PC2.30.100, i.e. an actual stiffness for the concrete lower than the theoretical prediction. Finally, test PC4.30.1000 seems to be well described by the mechanical model (Figure 3-141) when the moment is lower than half its ultimate value. But, as already said, a progressive buckling of the column flange in compression has been observed during the test and it has been previously pointed out that this failure mode is not included in the model. This probably explains the additional deformability reported during the test.

In conclusion, the agreement between the mechanical model and the experimentation can be considered as quite satisfactory, even good. Few discrepancies have been observed. These, however, can be explained and they do not put the general validity of the proposed rules in question again. It must not be forgotten that these rules have been rigorously derived, i.e. without a single empirical parameter, and are identical for the twelve tests being considered.

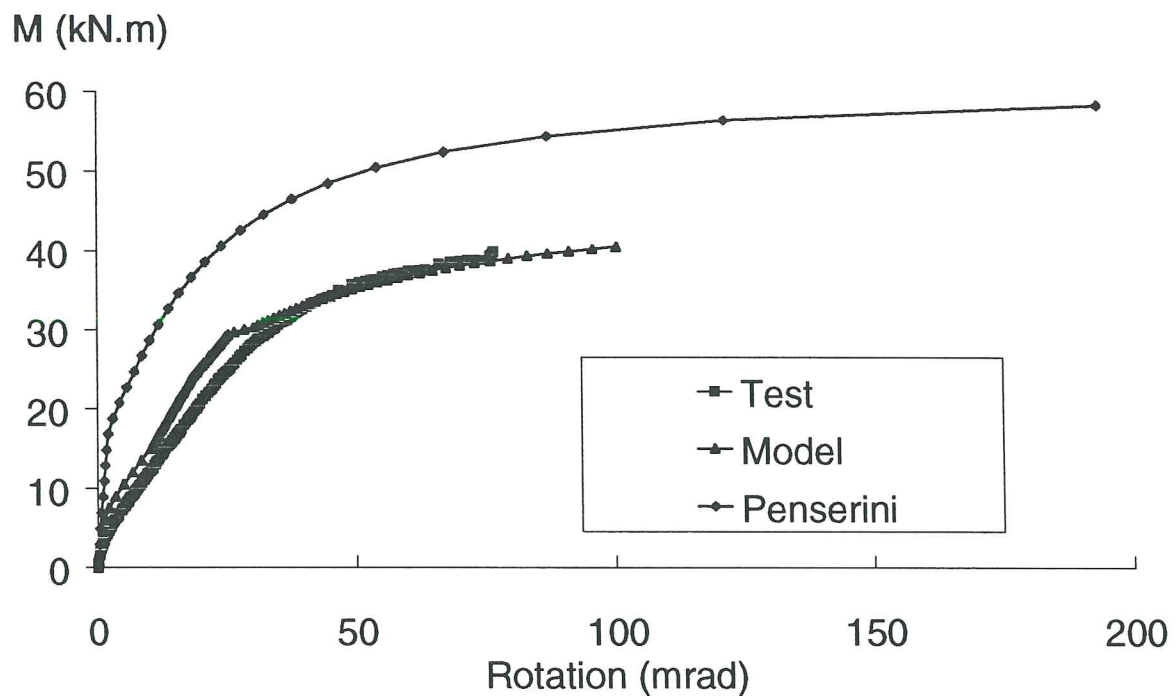


Figure 3-130 Comparison between the tests and the mechanical model. Test PC2.15.100

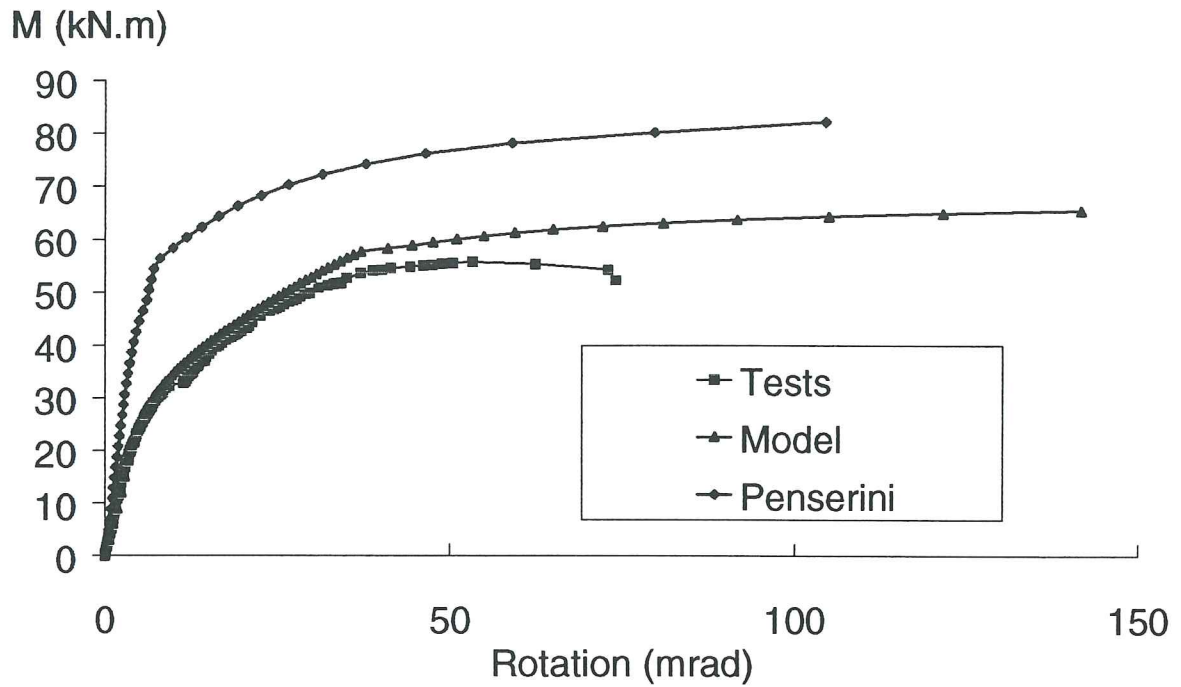


Figure 3-131 Comparison between the tests and the mechanical model. Test PC2.15.600

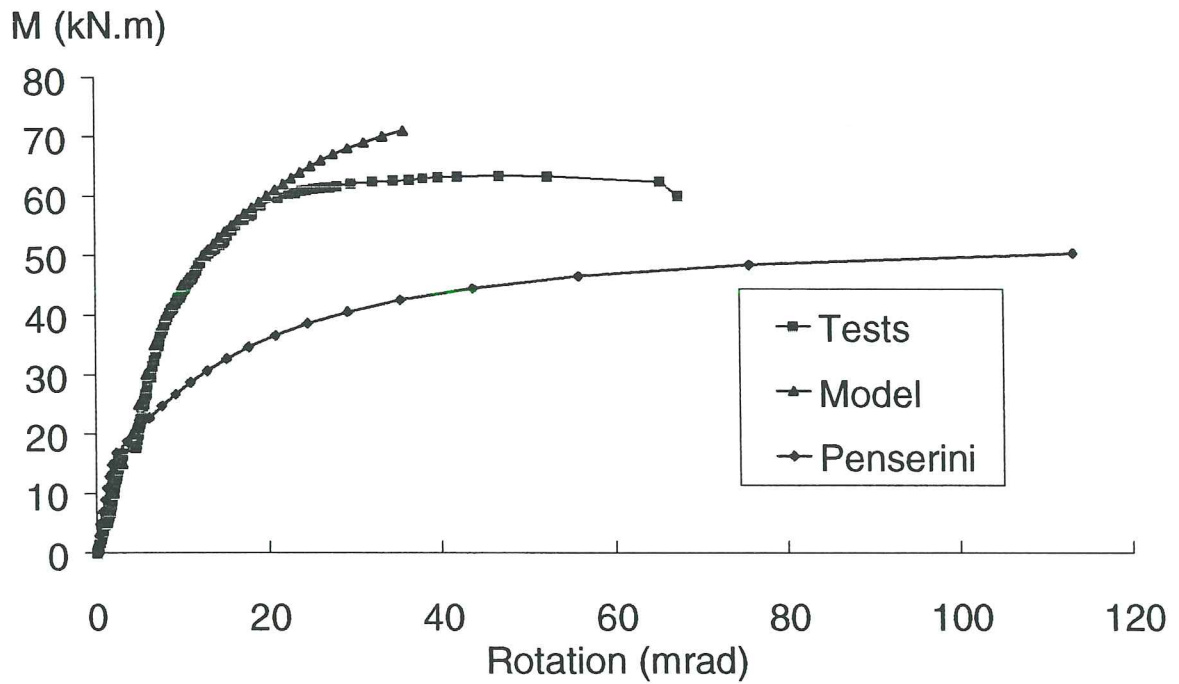


Figure 3-132 Comparison between the tests and the mechanical model. Test PC2.15.1000

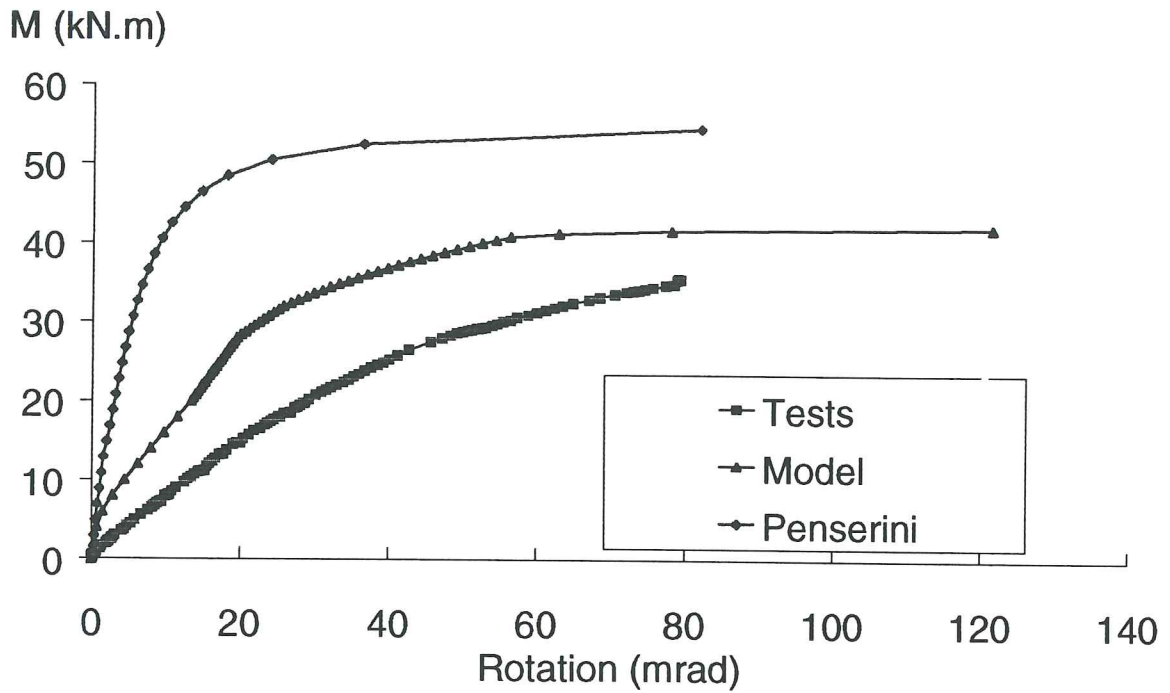


Figure 3-133 Comparison between the tests and the mechanical model. Test PC2.30.100

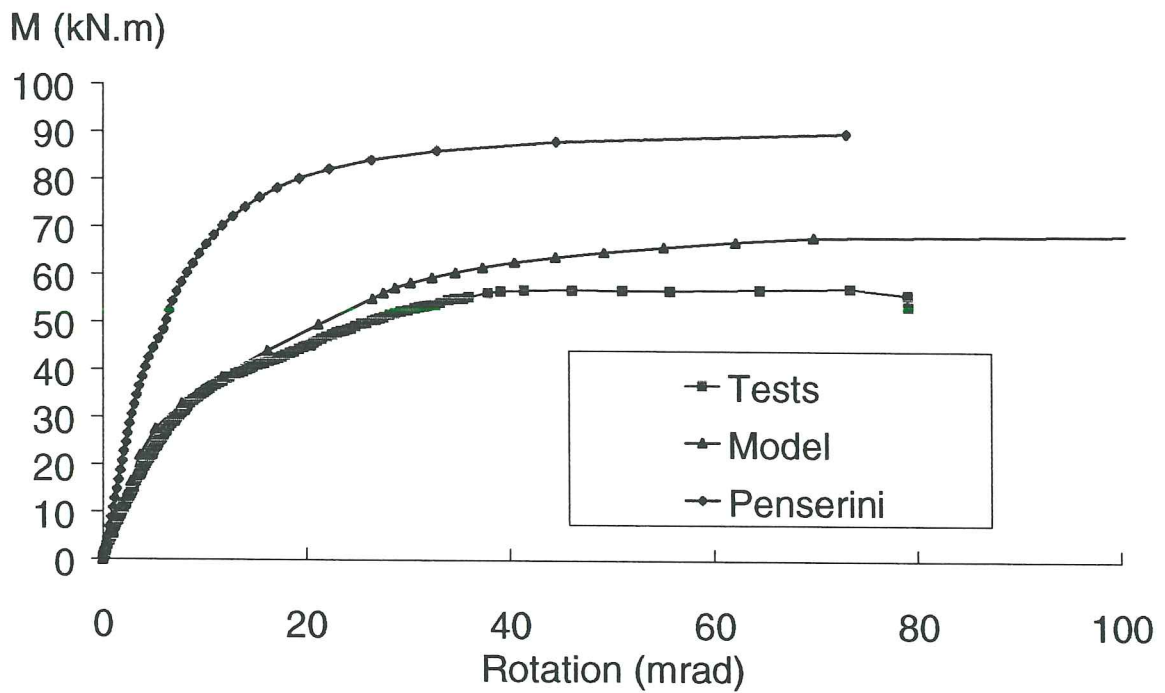


Figure 3-134 Comparison between the tests and the mechanical model. Test PC2.30.600

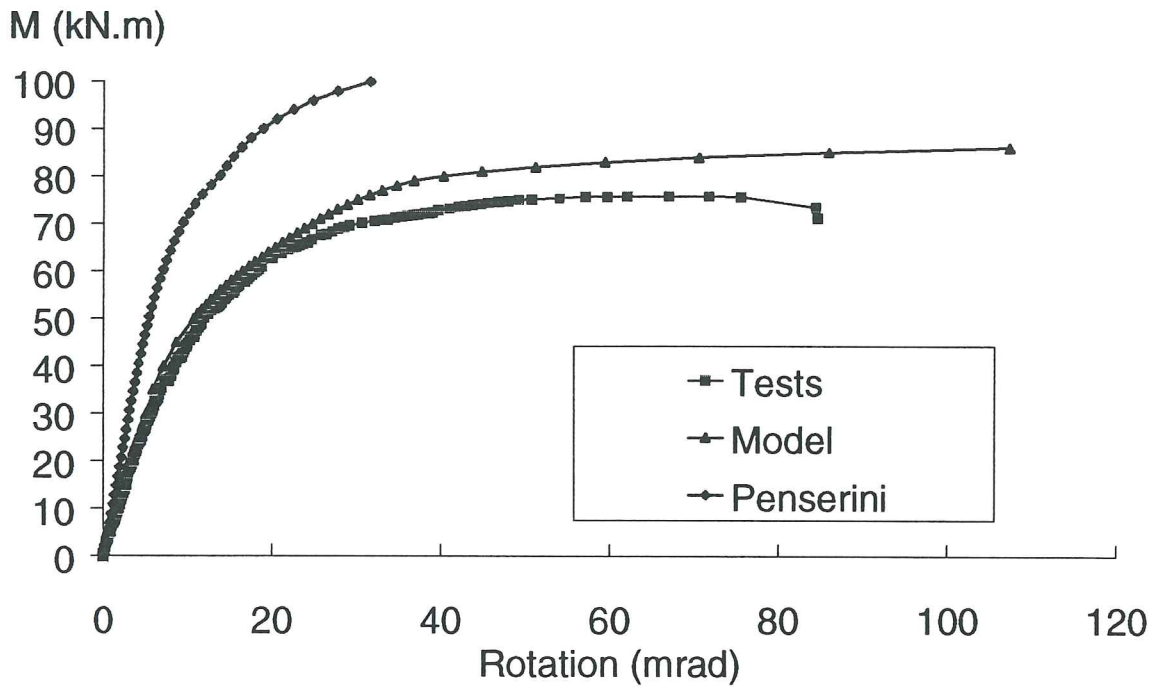


Figure 3-135 Comparison between the tests and the mechanical model. Test PC2.30.1000

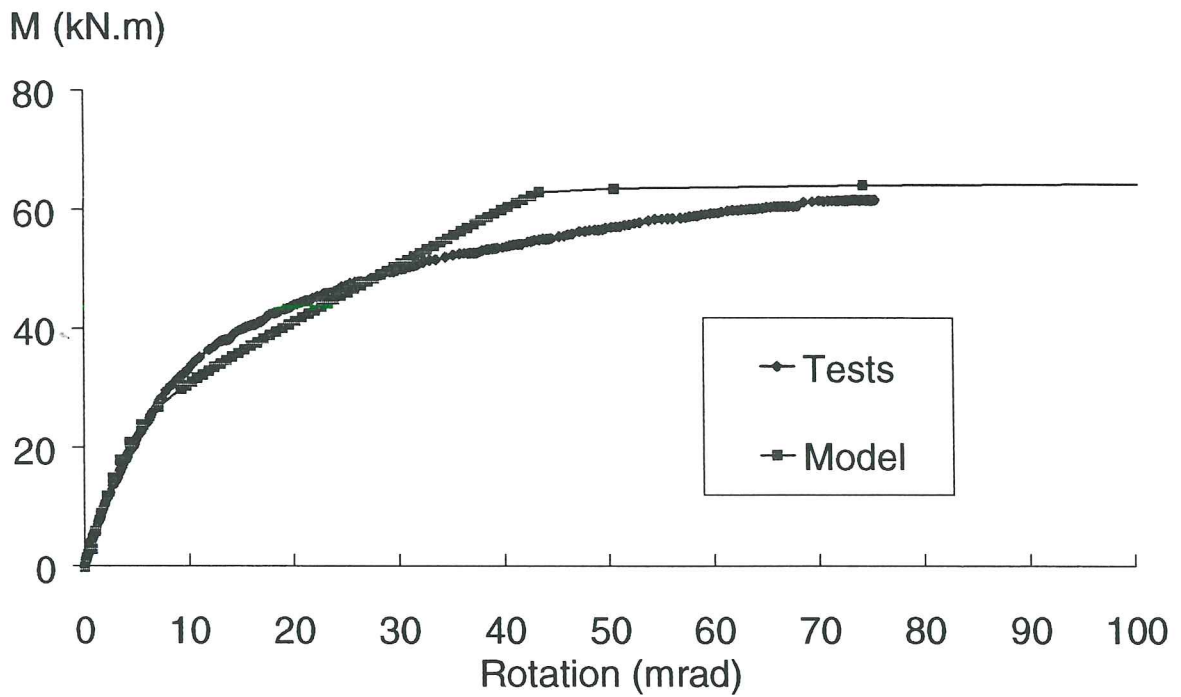


Figure 3-136 Comparison between the tests and the mechanical model. Test PC4.15.100

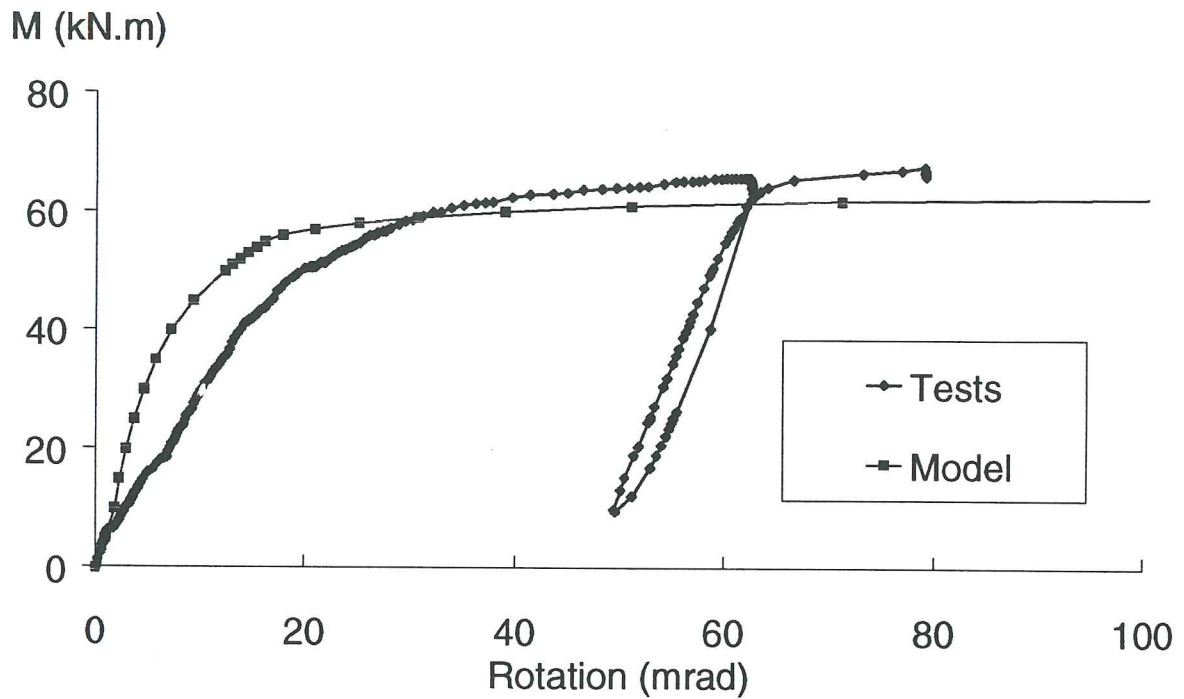


Figure 3-137 Comparison between the tests and the mechanical model. Test PC4.15.400

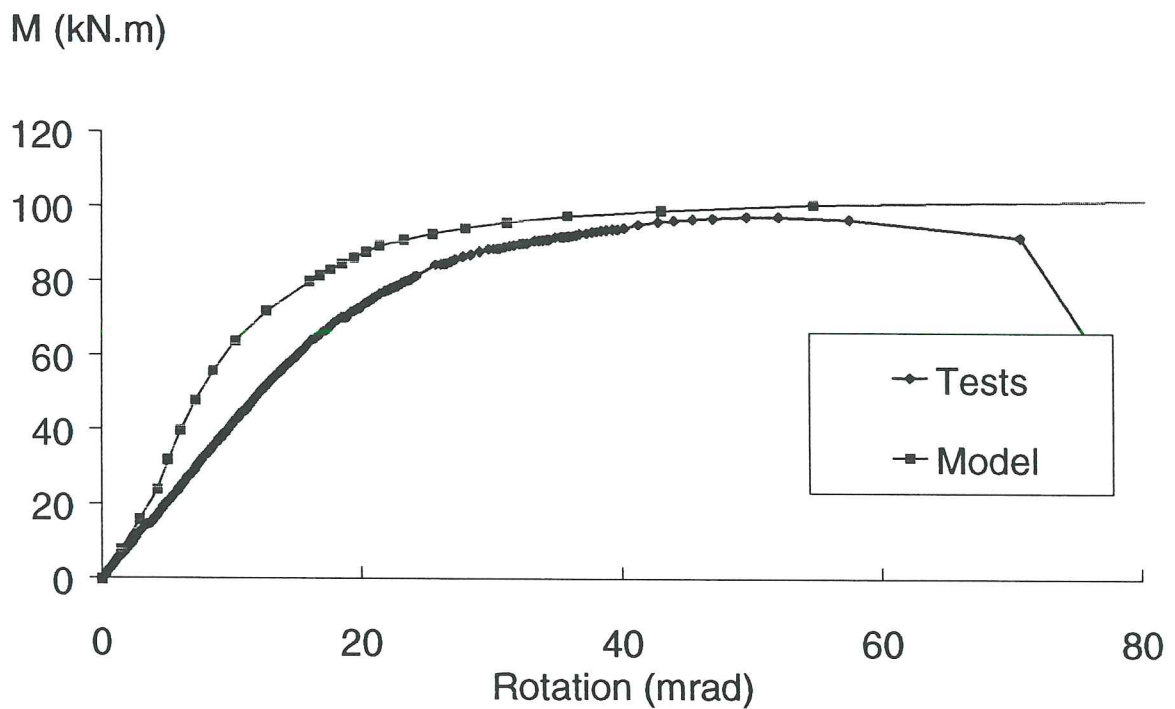


Figure 3-138 Comparison between the tests and the mechanical model. Test PC4.15.1000

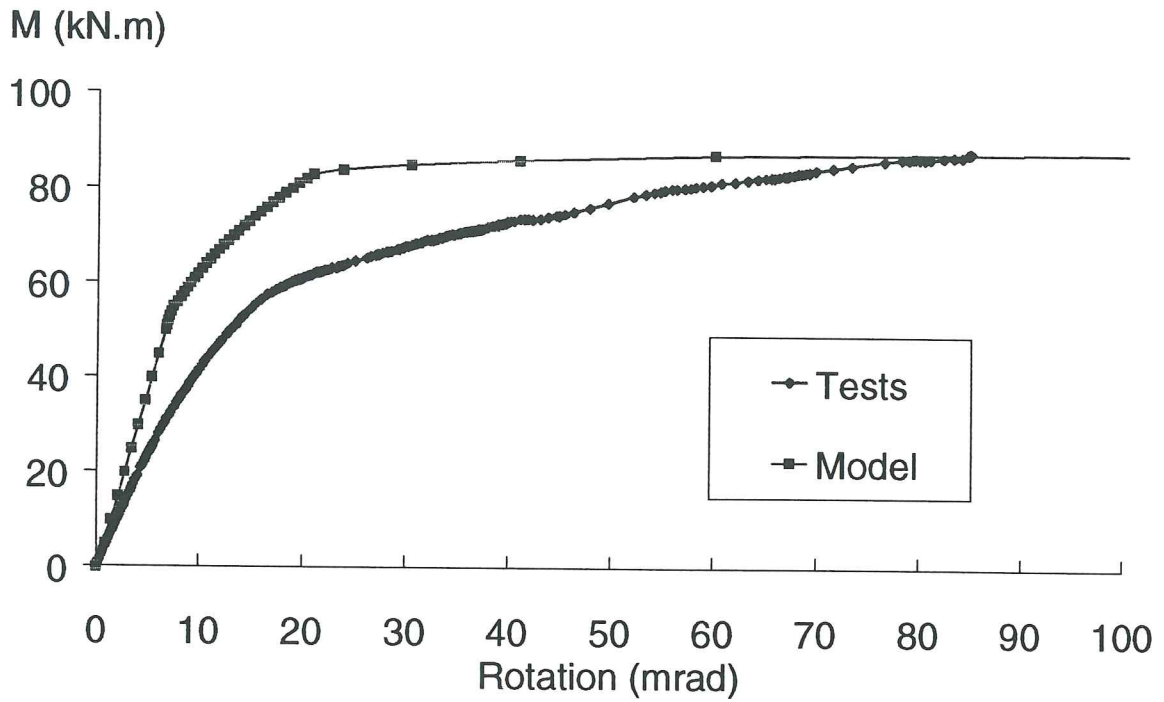


Figure 3-139 Comparison between the tests and the mechanical model. Test PC4.30.100

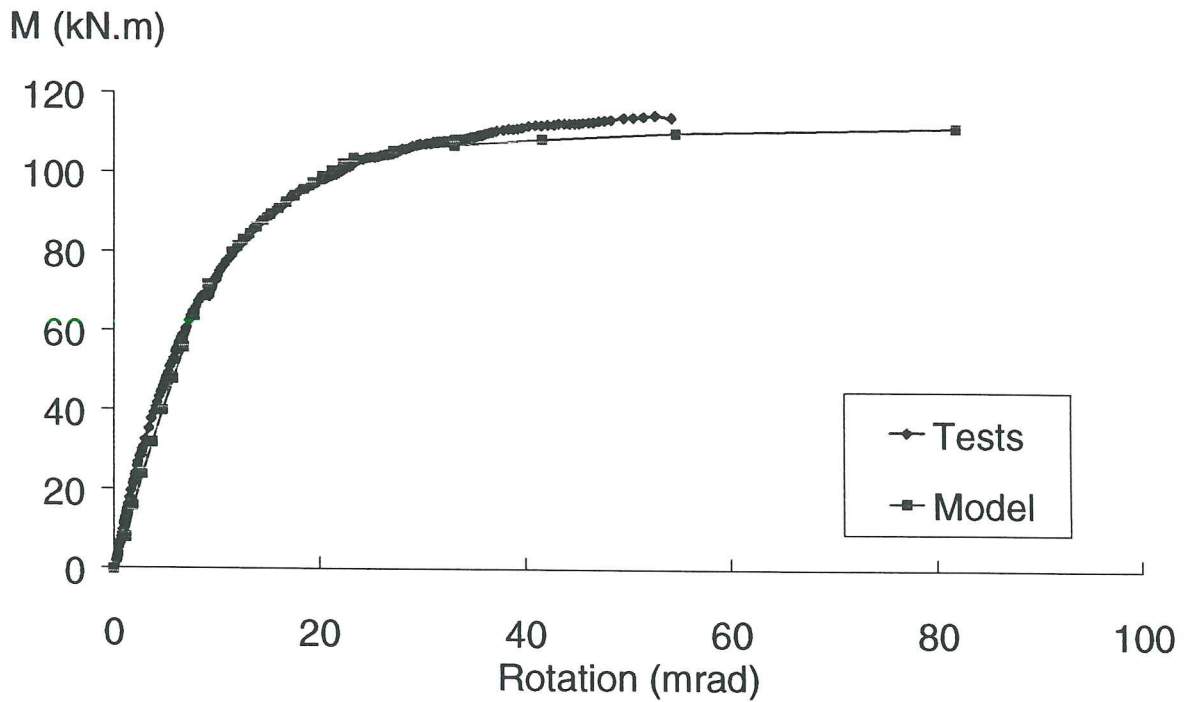


Figure 3-140 Comparison between the tests and the mechanical model. Test PC4.30.400

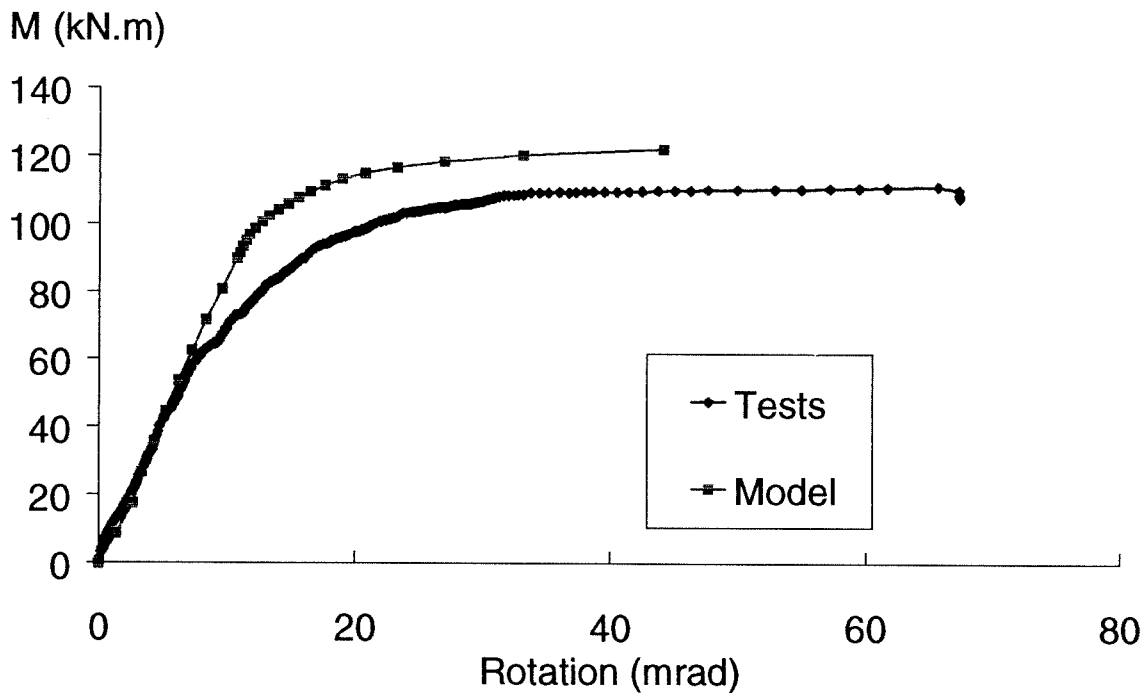


Figure 3-141 Comparison between the tests and the mechanical model. Test PC4.30.100.

3.4.5 CONCLUSIONS AND FURTHER DEVELOPMENTS

Twelve column bases constituted of welded plates connected to the concrete foundation by means of two or four anchor bolts have been tested in Liège in the frame of the COST C1 European Project. The results of these ones have been presented and the main influence of the selected parameters (number of anchor bolts, thickness of the base plates and ratio between bending moment and axial compressive force) has been extensively discussed.

On the basis of the knowledge got from these tests and from the available literature, a simple analytical model aimed at predicting the ultimate and design resistances has been developed and validated through comparisons with the experiments.

The model appears as an application of the principles of the component method, with references to annexes L and J of Eurocode 3 for what regards the characterization of the individual basic components.

A complete model requires also nowadays the prediction of the stiffness properties in rotation of the column bases.

However, the complexity of the problem is such that the development of a simple and reliable stiffness model appears still now as quite contingent. It has therefore been decided

to focus on the development of a scientific tool, i.e. a mechanical model, allowing, through rather long and iterative calculation procedures, to simulate accurately the non-linear response of the column bases from the first loading steps to failure.

Such a tool, the validity of which is demonstrated through comparisons with experiments, allows to deeply understand the behaviour of the column bases and of their constitutive components, the inherent interactions and the way failure occurs.

Through the use of this tool in parametric studies, the development of a reliable stiffness model may be contemplated in the future, and more especially in the frame of the present CRIF two-years projects on column bases where complementary experiments on column bases with two anchor bolts subjected to uniaxial major or minor axis bending have been recently performed.

3.5 Composite joints

3.5.1 Introduction

Composite construction is quite attractive from an economical point of view. To illustrate this statement, let us briefly comment the following design steps which reflect established practice in building construction :

- The steel frame is first designed by considering rather flexible - presumably pinned - links between the constitutive beam and column elements. The connection types may be selected so as to achieve economy in fabrication and erection.
- The slabs, at each storey, are then concreted; longitudinal and transverse steel reinforcement bars are placed (one or two layers) in the concrete and it is recommended not to interrupted the longitudinal rebars when crossing the internal columns (see Figure 3-142) so as to restore a continuity in the composite joints. Under hogging moments, tensile stresses develop in the longitudinal reinforcement bars, what results in a substantial rotational stiffness and moment resistance of the composite joint, even when rather flexible steelwork connections are used.

These good stiffness and resistance properties of the composite joints limit the mid-span deflection and the maximum sagging moments in the beams; this results in a reduction of the member sizes, and therefore of the building height.

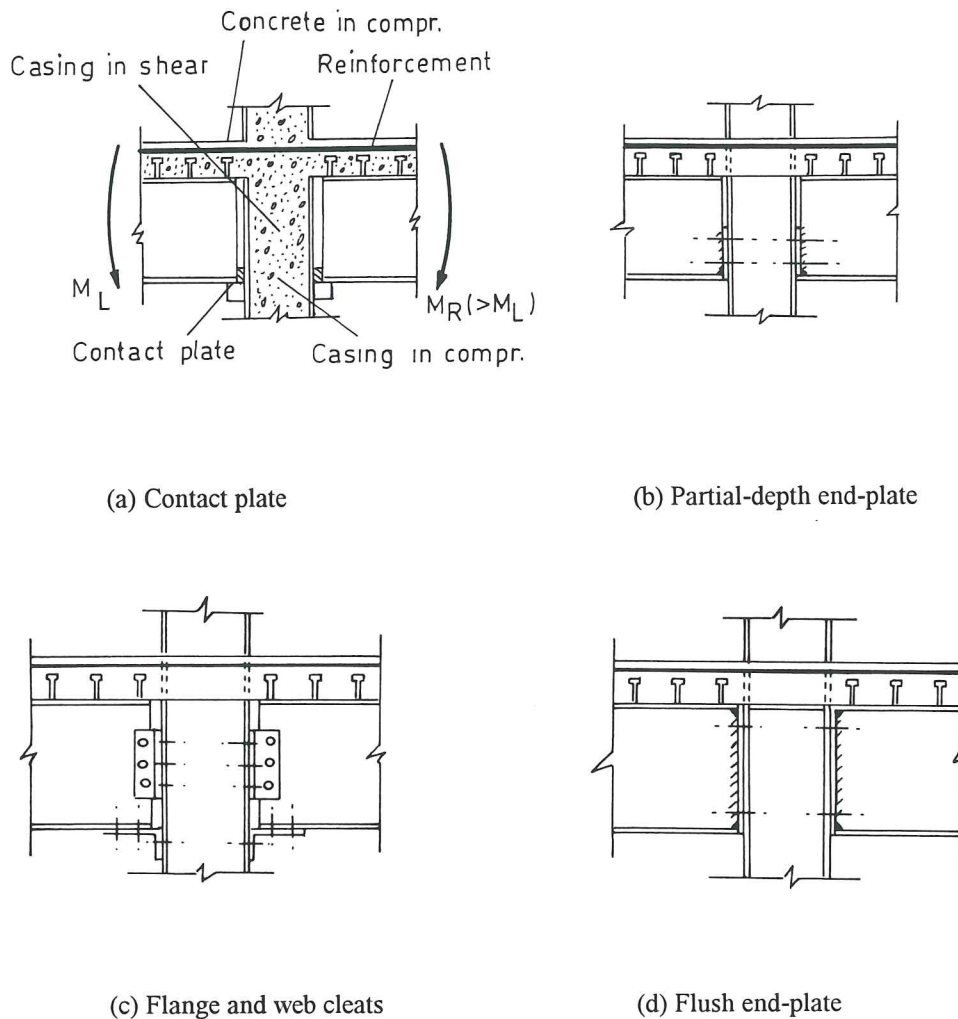


Figure 3-142 Composite joints

As steel joints (see Chapter 1), composite ones may be classified according to their resistance (partial strength/full strength), their stiffness (rigid/semi-rigid/pinned) and their rotation capacity (class 1, 2, or 3).

Their class helps in selecting the appropriate modelling (continuous, semi-continuous and simple) for frame analysis.

The idealization of the $M-\phi$ characteristics to which it has to be referred to is also depending on the type of frame analysis; the latter determines the properties of the joints which have to be evaluated.

Eurocode 4 [E7] recognizes the partial strength/full strength character of the composite joints. This classification is relevant in the cases where plastic design is performed; it allows to determine the location of the plastic hinges under hogging moments, in the joint or at the beam end-section.

On the other hand, no allowance is made for semi-rigid joints in cases where elastic frame design is carried out. Eurocode 4 only recognizes the use of rigid joints.

No specific guidelines are however provided in Eurocode 4 to the designers for the evaluation of the resistance and stiffness properties of the composite joints. At the time of drafting, the conclusions from research were judged not to be sufficiently well-established.

Since that time, the revised Annex J of Eurocode 3 has been prepared, where reference is made to a general design concept for joints, the component method, which is described in Chapter 2. Several researches progressed also throughout Europe and it was recently concluded that a sufficient knowledge was available so as to prepare a specific annex to Eurocode 4 on « Composite Joints in Building Frames » as well as a comprehensive background document where detailed information on the models, formulae, etc ... would be gathered. This work has been made possible through a collaboration between the C1 project of the programme for European Cooperation in the Field of Scientific and Technical Research (COST) and the Technical Committee 11 of the European Convention for Constructional Steelwork (ECCS).

The drafting group for both documents comprised the present author and the following colleagues : D. Anderson (Warwick), J.M. Aribert (Rennes), G. Huber (Innsbruck), H.J. Kronenberger (Kaiserslautern), J.W.B. Stark (Delft), F. Tschemmerneegg (Innsbruck), K. Weynand (Aachen) and Y. Xiao (Southampton).

In this group, we have reflected the knowledge we had acquired few years before in the frame of an ECSC (European Convention for Steel and Coal) research programme that we had carried out in collaboration with the Arbed company (Luxembourg), and where 56 experimental tests on steel and composite joints with cleated connections had been performed. But our main task, as one of the three drafters of the revised Annex J of Eurocode 3, was to ensure a perfect compatibility between the latter and the Annex J of Eurocode 4 being drafted.

The Eurocode 4 Annex J [E3] is now available as a CEN document (Comité Européen de Normalisation) and the background document should be published in early 1997 as a COST C1 document [C7].

In the next sections, the different aspects of the design of composite joints are briefly tackled.

3.5.2 Characterization

Here again reference is made to the component method as a composite joint is nothing else than a steel joint surmounted by a reinforced slab. Shear connectors are fully efficient or not according to their percentage. In the case of partial interaction between the steel beam and the slab, slip occurs, what may affect substantially the rotational behaviour of the composite joint. Guidelines on how to deal with partial interaction are provided by Eurocode 4 Annex J.

A slab in tension generates basically two new components : the concrete in tension and the reinforcement bars in tension. Contact plates constitute an original and quite economical way to ensure the transfer of compressive loads from the lower beam flange to the column (Figure 3. 142.a). Their use leads however locally to a reduced stiffness in comparison with that reported in other connection types such as end-plated ones.

Lastly encased columns exhibit higher properties as far as web panels in shear and compression are concerned. All these particularities are covered by Eurocode 4 Annex J.

3.5.2.1 Concrete in tension

This component is disregarded for sake of simplicity. The concrete is therefore assumed as cracked in tension all along the joint loading.

In composite joints with flange cleated connections (see Figure 3-142.c), the lower part of the concrete slab may be subjected to compressive forces, especially when slip occurs between the lower beam flange and the lower flange cleat, the centre of rotation being then located in the slab. Here again, the additional resistance of the concrete is disregarded.

This assumption is considered as conservative as it leads to calculated values of the stiffness and resistance properties lower than the actual ones.

3.5.2.2 Reinforcement bars in tension

Reinforcement bars are main components as they allow a composite action to take place in the joint. Stiffness and resistance evaluation formulae are provided in the Annex; the elongation of the rebars is assumed to extend over half-a-depth of the column cross-section. Beyond this limit, the elongation of the rebars is taken into consideration in the flexural stiffness of the beam under hogging moments. Tests show that a significant level of deformation may be supplied by rebars in tension, and that this available ductility is higher than that required in practical situations [L1]. It has however to be pointed out that the ductility of the reinforcement used in the tests was significantly better than the minimum specified in Eurocode 4 for even « high ductility » bars [A2].

As illustrated in Figure 3-142.a, an unbalanced loading ($M_R > M_L$) generates contact forces between the column and the concrete slab in the left-sided joint. Provisions are given in the code so as to avoid the crushing of the concrete in compression by privileging a premature failure of the rebars in tension in the right-sided joint. This is achieved by providing a sufficient amount of transverse reinforcement in the slab close to the column face.

3.5.2.3 Encased columns

The casing of the column is a mean, as far as joints are concerned, to stiffen and strengthen the column web panel in shear and the column web in compression.

As a result, encasement appears as a way to reinforce the column web and not as a new component.

Formulae are provided in the Annex so as to quantify the additional stiffness and resistance got through encasement, with regard to unreinforced steel webs.

3.5.2.4 Contact plate

The additional deformability resulting from the use of contact plates (see Figure 3-142.a) is covered by an appropriate stiffness coefficient. The resistance is limited by the design strength of the steel forming the plate, but this is under review [A2].

3.5.2.5 Assembly of the components

Similar procedures for stiffness and resistance assembly than those described in Section 3.2.3.2 are recommended in Eurocode 4 Annex J, the layer of reinforcement being considered as an additional bolt-row, the deformation capacity of which is sufficient to enable a full plastic redistribution of internal forces to take place in the joint.

3.5.3 Classification

3.5.3.1 Classification by stiffness

The same stiffness boundaries than those recommended by Eurocode 3 are referred to for composite joints. These boundaries have to be compared to the initial joint stiffness. This one should be evaluated by considering the contribution of the uncracked concrete in the tension part of the slab. For sake of simplicity - and this may be considered as a conservative approximation - the concrete is assumed to be cracked and does not contribute to the increase of the initial stiffness.

3.5.3.2 Classification by resistance

As for steel joints, the strength classification is achieved by comparing the design resistance of the joint to the weaker design moment resistance of the two connected members. As far as the beam is concerned, design moment resistance of the full composite beam under hogging moments is relevant.

3.5.3.3 Classification by ductility

The classification by ductility, as expressed for steel joints in Chapter 1, Section 1.7, remain unchanged and applies as well to composite joints.

3.5.4 Modelling

The local joint modelling of the composite joints is achieved, as for steel joints, according to the type of frame analysis and the stiffness and/or resistance class of the joint (see Figure 1-14 in Section 1.3.1).

In Eurocode 4, the selection of the appropriate joint modelling is however restricted with regard to steel joints as the use of semi-rigid joints is prohibited.

3.5.5 Idealization

Explicit references are made to Eurocode 3 Annex J as far as idealization is concerned. No specific additional information is required.

3.5.6 Conclusions

Substantial improvements of the stiffness and resistance properties of the joints in composite buildings may be achieved by taking into consideration the combined composite action of the steel connections and of the reinforcement bars in tension.

To benefit from this composite action, design rules for joint characterization, idealization, modelling and classification are required. The direct and rather easy extension of Eurocode 3 Annex J to composite joints has been made possible by referring to the principles of the component method. Under the auspices of the European Communities, an Annex J on « Composite Joints in Building Frames » has been prepared [E3] and a background document where the reader will find detailed information on how the rules included in Annex J have been derived and validated will be soon available [C7].

3.6 Extension to high strength steels (HSS)

3.6.1 Introduction

In the new revised Annex J of Eurocode 3 on "Steel Joints in Building Frames" , any joint is considered as a set of individual components and its mechanical properties (stiffness, resistance, ...) are evaluated accordingly.

The numerous components listed in Annex J allow to cover a wide range of structural joints.

For all these components, rules are given to evaluate their stiffness and resistance characteristics, as well as their deformation capacity. An assembly procedure is also described; it allows to derive the mechanical properties of the whole joint. The rules for the evaluation of the component properties have been validated through comparisons with experimental results. As the available experiments are not covering all the actual constructive possibilities (range of relative dimensions, steel grade, ...), some limitations have therefore been given so as to avoid the use of the Eurocode 3 rules outside these ranges of application.

The major limitation is that relative to the steel grade. In this section, the possible extension of the Eurocode 3 Annex J rules to higher steel grades up to S460 is discussed.

3.6.2 Steel grade limitation

The limitation of Eurocode 3 Annex J to S355 steel grades is a general statement for each constitutive component.

For some of them, however, its application is quite questionable :

Column web panel in shear : the limitation of the panel slenderness to $d / t_w \leq 69\varepsilon$ (see Section 3.2.1.6) is there to ensure that no shear buckling occurs. As $\varepsilon = \sqrt{235 / f_{ywc}}$ (with f_{ywc} = yield stress of the column web), the steel grade is already taken into consideration there and no other limitation is required; in other words, the formula given in Annex J for the plastic shear resistance of the panel is valid whatever is the steel grade, as long as $d / t_w \leq 69\varepsilon$. The limitation to S355 can therefore be removed.

No steel grade limitation should be expected from the rules discussed in Section 3.2.1.6 for slender web panels as the steel grade is explicitly taken into account in the post-critical range of application.

Beam flange and web in compression :

The strength calculation is based on the evaluation of the design resistance $M_{c,Rd}$ of the beam cross-section in bending. $M_{c,Rd}$ depends on the class of the beam profile and, as for the column web in shear, this one is influenced by ε . Once again, a limitation of the steel grade seems not needed for this component. Further studies are however planned in Liège so as to check his statement.

Bolts in bearing
Plate in tension and compression
Beam web in tension
Column web in tension

No instability is likely to occur in these components, even for the plate in compression, where the risk of instability is prevented through the use of appropriate bolt pitches. Their strength is linked to plasticity and a limitation to steel grade lower the S355 seems not justified.

End plate in bending
Column flange in bending
Flange cleat in bending

These components are idealized as T-stubs subjected to tension forces. At design failure, the resistance of the bolts in tension is exhausted, a plastic mechanism develops in the T-stub flange or a mixed failure involving bolt fracture and plasticity in the T-stub flange occurs.

Once again, the relative values of the yield stresses (bolts/plate) are taken into consideration in the strength calculations and no limitation of the yield stress for the connected plate (end plate, column flange or cleat) has to be considered for these components.

The only component for which an extending of the design rules to HSS is questionable is the column web in compression where the buckling and crippling resistances (not the crushing one) is highly dependent upon the web slenderness and on the longitudinal stresses in the column web resulting from bending moments and normal forces.

This point is discussed here below.

3.6.3 Column web in compression and HSS

3.6.3.1 Design resistance of a column web according to Eurocode 3 Annex J

In a strong axis joint between H or I hot-rolled profiles, the failure of the column web panel may occur in two different ways : shear yielding or crushing under the tension or compression forces carried over from the beam to the column by the connection (also called *load-introduction failure*). For slender webs, a third mode - web buckling or web crippling - can also be observed.

The failure mode of the web panel depends on its external loading; this topic, which has been extensively discussed in Section 3.2.2 of the present Chapter, is illustrated in Figure 3-32 where the loading of the panel is characterized by the ratio η between the left and right loads, P_l and P_r , which varies from 0 to 1.

The Eurocode 3 design rules for web panels in shear and load-introduction cover the possible stress interactions. We just reproduce here that relative to the column web in compression (Section 3.2.2.2), the validity of which should be checked in cases where HSS is used.

$$\begin{aligned}
 F_{wc,Rd} &= \rho \frac{f_{ywc} \cdot t_{wc} \cdot b_{eff}}{\gamma_{mo}} && \text{if } \bar{\lambda} \leq 0.673 \\
 &= \rho \frac{f_{ywc} \cdot t_{wc} \cdot b_{eff}}{\gamma_{mo}} \left[\frac{1}{\bar{\lambda}} \cdot \left(1 - \frac{0.22}{\bar{\lambda}}\right) \right] && \text{if } \bar{\lambda} > 0.673
 \end{aligned} \tag{3-118}$$

with :

$$\bar{\lambda} = 0.93 \sqrt{\frac{b_{eff} \cdot d_c \cdot f_{ywc}}{E \cdot t_{wc}^2}}$$

$$\rho = \rho_1 = \frac{1}{\sqrt{1 + 1.3 \left(\frac{b_{eff} \cdot t_{wc}}{A_{v,c}} \right)^2}} \quad \text{if } \eta = 0$$

with :

$$\rho_1 + (1 - \rho_1) \cdot 2 \cdot \eta \quad \text{if } 0 < \eta < 0.5$$

$$1 \quad \text{if } 0.5 \leq \eta \leq 1$$

t_{wc} is the web thickness and b_{eff} is the effective yielding width. d_c is the clear depth of the column web, E the Young modulus, f_{ywc} the yield stress of the column web and $A_{v,c}$ the shear area of the column web panel.

The effect of the longitudinal stresses $\sigma_{n,Ed}$ on the design resistance of the column web in compression is taken into account by multiplying Formula (3-118) by means of the reduction factor k_{wc} :

$$k_{wc} = 1.25 - 0.5 \frac{\sigma_{n,Ed}}{f_{ywc}} \leq 1 \quad (3-119)$$

$\sigma_{n,Ed}$ is the normal stress in the column web, at the root of the fillet or of the weld, due to axial force and bending moment. The minimum value of k_{wc} is 0.75 (when $\sigma_{n,Ed}$ is equal to f_{ywc}).

Formula (3-119), in itself, takes the risk of premature buckling of the web resulting from the use of HSS into consideration through the $\bar{\lambda}$ slenderness coefficient, but the validity of the formula has not been demonstrated.

In the following pages, its possible extension to HSS is discussed on the basis of comparisons with numerical simulations (Section 3.6.3.2) and experimental tests (Section 3.6.3.3).

3.6.3.2 Comparisons with numerical simulations

Available works with steel grades up to S355

In Section 3.2.2, we have extensively described numerical and experimental works aimed at verifying the accuracy of the design formulae provided by Eurocode 3 revised Annex J for the evaluation of the resistance of a column web in shear, tension and compression. In the next paragraphs, similar investigations are carried out for joints made of higher steel grades, up to S460.

Recent works with steel grades up to S460

Additional numerical simulations have been carried out on another double-sided joint configuration than those considered in Section 3.2.2.3 (C configuration in [C2]) so as to check the validity of the Eurocode 3 Formulae (3-118) and (3-119) for webs made of HSS up to S460.

These simulations cover cases with symmetrical loading ($\eta = 1$). The normal force in the column is first considered as zero ($\beta = 0$) and is progressively increased for each new simulation ($\beta = 0,1; \beta = 0,2; \beta = 0,3; \dots$).

The results of these simulations are compared in Figure 3-143 to the Eurocode 3 predictions.

From this figure, the safe character of the Eurocode 3 formula for load-introduction may be seen. For S460 simulations, the difference between the calculated and actual resistances appears to be a bit higher than for the other cases; it amounts 12.4 % for $\beta=0$. This difference is due to the reduction of 5 % of the calculated design resistance because of the web slenderness ($\bar{\lambda} = 0,73$) in the case of S460 steel grade.

The reduction of the web resistance because of the longitudinal stresses in the column (Formula 3-119) is not so marked than in Figures 3-41, 3-42, 3-47 and 3-48, where other joint configurations had been referred to.

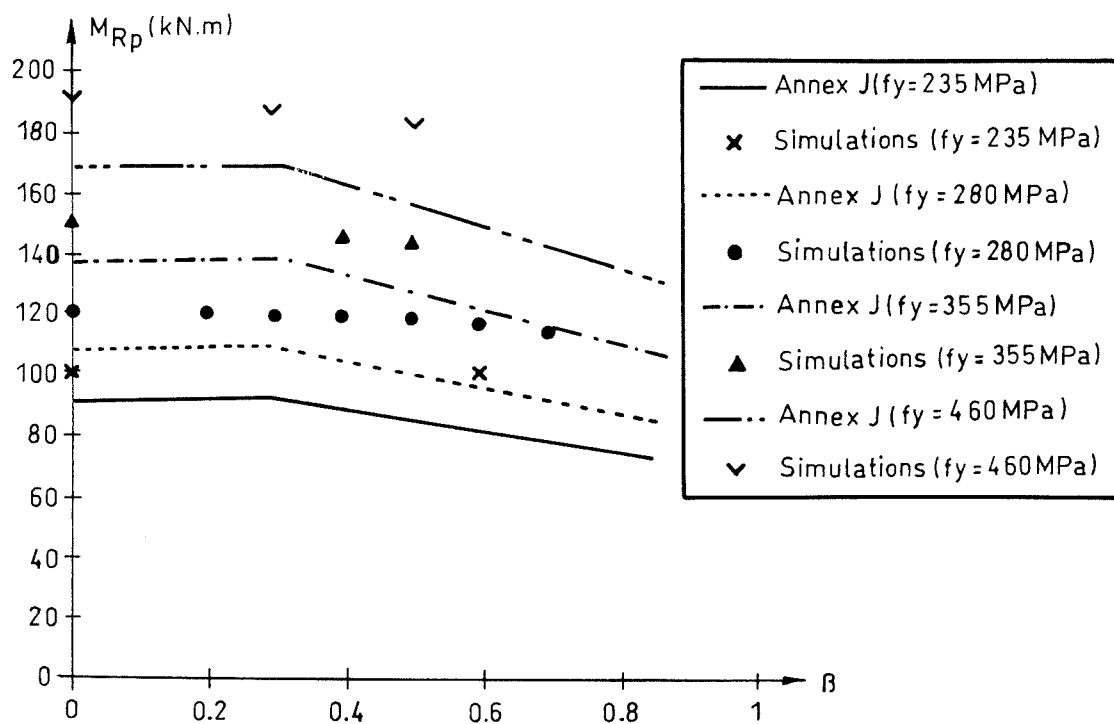


Figure 3-143 Variation of the joint resistance with the normal force in the column and the steel grade (up to S460). Double-sided joint configuration ($\eta = 1$)

3.6.3.3 Comparisons with experimental tests

Available works with steel grades up to S355

In Section 3.2.2.4, comparisons between experimental tests and Eurocode 3 design formulae for webs in shear and/or compression have been presented. Steel grades S235 and S355 were considered.

From these comparisons, it has been concluded that the Eurocode 3 Annex J design rules are safe and rather accurate. Only the reduction of the design resistance of the web in compression, because of the longitudinal stresses in the column, appears as conservative.

Recent works with steel grades up to S460

In [A1], Aribert reports on several "column web resistance" tests performed at INSA Rennes and TU Delft (see Figure 3-144). All the geometrical data are given in the aforementioned reference. In Table 3-9, the nominal and actual values of the yield stress of the web, f_{yw} , are indicated. It may be seen that all the MH tests carried out in Rennes are made of HSS. All the others are of a lower yield grade and fall within the scope of the present Annex J.

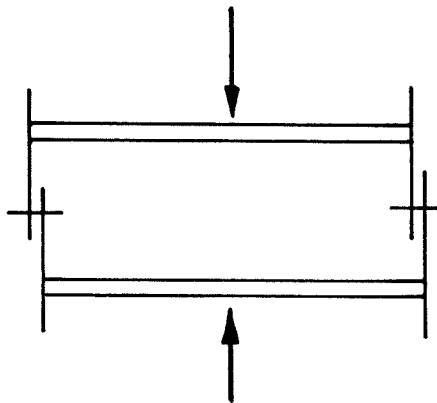


Figure 3-144 Compression tests on hot-rolled H or I profiles

In the case of symmetrical web loading, the experimental failure load $F_{Ru, test}$ corresponds (see Appendix 1 and Section 3.2.2.3) to the pseudo-plastic resistance of the web $F_{Rp, test}$ for normal web slendernesses and to its buckling resistance for more slender webs. It can therefore be directly compared to the Eurocode 3 Formulae (3-118) and (3-119) provided that the actual measured yield stress is used and the γ_{M0} factor is taken as equal to 1.0.

This Eurocode 3 strength $F_{Rp, model}$ is reported for each test in Table 3-9, together with the value of the reduced slenderness $\bar{\lambda}$. For tests in which $\bar{\lambda} \leq 0,67$, the failure is due to crushing (usually, crushing is directly followed by buckling in the case of symmetrical

loading; anyway, F_{Rp} is due first to crushing); for those where $\bar{\lambda} > 0,67$, buckling initiates the failure.

Finally, the ratio $F_{Rp, test} / F_{Rp, model}$ is given.

Similar comparisons have also been carried out on other tests performed in Delft [Z6]. They are reported in Table 3-10.

Through the examination of these results, the safe and rather accurate character of the Formulae (3-118) and (3-119) may be seen for steel grades up to S460.

3.6.4 Conclusions

The possible extension of Eurocode 3 Annex J to HSS up to S460 requires the validation of the strength evaluation formula for column webs in compression.

On the basis of new and already available numerical and experimental research results, the safe and rather accurate character of the Eurocode 3 approach is shown. Finally, the reduction of the resistance of the column web in compression because of longitudinal stresses in the column (through the k_{wc} coefficient - Formula (3-119)) is seen, sometimes, to be questionable. But as explained in Section 3.2.2, the use of this reduction coefficient is quite justified in some applications and, because of that, it is not recommended to remove it from the code as far as now. On the other hand, we have pointed out in Section 3.2.2.5 that the longitudinal stresses in the column were usually limited because of the risk of flexural instability in the column, what reduces strongly the number of practical applications where the k_{wc} coefficient is « active » and reduces the resistance of the web in compression.

References		Section	f_{yw} (MPa)		Experimental failure load	Eurocode 3		$F_{Rp,test} / F_{Rp,model}$
Laboratory	Test n°		Nom. values	Actual values	$F_{Rp,test}$ (kN)	$\bar{\lambda}$	$F_{Rp,model}$ (kN)	
INSA	L1	HEB 140	235	320	365	0,60	323	1,13
INSA	L2	HEB 200	235	320	770	0,64	545	1,41
INSA	L3	HEB 260	235	320	870	0,74	705	1,23
INSA	L4	HEB 140	235	320	375	0,65	375	0,99
INSA	L5	HEB 200	235	320	780	0,67	584	1,34
INSA	L6	HEB 200	235	320	825	0,68	609	1,35
INSA	L7	HEB 260	235	320	880	0,77	756	1,16
INSA	N1	HEB 160	235	275	550	0,57	391	1,41
INSA	T1	HEB 200	235	265	760	0,64	531	1,43
INSA	T2	HEB 200	235	265	800	0,65	555	1,44
INSA	T3	HEB 200	235	265	840	0,66	579	1,45
INSA	T4	HEB 200	235	265	940	0,69	618	1,52
INSA	M1	IPE 140	235	303	175	0,72	142	1,23
INSA	M2	HEA 260	235	335	608	0,95	455	1,34
INSA	M3	IPE 220	235	284	300	0,85	205	1,46
INSA	M4	IPE 360	235	326	530	1,04	377	1,41
T.U. DELFT	1,1	IPE 240	275	367	380	1,11	269	1,41
T.U. DELFT	2,1	IPE 240	355	425	320	1,20	295	1,08
T.U. DELFT	3,1	HEA 240	235	317	483	0,89	413	1,17
T.U. DELFT	4,1	HEA 300	275	357	630	1,02	571	1,10
T.U. DELFT	5,1	HEA 500	235	286	980	0,96	797	1,23
INSA	MH1	HEA 140	460	484	365	0,88	312	1,17
INSA	MH2	HEA 160	460	481	530	0,84	417	1,27
INSA	MH3	HEA 160	460	475	522	0,84	405	1,29
INSA	MH4	HEA 200	460	542	760	0,96	594	1,28
INSA	MH5	HEA 200	460	542	740	0,95	613	1,21
INSA	MH6	HEAA 200	460	610	402	1,33	373	1,08
INSA	MH7	HEAA 300	460	544	588	1,50	467	1,26
INSA	MH8	IPE 240	460	566	454	1,35	330	1,38
INSA	MH9	IPEA 360	460	524	490	1,63	323	1,52
INSA	MH10	HEA 160	460	481	580	0,89	457	1,27
INSA	MH11	HEA 160	460	481	620	0,92	475	1,31
INSA	MH12	HEA 160	460	481	664	0,94	493	1,35

Table 3-9 Test evaluation (Rennes database)

References		Section	f_{yw} (MPa)		Experimental failure load $F_{rp, test}$ (kN)	Eurocode 3		$F_{Rp, test} /$ $F_{Rp, model}$
Laboratory	Test n°		Nom. values	Actual values		$\bar{\lambda}$	$F_{Rp, model}$ (kN)	
T.U. DELFT	A00	HE300A	235	357	660	1,02	571	1,16
T.U. DELFT	A9	HE300A	235	357	599	1,02	571	1,05
T.U. DELFT	A10	HE300A	235	357	682	1,02	571	1,19
T.U. DELFT	18, 19	IPE240	235	425	335	1,20	295	1,14
T.U. DELFT	17	IPE240	235	425	322	1,20	285	1,09
T.U. DELFT	16	IPE240	235	425	283	1,20	275	1,03

Table 3-10 Test evaluation (extra Delft tests)

**PART III : IDEALIZATION AND
CLASSIFICATION OF THE
JOINTS**

Chapter 4 : IDEALIZATION

Chapter 5 : CLASSIFICATION

4. IDEALIZATION

4.1 Introduction

As expressed in Chapter 1, the elastic analysis of a steel frame with semi-rigid joints requires the idealization of the behaviour laws for the beam and column elements as well as for the structural joints in bending.

The idealization of the response for the beam and column elements is achieved through the definition of the so-called flexural rigidity EI/L (I denotes the inertia and L the length of the considered element). As shown in Figure 4-1, EI/L is expressed as the ratio between the applied bending moment and the resultant rotation ϕ .

The range of application of this idealized rotational behaviour is the elastic domain.

In this respect, two different approaches can be followed:

- *Elastic verification of the cross-section*

Further to the elastic frame analysis, the maximum applied bending moment in each element is compared to the maximum elastic resistant moment $M_{e,Rd}$ of the cross-section (Figure 4-1.a). $M_{e,Rd}$ corresponds to the first onset of plasticity in the most stressed fiber of the cross-section.

- *Plastic verification of the cross-section*

The plastic verification consists in limiting the value of the maximum applied bending moment in each element to the plastic moment resistance $M_{pl,Rd}$ of the cross-section (Figure 4-1.b).

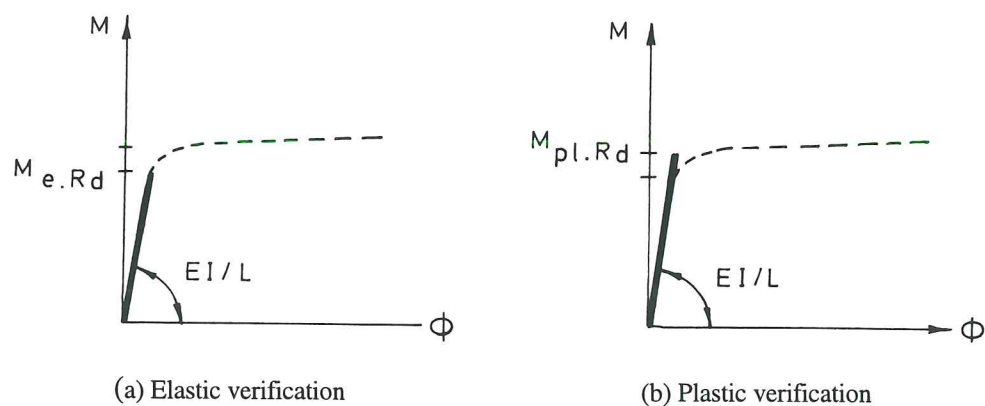


Figure 4-1 Linear idealizations of the beam and column flexural response

The second approach requires class 1 or 2 cross-sections [E1] in which local plate buckling is likely to occur only after the plastic moment resistance is reached. $M_{e,Rd}$ and $M_{pl,Rd}$ values may be reduced, if necessary, to take into consideration any possible interaction with normal or shear forces in the cross-section.

Quite similar idealizations are required for structural joints.

For consistency in the frame analysis, the moment-rotation curves of the joints have also to be linearly idealized (Figure 4-2). The corresponding stiffness S_j characterizes the rotational spring which allows to take the semi-rigid behaviour of the joint into consideration when analyzing the structure.

As for beam and column elements, two approaches may be considered for class 1 and 2 joints :

- Elastic verification of the joint ;
- Plastic verification of the joint.

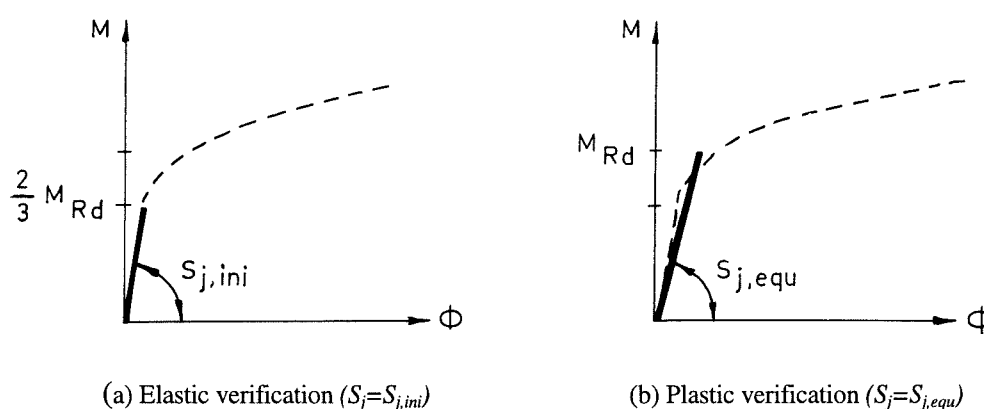


Figure 4-2 Linear idealizations of the joint flexural response

When a plastic analysis of the frame is contemplated, it is usually recommended, for beams and column cross-sections, to refer to the so-called « plastic hinge idealization ». A similar concept also applies to joints; it is described and commented in Appendix 2 of the present thesis. In the present chapter, the linear idealization of the joint response in view of an elastic structural analysis is discussed.

4.1.1 Elastic verification of the joint

In the case of an elastic verification of the joint, the linearized $M-\phi$ response is to be characterized by the initial elastic stiffness $S_{j,ini}$ (Figure 4-2.a). The maximum bending moment to be reached in the joint is the elastic moment resistance which is defined in Eurocode 3 Annex J [E2] as equal to 2/3 of the design resistance M_{Rd} .

This idealization may be referred to when considering serviceability or ultimate limit-states for the frame. It is anyway of particular interest for severe serviceability conditions; in such a case, the use of the initial stiffness is likely to reduce the transverse displacement of the beams as well as the lateral drift of the storeys and of the whole frame.

The designer may also take profit of the full resistance of the joint by accepting to reach M_{Rd} in the joint subjected to the highest loads in the structure. The verification of the joint is then said "plastic".

4.1.2 Plastic verification of the joint

In beam and column elements made of H or I sections, the ratio between $M_{pl,Rd}$ and $M_{e,Rd}$ (see Figure 4-1) is so limited ($\approx 1,14$) that the plastic verification of the most loaded section may be simply based on the diagram of internal forces resulting from the elastic global analysis in which the flexural behaviour of the members is characterized by the elastic stiffness EI/L . This is no more possible for joints where the use of the initial elastic stiffness $S_{j,ini}$ beyond the elastic limit $2/3 M_{Rd}$ leads to unacceptable overestimations of the joint stiffness and resistance properties.

An idealized joint response characterized by a reduced elastic stiffness $S_{j,equ}$ has therefore to be substituted to the complex and non-linear actual $M-\phi$ curve (Figure 4-2.b) but in such a way that the resulting global frame response is not significantly affected compared to the actual one.

This equivalent reduced stiffness $S_{j,equ}$ is to be used in the global frame analysis in view of a consistent determination of the internal forces in the frame.

The type of verification - elastic or plastic - is therefore seen to influence the joint stiffness which has to be introduced in the global frame analysis.

4.1.3 Equivalent elastic stiffness for plastic joint verification

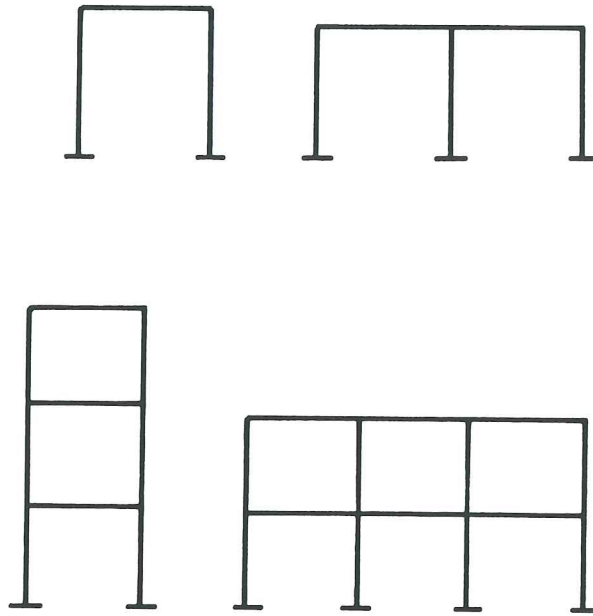
With a view to determine the equivalent stiffness $S_{j,equ}$, different rectangular and pitched-roof structures (Figure 4-3) have been numerically studied (for different types of joints) by means of the non-linear finite element program FINELG [F1] and this, in the two following cases :

- *exact numerical simulation*, i.e. actual non-linear behaviour of the joint;
- *numerical simulation with an idealized joint response*, i.e. linearized joint response.

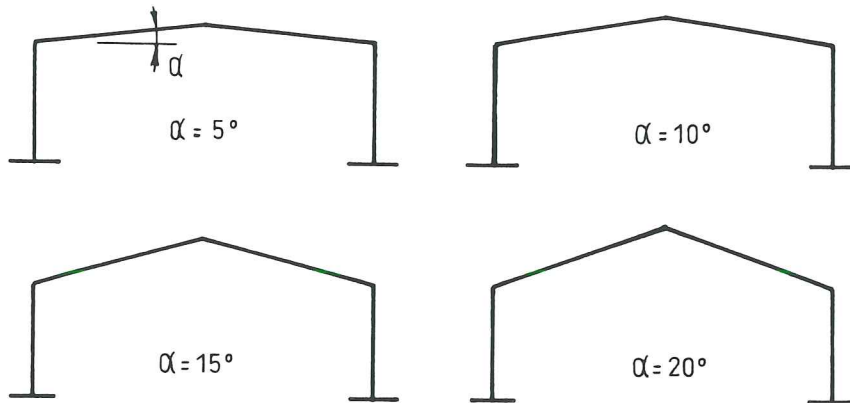
The equivalent stiffness recommended in the old Annex J for beam-to-column joints was the secant stiffness corresponding to the design resistance M_{Rd} (see Figure 4-4.a.). In the new revised Eurocode 3 Annex J, on the other hand, a value of $S_{j,ini}/2$ is recommended (Figure 4-4.b).

The secant stiffness corresponding to M_{Rd} is defined in the new revised Annex J as equal to $S_{j,ini}/\mu$ with, for instance, μ equal to 3 for welded joints and bolted joints with end-plates. In the present paper, μ is first taken as equal to 3 for simplicity. The generalization to other values of μ is then made afterwards.

The numerical simulations have been performed by considering successively these two different recommendations so as to evaluate their respective accuracy.



(a) Rectangular



(b) Pitched-roof

Figure 4-3 Reference frames

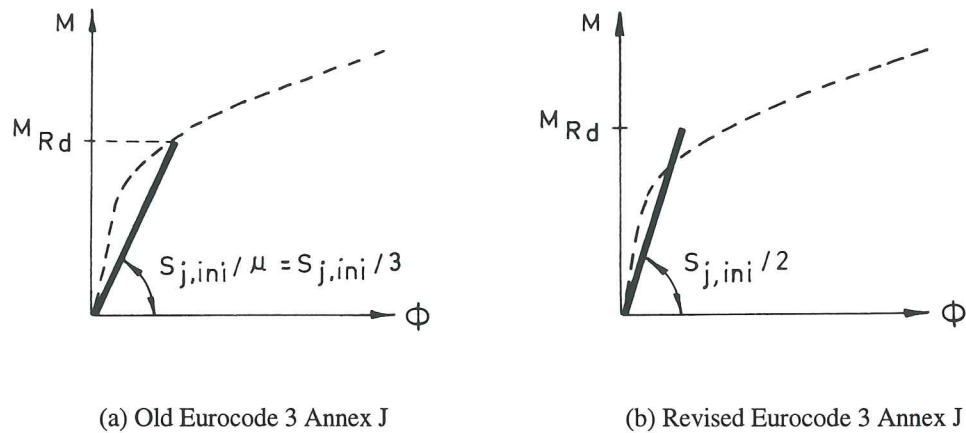


Figure 4-4 Recommended linear idealizations of the joint response for plastic verification

For non-sway frames, the structural response under service loads and at collapse is seen to be not highly affected by the definition of the equivalent stiffness, $S_{j,ini}/3$ or $S_{j,ini}/2$. In both cases, the frame with idealized joint response exhibits a safe and relatively accurate response in comparison to the exact one. This point has been largely discussed in [J1].

For sway frames, on the other hand, the numerical simulations show that the use of $S_{j,ini}/3$ is unsatisfactory; it leads to large and uneconomical overestimations of the frame displacements [J1]. The value of $S_{j,ini}/2$ is better, generally safe, but can sometimes lead to underestimations of the transverse displacements. In both cases, the response of the frame at collapse is seen to be less significantly affected by the value of the equivalent stiffness.

In the present chapter, an original and simple formula for the assessment of the equivalent stiffness $S_{j,equ}$ is proposed for beam-to-column joints. Its derivation is first made in the case of rectangular building frames. It is then extended to pitched-roof portal frames where beam and columns - with constant geometrical properties over the length - are no more perpendicular.

4.2 Rectangular frames

The derivation of a formula for the assessment of the equivalent stiffness $S_{j,equ}$ is based on a two-step procedure described in the following paragraphs.

Step 1 : Evaluation of the rotation Φ_{max}

The rotation Φ_{max} is defined as an estimation of the mean rotation in the joints acting at the ends of the considered beam. It is determined, as shown in Figure 4-5 by similarity with the so-called "wind connection method" as far as it is assumed to result from the beam deformability only (the column being considered as rigid) :

$$\phi_{mean} = \frac{qL_b^3}{24 EI_b} - \frac{ML_b}{2 EI_b} \quad \text{in the case of distributed load } q \quad (4-1)$$

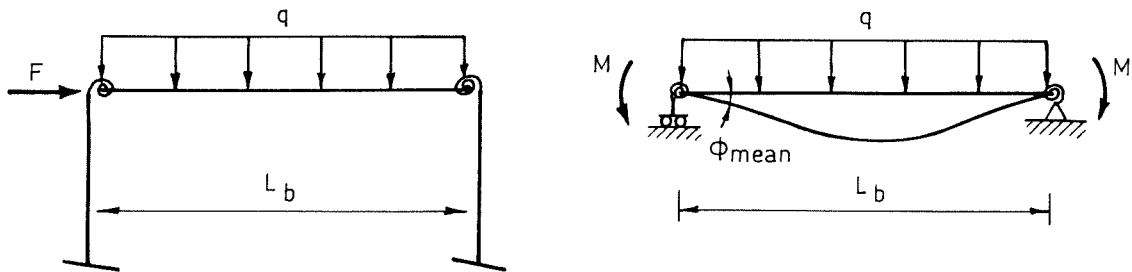
$$\phi_{mean} = \frac{PL_b^2}{16 EI_b} - \frac{ML_b}{2 EI_b} \quad \text{in the case of concentrated load } P \quad (4-2)$$

at mid-span

where I_b is the beam inertia;

L_b is the length of the beam;

M is the moment at beam end.



(a) Rectangular frame

(b) Idealized beam

Figure 4-5 Definition of ϕ_{max} (distributed load)

In the present procedure, the equivalent stiffness is defined as the actual secant stiffness corresponding to ϕ_{mean} (Figure 4-6), so $M = S_{j, equ} \phi_{mean}$. By introducing this expression into equations (4-1) and (4-2), the following value of ϕ_{mean} is derived :

$$\phi_{mean} = \frac{qL_b^2}{12 \left(\frac{2 EI_b}{L_b} + S_{j, equ} \right)} \quad \text{distributed load } q \quad (4-3)$$

$$\phi_{mean} = \frac{PL_b}{8 \left(\frac{2 EI_b}{L_b} + S_{j, equ} \right)} \quad \text{concentrated load } P \quad (4-4)$$

at mid-span

Step 2 : Derivation of $S_{j, equ}$

For each value of ϕ_{mean} , the actual corresponding moment M may be estimated by referring to the approximated tri-linear moment-rotation curve (see Figure 4-6). The

equivalent stiffness $S_{j, equ}$ can then be derived by expressing $S_{j, equ}$ as the ratio between M and ϕ_{mean} . In this procedure, three different cases have to be identified :

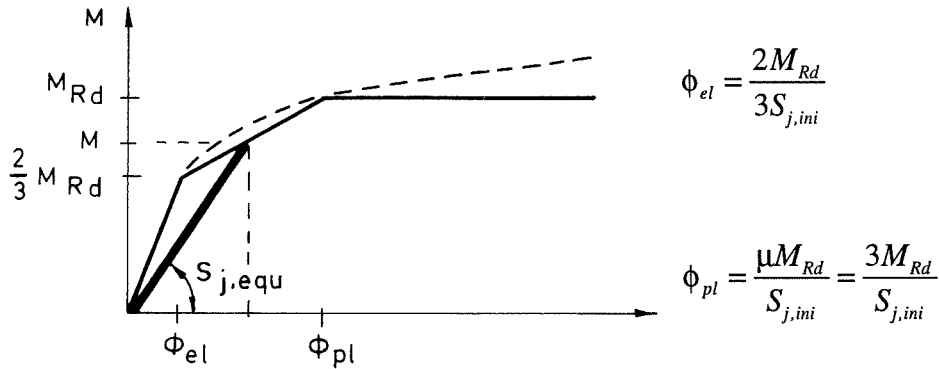


Figure 4-6 Definition of $S_{j, equ}$ as dependent of M and ϕ_{mean}

- $\phi_{mean} \leq \phi_{el}$

In this elastic range of joint behaviour :

$$S_{j, equ} = S_{j, ini} \quad (4-5)$$

- $\phi_{el} < \phi_{mean} \leq \phi_{pl}$

The straight line characterizing the intermediate part of the tri-linear M - ϕ curve in Figure 4-6 has the following equation :

$$\frac{M - \frac{2}{3} M_{Rd}}{M_{Rd} - \frac{2}{3} M_{Rd}} = \frac{\phi_{mean} - \phi_{el}}{\phi_{pl} - \phi_{el}} \quad (4-6)$$

By replacing M by $S_{j, equ} \cdot \phi_{mean}$ and ϕ_{mean} by expressions (4-3) and (4-4), the following values of $S_{j, equ}$ may be obtained.

$$S_{j, equ} = \frac{qL_b^2 S_{j, ini} + 96 \frac{EI_b}{L_b} M_{Rd}}{7 qL_b^2 - 48 M_{Rd}} \quad \text{distributed load } q \quad (4-7)$$

$$S_{j, equ} = \frac{PL_b S_{j, ini} + 64 \frac{EI_b}{L_b} M_{Rd}}{7 PL_b - 32 M_{Rd}} \quad \text{concentrated load } P \text{ at mid-span (4-8)}$$

The two expressions of S_j may be written in the following format :

$$S_{j, equ} = \frac{S_{j, i} M_{fixed} 4 R M_{Rd}}{7 M_{fixed} - 4 M_{Rd}} \quad (4-9)$$

where M_{fixed} is the end moment at the fixed ends of a symmetrically loaded beam;

R is the beam stiffness ($2EI_b/L_b$).

- $\phi_{mean} > \phi_{pl}$

In this plastic range of behaviour, $S_{j, equ}$ is taken as equal to the secant joint stiffness corresponding to M_{Rd} so :

$$S_{j, equ} = S_{j, ini} / \mu = S_{j, ini} / 3 \quad (4-10)$$

For practical applications, the procedure is simply used as follows :

- $S_{j, equ}$ is calculated through the following formula :

$$S_{j, equ} = \frac{S_{j, ini} + 2(\mu - 1)R\rho}{(3\mu - 2) - 2(\mu - 1)\rho} \quad (4-11)$$

which generalizes formula (4-9) for any value of μ ; the value obtained through formula (4-11) is considered as correct if :

$$S_{j, ini} / \mu \leq S_{j, equ} \leq S_{j, ini} \quad (4-12)$$

In expression (4-11), ρ is defined as M_{Rd}/M_{fixed} .

- If condition (4-12) is not fulfilled and $S_{j, equ}$ calculated through formula (4-11) is greater than $S_{j, ini}$, then $S_{j, equ} = S_{j, ini}$.
- If condition (4-12) is not fulfilled and $S_{j, equ}$ calculated through formula (4-11) is lower than $S_{j, ini}/\mu$, then $S_{j, equ} = S_{j, ini}/\mu$.

4.3 Pitched-roof portal frame

The expression derived for rectangular frames can not be directly extended to pitched-roof portal frames. The concept of equivalent stiffness and the global procedure followed in section 4.2 for rectangular frames can however, as demonstrated hereafter, be applied to pitched-roof portal frames.

Step 1 : Evaluation of the rotation ϕ_{mean}

The beam to analyse in this specific case is that represented at Figure 4-7.b. As for rectangular frames, the mean rotation ϕ_{mean} is assumed only to result from the beam deformability (columns considered as rigid in bending) :

$$\phi_{mean} = \frac{q \cos \alpha \ell_b^3}{3EI_b} - \frac{M\ell_b}{EI_b} \quad \text{distributed load } q \quad (4-13)$$

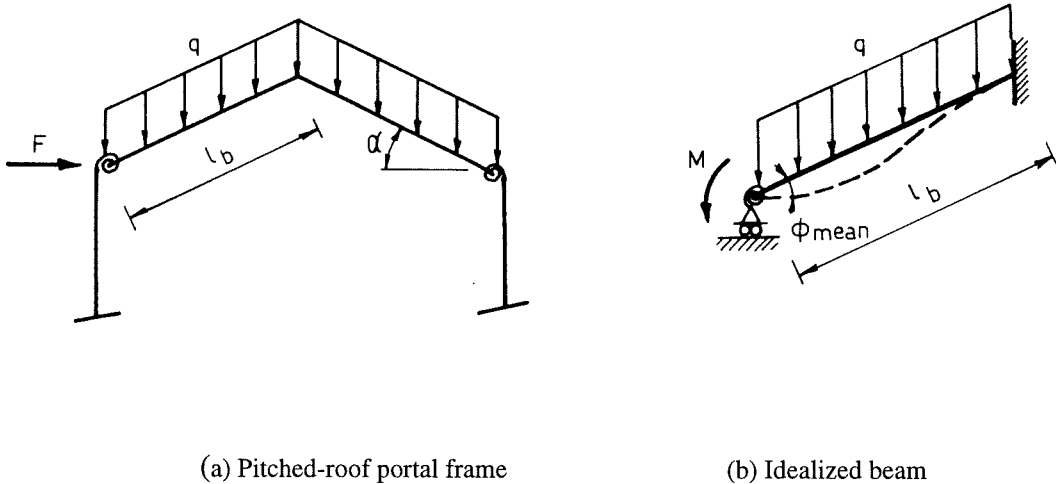
$$\phi_{mean} = \frac{P \cos \alpha \ell_b^2}{4EI_b} - \frac{M\ell_b}{EI_b} \quad \text{concentrated load } P \text{ at roof ridge} \quad (4-14)$$

where I_b is the beam inertia;

ℓ_b is the length of the inclined parts of the rafter as defined in Figure 4-7.a;

M is the moment in the joint;

α is the inclination of the beams.



(a) Pitched-roof portal frame

(b) Idealized beam

Figure 4-7 Definition of ϕ_{mean} (distributed load)

If a generalized definition of the length of the whole beam is taken as :

$$L_b = 2\ell_b \quad (4-15)$$

as shown in Figure 4-7, expressions (4-13) and (4-14) so become :

$$\phi_{mean} = \frac{q \cos \alpha L_b^3}{24EI_b} - \frac{ML_b}{2EI_b} \quad \text{distributed load } q \quad (4-16)$$

$$\phi_{mean} = \frac{P \cos \alpha L_b^2}{16EI_b} - \frac{ML_b}{2EI_b} \quad \text{concentrated load } P \text{ at roof ridge} \quad (4-17)$$

These two expressions are quite similar to the (4-1) and (4-2) ones, except that the vertical load q (expressed by unit length of the inclined parts of the beam) is multiplied by $\cos \alpha$.

Step 2 : Derivation of $S_{j, equ}$

The evaluation of $S_{j, equ}$ proceeds exactly as explained in Section 4-2 and, as for rectangular frames, it can be concluded, when $\phi_{el} < \phi_{mean} \leq \phi_{pl}$, that :

$$S_{j, equ} = \frac{S_{j, ini} M_{fixed} + 4RM_{Rd}}{7M_{fixed} - 4M_{Rd}} \quad (4-18)$$

where : M_{fixed} is the end moment at the fixed ends of an equivalent straight beam of length $L_b = 2\ell_b$ symmetrically loaded;

R is the stiffness of the equivalent straight beam ($R=2EI_b/L_b$ with $L_b = 2\ell_b$)

Cases where $\phi_{mean} \leq \phi_{el}$ and $\phi_{mean} > \phi_{pl}$ are similar to those described in section 4.2.

As for rectangular frames, the expression of the equivalent stiffness may be generalized to any value of μ .

4.4 Accuracy of the proposed formulae

To check the validity of the proposed expressions, comparisons have been made, for the non-sway reference frames, between the transverse displacement, under service loads, obtained respectively through two types of numerical simulations :

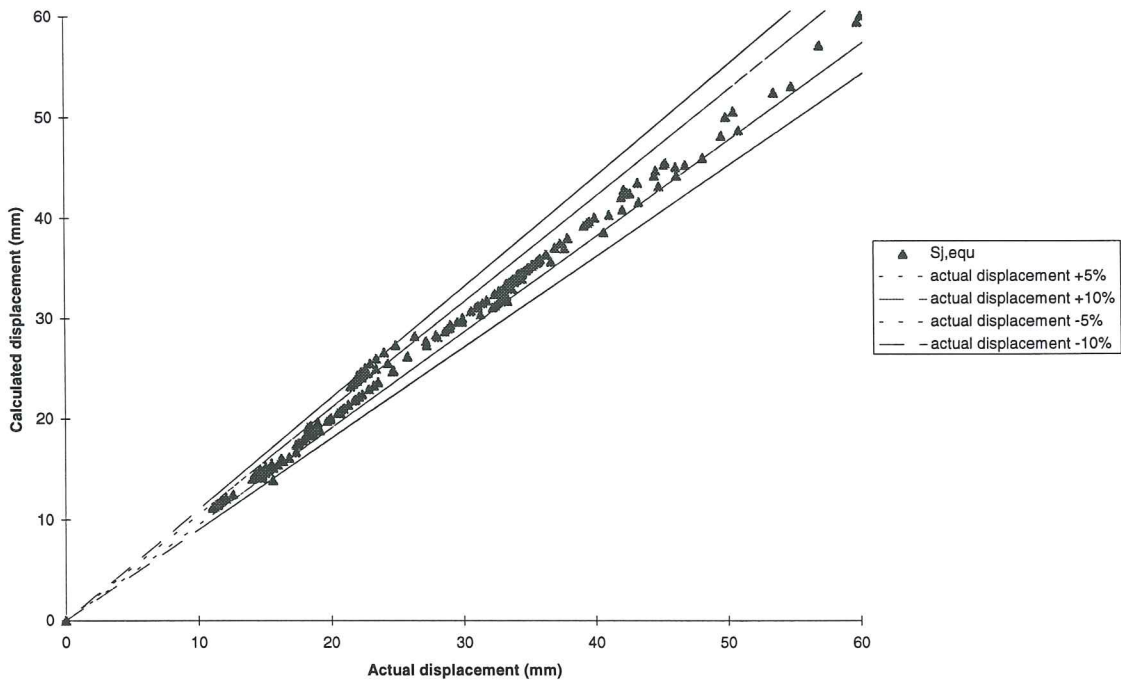
- numerical simulation with actual joint response;
- numerical simulation with the linearized joint response.

4.4.1 Rectangular frames

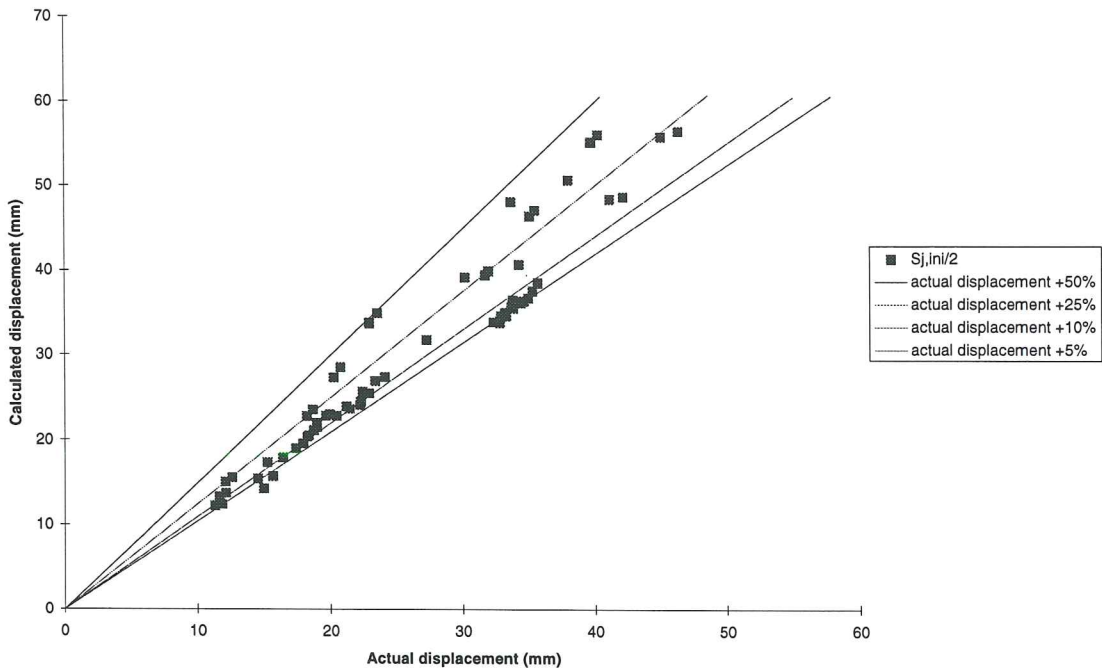
The comparisons have been performed for all the four considered sway structures (Figure 4-3.a) with different joint types (extended end-plates, flush end-plates, ...) so justifying the number of data reported in Figure 4-8.a and Figure 4-8.b. The interested reader is begged to refer to [C1] for detailed information about this work.

It can be seen from Figure 4-8.a where the proposal expressed in Section 4.2 is checked that the majority of the calculated displacements differ of less than 5 % from the actual ones. This accuracy is of primary importance but in view of a practical application, the simple format of the proposed approach has also to be highlighted.

As already mentioned, a value of $S_{j, equ} = S_{j, ini}/2$ has been selected in Eurocode 3 Annex J. Figure 4-8.b shows how the displacements obtained through this way compare with the actual ones. An overestimation up to 50 % of the transverse displacements may be observed, but in many cases it does not exceed 25 %.



(a) $S_{j,eq}$ according proposal in Section 4.2

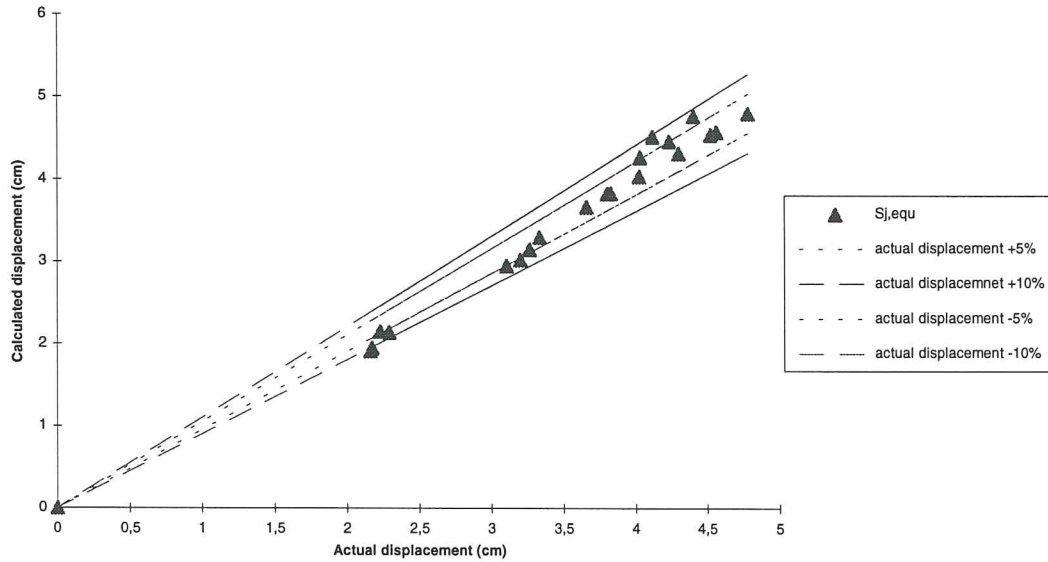


(b) $S_{j,eq} = S_{j,ini}/2$

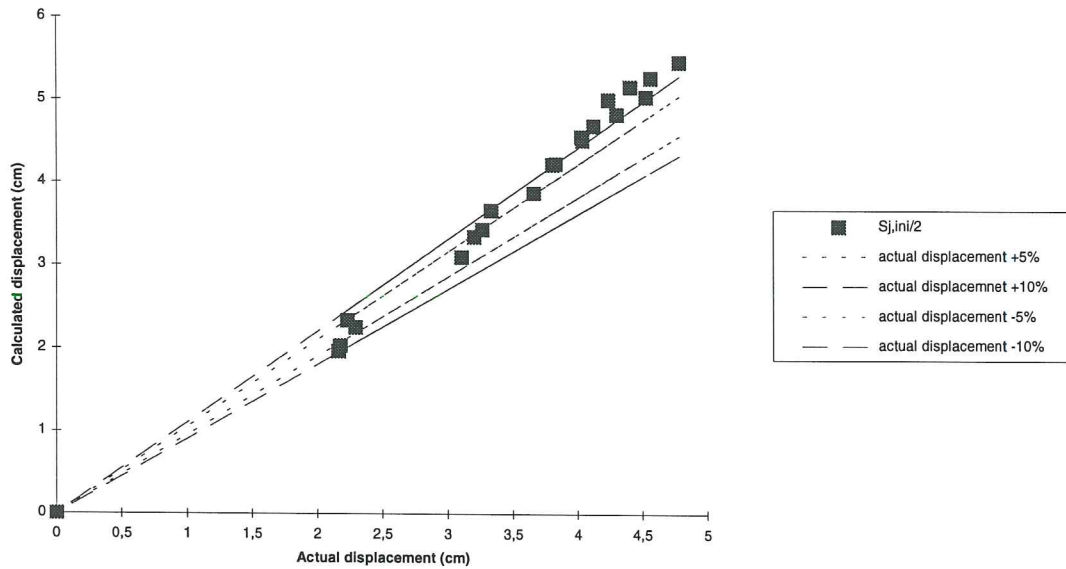
Figure 4-8 Comparisons between actual and calculated frame transverse displacements under service loads - Rectangular frames

4.4.2 Pitched-roof portal frames

Similar comparisons have been performed on pitched-roof portal frames (Figure 4-3.b) for different types of joints and loadings (distributed loads and concentrated ones). The conclusions (Figure 4-9) are seen to be quite similar to those drawn in the case of rectangular frames.



(a) $S_{j, equ}$ according to proposal in Section 4.2



(b) $S_{j, equ} = S_{j, ini}/2$

Figure 4-9 Comparisons between actual and calculated frame transverse displacements under service loads - Pitched-roof portal frames

4.5 Conclusions

In view of a structural elastic linear analysis, the joint $M-\phi$ curves have to be linearized. Further to the frame analysis, the sufficient resistance of the joints has to be checked. In this respect, two classical check procedures - the elastic one and the plastic one - are available. The way to linearize the $M-\phi$ curves in both cases has been shown and a simple and reliable procedure to derive the elastic stiffness to be used for joint plastic verification has been suggested. It applies to beam-to-column joints belonging to rectangular and pitched-roof portal frames where the possible beam splices or ridge connections are assumed to be rigid, what is not very restrictive from a practical point of view.

5. CLASSIFICATION

5.1 Introduction

The analysis of a building frame is aimed at evaluating the value of the internal forces acting in the beam and column cross-sections as well as in the joints. It requires first the idealization of the structural systems and support conditions, and the modelling of the constitutive elements : beams, columns and joints.

The modelling of the joint is dealt with in Chapter 1 (Section 1.3), where three different types of modellings are defined :

- continuous modelling;
- semi-continuous modelling;
- simple modelling.

The procedure on how to select the appropriate type of modelling according to Eurocode 3 is presented in Figure 1-13, it is highly dependent on the type of analysis which is planned and the stiffness and/or resistance classes to which the joints belong.

Eurocode 3 criteria for stiffness and resistance classification of beam-to-column joints are described in Section 1.6.

The resistance classification system of Eurocode 3 is quite simple and is not often criticized. Things are different as far as stiffness classification is concerned.

In this chapter, the background of the Eurocode 3 stiffness classification system is first briefly recalled and the actual research streams in this field are then discussed. Finally, the way to extend the Eurocode 3 classification systems to joints in pitched-roof portal frames is introduced and validated.

5.2 Eurocode 3 stiffness classification

As explained in Section 1.6.2, the stiffness classification is achieved in Eurocode 3 Annex J by comparing the initial joint stiffness $S_{j,ini}$ to stiffness boundaries :

• Pinned joint :
$$S_{j,ini} \leq 0,05 EI_b / L_b \quad (5-1)$$

• Semi-rigid joint :
$$S_{j,ini} \leq 8 EI_b / L_b \quad (\text{braced frames}) \quad (5-2.a)$$

$$25 EI_b / L_b \quad (\text{unbraced frames}) \quad (5-2.b)$$

• Rigid joint :
$$S_{j,ini} > 8 EI_b / L_b \quad (\text{braced frames}) \quad (5-3.a)$$

$$> 25 EI_b / L_b \quad (\text{unbraced frames}) \quad (5-3.b)$$

where I_b and L_b are respectively the second moment of inertia and the length of the connected beam.

These criteria are illustrated in Figure 5-1 in the particular case of unbraced frames.

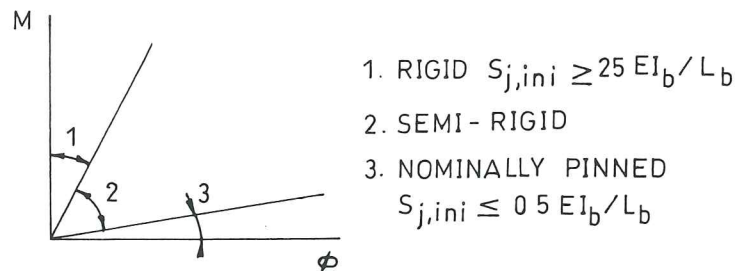


Figure 5-1 Eurocode 3 criteria for stiffness classification
(joints in an unbraced frame)

The boundary to distinguish rigid joints from semi-rigid ones differs for braced and unbraced frames. This specific point is discussed later in 5.3.

The stiffness classification of Eurocode 3 originates in the Netherlands and its background has been published some years ago by F. Bijlaard and M. Steenhuis in [B4]. Let us follow them in the justification of the stiffness boundaries between the rigid and semi-rigid domains.

The distribution of forces and moments in a structure is influenced by the flexibility of the joints. This also holds for the stability.

According to F. Bijlaard and M. Steenhuis, the influence of the joint flexibility on the global frame response may be neglected until it does not lead to a decrease of the Euler buckling load of the frame higher than 5 %. In other words, the Euler buckling loads of the frame with joints assumed to be rigid ($F_{cr,r}$) and actual semi-rigid ones ($F_{cr,sr}$) have to be evaluated and the actual joints may be considered as fully rigid as long as :

$$\frac{F_{cr,sr}}{F_{cr,r}} \geq 0,95 \quad (5-4)$$

To evaluate the related stiffness boundaries, the single-bay single-storey frame illustrated in Figure 5-2 is selected; it is assumed to be braced or unbraced according to the case being considered.

As shown by Meijer [M1], the criterion (5-4) may be expressed in the form of a mathematical relationship between \bar{c} and ρ where :

$$\bar{c} = S_{j,ini} \frac{L_b}{EI_b} \tag{5-5}$$

and

$$\rho = \frac{EI_b H_c}{L_b EI_c} \tag{5-6}$$

In these expressions, EI_b/L_b and EI_c/H_c are the flexural stiffnesses of the connected beam and column respectively.

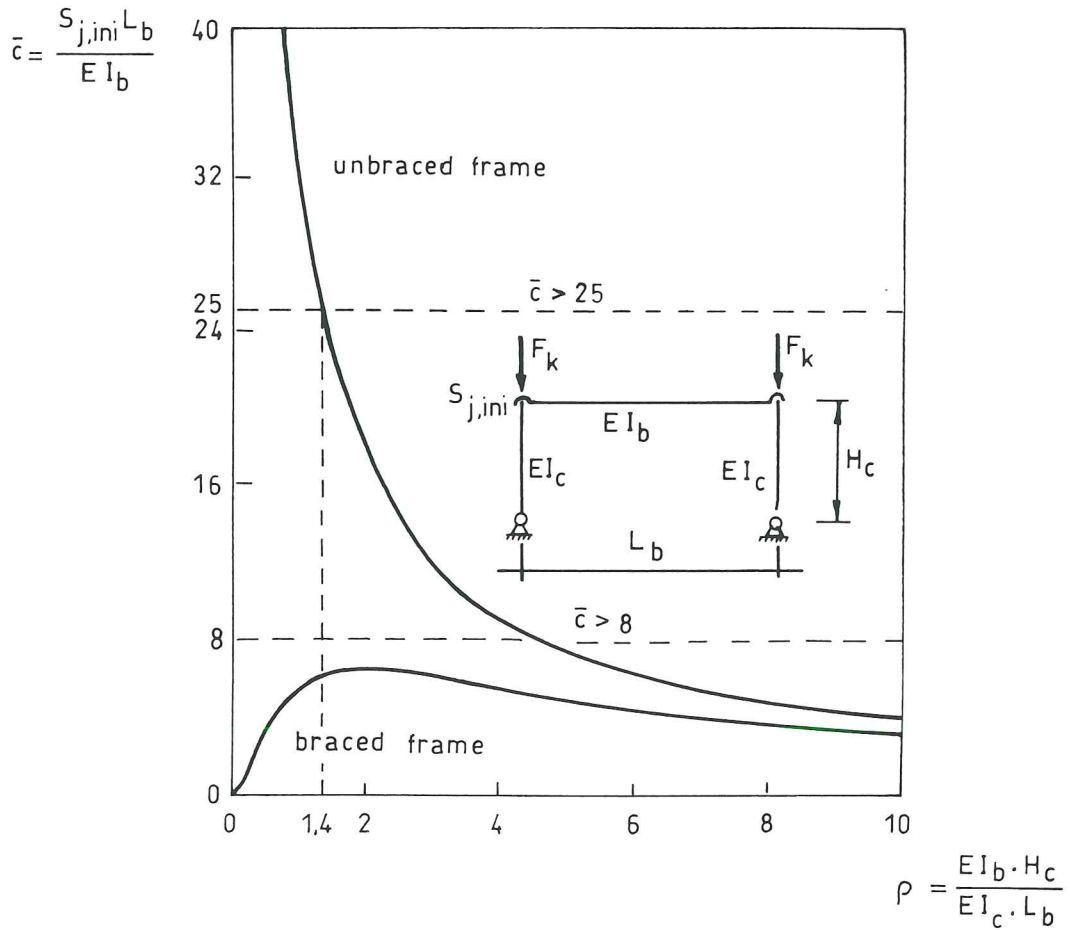


Figure 5-2 Relationship between \bar{c} and ρ

Criterion (5-4) applies to the Euler buckling loads, whereas it could appear more justified to limit the influence of the joint flexibility on the design carrying capacity F_{Rd} of the frame.

In fact that is what happens. On the basis of the well-known Merchant-Rankine formula [W3] :

$$F_{Rd} = \left(\frac{1}{F_{pl}} + \frac{1}{F_{cr}} \right)^{-1} \quad (5-7)$$

it may be shown that the design carrying capacity F_{Rd} will drop by no more than 5 % as soon as the criterion (5-4) is satisfied. F_{pl} is the first order rigid-plastic resistance of the frame.

From a practical point of view, the use of the mathematical relationship illustrated in Figure 5-2 is rather tedious; it also requires the evaluation of the ρ parameter which is often unknown in the preliminary design steps. In Eurocode 3, a further simplification has therefore been achieved.

A constant boundary value has been selected for the parameter factor \bar{c} , which becomes so independent of the parameter ρ . For braced frames the boundary value is $\bar{c} = 8$ and for unbraced frames this boundary value is $\bar{c} = 25$.

The lines of $\bar{c} = 8$ and $\bar{c} = 25$ are drawn in Figure 5-2. In this figure, it may be seen that the boundary value $\bar{c} = 8$ covers completely the ρ - \bar{c} relationship for braced frames. The boundary value $\bar{c} = 25$ for unbraced frames covers the ρ - \bar{c} relation only if $\rho \geq 1,4$. For $\rho < 1,4$, the boundary value $\bar{c} = 25$ is in principle unsafe. This is not really a problem; in [B5], it has been shown that at the value of $\rho = 0,1$ the Euler buckling load based on $\bar{c} = 25$ would be no more than 85 % of the Euler buckling load if the value for $\bar{c} = 25$ would be $\bar{c} = \infty$. For relative slender frames, this means that the carrying capacity of the frame based on the Merchant-Rankine formula drops as follows :

$$F_{cr(\bar{c}=25)} = F_{pl} \Rightarrow 8\% \quad (5-8)$$

$$F_{cr(\bar{c}=25)} = 2 \cdot F_{pl} \Rightarrow 5,6\% \quad (5-9)$$

Frames such that $\rho < 0,1$ are not very realistic, so the value $\rho < 0,1$ can be used as a boundary. It can be concluded that $\bar{c} = 25$ is a sufficiently safe boundary as long as $F_{cr}/F_{pl} \geq 1$.

5.3 Ongoing research works on classification

Several criticisms are regularly addressed to the Eurocode 3 stiffness classification systems. Amongst these, let us mention the following ones :

- Several authors have demonstrated the rather safe character of the stiffness boundaries. According to them, the criteria could be relaxed in some occasions.

- The criteria are expressed on the basis of a single-bay single-storey frame. How can the stiffness boundary for unbraced frames be extended to multi-bay or multi-storey frames?
- The stiffness criteria illustrated in Figure 5-2 require the evaluation of a frame parameter ρ and the ρ - \bar{c} mathematical expression is rather complex. Eurocode 3 makes the classification more easy, but probably less accurate, by expressing the stiffness boundary in terms of EI_b/L_b only. Some authors suggest to go further and to make the stiffness boundary independent of the frame.
- To limit the influence of the joint flexibility to 5 % of the ultimate carrying capacity of the rigidly-connected frame does not necessarily mean that a so low influence is also recorded under service loads where the displacements of the structure may be significantly influenced. When deriving classification criteria, both serviceability and ultimate limit states should be considered.

In the frame of the COST C1 European Project, and more especially of the "Steel and Composite" Working Group that we chair, one of the main objectives is to clarify all these points and to try to suggest new classification criteria where a good balance would be achieved between accuracy - what the scientists are searching for - and user's friendly character - required by designers for practical applications.

Some ideas have been recently developed. Let us mention two of them :

- Eurocode 3 classifies the frames as braced/unbraced and sway/non sway. A sway frame is such that F_{Sd}/F_{cr} is greater than 0,1, where F_{Sd} designates the loading of the frame at ultimate state. In a sway frame, the second order effects affect the lateral stability of the structural system.

In the stiffness classification for joints as it is now in Eurocode, reference is made to the braced/unbraced character of the frame to select the appropriate stiffness boundary ($\bar{c} = 8$ or 25).

For braced frames, the boundary $\bar{c} = 8$ is derived by considering that the Euler load corresponds to the local buckling of an individual column; for unbraced frames, it corresponds to the global frame instability.

In reality, an unbraced frame may be classified as "non-sway" and a global instability of the frame is then not likely to occur.

In these conditions, the question has to be raised whether the braced or unbraced character of the frame is an appropriate criterion to select the stiffness boundary for joint classification.

In [G7], Gomes suggests an interesting concept where :

- the sway/non-sway character of the frame is substituted to the braced/unbraced one;

- the stiffness boundary between the semi-rigid and rigid fields writes :

$$S_{j,ini} = 114 \frac{F_{sd}}{F_{cr,r}} \quad \text{but } \bar{S}_b \geq 8 \quad (5-10)$$

This definition does not require any classification of the frame and allows a continuous variation of the boundary according to the $F_{sd}/F_{cr,r}$ value. It allows also to classify the joint as part of a whole frame, and not as part of a sub-frame constituted of simple one-storey one-bay frame, as it is now in Eurocode.

This approach seems more in agreement with the background of the stiffness classification given in 5.2 but requires the pre-evaluation of $F_{cr,r}$.

- In the case of a multi-bay frames, C. Briquet and al [B6] propose to substitute, according to [J4], the actual frames by an equivalent single-bay one where the stiffness classification system of Eurocode 3 may, in principle, be applied. This approach raises however some other questions, as explained in [B6]. In this paper, the aspects of classification at serviceability limit state are also discussed.

In COST C1, links have also been established with Italian experts who derived original solutions for joint classification in aluminium alloy structures [M2].

The outcome of these exchanges should be published in a forthcoming COST publication to be issued in 1998.

5.4 Classification criteria for joints in pitched-roof portal frames

5.4.1 Objectives

Even if nothing is clearly specified in Eurocode 3, it appears clearly from the background of the classification system described in Section 5.2 that the latter applies to frames where the constitutive beams and columns are perpendicularly connected, i.e. to so-called rectangular frames.

As for the idealization discussed in Chapter 4, recommendations on joint classification are required for pitched-roof portal frames which constitute a significant part of the activity of steel constructors.

The present Section is there to reflect some works that we carried out recently in order not to derive a full new brand classification system - as we explained, this work is in progress in the COST C1 project - but to bring an answer allowing to apply the new design concepts right now to pitched-roof portal frames with a sufficient degree of accuracy, at least not lower than that associated to the design of rectangular frames.

As explained in Chapter 1, three classification systems have to be considered :

- classification by stiffness;
- classification by resistance;
- classification by ductility.

The two last ones are valid whatever is the type of frame and remain unchanged when applied to joints belonging to pitched-roof portal frames.

The only classification system to consider is then the stiffness one. Pitched-roof portal frames being traditionally unbraced, the scope of our investigations reduced to the derivation of a boundary enabling to differentiate semi-rigid joints from rigid ones; the use of rather flexible joints being quite unrealistic because of the design requirements on frame displacements under service loads.

In other words, the only question we had to bring an answer was :

"Is the Eurocode 3 criteria $\bar{c} \geq 25$ for stiffness classification also applicable to joints in pitched-roof portal frames ?"

5.4.2 Stiffness classification boundary

The different steps of our works are listed hereafter :

- In [D1], Davies presents the Merchant-Rankine formula as a reliable tool to evaluate the failure load of a pitched-roof portal frame. The field of application of the formula is seen to be similar to that recommended by Merchant and Rankine for rectangular frames.

In this application range, it has been explained in Section 5.2 that a decrease of 5 % of the elastic critical load was never leading to a higher decrease of the failure load of the structure. This applies therefore also to pitched-roof portal frames.

- On the basis of the Davies work, it may be concluded that the criterion (5-4) on which the Eurocode 3 stiffness classification is leaning may be kept for a further application to pitched-roof portal frames.
- In Figure 5-3, the $\bar{c} - \rho$ relationship for rectangular frames (see Section 5.2) is reported. A similar one may be drawn for pitched-roof portal frames, but because of the lack of sufficiently reliable and validated mathematical expressions to evaluate the elastic critical load of pitched-roof portal frame with rigid or semi-rigid joints, we decided to perform a numerical study.

First, realistic pitched-roof portal frames and loading conditions were selected; amongst the parameters differentiating the frames, let us mention the rafter inclination (5°, 10°, 15° and 20°), the support conditions (pinned and rigid column bases) and the ratio between horizontal and vertical applied loads.

For each frame, the elastic critical load was computed by assuming rigid beam-to-column joints. A full continuity was assumed at the ridge connection.

The flexibility of the joint was then progressively increased until the elastic critical load of the frame amounts 95 % of the critical load obtained by assuming a full rotational continuity in the beam-to-column joints.

The corresponding stiffness $S_{j,ini}$ was then used to compute the \bar{c} ratio while the characteristics of the beam and column elements enabled to derive ρ .

To each frame corresponds therefore a dot of coordinates (ρ, \bar{c}) in Figure 5-3.

To evaluate the flexural stiffness of the beam, EI_b/L_b , the developed length of the beam was selected, (see Formula 4-15), as in Chapter 4 on idealization.

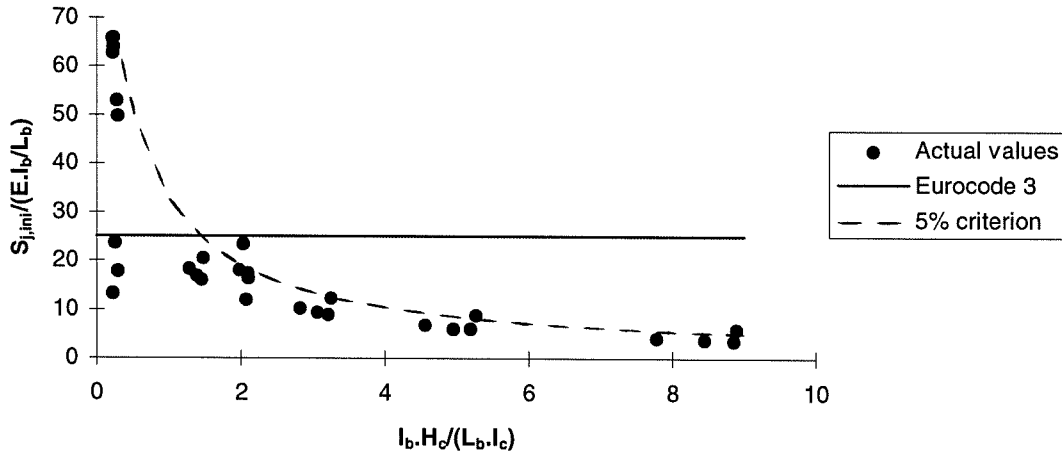


Figure 5-3 \bar{c} and ρ relationship for pitched-roof portal frames

In the diagram of Figure 5-3, most of the dots are located close to the theoretical "5 % curve" derived for rectangular frames. Most of the dots are also located below the "5 % curve", what means that the actual stiffness requirement for rigid joints is a bit less severe than that derived analytically for joints belonging to rectangular frames.

From these results, it may be concluded that the boundary $\bar{c} = 25$ proposed in Eurocode 3 may be applied to joints in pitched-roof portal frames with a similar level of accuracy than for joints in rectangular frames. This conclusion applies as long as the developed length of the beam is considered and the ridge connection is designed in such a way that it may be considered as rigid. This latter requirement is not very restrictive in practical applications.

5.5 Conclusions

Eurocode 3 revised Annex J proposes criteria for stiffness, resistance and ductility classification of beam-to-column joints in rectangular frames. The resistance and ductility classification systems are rather well accepted whereas criticisms are addressed to the stiffness classification.

In the frame of the COST C1 European Project, proposals for alternative stiffness classification criteria are in discussion amongst the scientific community and new recommendations could be suggested as an outcome of the ongoing studies.

In the present chapter, the background of the Eurocode 3 stiffness classification system has been described and its possible extension to joints belonging to pitched-roof portal frames has been demonstrated.

PART IV : DESIGN TOOLS FOR PRACTITIONERS

Chapitre 6 : DESIGN TOOLS FOR PRACTITIONERS

6. DESIGN TOOLS FOR PRACTITIONERS

6.1 Introduction

In the last decades, many research works have been devoted to the improvement of the design and analysis procedures for structural frames and for their constitutive beam and column elements. More and more refined design procedures have been developed and progressively introduced in the national and international design codes. Comparatively less works have been devoted to structural joints which are still traditionally considered, in most of the national design codes, as pinned or rigid.

Since a bit more than ten years however, the situation has changed. It is now well recognized that the design of actual pinned or rigid joints is often leading to high fabrication and erection costs [4]. It is well known that a strong reduction of these costs may result from the use of so-called semi-rigid and partial-strength joints but it has also to be said that, till now, the knowledge on how to design semi-rigid joints and on how to design structural frames including such joints is mainly in the hands of the scientists who deeply investigated these problems in the last decade.

In this context, the drafters of Eurocode 3 have been faced to the following situation : "do we open or not the door to semi-rigid design in Eurocode 3 ?". The reply was "yes!". As a matter of fact, it has been thought that Eurocode 3 had not to prevent designers from designing frames and joints for economy.

It has however to be recognized that the present situation is quite unusual in the sense that new design rules and procedures which have almost never been used in practical applications are now codified, at the European level, in the recently revised Annex J of Eurocode 3 [E2].

The task of the scientists is now to disseminate the new design techniques by organizing workshops, seminars and conferences, by preparing design handbooks and simplified design guidelines and by teaching the new concepts in the universities.

In this Chapter, a design handbook for designers of steel building frames is first presented. This handbook gives a quite complete overview of the design procedures for frames, including joint behaviour, according to Eurocode 3 Part 1-1. In its first part, a background information is given. The second part focuses on application rules for daily practice; a particular attention is paid to structural joints. Finally, worked examples covering frame and joint design are presented in the third part.

The drafting of the design handbook has been sponsored by the European Community in the frame of an ECSC project (contracts 720-SA/212 and 320). The partners in this project were the University of Liège in Belgium as co-ordinator (R. Maquoi and J.P. Jaspart), CTICM in France (B. Chabrolin, I. Ryan and A. Soua), CRIF in Belgium (D. Vandegans), TNO Delft in the Netherlands (M. Steenhuis) and RWTH Aachen in Germany (K. Weynand).

6.2 Contents of the design handbook

The ECSC user's manual covers [E4] the following three main aspects :

- The design of commonly used beam-to-column joint configurations such as welded ones or bolted end-plate and flange cleated ones. Beam splices are also considered.
- Guidelines on how to incorporate the joint behaviour in the structural analysis (both first order and second order, elastic and plastic).
- Design checks for the ultimate limit states (frame and member resistance and stability, member and joint cross-section checks, ...).

It includes three main parts which all deal with each of the three above-mentioned aspects :

- *Part 1 - Technical Background*

A primary objective of the manual is to facilitate the use of Eurocode 3 and it has so been thought that this was requiring explanations about the general design philosophy to adopt and the successive steps to follow in the design and analysis process, the assumptions to make and the formulae to use.

- *Part 2 - Application Rules*

In this section, practical guidelines are given in a straightforward manner. The designer should find there the recommendations he needs to perform frame analysis, joint design and structural verifications. All the formulae are expressed together with their limitations and their implications on further steps. For joints, three different design approaches are proposed, as described in Section 3 of the present chapter.

- *Part 3 - Worked Examples*

Three different worked examples are included in the manual. They cover the whole frame and joint design procedure and not only some specific aspects as the joint characterization or the frame analysis. They should help the designer in understanding the different steps of a semi-rigid frame design, and the sequence of these steps according to the practical situation to which he is faced : engineer or constructor responsible for both frame and joint design or share of the responsibilities between the engineer (frame design) and the constructor (joint design).

All the scientific aspects have been disregarded and the contents of all the chapters has been limited to the minimum but sufficient information which appears to be strictly useful to practitioners.

6.3 Design of the structural joints

An important step in the design process is the determination of the mechanical properties of the joints in terms of rotational stiffness, moment and shear resistances and rotation capacity.

For what regards this characterization, three approaches - illustrated in Section 6.6, are followed :

- *Design Sheets*

These are short documents containing very simple rules allowing to calculate in an easy and quick way the stiffness and resistance properties of some well-defined types of joints.

These simplified procedures described in Section 6.4 strongly reduce the amount of calculation in comparison with the application of Eurocode 3 Annex J but are anyway in agreement with the Eurocode 3 design philosophy.

- *Design Tables*

These are tables covering standardized joints and providing the user with joint detailing and stiffness/resistance properties (see Section 6.4); information allowing to classify the joints as pinned, semi-rigid or rigid, partial strength, full strength or pinned is also given.

- *Software*

This PC software called DESIMAN is able to characterize the mechanical properties of a wide range of usual or non-usual types of joints subjected to bending moments and shear forces. It includes graphical pre- and post-processors (see Section 6.5).

6.4 Design sheets and design tables

6.4.1 The SPRINT project

Through the so-called component method described in Chapter 2, Annex J allows the designer to cover a wide range of usual structural joints. The understanding of the component method philosophy and of its application requires anyway some time and efforts from the designer; it has therefore been felt that simplified design guidelines should be prepared so as to allow him to profit directly and in an easy way from the advantages linked to the new design concepts on joints.

Design tools have therefore been prepared in the frame of a three years European SPRINT project RA351 involving CRIF (J. Janss) as co-ordinator and the University of Liège (R. Maquoi and J.P. Jaspert) in Belgium, CTICM (B. Chabrolin, I. Ryan and A. Soua) and ENSAIS Strasbourg (A. Colson) in France, the University of Trento (R. Zandonini, O. Bursi) in Italy and LABEIN Bilbao (W. Azpiazu) in Spain.

6.4.2 The SPRINT document

The SPRINT document [S1] contains the six following chapters :

Chapter 1 : Description of a simple design model for joint stiffness and resistance calculation

Chapter 2 : Stiffness and resistance calculation for major axis beam-to-column joints with extended end-plate connections

Chapter 3 : Stiffness and resistance calculation for major axis beam-to-column joints with flush end-plate connections

- a) End-plate height smaller than beam depth
- b) End-plate height larger than beam depth

Chapter 4 : Stiffness and resistance calculations for beam splices with flush end-plate connections

- a) End-plate height smaller than beam depth
- b) End-plate height larger than beam depth

Chapter 5 : Stiffness and resistance calculation for major axis beam-to-column joints with flange cleated connections

Chapter 6 : Elastic global analysis of frames with semi-rigid joints.

The first part of Chapter 1 gives general indications about the semi-rigid behaviour of the joints, their modelling for frame analysis, their characterization through the component method, the idealization of their characteristic $M-\phi$ curves and their classification, in terms of stiffness, as pinned, semi-rigid and rigid.

The second part of Chapter 1 gives guidelines on how to use the design tools for joints described in Chapters 2 to 5.

How to perform the global structural analysis of a frame, the constitutive joints of which have been classified as semi-rigid, is explained in a simple way in Chapter 5. In this chapter, the designer's attention is turned to elastic methods of global analysis which are of first interest in daily practice.

6.4.3 The SPRINT design tools for joints

For design purposes, design aids for joints are detailed in Chapters 2 to 5 of the SPRINT document. Each of these chapters is devoted to a specific type of joint. It is composed of two parts :

- a. a calculation procedure, presented in the format of design sheets;

b. design tables.

An example of such calculation procedures and design tables are reproduced in Section 6.6. of the present chapter.

The calculation procedure is aimed at assisting the designer who is willing to take account of all the capacities of the semi-rigidity, without having to go through the more complex approach of Eurocode 3 Annex J.

For a specific joint, a first design sheet is devoted to the useful mechanical and geometrical characteristics of the joint being considered. In the following sheets, the calculation procedure gives the expressions of both stiffness and resistance for all the components of the joint. How to derive the global properties of the whole joint, i.e. its nominal stiffness and its design moment resistance, is summarized at the end of the design sheet. Additional design considerations are given in Chapter 1 of the SPRINT document.

Of course the shear resistance of the joint is of major importance for the design. It is not given in the design sheets for sake of clarity. Relevant information in this respect is however provided in Chapter 1 (as well as information on weld design).

The second part of each of the Chapters 2 to 5 of the SPRINT document consists in design tables, which can be used in a straightforward manner as an alternative to the design sheets. These design tables are established for standard combinations of connected members and provide the designer with the values of:

- the initial stiffness $S_{j,ini}$ and the reduced stiffness $S_{j,ini}/2$ to be possibly used for elastic design;
- the design moment M_{Rd} and the shear resistance V_{Rd} of the joint;
- the component of the joint which is governing the moment resistance;
- the reference lengths in case of a braced (L_{bb}) or unbraced (L_{bu}) structural system.

The knowledge of the "governing component" at failure, and of its ductility, allows to determine the level of rotation capacity for the joint while the reference length allows to classify the joint as pinned, semi-rigid or rigid. Reference lengths are boundaries to which the actual beam span (beam to which the considered joint is attached) has to be compared. Too such reference lengths exist for each joint:

- one to distinguish between a rigid and a semi-rigid joint;
- one to distinguish between a semi-rigid and a pinned joint.

The design tables have been obtained from the expressions given in the design sheets but by taking some options which generally give conservative results. There are however some extreme situations where the use of the design tables cannot be furthermore

recommended. These situations are mostly related to the stress state which exists in the column web panel. How to combine the calculation procedure and the design tables in such cases is explained in Chapter 1 of the SPRINT document.

In the design tables, information on joint classification is also provided to the designer :

- a number followed by the label *R*: the number is the reference length; the label *R* means that the reference length is the upper boundary between the rigid and semi-rigid stiffness classes;
- a label *P* followed by a number: the number is the reference length; the label *P* means that the reference length is the lower boundary between the pinned and semi-rigid stiffness classes.

In the case of non-reasonable values for the reference length, only an ad-hoc indication *P*, *R* or *S* is given (*S* for semi-rigid).

6.4.4 The different ways to use the SPRINT design tools

The SPRINT design sheets and tables can be used in isolation or in combination so as to assist efficiently the designer in different situations which can result from the design procedure he has decided to follow. Some examples are discussed hereafter.

- The predesign and the design of the frame is based on the assumption that the constitutive joints are rigid or pinned. At the end of the design procedure, the joints have to be designed so as to resist the internal forces resulting from the structural analysis and to fulfil the stiffness requirements (pinned or rigid). In such a case, the tables can be used to select an approximate joint.
- To get rigid joints, transverse stiffeners are traditionally welded on the columns, at the level of the beam flanges. In the tables, it is seen that several unstiffened joints (mainly joints with extended end-plates) may be considered as rigid for frame analysis. In this respect, the tables allow the designer to profit from a substantial economy on the joint fabrication (no stiffeners) without altering at all the design procedure he is used to apply (rigid design).
- When predesigning a frame, economical benefit from the semi-rigid design may be achieved more easily by selecting, through the use of the design tables, the most convenient joint for fabrication and erection as well as the corresponding structural properties.
- For joints, components of which are different from these listed in the tables, a combined use of the design sheets and tables can strongly reduce the amount of calculations to be done to characterize the response of the joints.

6.5 PC software DESIMAN for the design of joints

6.5.1 Need for a software

The use of the SPRINT design tables is the most convenient way to design structural joints as it requires no calculation at all. These ones are seen to be useful, but their scope is limited to specific joint configurations, connection types, steel grades, bolt diameter, ...

As soon as the joints to be designed are out of the scope of the tables, the SPRINT design sheets have to be used. Their scope is wider and allows to cover a larger range of bolt diameter, steel grades, steel profiles, ...

The type of connections covered remain however the same than for the design tables. Obviously, for any other type of connections, specific simplified design sheets may be produced and new corresponding design tables may also be prepared.

Otherwise, for all the possible joint configurations and connection types not covered by the SPRINT design tables and sheets, reference has to be made to Eurocode 3 Annex J. But the definition of the constitutive components, the characterization of their local response and the assembly procedure require often some expertise and can sometimes not be achieved in a reasonable time compatible with the requirement of rentability inherent to any actual design project.

The need for an appropriate design tool covering all these situations where the simplified design procedures were of no help has been clearly understood by the above-mentioned ECSC partners when drafting the design handbook presented in Section 6.2 and that is why the Department MSM of the University of Liège (J.P. Jaspart), the CRIF Research Centre (D. Vandegans) and the University of Aachen (K. Weynand) joined to develop the PC software DESIMAN.

6.5.2 Scope of DESIMAN

DESIMAN enables the user to take full profit of the component method by offering the possibility to combine components without any restriction, so as to cover a wide range of joint configurations.

In its basic version developed in the frame of the above mentioned ECSC project, the scope of the software is as follows :

- The components available are those of Eurocode 3 Annex J. One extra component has been added because of its frequent use in industrial buildings : the haunch. The rules for the characterization of the components are also those of Eurocode 3 Annex J. For the haunches, reference is made to Section 3.2.1.4. of the present thesis. The SPRINT procedures are also available in DESIMAN, for the relevant connection types.
- The assembly proceeds as specified in Eurocode 3 Annex J. The scope is therefore restricted to joints subjected to bending moments and shear forces.

Through a collaboration between the ASTRON company in Diekirch (Luxembourg) and the Department MSM (J.P. Jaspart), progress on new components (see Section 3.2.1) and assembly procedures (see Section 3.2.3.3.) have been made and the scope of DESIMAN has been extended to :

- Joints with so-called intermediate stiffeners, stiffeners on the extended parts of end-plates, non-symmetrical beam cross-sections, slender web panels, haunches without stiffeners, ...
- Joints subjected to combined bending moments, shear forces and axial compressive or tensile forces.

6.5.3 DESIMAN, a user's friendly software

DESIMAN is constituted of three well integrated parts :

- The graphical pre-processor allows a user's friendly introduction of the geometrical and mechanical data. It is connected to bolt, plate, material and profile databases, so allowing a substantial decrease of the time required to introduce the data. It is also connected to another database in which the data for all the joints treated by a specific designer may be stored, in order to be used further if needed. A characteristic screen of the pre-processor is shown in Section 6.6.3.
- A calculation module which is hidden for the user.
- The post-processor first reduces to a single screen (see Section 6.6.3) where the main results of the computation are summarized : design resistance in bending and shear in the basic version of DESIMAN, rotational stiffness, collapse mode, ductility as well as stiffness and resistance classes for frame analysis. But besides this screen, four separate files may be visualized on the screen or printed on paper :
 - A short one just giving the same results than those appearing on the output screen (1/2 page).
 - The previous one to which the resistance and the stiffness of all the constitutive joint components are added. Such a file allows the designer to modify in an optimum way its joint when the design requirements are not fulfilled (1 page).
 - A calculation note (± 5 pages) presenting more detailed results of the calculations, for each component and for the joint. This note is useful when, for instance, the design has to be checked by a control office.
 - A full calculation note just like that which could be produced by hand, and in which the results of all the intermediate calculations are given.

6.5.4 How to use DESIMAN

The possible applications of DESIMAN are quite large :

- Evaluation of the properties of a specific joint, in terms of stiffness, resistance and rotation capacity.
- Design of a joint for specific requirements. As no predesign rules are introduced in the software, the design process is an iterative one in which a configuration is first introduced and then improved or optimized by modifying the geometrical or mechanical properties of the constitutive components. The starting configuration results from previous calculations stored in the attached databank, from the SPRINT tables or from the own designer's experience. The iterative process is quite convenient because of the rapidity of the computation and the user's friendly character of the software enabling quick modifications of the data and quick check of the influence of these modifications on the overall joint response.
- DESIMAN may be used to produce new design tables for joints of particular interest for a specific constructor.
- DESIMAN may also be used as a development tool for innovative connections. It so replaces quite expensive experimental campaigns usually aimed at investigating the general behaviour of a new developed connection type. If all the components are not known, experimental tests on individual components are often sufficient to define the component properties which are then introduced in the software. This process saves so money and time.

6.6 Screens of DESIMAN and examples of design sheets and tables

6.6.1 Example of simplified design procedure

<i>Mechanical characteristics</i>		
	Yield stresses	Ultimate stresses
Beam web	f_{ywb}	-
Beam flange	f_{yfb}	-
Column web	f_{ywc}	-
Column flange	f_{vfc}	f_{ufc}
End-plate	t_{yp}	f_{up}
Bolts	-	f_{ub}
If hot-rolled profiles : $f_{ywc} = f_{vfc}$ and $f_{ywb} = f_{yfb}$		
<i>Geometrical characteristics</i>		
Joint		
Column		
		<p>$s = r_c$ for a rolled section</p> <p>$s = \sqrt{2} a_c$ for a welded section</p>
$A_{vc} = A_c - 2 b_c t_{fc} + (t_{wc} + 2 r_c) t_{fc}$ with $A_c =$ column section area	$A_{vc} = (h_c - 2 t_{fc}) t_{wc}$	
Beam		
	End-plate	
Bolts		
d_w :	see figure or = d_f if no washer	
A_s :	resistance area of the bolts	

	STIFFNESS	RESISTANCE
Column web panel in shear	$k_1 = \frac{0,385 A_{vc}}{\beta h}$	$F_{Rd,1} = \frac{V_{wc,Rd}}{\beta} \text{ with } V_{wc,Rd} = \frac{0,9 A_{vc} f_{yw}}{\sqrt{3} \gamma_{Mo}}$
	<p>$\beta =$ 1 for one-sided joint configurations; 0 for double sided joint configurations symmetrically loaded; 1 for double-sided configurations non-symmetrically loaded with balanced moments; 2 for double-sided joint configurations non-symmetrically loaded with unbalanced moments.</p> <p>For other values, see 1.2.2.1 in chapter 1.</p>	
Column web in compression	$k_2 = \frac{0,7 b_{eff,wc,c} t_{wc}}{d_c}$	$F_{Rd,2} = k_{wc} \rho_c b_{eff,wc,c} t_{wc} f_{yw} / \gamma_{Mo}$ <p style="text-align: center;">if $\bar{\lambda}_{wc} \leq 0,67$</p> $F_{Rd,2} = k_{wc} \rho_c b_{eff,wc,c} t_{wc} f_{yw} \left[\frac{1}{\bar{\lambda}_{wc}} \left(1 - \frac{0,22}{\bar{\lambda}_{wc}} \right) \right] / \gamma_{Mo}$ <p style="text-align: center;">if $\bar{\lambda}_{wc} > 0,67$</p> <p>with $\bar{\lambda}_{wc} = 0,93 \sqrt{\frac{b_{eff,wc,c} d_c f_{yw}}{E t_{wc}^2}}$</p> $k_{wc} = \min [1,0 ; 1,25 - 0,5 \frac{\sigma_{n,wc}}{f_{yw}}] (*)$ <p>$\rho_c = 1$ if $\beta = 0$ $= \rho_{c1}$ if $\beta = 1$ $= \rho_{c2}$ if $\beta = 2$</p> <p>where $\rho_{c1} = \frac{1}{\sqrt{1 + 1,3 (b_{eff,wc,c} t_{wc} / A_{vc})^2}}$ $\rho_{c2} = \frac{1}{\sqrt{1 + 5,2 (b_{eff,wc,c} t_{wc} / A_{vc})^2}}$</p> <p>$\sigma_{n,wc}$: normal stresses in the column web at the root of the fillet radius or of the weld</p> $b_{eff,wc,c} = t_{fb} + a_f \sqrt{2} + t_p + \min(u ; a_f \sqrt{2} + t_p) + 5(t_{fc} + s)$
	<p>(*) see 1.2.2.2 in chapter 1.</p>	
Beam flange in compression	$k_3 = \infty$	$F_{Rd,3} = M_{c,Rd} / (h_b - t_{fb})$ $M_{c,Rd}$: beam design moment resistance

Bolts in tension	$k_A = 3,2 \frac{A_s}{L_b}$	$F_{Rd,A} = 4 B_{t,Rd} \text{ with } B_{t,Rd} = F_{t,Rd}$ $F_{t,Rd} = \frac{0,9 f_{ub} A_s}{\gamma_{Mb}}$
Column web in tension	$k_5 = \frac{0,7 b_{eff,wc,t} t_{wc}}{d_c}$	$F_{Rd,5} = \rho_t b_{eff,wc,t} t_{wc} f_{ywc} / \gamma_{Mo}$ <p>with $\rho_t = 1$ if $\beta = 0$ $= \rho_{t1}$ if $\beta = 1$ $= \rho_{t2}$ if $\beta = 2$</p> <p>where $\rho_{t1} = \frac{1}{\sqrt{1 + 1,3 (b_{eff,wc,t} t_{wc} / A_{vc})^2}}$ $\rho_{t2} = \frac{1}{\sqrt{1 + 5,2 (b_{eff,wc,t} t_{wc} / A_{vc})^2}}$</p> $b_{eff,wc,t} = \min [4\pi m ; 8m + 2,5e ; p + 4m + 1,25e]$
Column flange in bending	$k_6 = \frac{0,85 l_{eff,fc,t}^3 t_{fc}^3}{m^3}$	$F_{Rd,6} = \min [F_{fc,Rd,t1} ; F_{fc,Rd,t2}]$ $F_{fc,Rd,t1} = \frac{(8n - 2e_w) l_{eff,fc,t} m_{pl,fc} k_{fc}}{2mn - e_w(m + n)} k_{fc}$ $F_{fc,Rd,t2} = \frac{2 l_{eff,fc,t} m_{pl,fc} k_{fc} + 4 B_{t,Rd} n}{m + n}$ <p>$k_{fc} = 1$ if $\sigma_{n,fc} \leq 180 \text{ N/mm}^2$ (**) $= (2f_{yfc} - 180 - \sigma_{n,fc}) / (2f_{yfc} - 360) \leq 1$ if $\sigma_{n,fc} > 180 \text{ N/mm}^2$</p> <p>$\sigma_{n,fc}$: normal stresses in the centroid of the column flange</p> <p>$n = \min [e ; 1,25m ; (b_p - w)/2]$</p> <p>$e_w = d_w / 4$</p> <p>$m_{pl,fc} = 0,25 t_{fc}^2 f_{yfc} / \gamma_{Mo}$</p> <p>$l_{eff,fc,t} = b_{eff,wc,t}$</p> <p>(**) see 1.2.2.3 in chapter 1</p>

<p>End-plate in bending</p>	$k_7 = \frac{0,85 l_{eff,p,t}^3}{m_p^3}$	$F_{Rd,7} = \min [F_{ep,Rd,1} ; F_{ep,Rd,2}]$ $F_{ep,Rd,1} = \frac{(8n_p - 2e_w) l_{eff,p,t} m_{pl,p}}{2m_p n_p - e_w(m_p + n_p)}$ $F_{ep,Rd,2} = \frac{2 l_{eff,p,t} m_{pl,p} + 4 B_{t,Rd} n_p}{m_p + n_p}$ $n_p = \min [e_p ; 1,25m_p]$ $m_{pl,p} = 0,25 t_p^2 f_{yp} / \gamma_{Ho}$ $l_{eff,p,t} = \min [4\pi m_p ; 8m_p + 2,5e_p ; w + 4m_p + 1,25e_p ; b_p]$
<p>JOINT</p>	<p>Initial stiffness :</p> $S_{j,int} = E h^2 / \sum_{i=1}^7 1/k_i$ <p>Nominal stiffness :</p> $S_j = S_{j,int} / 2$	$F_{Rd} = \min [F_{Rd,i}]$ <p>Plastic design moment resistance :</p> $M_{Rd} = F_{Rd} h$ <p>Elastic moment resistance :</p> $\frac{2}{3} M_{Rd}$

6.6.2 Example of design table for standardized joints

$\beta = 1$

$\gamma_{M0} = 1.10$

$k_{wc} = 1$

$k_{fc} = 1$

$\gamma_{Mb} = 1.25$

Column	Beam	Bolts hr88	End-plate: S235 (mm)															Connection detail (mm)				Welds (mm)			Rotational stiffness (kNm/rad)			Resistance			Failure mode		Reference length(m)	
			t _p	b _p	h _p	e _p	p	P	P _p	e _{pI}	u ₁	w	w ₁	u	a _w	a _f	S _{j,ini}	S _{j,ini/2}	MRd	2/3MRd	VRd	Code	L _{pb}	L _{bu}	Code	L _{pb}	L _{bu}							
																												Failure mode	Code	Failure mode	Code	Moment (kNm)	Shear (kN)	failure mode
HEB140	IPE220	M16	15	140	305	35	90	120	60	40	90	25	10	3	5	10618	5309	30.6	20.4	157	CWS	4.4-R	S	CWS	4.4-R	S								
	IPE240	M16	15	140	325	35	90	140	60	40	90	25	10	4	5	12136	6068	33.4	22.3	157	CWS	5.4-R	S	CWS	5.4-R	S								
	IPE270	M16	15	140	355	35	95	160	65	40	90	25	10	4	6	14740	7370	37.7	25.1	157	CWS	6.6-R	S	CWS	6.6-R	S								
HEB160	IPE220	M16	15	140	305	35	90	120	60	40	90	25	10	3	5	12928	6464	41.2	27.4	157	CWS	3.6-R	S	CWS	3.6-R	S								
	IPE240	M16	15	140	325	35	90	140	60	40	90	25	10	4	5	14835	7418	45.0	30.0	157	CWS	4.4-R	S	CWS	4.4-R	S								
	IPE270	M16	15	154	355	35	95	160	65	40	90	32	10	4	6	18351	9175	50.7	33.8	157	CWS	5.3-R	S	CWS	5.3-R	S								
		M20	20	154	365	45	95	160	65	40	90	32	10	4	6	20161	10081	50.7	33.8	245	CWS	4.8-R	S	CWS	4.8-R	S								
	IPE300	M16	15	160	385	35	95	190	65	40	90	35	10	4	6	21630	10815	56.5	37.7	157	CWS	6.5-R	S	CWS	6.5-R	S								
		M20	20	160	395	45	95	190	65	40	90	35	10	4	6	23591	11796	56.5	37.7	245	CWS	6.0-R	S	CWS	6.0-R	S								
	IPE330	M16	15	160	415	35	95	220	65	40	90	35	10	4	6	24908	12454	62.2	41.5	157	CWS	7.9-R	S	CWS	7.9-R	S								
		M20	20	160	425	45	95	220	65	40	90	35	10	4	6	27044	13522	62.2	41.5	245	CWS	7.3-R	S	CWS	7.3-R	S								
HEB180	IPE220	M16	15	140	305	35	90	120	60	40	90	25	10	3	5	13692	6846	47.4	31.6	157	CWS	3.4-R	S	CWS	3.4-R	S								
	IPE240	M16	15	140	325	35	90	140	60	40	90	25	10	4	5	15761	7881	51.7	34.5	157	CWS	4.1-R	S	CWS	4.1-R	S								
	IPE270	M16	15	154	355	35	95	160	65	40	90	32	10	4	6	19609	9804	58.4	38.9	157	CWS	5.0-R	S	CWS	5.0-R	S								
		M20	20	154	365	45	95	160	65	40	90	32	10	4	6	21718	10859	58.4	38.9	245	CWS	4.5-R	S	CWS	4.5-R	S								
	IPE300	M16	15	170	385	35	95	190	65	40	90	40	10	4	6	23353	11677	65.0	43.3	157	CWS	6.0-R	S	CWS	6.0-R	S								
		M20	20	170	395	45	95	190	65	40	90	40	10	4	6	25586	12793	65.0	43.3	245	CWS	5.5-R	S	CWS	5.5-R	S								
	IPE330	M16	15	180	415	35	95	220	65	40	90	45	10	4	6	27122	13561	71.6	47.7	157	CWS	7.3-R	S	CWS	7.3-R	S								
		M20	20	180	425	45	95	220	65	40	90	45	10	4	6	29497	14748	71.6	47.7	245	CWS	6.7-R	S	CWS	6.7-R	S								
		M24	20	180	440	50	115	200	75	50	110	35	10	4	6	27626	13813	71.6	47.7	352	CWS	7.2-R	S	CWS	7.2-R	S								

6.6.3 Input and output screens of DESIMAN software

DesiMan 2.3 [welded joint]

File Design Databases Help

Input joint characteristics

Name: welded joint

	Section	Size	Material
Beam	IPE	80	S 235
Column	HEB	100	S 235

Joint configuration: Single sided beam-to-column joint configuration

Type of joint: Welded connection

Calculation according to: EC 3 - Annex J

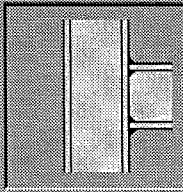
Stiffened column web Backing plates
 Supplementary web plate

OK

Cancel

Input more data...

Check data



DesiMan 2.3 [welded joint]

File Design Databases Help

DesiMan
Version 2.3

Input data

Results

Design moment resistance:
6.99 kNm

Initial rotational stiffness:
3710.2383 kNm/rad

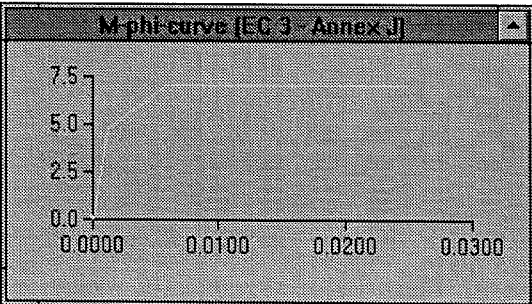
Strength classification:
PARTIAL STRENGTH Joint

Stiffness classification:
RIGID Joint

Rotation capacity:
.F.

Failure due to:
Collapse in compression zone

M-phi curve [EC 3 - Annex J]



6.7 Conclusions

To achieve an economical design of the frames and of the constitutive joints - as it is now possible through the new possibilities offered by Eurocode 3 - the designers require design tools adopted to their search of efficiency and profitability. This need has been met through the drafting of a design handbook covering the different aspects of the frame analysis and design and showing how the new concepts for joint design introduced in Eurocode 3 may be used to design frames and joints for economy. The RA 351 SPRINT has also widely contributed to the dissemination of the new concepts towards practitioners. In this project, design tables and design sheets for commonly used types of beam-to column joints and beam splices have been established. These design aids allow the designers to select the well known fully rigid joints or fully pinned joints or to select semi-rigid joints which generally give a significant benefit by simplifying joint details, thereby reducing shop and erection costs.

Finally, the development of the software DESIMAN is a natural complement to the set of already available design tools for joints. Its use is not restricted to specific connection types. Its user's friendly and flexible character makes it quite suitable for design or pre-design as well as in the frame of a development process.

PART V : GENERAL CONCLUSIONS

Chapter 7 : General conclusions

7. CONCLUSIONS

To consider the actual response of the structural joints in the design and analysis process of a frame requires, in any case :

- the characterization;
- the classification;
- the modelling;
- the idealization;

of the rotational behaviour of the joints as well as :

- the analysis of the frame including the joint response;
- the verification of the limit states.

In the present thesis, the local behaviour of the joint, i.e. the four first points only, is studied. We had the feeling that there was still a significant lack of available information in this field whereas well-established procedures and design tools for frame analysis and verification of the serviceability and ultimate limit states are nowadays available. The interested reader may find this information in a design handbook on «Frame Design including Joint Behaviour» to which we have contributed and which is presented in Chapter 6 of the present thesis.

The characterization, the classification, the modelling and the idealization are four topics which are addressed in the recent version of the so-called revised Annex J of Eurocode 3 to which we have largely contributed.

To characterize the joint properties, the so-called component method has been introduced. According to the latter, each joint is considered as a set of individual basic components and the calculation of the stiffness and resistance properties of the joints proceeds as follows :

- identification of the constitutive components;
- characterization of the stiffness and/or resistance properties of the individual components;
- assembly of the components so as to derive the stiffness and/or resistance properties of the whole joints.

The list of available components in the revised Annex J of Eurocode 3 allows nowadays to cover a wide range of commonly used joint configurations with welded connections or bolted connections with end-plates or flange cleats subjected to bending moments and shear forces.

For these joints, simplified calculation procedures more in agreement with the designer's expectation, in his daily practice, have also been developed, together with design tables for standardized joints where all the joint characteristics, in terms of bending and shear resistance, rotational stiffness, failure mode and stiffness and resistance classes are given. These design tools, presented in Chapter 6, have been prepared in the frame of a European SPRINT project in which CRIF and the Department MSM of the University of Liège were the two Belgian partners. We also contributed to the development of a computer software, DESIMAN (introduced in Chapter 6), allowing a simple and quick evaluation of the joint properties through appropriate calculation procedures and graphical pre- and post-processors.

Besides our activity in these different actions, we realized that a wide acceptance of the new design concepts for frames and joints introduced by Eurocode 3 required to make calculation procedures available to designers for a wider range of joint configurations.

This means that new components have to be added to the list of already available ones and procedures for assembly had to be extended to cover other loading cases.

In the next paragraphs, the contributions brought by the present thesis are reviewed.

1. Most of the researches carried out in the past focus on major axis beam-to-column joints between hot-rolled cross-sections connected perpendicularly.

In pitched-roof portal frames, where hot-rolled sections are used, haunched beams may increase the inertia of the rafters at the beam-to-column intersections. Guidelines on how to design end-plated joints with haunched beams are described.

2. Another solution consists in replacing haunched beams and rolled columns by tapered built-up profiles. The slenderness of the joint components is often likely to generate instabilities, mainly in the column web panel in shear. As the post-critical resistance of these panels is significant, specific design models have to be established. Some existing ones are discussed in the thesis and improvements are suggested.
3. Specific stiffening and strengthening systems such as so-called intermediate stiffeners are commonly used in connections between slender built-up profiles. To assess their degree of efficiency and to decide whether their use has or not to be recommended, design rules for end-plates and column flanges in bending fitted with intermediate stiffeners are expressed.
4. The stiffening of the extended part of the end-plates is another usual way to reinforce connections; this one is also dealt with in the thesis.
5. Modifications to the existing design rules for joints are presented so as to allow them to cover cases where the structural elements are not perpendicularly connected as in ridge connections and beam-to-column joints belonging to pitched-roof portal frames.
6. The inclination of the rafters in pitched-roof portal frames generate often significant axial forces in the joints in addition to bending moments and shear forces. The

properties of the individual components are not affected by the external loading acting on the joint but things are different as far as distributions of internal forces within the joint are concerned.

No hand calculation procedure is available nowadays. A software procedure to distribute the internal forces has been developed some years ago in The Netherlands; it uses a static approach which is recognized as safe as long as the deformation capacity of the constitutive components is not exceeded, what is not checked by the software.

Our contribution consists in writing a software procedure satisfying all the necessary requirements in terms of equilibrium and displacement compatibility between the components, but in which the resistance, but also the deformation capacity of the components, is not exceeded. Inside the software, the deformation of each component is checked at each loading step and the computation stops as soon as the maximum deformation capacity is obtained in one of the constitutive components.

This iterative calculation procedure is applied to some joints and, through these cases, the validity of the Eurocode 3 requirement which limits the use of Annex J to joints in which the axial force is lower than 10 % of the design resistance of connected beam in compression or tension is seen quite questionable.

The software should be used in a near future as a reference for the development of less sophisticated calculation procedures, some being possibly applicable by hand.

7. In the component method, one speaks about individual components. Anyway some of them are interacting as column web panels in shear and webs subjected to compressive or tensile forces. In the revised Annex J, we have introduced reduction factors taking the detrimental effect of these interactions into account.

Some other reduction factors were already existing in the old Annex J and have been kept in the revised draft. They cover the effect of longitudinal stresses in the column on the webs in compression and the column flanges in bending (bolted connections). Few background information exists for these two last reduction factors.

Through extensive numerical and experimental investigations, we confirm the need for such reduction factors, even if some further improvements could be contemplated.

8. Minor axis beam-to-column joints are those where the beam is connected to the column web. Most of the constitutive components are similar to those of major axis joints (end-plate, cleats, bolts, ...), but the component which mostly contributes to the overall joint deformability is the column web subjected to transverse tensile and compressive forces carried over by the connection. The study of this component is the subject of a doctoral thesis in preparation. We reflect in the present thesis the resistance model in the development of which we have been involved.
9. Column bases transfer reactions from the structural system to the foundation and their rotational stiffness influences significantly the response of the whole frame, especially for what regards transverse displacements in unbraced frames. A quite extensive study

of their behaviour is presented, on the basis of 12 experimental tests carried out on base plate configurations with two and four anchor bolts.

An analytical model for strength evaluation and a mechanical model for the prediction of the whole behaviour from the first loading steps to failure are described and validated through comparisons with experimentation.

10. We were amongst the first to be convinced that the extension of the component method to composite joints could be easily contemplated.

Therefore we were quite pleased to contribute to the activities of the European working group - we report on these ones in the thesis - which drafted in the two last years an Annex J on « Composite Joints in Building Frames » for Eurocode 4 and a background document giving detailed information about the design rules included in the annex.

11. Through a component-by-component approach, the possible extension of the Eurocode 3 Annex J design rules to high strength steels up to S460 is demonstrated.

Some complementary investigations are however planned for final confirmation.

In view of an elastic linear frame analysis combined with a plastic verification of the member or joint section subjected to the highest loading, in comparison with its proper design resistance, the moment-rotation characteristic of the joints has to be linearized. Eurocode 3 revised Annex J recommends a value equal to the initial elastic stiffness of the joint divided by two. In Chapter 4, we have proposed an original expression, the validity of which has been largely demonstrated through comparisons with numerical results on rectangular and pitched-roof portal frames. The Eurocode 3 recommendation, derived for rectangular frames, may anyway still be kept as far as a rather high degree of accuracy is not requested.

Guidelines are also given on how to apply the Eurocode 3 recommendation to pitched-roof portal frames so as to obtain a similar level of accuracy than for rectangular frames.

Finally the problem of classification is raised in Chapter 5. The background of the stiffness classification boundaries according to Eurocode 3 is described and we demonstrate how to extend them to joints belonging to pitched-roof portal frames. This last point being solved, nothing prevents right now to apply all the new available design concepts for joints and frames to pitched-roof portal frames which constitute a significant part of the activity in steel construction.

Lastly new research orientations to improve the existing stiffness classification system are briefly discussed. They are now in discussion in the COST C1 European project.

As a conclusion now, we would like to enumerate some different topics which appear to us of high interest for further research works, in the sense that they could bring answers to some questions still in suspense and would help in developing further practical design

tools for other types of joint configurations such as column bases or minor axis joints. Some of these works are already in progress.

These are :

- further verifications for the extension of the design rules for joints to high strength steels;
- improvement of the design models for slender column web panels in shear;
- refinement of the boundaries for stiffness classification;
- development of simplified design procedures for the distribution of internal forces in joints subjected to axial forces in addition to bending moments and shear forces;
- practical design guidelines for the design of column bases;
- development of a stiffness model for weak axis joints.

Lastly, I would like to mention two topics where the use of the component method could bring some good progress in the future : the fire response of structural joints and the behaviour of the joints in so-called slim floor systems.

And if we think that, in the frame of the COST C1 project, an application to concrete, precast concrete and timber joints is now contemplated, ...

REFERENCES

References

A

[A1] Aribert, J.M., Lachal, A. and Moheissen

Interaction du voilement et de la résistance plastique de l'âme d'un profilé laminé soumis à une double compression locale (nuance allant jusqu'à Fe 360).

Construction métallique, n° 2, 1990.

[A2] Anderson, D.

European rules for the design of composite joints.

Report of the IABSE Colloquium on Semi-Rigid Connections, Istanbul, Turkey, September 1996, pp. 171-182.

References

B

- [B1] Bursi, O.
Behaviour and modelling of semi-rigid beam-to-column steel joints.
Sprint Contract RA351, University of Trento (I), University of Liège (B), CRIF (B), CTICM (B), ENSAIS Strasbourg (F), LABEIN (E)
- [B2] Bursi, O. and Jaspart, J.P.
Benchmarks for finite element modelling of bolted steel connections.
To appear in the Journal of Constructional Steel Research.
- [B3] Bursi, O. and Jaspart, J.P.
Calibration of a finite element model for bolted end-plate steel connections.
To appear in the Journal of Constructional Steel Research.
- [B4] Bijlaard, F.S.K. and Steenhuis, M.
Prediction of the influence of connection behaviour on the strength, deformations and stability of frames by classification of connections.
Proceedings of the Second AISC and ECCS Workshop on Connections, Pittsburgh, U.S.A., 1991, pp. 307-318.
- [B5] Bijlaard, F.S.K. et al
SG Course about new codes EC3 and TGB-Steel (in Dutch).
TNO Building and Construction Research, March 1991.
- [B6] Briquet, C., Guisse, S., Jaspart, J.P., Lognard, B. and Maquoi, R.
Research activities under COST C1 at the Department MSM of the University of Liège.
Proceedings of the Second State-of-the-Art, COST C1 Workshop, Prague, October 26-28, 1994, pp. 75-88.

C

- [C1] COST C1 European Action - Belgian Project between University of Liège and the Walloon Region on "Semi-Rigid Behaviour of Structural Joints".
Interim Report n° 4, Department MSM, University of Liège, December 1994.
- [C2] COST C1 European Action - Belgian Project between University of Liège and the Walloon Region on "Semi-Rigid Behaviour of Structural Joints".
Interim Report n° 2, Department MSM, University of Liège, December 1993.
- [C3] COST C1 European Action - Belgian Project between University of Liège and the Walloon Region on "Semi-Rigid Behaviour of Structural Joints".
Interim Report n° 1, Department MSM, University of Liège, Juin 1993.
- [C4] Cerfontaine, F.
Dimensionnement et conception économiques des assemblages boulonnés entre profilés métalliques reconstitués par soudage.
Diploma work, Department MSM, University of Liège, 1996.
- [C5] COST C1 European Action - Belgian Project between University of Liège and the Walloon Region on "Semi-Rigid Behaviour of Structural Joints".
Interim Report n° 5, Department MSM, University of Liège, Juin 1995.
- [C6] COST C1 European Action - Belgian Project between University of Liège and the Walloon Region on "Semi-Rigid Behaviour of Structural Joints".
Interim Report n° 6, Department MSM, University of Liège, December 1995.
- [C7] COST C1/ECCS Drafting Group on Composite Connections.
Proposed document on Connection Behaviour and Design.
To appear as a COST C1 publication.

References

D

[D1] Davies, J.M.

Inplane stability in portal frames

The Structural Engineer, Vol. 68, N° 8, April 17, 1990, pp. 141-147.

References

E

- [E1] Eurocode 3
Design of Steel Structures. Part 1.1 : General Rules and Rules for Buildings.
European Prestandard - ENV 1993-1-1, February 1992.
- [E2] Eurocode 3. Revised Annex J on « Steel Joints in Building Frames ».
Paper CEN/TC250/SC3-N-419 E, Brussels, June 1994
- [E3] Eurocode 4. Annex J on « Composite Joints in Building Frames ».
Paper N123, CEN/TC250/SC4, 1996.
- [E4] ECSC Research Contracts 7210-SA/212 and 320.
Elaboration of a design handbook in view of the application of the semi-rigid concept for connections to the structural analysis.
University of Liège (B), CTICM (F), CRIF (B), RWTH Aachen (D) and TNO Delft (NL), 1993-1996.
- [E5] ECCS Technical Committee 8 on Structural Stability - Technical Working Group 8.3 on Plated Structures.
Behaviour and Design of Steel Plated Structures.
ECCS Publication n° 44, Edited by P. Dubas and E. Gehri, 1986.
- [E6] Eurocode 3, Annex L on "Design of Column Bases".
European Prestandard - Env 1993-1-1, February 1992.
- [E7] Eurocode 4
Design of Composite Steel and Concrete Structures. Part 1.1 : General Rules and Rules for Buildings.
European Prestandard, ENV 1994-1-1, CEN, Brussels, 1992.

References

F

- [F1] Frey, F., De Ville de Goyet, V. et al
FINELG - Non-linear Finite Element Analysis Program - *User's Manual*
Version 5.2., University of Liège, March 1990.
- [F2] Finet, L.
Influence de l'effort normal sur le calcul des assemblages semi-rigides.
Diploma work, CUST, Clermont-Ferrand, France, July 1994.

G

- [G1] Guisse, S. and Jaspart, J.P.
Stress interactions in column webs.
Proceedings of the IX International Conference on Metal Structures, Krakow, Poland, June 26-30, 1995, pp. 147-156.
- [G2] Gomes, F.C.T., Jaspart, J.P. and Maquoi, R.
Behaviour of minor axis joints and 3-D joints.
Proceedings of the Second State of the Art Workshop COST C1 on Semi-Rigid Connections, F. Wald Ed., Czech Technical University, Prague, 26-28.10.1994, pp. 111-120.
- [G3] Gomes, F.C.T.
Comportement semi-rigide de noeuds poutre-colonne d'axe faible et résistance de noeuds tridimensionnels en acier.
Doctoral thesis (to be submitted at the University of Liège)
- [G4] Gomes, F.C.T. and Jaspart J.P.
Experimental research of minor axis joints. Comparison with theoretical predictions.
COST C1-WG2 "Steel and Composite" Meeting, Doc. C1/WD2/94-13, Coimbra, 25-26/11/1994.
- [G5] Gomes, F.C.T.
Etat limite ultime de la résistance de l'âme d'une colonne dans un assemblage semi-rigide d'axe faible.
Internal Report n° 203, Dept. MSM, University of Liège, 1990.
- [G6] Guisse, S., Vandegans, D. and Jaspart, J.P.
Application of the component method to column bases. Experimentation and development of a mechanical model for characterization.
Rapport CRIF, MT 295, CRIF, Liège, 1997

References

[G7] Gomes, F.C.T.

Proposal for the classification of beam-to-column joints.

Document C1/WG2/95-20, COST C1 Working Group 2 «Steel and Composite », Graz, December 15, 1995.

References

H

[H1] Hoffmann, J.P.

Eurocode 3. Calcul d'assemblages de portiques rigides faits de profilés reconstitués soudés.

Diploma work, CUST, Clermont-Ferrand, France, July 1993.

References

J

[J1] Jaspert, J.P.

Etude de la semi-rigidité des assemblages poutre-colonne et de son influence sur la résistance et la stabilité des ossatures en acier.

Ph.D. Thesis (in French), Department MSM, University of Liège, Belgium, 1991.

[J2] Jaspert, J.P.

Material identified as significant for Eurocode 3 at the University of Liège.

Report n° 206, Department MSM, University of Liège, 1992.

[J3] Janss, J., Jaspert, J.P. and Maquoi, R.

Strength and behaviour of in-plane weak axis joints and 3-D joints.

Proceedings of a State-of-the-Art Workshop on Connections and the Behaviour, Strength and Design of Steel Structures, Cachan, France, May 25-27, 1987.

[J4] Jaspert, J.P.

Extending of the Merchant-Rankine formula for the assessment of the ultimate load of frames with semi-rigid joints.

Journal of Constructional Steel Research, n° 11, 1988, pp. 283-312.

References

K

[K1] Klein

Das elastisch-plastische Last-Verformung Verhalten $M_b-\theta$ steifenlosen, geschweisster Knoten für die Berechnung von Stahlrahmen mit HEB-Stützen.

Ph.D. Thesis, University of Innsbruck, 1985.

References

L

[L1] Lawson, R.M. and Gibbons, C.

Moment connections in composite construction : Interim guidance for end-plate connections.

Steel Construction Institute, Ascot, 1995.

References

M

[M1] Meijer, H.S.

Influence of the rotational stiffness of column-beam connections on the behaviour of braced and unbraced frames (in Dutch).

Diploma work, Technical University of Eindhoven, August 1990.

[M2] Mazzolani, F.M., De Matteis, G. and Mandara, A.

Classification system for aluminium alloy connections.

Report of IABSE Colloquium on Semi-Rigid Structural Connections, Istanbul, Turkey, 1996, pp. 83-94.

References

N

- [N1] Nethercot, D.A. and Zandonini, R.
Methods of prediction of joint behaviour - Beam-to-column connections.
Chapter of a volume in the "Stability and Strength" series published by Elsevier.
- [N2] Neves, L.F.C., Gomes, F.C.T.
Semi-rigid behaviour of beam-to-column minor axis joints.
Proceedings of the IABSE Colloquium, Istanbul, Turkey, September 25-27, 1996, pp. 207-216.
- [N3] Neves, L.F.C.
Nos semi-rígidos em estruturas metálicas. Avaliação da rigidez em configurações de eixo fiaco.
Master Thesis, University of Coimbra, 1996.

References

P

[P1] Packer, J.A., Morris, G.A. and Davies, G.

A limit state design method for welded tension connections to I-sections webs.

Journal of Constructional Steel Research, vol. 92, 1989, pp. 33-53.

[P2] Penserini, P.

Caractérisation et modélisation du comportement des liaisons structure métallique - fondation.

Ph.D. Thesis, University Pierre and Marie Curie, Paris 6, 1991.

S

- [S1] SPRINT Contract RA351.
- Steel moment connections according to Eurocode 3. Simple design aids for rigid and semi-rigid joints.
- CRIF(B), University of Liège (B), CTICM (F), University of Trento (I), LABEIN Bilbao (SP), 1992-1996.
- [S2] SERICON
- International databank system for semi-rigid connections.
- ECCS TC10 and Cost C1, Version 1.5, RWTH Aachen Germany, 1995.
- [S3] Scheer, J., Pasternak, H. and Schween
- Ermittlung der Traglast von geschweissten Rahmenecken mit Hilfe von Zugfeld-Modellen.
- Report n° 6202/2, Institut für Stahlbau, Technische Universität Braunschweig, 1992.
- [S4] Schween
- Ermittlung der Tragfähigkeit von Rahmenecken mit Hilfe von Zugfeldmodellen (Fortsetzung).
- Report n° 6207, Institut für Stahlbau, Technische Universität Braunschweig, 1995.
- [S5] Steenhuis, M., Dol, C. and Van Gorp, L.
- Computerized calculation of force distributions in bolted end-plate connections according to Eurocode 3.
- Journal of Constructional Steel Research, vol. 31, n° 1, 1994, pp. 135-144.

References

T

[T1] Taquet, F.

Analyse de la capacité portante de noeuds d'angle.

Diploma work, Department MSM, University of Liège, 1988.

References

V

[V1] Vandegans, D.

Use of Threaded Studs in Joints between I-beams and RHS columns.

Proceedings of the Istanbul Colloquium, Turkey, September 25-27, 1996,
pp. 53-62.

[V2] Vayas, I., Ermopoulos, J. and Pasternak, H.

Design of Steel Frames With Slender Joint Panels.

Journal of Constructional Steel Research, vol. 35, n° 2, 1995.

References

W

- [W1] Weynand, K., Jaspart, J.P. and Steenhuis, M.
The Stiffness Model of Revised Annex J of Eurocode 3.
Connections in Steel Structures II, Proceedings of the Third International Workshop, Trento, Italy, May 29-31, 1995, Pergamon Press, pp. 441-452.
- [W2] Wald, F.
Patky sloupu - Column Bases.
CVUT - Czech Technical University, Prague 6, 1995.
- [W3] Wood, R.H.
Effective length of columns in multi-storey buildings - Part 3.
The Structural Engineer, vol. 52, 1974, pp. 341-346.

Z

[Z1] Zoetemeijer, P.

Een rekenmethode voor het ontwerpen van geboute hoekverbindingen met een kolomschot in the trekzone van de verbinding en een niet boven de ligger uitstekende kopplaat.

Report 6-81-4, Stevin Laboratory, TU Delft, June 1982.

[Z2] Zoetemeijer, P.

Bolted beam-to-column knee connections with haunched beams. Tests and computations.

Report 6-81-23, Stevin Laboratory, TU Delft, 1992.

[Z3] Zoetemeijer, P.

Summary of researches on bolted beam-to-column connections.

Report 6-85-7, TH Delft, November 1983.

[Z4] Zoetemeijer, P.

Bolted connections with flush end-plates and haunched beams. Tests and limit state design methods.

Report 6-81-15, Stevin Laboratory, TU Delft, June 1981.

[Z5] Zoetemeijer, P.

Influence of normal-, bending- and shear stresses in the web of European rolled sections.

Report n° 6-75-18, Stevin Laboratory, TU Delft, 1975.

[Z6] Zoetemeijer, P.

The influence of normal-, bending-, and shear stresses on the ultimate compression force exerted laterally to European rolled sections.

Report n° 6-80-5, Stevin Laboratory, Delft University of Technology, 1980.